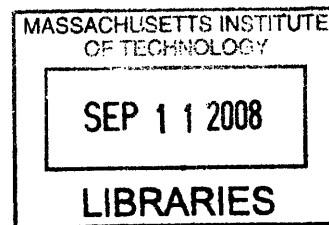


**Photo-Cross-Linking and Identification of Nuclear Proteins that Bind to DNA  
Containing a Site-Specific Adduct of *cis*-[Pt(NH<sub>3</sub>)(*N*-(6-aminohexyl)-4-  
benzophenamide)Cl<sub>2</sub>].**

by

Evan Ross Guggenheim

B.S. High Honors, Chemistry (2003)  
Brandeis University



Submitted to the Department of Chemistry in Partial Fulfillment of the Requirements for the  
Degree of

Doctor of Philosophy in Inorganic Chemistry  
at the  
Massachusetts Institute of Technology

September 2008

© 2008 Massachusetts Institute of Technology  
All rights reserved

Signature of Author: \_\_\_\_\_

A handwritten signature in black ink, appearing to be "Evan Ross Guggenheim", written over a horizontal line.

Department of Chemistry  
June 25, 2008

Certified by: \_\_\_\_\_

Stephen J. Lippard  
Arthur Amos Noyes Professor of Chemistry  
Thesis Supervisor

Accepted by: \_\_\_\_\_

Robert W. Field  
Chairman, Departmental Committee on Graduate Studies

**ARCHIVES**

This doctoral thesis has been examined by a committee of the Department of Chemistry as follows:

---

Richard R. Schrock  
Frederick G. Keyes Professor of Chemistry  
Committee Chairman

---

Stephen J. Lippard  
Arthur Amos Noyes Professor of Chemistry  
Thesis Supervisor

---

Stuart S. Licht  
Samuel A. Goldblith Career Development Professor of Chemistry

# Photo-Cross-Linking and Identification of Nuclear Proteins that Bind to DNA Containing a Site-Specific Adduct of *cis*-[Pt(NH<sub>3</sub>)(*N*-(6-aminohexyl)-4-benzophenonamide)Cl<sub>2</sub>].

by  
Evan Ross Guggenheim

Submitted to the Department of Chemistry on June 25, 2008  
in Partial Fulfillment of the Requirements for the Degree of  
Doctor of Philosophy in Inorganic Chemistry at the  
Massachusetts Institute of Technology

## ABSTRACT

*cis*-Diamminedichloroplatinum(II), or cisplatin, is the most successful cancer drug ever discovered. It has been used for over 30 years in the treatment of several types of malignancies, with the highest success rates in testicular cancer patients. Despite the triumphs of this drug, the exact mechanisms of cell-killing by cisplatin are not fully understood. A more complete understanding of the ability of this drug to target and destroy cancer cells will lead to advances in overcoming the intrinsic and acquired resistance that many cancer patients encounter with cisplatin. Cisplatin can form several distinct DNA adducts, which are toxic to cells if not repaired. By identifying proteins that bind to platinum-modified DNA, the work in this thesis focuses on the early stages of DNA adduct processing.

The first chapter of this thesis gives a review of the identification of proteins with an affinity for platinum-modified DNA in the literature. Different techniques are discussed, and the proteins identified by these methodologies are discussed.

The methodologies previously used to identify proteins with an affinity for platinum-modified DNA have led to important advances in our knowledge of the cellular processing of these adducts. The development of an assay that can survey the entire nuclear milieu, allowing for multiprotein complexes to stay intact and proteins to compete for binding to the damaged DNA has been difficult. These challenges were addressed by using a photo-active cisplatin analogue, *cis*-[Pt(NH<sub>3</sub>)(*N*-(6-aminohexyl)-4-benzophenonamide)Cl<sub>2</sub>] (PtBP6). Site-specifically modified DNA probes were synthesized and used to identify proteins photo-cross-linked by the benzophenone-modified platinum complex. A 25-bp probe containing a 1,2-d(GpG) and 1,3-d(GpTpG) intrastrand adduct of PtBP6 were synthesized and used in photo-cross-linking experiments. The results demonstrated that the 1,2-d(GpG) adduct binds more strongly to HMG-domain proteins, and the 1,3-d(GpTpG) adduct exclusively binds a nucleotide excision repair protein RPA1. A probe containing a mismatched 1,2-d(GpG) adduct was also synthesized, and this DNA photo-cross-linked more strongly to the mismatch repair protein, Msh2.

These results demonstrate that PtBP6-modified DNA mimics the behavior of cisplatin-modified DNA published in the literature. These experiments also identify PARP-1 as a protein with an affinity for platinum-modified DNA. This protein will bind to other types of DNA damage, but had not been previously implicated in platinum-DNA

damage binding. Photo-cross-linking experiments were carried out using nuclear extracts from cancer cells with varying sensitivity to cisplatin. The results indicate that expression levels of PARP-1 may effect the cell's ability to survive cisplatin exposure. The proteins photo-cross-linked by different nuclear extracts were consistent, however, indicating that DNA damage recognition is not the mechanism for cisplatin resistance in these cell lines.

In order to ensure that the proteins identified using the 25-bp probe were not binding to the blunt ends of the DNA and being photo-cross-linked, a 90 base dumbbell probe was synthesized. In this probe, the DNA contains no blunt ends but two loops, which are 19 bases from the platinum adduct. Photo-cross-linking experiments using this probe confirmed the binding of each of the proteins identified using the 25-bp probe. The photo-cross-linking of DDB1, RFC1 and RFC2 demonstrates that a longer platinum-modified DNA probe is a better substrate for recognition by nucleotide excision repair proteins. This work also indicates that both mismatch repair recognition complexes Msh2/Msh3 and Msh2/Msh6 bind to platinum-damaged DNA. The affinity of chromatin remodeling proteins for platinum-damaged DNA was also established in this work.

The characterization of PARP-1 as a protein with an affinity for platinum-damaged DNA was first discovered using photo-cross-linking experiments with PtBP6. Prior to this discovery, the ability of PARP inhibitors to sensitize cells to cisplatin had already been investigated. Conflicting results are reported in the literature about the efficacy of these inhibitors as potentiators of cisplatin toxicity. In order to probe the mechanism of the interaction, assays were carried out using PARP inhibitors synthesized by Alison Ondrus of the Movassaghi lab. These experiments indicated that the activity of PARP proteins following exposure to platinum-modified DNA may be cell-line dependent. We were unable to detect a significant increase in PARP activity following exposure to cisplatin, however, in any cell line tested. These results suggest that more mechanistic studies into the effect of the activity of PARP proteins on cancer cells exposed to cisplatin are warranted.

Initial photo-cross-linking experiments using a duplex containing a benzophenone moiety on the DNA indicated that this type of probe could be used to identify proteins with an affinity for various types of DNA lesions. Also, photo-cross-linking using a 157-bp probe, site-specifically modified with PtBP6, indicated that there are some obstacles to overcome when performing these types of experiments with longer DNA probes. Initial NMR spectroscopic studies of a PtBP6-modified d(GpG) were carried out to characterize the orientational isomers of this type of DNA lesion.

Thesis Supervisor: Stephen J. Lippard  
Title: Arthur Amos Noyes Professor of Chemistry

*I know you were here with me,  
because I couldn't have done it without you*

## ACKNOWLEDGEMENTS

It is hard to imagine boiling down five years of inspiration, encouragement, sympathy, empathy, and a whole lot of hard work into a few paragraphs. But it would be an injustice to not thank those people who have helped me grow, learn, and sometimes survive, through this program. This has been the most difficult thing I have ever accomplished in my life, and my success is in no small part due to those who helped me. Firstly, I have to thank Steve. Thank you for having faith in a synthetic inorganic chemist who didn't know a gel from an eppendorf tube, and letting me develop an understanding of bioinorganic chemistry that will no doubt mold the rest of my career in science. Through many sessions of editing year-end reports and manuscripts, you have improved my ability to write my results so that others can learn from my work. You have taught me how to think through a problem, and not leave one rock unturned. You taught me to never trust a "kit" without understanding what goes into it. No matter where my career and life take me, I will always feel a part of the Lippard Lab Family. I also want to thank the Chemistry Department at MIT, specifically my committee, Dan Nocera, Dick Schrock, John Essigmann, and Stuart Licht. I want to thank Susan Brighton from the Chemistry Office, you have been incredibly helpful in guiding me through this program, and I have enjoyed our many conversations about graduate school and otherwise.

That Lippard Lab Family has been tremendously important in my becoming a better scientist, and helping me through those inevitable tough times in my graduate school life. Mike McCormick, my partner in crime; we started this program together, helped each other through classes, "cumes," exams, seminars, subgroups, group meetings, and I really could not have done it without you. You helped me stay sane when things seemed to be stacked up against me. Also Jeremy Kodanko, who had the wisdom of an old man, despite only being sort of an old man. We had some great times here, those coffee breaks got me through some hard days. Going to lunch, talking with Mike and Jeremy about anything from science to sports to things I shouldn't mention here, were great memories that I will think back on forever. The rest of the cool crew, Matt Wallace and Ryan Todd, it has been quite a ride, and I am glad you two were a part of it. Also, the rest of the basketball squad, Laurance Beauvais and Leslie Murray, despite the bumps and bruises, we played some good games.

To the Cisplatin Subgroup, past and present, Katie Lovejoy, Shanta Dhar, Sumi Mukhopadhyay, Guangyu Zhu, Wee Han Ang, Dong Wang, Matthias Ober, Rodney Feazell, and Christiana Zhang. To those members of the subgroup who guided me through my first two years, when I needed it most, Katie Barnes, Yongwon Jung, Andrew Danford, and Dong Xu. You are great co-workers and great friends. Other members of the Fam who made this possible, Emily Carson, Viviana Izzo, Andy Tennyson, Todd Harrop, Mi Hee "focus!" Lim, Liz Nolan and Erwin Reisner. Current members who helped me through the series of anxiety attacks that you could call my thesis writing and defense, Simone Friedle, Brian Wong, Rachel Behan, Elisa Tomat, Christy Tinberg, Woon-Ju Song, Lindsey McQuade, Julia Kozhukh, Zach Tonzetich, and Xiao-An Zhang. To those members of the Dead Man Piano Movers that I haven't mentioned yet, Erik Dill, Joel Rosenthal, Matt Sazinsky, Chris Goldsmith, and John Robblee. I worked with two great UROPs at MIT, Noel Lee and Cindy Yuan. I also would like to thank Steve Tardivo, Maddy Eibner-Siwiek, Stephen Buchwald and Tim Jamison for many

pleasurable chats in and around the halls of MIT. I wish the best of luck to all of you at MIT and beyond.

While I had so much help in getting through this program at work, I never would have been successful without my friends and family. I want to thank Nathan Speed for being a great friend through this whole experience. We have gotten each other through some tough times, and helped each other celebrate the good times. I have other incredible friends to help me stay focused on the important things in life in Tim Torrisi, Mike Stier, Jeremy Lechan, Jen Gueguen, Gretchen Chick, Casey Barrieau and Justin Moore. I do not know how I could have made it through this without you all by my side. I've had some great rotating roommates throughout the years at MIT, and I would like to thank Vince DeMore, Pete Dempsey, Marty Newman, Colin Rowan and Dave McMenemy for being there to help me chill out after a long day at work. I also cannot forget to thank other wonderful friends who have helped me throughout this journey, Vari Kamberkar, Seth Woolf, Pete Sloan, Erik Kolovson, Holly Ricci, and Jen and Josh Segal. When things got really tough, I found inspiration in an amazing person that I wish I could have known better, Laurel Bowron.

I am blessed to have an amazing family to support me through these times. Mom, you are unbelievably brave and strong, and your strength has inspired me to march on through the bumps in the road. My brothers David and Jacob, my grandparents Margot Goldstein and Sydney and Hank Guggenheim. My uncles Seth Guggenheim, and Gerson and Josh Goldstein. Seeing your smiling faces is enough reward to make it all worth it. I want to thank my aunt Jana Guggenheim, one of the smartest and wittiest people I ever knew, for being an intellectual inspiration, and for watching over me when I needed it most. My grandfather Melvin Goldstein, for teaching me how to really enjoy learning. Between his love for Judaism, Shakespeare, music, dance and most importantly, his grandchildren, my memories of days with Poppy are the fondest of my childhood. And to round out the all-star squad of those watching over me from above, I would like to thank Dad. The things Dad did with his life and the way he lived it were an inspiration to everyone around him. But no one could be more blessed by his wonderful influence than his children. Dad and I had a connection that can never be replaced, and it lives on even today. I don't know how people can grow up to appreciate what is really important in life without a dad like Bob, but I am sure glad I didn't have to. Dad used to say that he was "rich with love," and the people in my life have made me feel downright greedy.

Lastly, I'd like to thank my amazing girlfriend Jocelyn. You've been my closest friend and my rock through the many obstacles that have been thrown my way over the last five years. Your patience, understanding, love, and advice have kept me going and inspired me to do my best. I am so lucky to have you here for me, and I cannot imagine someone with whom I would rather spend this next phase of my life.

## TABLE OF CONTENTS

<b>ABSTRACT</b>	<b>3</b>
<b>ACKNOWLEDGEMENTS</b>	<b>6</b>
<b>TABLE OF CONTENTS</b>	<b>8</b>
<b>LIST OF TABLES</b>	<b>15</b>
<b>LIST OF SCHEMES</b>	<b>16</b>
<b>LIST OF FIGURES</b>	<b>17</b>
<b>ABBREVIATIONS</b>	<b>21</b>
<b>Chapter 1: Nuclear Proteins with an Affinity for Platinum-Modified DNA.</b>	<b>24</b>
I. INTRODUCTION	25
II. METHODS USED TO IDENTIFY PLATINUM-DNA BINDING PROTEINS	26
III. HUMAN PROTEINS THAT BIND PLATINUM-MODIFIED DNA AND IMPLICATIONS IN DNA REPAIR	31
Nucleotide excision repair (NER) proteins	31
HMG-domain proteins	32
Transcription factors lacking an HMG-domain	34
Mismatch repair (MMR) proteins	35
DNA protein kinase (DNA-PK)	36
3-Methyladenine DNA glycosylase (AAG)	37
Poly(ADP-ribose) polymerase 1 (PARP-1)	37
IV. SUMMARY OF CONSEQUENCES OF PROTEINS BINDING TO PLATINUM-MODIFIED DNA	38
V. NEW PLATINUM ANTICANCER COMPOUNDS	40
VI. ORGANIZATION AND SCOPE OF THESIS	43
VII. REFERNCES	47
VIII. TABLES	51
IX. FIGURES	52
<b>Chapter 2: Optimization of Photo-Cross-Linking Conditions for Identification of Proteins with an Affinity for a 25-bp Duplex DNA Containing a 1,2-d(GpG) Adduct of cis-[Pt(NH<sub>3</sub>)(N-(6-aminohexyl)-4-benzophenonamide)Cl<sub>2</sub>].</b>	<b>56</b>
I. INTRODUCTION	57
II. MATERIALS AND METHODS	61



Cell culture	60
Nuclear extraction	60
Synthesis of PtBP6	61
Synthesis of cis-Diamminediiiodoplatinum(II) (1)	61
Synthesis of cis-Diamminedichloroplatinum(II) (2)	62
Synthesis of (Ph <sub>4</sub> P)[PtCl <sub>3</sub> (NH <sub>3</sub> )] (3)	62
Synthesis p-Benzoylbenzoic acid N-hydroxysuccinimide ester (4)	62
Synthesis of [(4-Benzoyl-benzoylamino)-hexyl]-carbamic acid tert-butyl ester (5)	63
Synthesis of N-Aminoethyl-4-benzoyl-benzamide (5b)	63
Synthesis of [PtCl <sub>2</sub> (NH) <sub>2</sub> (BP6)] (6)	63
DNA Synthesis	64
Preparation of a 25 base DNA containing a site-specific PtBP6 adduct	65
Characterization of 25 base DNA containing a 1,2-d(GpG) adduct of PtBP6	65
Radiolabeling of 25 base DNA	67
Synthesis of duplex probes	67
Optimization of analytical-scale photo-cross-linking with a 1,2-d(GpG)-PtBP6 probe	68
Optimization of preparative-scale photo-cross-linking of probes	68
Preparative scale photo-cross-linking	69
III. RESULTS	71
Synthesis and characterization of cis-[Pt(NH <sub>3</sub> )(N-(6-aminoethyl)-4-benzophenonamide)Cl <sub>2</sub> ] (PtBP6)	71
Synthesis and characterization of a 25 base 1,2-d(GpG) intrastrand probe	71
Duplex 25-bp probes	73
Analytical-scale photo-cross-linking of a 25-bp duplex containing a 1,2-d(GpG) adduct of PtBP6	73
Analysis of protein retention on streptavidin-coated magnetic beads	74
Preparative-scale photo-cross-linking of a 25-bp duplex containing a 1,2-d(GpG) intrastrand PtBP6 adduct with HeLa nuclear extracts	74
IV. DISCUSSION	75
Optimization of photo-cross-linking experiments	76
Protein carryover	77
Detection limits of photo-cross-linking	77
Consideration of the end effect	78
PtBP6 versus cisplatin adducts	78
DNA repair proteins	79
HMG-domain proteins	80
V. CONCLUSIONS	80
VI. REFERENCES	82
VII. TABLES	84
VIII. SCHEMES	88
IX. FIGURES	89

<b>Chapter 3: Photo-cross-linking and identification of nuclear proteins that bind to constructs of a 25-bp probe containing a site-specific adduct of PtBP6.</b>	<b>103</b>
I. INTRODUCTION	104
II. MATERIALS AND METHODS	104
Cell culture	105
Short hairpin RNA (shRNA)-induced RNAi on PARP-1 in HeLa cells	105
Nuclear extraction	106
Cytotoxicity assays	106
Synthesis of a 25-base single stranded DNA containing a 1,3-d(GpTpG) intrastrand PtBP6 cross-link	106
Characterization of 1,3-d(GpTpG) intrastrand PtBP6-modified 25-base DNA probes	107
Synthesis of duplex DNA	107
Analytical-scale photo-cross-linking	108
Preparative-scale photo-cross-linking of 25-bp duplex containing a 1,3-d(GpTpG) adduct of PtBP6	109
Western blot for PARP-1 in HeLa and Ntera2 nuclear extracts	109
III. RESULTS	110
Preparation of nuclear extracts	110
Cytotoxicity assays	110
Preparation and characterization of 25-base DNA containing a 1,3-d(GpTpG) adduct of PtBP6	111
Synthesis of duplex DNA	111
Silencing of PARP-1 in HeLa cells	112
Photo-cross-linking of 25-bp duplex containing a 1,3-d(GpTpG) adduct of PtBP6	112
Analytical-scale photo-cross-linking using nuclear extracts from HeLa cells in which PARP-1 was silenced by RNAi	112
Analytical-scale photo-cross-linking of a 25-bp duplex containing a mismatched 1,2-d(GpG) intrastrand adduct	112
Analytical-scale photo-cross-linking using nuclear extracts from different cancer cell lines	113
Western blot of analysis PARP-1 in HeLa and Ntera2 cells	113
IV. DISCUSSION	114
Protein identification	114
Consideration of the end effect	114
Photo-cross-linking with nuclear extracts from different cancer cell lines	115
HMG-domain proteins and the 1,3-d(GpTpG) adduct	115
Nucleotide excision repair protein, RPA1	116
Platinum-modified DNA containing a mismatch	117
PARP-1 and DNA ligase III	117
V. CONCLUSIONS	120
VI. REFERENCES	121

VII. TABLES	123
VIII. FIGURES	125
<b>Chapter 4: Photo-Cross-Linking and Identification of Nuclear Proteins that Bind to a PtBP6-Modified 90-base DNA Dumbbell Probe.</b>	<b>134</b>
I. INTRODUCTION	135
II. MATERIALS AND METHODS	136
Cell culture	136
Synthesis and characterization of a site-specifically platinated 25-base DNA	136
Synthesis of a biotinylated 65-base DNA	136
Synthesis of site-specifically modified 90-base probe	137
Characterization of site-specifically modified 90-base probe	137
Analytical-scale photo-cross-linking of 90-base probe	138
90-base probe repair assay	139
Preparative-scale photo-cross-linking of 90-base probe	139
III. RESULTS	139
Synthesis of a site-specifically platinated 90-base probe	139
Characterization of the site-specifically platinated 90-base probe	140
90-base probe repair assay	141
Analytical-scale photo-cross-linking of 90-base probe	141
Preparative-scale photo-cross-linking of 90-base probe	141
IV. DISCUSSION	142
Mung bean nuclease analysis of 90-base dumbbell probe	142
The photo-cross-linking of PARP-1 is not due to an affinity for DNA ends	143
Mismatch repair recognition complexes Msh2/Msh3 and Msh2/Msh6 both bind to platinum-modified DNA	144
The photo-cross-linking of SPT16 gives structural information about the binding of the FACT complex to platinum-modified DNA	144
Proteins implicated in nucleotide excision repair bind to PtBP6-modified DNA	144
Chromatin remodeling proteins bind to platinum-modified dumbbell DNA	146
PtBP6-modified DNA is able to photo-cross-link proteins with low cellular abundance	147
Recognition of platinum-modified DNA is consistent between cancer cell lines	147
V. CONCLUSIONS	148
VI. REFERENCES	150
VII. TABLES	153
VIII. FIGURES	155
<b>Chapter 5: The activity of PARP proteins following cisplatin exposure in cancer cells is cell line-dependent.</b>	<b>162</b>
I. INTRODUCTION	163
II. MATERIALS AND METHODS	166

Synthesis of CEP-A and CEP-6800	167
Cell culture	167
MTT assays	167
Density-dependent cytotoxicity assay	167
Photo-cross-linking in the presence of PARP inhibitors	168
Preparation of nuclear extracts from cisplatin-treated cells	168
Preparation of cisplatin-treated cell lysates	168
Nuclear extract-based PARP activity assay	169
Lysed cell-based PARP activity assay	169
Western blot for PAR	169
<b>III. RESULTS</b>	<b>170</b>
Synthesis of CEP-A and CEP-6800	170
Cytotoxicity assays	170
Photo-cross-linking in the presence of the PARP inhibitor CEP-A	171
PARP activity assay with nuclear extracts	172
Cell-based PARP activity assay	172
<b>IV. DISCUSSION</b>	<b>173</b>
The cell lines tested do not show density-dependent cytotoxicity	173
NTera2 cells are sensitive to PARP inhibition	174
PARP inhibitors potentiate the cytotoxicity of cisplatin in certain cancer cell lines	175
PARP-1 activity dissociates proteins from platinum-modified DNA in nuclear extracts	176
There is no significant change in poly(ADP-ribosyl)ation following cisplatin treatment of the cell lines tested	177
<b>V. CONCLUSIONS</b>	<b>178</b>
<b>VI. REFERENCES</b>	<b>180</b>
<b>VII. TABLES</b>	<b>182</b>
<b>VIII. FIGURES</b>	<b>183</b>
<b>Appendix A: Synthesis and characterization of a benzophenone-modified DNA probe.</b>	<b>199</b>
<b>I. INTRODUCTION</b>	<b>200</b>
<b>II. MATERIALS AND METHODS</b>	<b>201</b>
Synthesis of amino-modified DNA	201
Synthesis of a benzophenone-modified DNA strand	202
Characterization of benzophenone-modified DNA	202
Synthesis of cisplatin-modified 25-base top strand	202
Characterization of cisplatin-modified 25-base top strand	203
Preparation of double-stranded probes	203
Analytical-scale photo-cross-linking experiments	203
<b>III. RESULTS</b>	<b>204</b>
Synthesis and characterization of benzophenone-modified DNA	204

Synthesis and characterization of cisplatin-modified DNA	205
Synthesis of 25-bp duplexes	205
Analytical-scale photo-cross-linking of benzophenone-modified DNA	205
IV. DISCUSSION	206
V. REFERENCES	207
VI. SCHEMES	208
VII. FIGURES	209
<b>Appendix B: Synthesis and characterization of a benzophenone-modified 157-base pair probe.</b>	<b>217</b>
I. INTRODUCTION	218
II. MATERIALS AND METHODS	218
Synthesis and characterization of a site-specifically platinated 25-base DNA	218
Synthesis of a 157-bp duplex containing a 1,2-d(GpG) intrastrand adduct of PtBP6	219
Analytical-scale photo-cross-linking of 157-bp duplex containing a 1,2-d(GpG) intrastrand adduct of PtBP6	219
Exonuclease digestion of 157-bp duplex	220
Enzymatic digestion-coupled analytical-scale photo-cross-linking of 157-bp duplex containing a 1,2-d(GpG) intrastrand adduct of PtBP6	220
III. RESULTS	220
Synthesis of a 157-bp duplex containing a 1,2-d(GpG) intrastrand adduct of PtBP6	221
Analytical-scale photo-cross-linking of 157-bp duplex containing a 1,2-d(GpG) intrastrand adduct of PtBP6	221
Exonuclease digestion of 157-bp duplex	221
Exonuclease digestion-coupled photo-cross-linking	222
IV. DISCUSSION	222
V. REFERENCES	224
VI. FIGURES	225
<b>Appendix C: Synthesis of PtBP6-modified d(GpG).</b>	<b>230</b>
I. INTRODUCTION	231
II. MATERIALS AND METHODS	231
Synthesis of d(GpG) dinucleotide	232
Purification of the d(GpG) dinucleotide	233
Characterization of d(GpG) dinucleotide	233
Synthesis of PtBP6-modified d(GpG) dinucleotide	234
Characterization of PtBP6-modified d(GpG) dinucleotide	234
III. RESULTS	235
Synthesis and characterization of d(GpG) dinucleotide	235

Synthesis of PtBP6-modified d(GpG) dinucleotide	235
Characterization of PtBP6-modified d(GpG) dinucleotide	235
IV. DISCUSSION	236
Assignment of NMR spectroscopic peaks	237
pH-Dependent NMR of PtBP6-d(GpG)	238
V. CONCLUSIONS AND FUTURE DIRECTIONS	239
VI. REFERENCES	240
VII. SCHEMES	241
VIII. FIGURES	242
<b>Curriculum Vitae</b>	<b>250</b>

## LIST OF TABLES

Table 1.1: Proteins with an affinity for cisplatin-damaged DNA	50
Table 2.1: Proteins identified by preparative scale photo-cross-linking of a 25-bp duplex containing a 1,2-d(GpG) intrastrand PtBP6 adduct.	84
Table 3.1: Proteins identified by preparative scale photo-cross-linking of a 25-bp duplex containing a 1,3-d(GpTpG) intrastrand PtBP6 adduct.	123
Table 3.2: Ratios of normalized intensities of photo-cross-linking using a mismatched 1,2-d(GpG) intrastrand adduct of PtBP6 to a correctly matched 1,2-d(GpG) intrastrand adduct of PtBP6.	124
Table 4.1. Proteins identified by preparative scale photo-cross-linking of a 90-base DNA containing a 1,2-d(GpG) intrastrand PtBP6 adduct.	153
Table 5.1: Maximum tolerated dose of three PARP inhibitors in four cancer cell lines	182
Table 5.2: IC <sub>50</sub> values for cDDP co-treated with maximum tolerated dose of three PARP inhibitors in four cancer cell lines	182
Table 5.3: Density-dependent IC <sub>50</sub> values for cDDP in four cancer cell lines	182

## LIST OF SCHEMES

Scheme 2.1. Synthesis of cis-[Pt(NH <sub>3</sub> )(N-(6-aminohexyl)-4-benzophenonamide)Cl <sub>2</sub> ], PtBP6.	88
Scheme A.1. Synthesis of benzophenone-modified DNA from commercially available starting materials.	208
Scheme C.1. Synthesis of d(GpG).	241



## LIST OF FIGURES

Figure 1.1. The four steps of cisplatin anticancer activity.	51
Figure 1.2. Structures of three adducts of cisplatin on DNA.	52
Figure 1.3. Methodologies developed for the characterization and identification of proteins with an affinity for damaged DNA.	53
Figure 1.4. Platinum compounds with anticancer activity.	54
Figure 2.1. Chemical structures of cisplatin and PtBP6.	89
Figure 2.2. Photo-cross-linking with a PtBP6-modified DNA probe.	89
Figure 2.3. Isolation of photo-cross-linked proteins using streptavidin-coated magnetic beads.	90
Figure 2.4. <sup>1</sup> H NMR spectroscopic analysis of cis-[Pt(NH <sub>3</sub> )(N-(6-aminohexyl)-4-benzophenonamide)Cl <sub>2</sub> ] (PtBP6) in DMF.	91
Figure 2.5. RP-HPLC purification of platinated 25 base DNA.	92
Figure 2.6. Nuclease digestion of 25 base DNA.	93
Figure 2.7. Analysis of the reaction between activated PtBP6 and deoxyguanosine.	94
Figure 2.8. ESI-MS analysis of 25-base DNA containing a 1,2-d(GpG) adduct of PtBP6.	95
Figure 2.9. Maxam-Gilbert analysis of 25 base probe.	96
Figure 2.10. Native PAGE analysis of 25-bp duplexes.	97
Figure 2.11. Effect of varying the UV irradiation time on photo-cross-linking of PtBP6-modified 25-bp duplex.	98
Figure 2.12. Effect of varying the pre-irradiation incubation time on photo-cross-linking of PtBP6-modified 25-bp duplex.	99
Figure 2.13. Effect of temperature on photo-cross-linking.	100
Figure 2.14. Analysis of washing conditions of the streptavidin-coated magnetic beads.	101
Figure 2.15. Analytical-scale photo-cross-linking of 25-bp duplex containing a 1,2-d(GpG) adduct of PtBP6.	102
Figure 3.1. Cytotoxicity assays of HeLa, NTERA2, BxPC3, U2OS and HeLa YS cancer cell lines with increasing concentrations of cisplatin.	125
Figure 3.2. RP-HPLC purification of the reaction between a 25-base DNA fragment and the activated form of PtBP6.	126
Figure 3.3. Nuclease digestion analysis of products from the reaction of PtBP6 with DNA containing a 1,3-d(GpTpG) site.	127

Figure 3.4. ESI-MS analysis of 25-base DNA containing a 1,2-d(GpTpG) adduct of PtBP6.	128
Figure 3.5. Native PAGE analysis of 25-bp duplexes.	129
Figure 3.6. Western blot analysis of single clones of HeLa cells transfected with the plasmid for RNAi of PARP-1.	130
Figure 3.7. Analytical-scale photo-cross-linking results of the 1,2-d(GpG), 1,3-d(GpTpG) and mismatched 1,2-d(GpG) intrastrand adduct-containing probes, and photo-cross-linking using nuclear extracts from HeLa YS cells.	131
Figure 3.8. Photo-cross-linking of 25-bp PtBP6 probes with nuclear extracts from various cell lines.	132
Figure 3.9. Western blot analysis of PARP-1 expression using HeLa and Ntera2 nuclear extracts.	133
Figure 4.1. Synthesis of 90-base dumbbell DNA from a PtBP6-modified 25-base DNA and biotinylated 65-base DNA.	155
Figure 4.2. 6% urea-PAGE analysis of synthesis of 90-base DNA.	156
Figure 4.3. Nuclease digestion of the 90-base DNA probe.	157
Figure 4.4. Mung bean nuclease digestion of 90-base DNA.	158
Figure 4.5. Analysis of purified 90-base DNA probe.	159
Figure 4.6. 90-base probe repair assay.	160
Figure 4.7. Photo-cross-linking with 90-base DNA probe using nuclear extracts from various cancer cell lines.	161
Figure 5.1. The catalytic activity of PARP proteins.	183
Figure 5.2. Three pathways of PARP activity.	184
Figure 5.3. Chemical structures of four PARP inhibitors.	185
Figure 5.4. <sup>1</sup> H NMR of PARP inhibitor CEP-A.	186
Figure 5.5. <sup>1</sup> H NMR of PARP inhibitor CEP-6800.	187
Figure 5.6. Cytotoxicity assays of PARP inhibitors in HeLa, Ntera2, BxPC3 and U2OS cancer cell lines.	188
Figure 5.7. Cytotoxicity assays of cisplatin co-treated with PARP inhibitors in HeLa, Ntera2, BxPC3, and U2OS cells.	189
Figure 5.8. Density-dependent cytotoxicity assays for cisplatin in four cell lines.	190
Figure 5.9. High density cytotoxicity assays for cisplatin in HeLa YS and HeLa pcDNA cell lines.	191
Figure 5.10. Structure of zeocin selection reagent.	192
Figure 5.11. Photo-cross-linking of PtBP6-modified 25-bp duplexes with increasing concentrations of the PARP inhibitor, CEP-A.	193

Figure 5.12. Photo-cross-linking of 25-bp duplex containing a 1,2-d(GpG) adduct of PtBP6 in various cancer cell extracts in the presence of the PARP inhibitor, CEP-A.	194
Figure 5.13. Photo-cross-linking of 25-bp duplex containing a 1,3-d(GpTpG) adduct of PtBP6 in various cancer cell extracts in the presence of the PARP inhibitor, CEP-A.	195
Figure 5.14. Intensity of total photo-cross-linking for site-specifically platinated DNA, with or without addition of the PARP inhibitor CEP-A.	196
Figure 5.15. Nuclear extract-based PARP activity assay for HeLa and NTERA2 cells.	197
Figure 5.16. Cell lysis-based PARP activity assay.	198
Figure A.1. Photo-cross-linking using benzophenone-modified DNA.	209
Figure A.2. Amino-modified bases prepared from commercially available starting materials.	210
Figure A.3. The sites of benzophenone attachment used in these experiments.	211
Figure A.4. RP-HPLC purification of benzophenone-modified DNA.	212
Figure A.5. Nuclease digestion analysis of unmodified and benzophenone-modified DNA probe.	213
Figure A.6. Maxam-Gilbert analysis of amino- versus benzophenone-modified DNA.	214
Figure A.7. Nuclease digestion analysis of cisplatin-modified DNA.	215
Figure A.8. Photo-cross-linking of DNA-BP duplexes.	216
Figure B.1. The 157-bp duplex is synthesized from six shorter DNA fragments.	225
Figure B.2. 6% urea-PAGE analysis of 157-base DNA probe.	226
Figure B.3. Analytical-scale photo-cross-linking of 157-bp probe with HeLa nuclear extracts.	227
Figure B.4. Exonuclease III digestion of 157-bp duplexes.	228
Figure B.5. Exonuclease-coupled photo-cross-linking experiment with 157-bp duplex.	229
Figure C.1. Orientational isomers of PtBP6 on DNA.	242
Figure C.2. Conformers of d(GpG).	243
Figure C.3. <sup>1</sup> H NMR spectrum of d(GpG).	244
Figure C.4. RP-HPLC purification of d(GpG)-PtBP6.	245
Figure C.5. <sup>1</sup> H NMR spectrum of d(GpG)-PtBP6.	246
Figure C.6. pH-dependent <sup>1</sup> H NMR spectra of d(GpG)-PtBP6.	247
Figure C.7. <sup>1</sup> H COSY of d(GpG)-PtBP6.	248
Figure C.8. H8 proton chemical shifts at low and high pH.	249

## ABBREVIATIONS

15G-BP	benzophenone-modified guanine at the 15 <sup>th</sup> base
4-ANI	4-amino-1,8-naphthalimide
6-AN	6-aminonicotinamide
AAG	3-methyladenine DNA glycosylase
AAS	atomic absorption spectroscopy
AIF	apoptosis-inducing factor
ATP	adenosine triphosphate
BCA	bicinchoninic acid
BER	base excision repair
BRCA	breast cancer gene
BSA	bovine serum albumin
cDNA	complementary deoxyribonucleic acid
CHO	Chinese hamster ovary
CIP	calf intestinal phosphatase
Cisplatin (cDDP)	<i>cis</i> -diamminedichloroplatinum(II)
COSY	two dimensional correlation spectroscopy
CSD	cold shock domain
CTR	copper transporter protein
DACH	diaminocyclohexane
DDB1	DNA damage binding protein-1
DDB2	DNA damage binding protein-2
DMEM	dulbecco's modified eagle's medium
DMF	dimethylformamide
DMSO	dimethyl sulfoxide
DNA topo I	DNA topoisomerase I
DNA	deoxyribonucleic acid
DNA-PK	DNA protein kinase
DNA-PKcs	DNA protein kinase catalytic subunit
DRP	damage response protein
DSB	DNA double-strand break
DTT	dithiothreitol
EDTA	ethylene diamine tetraacetic acid
EMSA	electrophoretic mobility shift assay
ESI-MS	electrospray ionization mass spectrometry
ESI-TOF	electrospray ionization time-of-flight mass spectrometry
Exo III	exonuclease III
FACT	facilitates chromatin transcription complex
FBS	fetal bovine serum
FDA	U.S. food and drug administration
GGR	global genome repair
HEPES	4-(2-hydroxyethyl)-1-piperazineethanesulfonic acid

HMG	high-mobility group
HMGB	high-mobility group box protein
HR	homologous recombination
HRP	horseradish peroxidase
IE-HPLC	ion-exchange high performance liquid chromatography
LEF-1	lymphoid enhancer binding factor
MAPK	mitogen-activated protein kinase
MBN	mung bean nuclease
MDB	minimal DNA-binding domain
MEF	mouse embryonic fibroblasts
MMR	mismatch repair
MNNG	<i>N</i> -methyl- <i>N</i> -nitro- <i>N</i> -nitrosoguanidine
Msh	MutS homolog
mtTFA	transcription factor A, mitochondrial precursor
MTT	3-(4,5-Dimethylthiazol-2-yl)-2,5-diphenyltetrazolium bromide
MWCO	molecular weight cutoff
NAD	nicotinamide adenine dinucleotide
NCI	national cancer institute
NER	nucleotide excision repair
NHEJ	nonhomologous end-joining
NHS	<i>N</i> -hydroxysuccinimide
NMR	nuclear magnetic resonance
NOESY	Nuclear Overhauser Enhancement Spectroscopy
OCT	organic cation transporter
Oxaliplatin	(1,2-diaminocyclohexane)(oxalato)platinum(II)
PAGE	polyacrylamide gel electrophoresis
PAR	poly(ADP-ribose)
PARG	poly(ADP-ribose) glycohydrolase
PARP	poly(ADP-ribose) polymerase
PB-1	protein polybromo-1
PBS	phosphate buffered saline
PCNA	proliferating cell nuclear antigen
PMSF	phenylmethanesulphonylfluoride, a protease inhibitor
PNK	polynucleotide kinase
Pol I	RNA polymerase I
PtBP6	<i>cis</i> -[Pt(NH <sub>3</sub> )( <i>N</i> -(6-aminohexyl)-4-benzophenonamide)Cl <sub>2</sub> ]
PVDF	polyvinylidene flouride
rDNA	ribosomal DNA
RFC	replication factor C
RNA	ribonucleic acid
RNAi	RNA interference
RNA pol	RNA polymerase
RPA	replication protein A
RP-HPLC	reverse-phase high performance liquid chromatography
rpm	revolutions per minute
rRNA	ribosomal RNA

Satraplatin	<i>cis-trans-cis</i> -[Pt(NH <sub>3</sub> )(cyclohexylamine)Cl <sub>2</sub> (O <sub>2</sub> CCH <sub>3</sub> ) <sub>2</sub> ]
SDS	sodium dodecyl sulfate
SMARC	SWI/SNF-related matrix-associated actin-dependent regulator of chromatin
SPT16	suppressor of Ty 16 homolog
SRY	sex-determining factor
SSRP1	structure specific replication protein-1
TBP	TATA-box binding protein
TCA	trichloroacetic acid
TC-NER	transcription coupled nucleotide excision repair
TEAA	triethylammonium acetate
TEG	triethylene glycol
TFIID	transcription factor II D
THF	tetrahydrofuran
TLC	thin layer chromatography
Topo I	DNA topoisomerase I
t-PBS	phosphate buffered saline containing 0.1% tween-20
tsHMG	testis-specific HMG-domain protein
UBF	upstream binding factor
UV	ultraviolet
WT-1	wilms tumor suppressor
XPA	xeroderma pigmentosum complementation group A
XPC	xeroderma pigmentosum complementation group C
XPE	xeroderma pigmentosum complementation group E
XRCC1	X-ray repair cross-complementing protein-1
YB-1	Y-box-binding protein-1

## **Chapter 1: Nuclear Proteins with an Affinity for Platinum-Modified DNA.**

## I. INTRODUCTION

The anticancer drug *cis*-diamminedichloroplatinum(II) (cisplatin) was FDA-approved for the treatment of testicular cancer over 30 years ago. Today, this drug is still first-line chemotherapy for several types of malignancies.<sup>1</sup> Despite years of study, the mechanism of antitumor activity of cisplatin is still not fully understood. Cisplatin continues to be the subject of intense investigation because the drug is not effective on all tumors, and patients treated with the drug may develop resistance to platinum-based therapy.<sup>1</sup> In order to identify factors that lead to resistance to cisplatin, it is important to understand the four steps of the antitumor activity of cisplatin (Figure 1.1).

Cisplatin enters the cell by both passive and active transport mechanisms (Figure 1.1i). While it was originally thought that cisplatin enters the cell by passive diffusion, the role of the copper transporter protein CTR1 in cisplatin uptake has recently been established.<sup>2</sup> The low intracellular concentration of chloride ions induces the aquation of cisplatin, referred to as the activation step (Figure 1.1ii). For another FDA-approved anticancer drug, oxaliplatin, these two steps occur simultaneously, due to non-chloride leaving groups of the drug and the ability of the organic cation transporters OCT1 and OCT2 to transport the activated form of the oxaliplatin (Figure 1.1i).<sup>3</sup> Once activated, the compounds  $[\text{Pt}(\text{NH}_3)_2(\text{H}_2\text{O})_2]^{2+}$  and  $[\text{Pt}(\text{NH}_3)_2(\text{H}_2\text{O})\text{Cl}]^+$ , will bind to several intracellular targets.

One important target of these aquated platinum compounds is the nucleophilic N7 of purine residues. An interaction between an ammine hydrogen atom and the C6 oxo of guanine make this base the more favorable for binding than adenine.<sup>4</sup> These DNA-bound platinum complexes will then bind to a second target on the DNA, resulting in DNA adducts. The most common adduct is the 1,2-d(GpG) intrastrand cross-link in which cisplatin binds to the N7



positions of two consecutive guanosine residues. Cisplatin can also form a 1,3-d(GpNpG) intrastrand cross-link in which the bound guanosine residues are separated by one nucleotide, and an interstrand adduct where cisplatin binds to residues on opposite strands of the DNA (Figure 1.2). All of these platinum adducts cause bending and unwinding of the DNA.<sup>1</sup> The bulky lesions are a recognition site for nuclear factors<sup>5</sup> and will block polymerases.<sup>6</sup> Consequentially, processing of the DNA-damage must result in repaired DNA in order for the cell to survive.

The resistance mechanisms which make cisplatin ineffective in certain patients may derive from each of the four steps of cisplatin cytotoxicity. For example, cisplatin uptake is reduced when the gene encoding the copper uptake transporter CTR1 is mutated or deleted.<sup>2</sup> An increase in “decoy” binding sites for the platinum inside the cell, such as glutathione, can decrease the number of platinum-DNA adducts that form, reducing cytotoxicity.<sup>7</sup> This chapter will focus on the processing of platinum adducts following DNA-binding. The signaling pathways that are initiated following recognition of platinum-DNA adducts may have an important effect on the ability of the cell to repair damaged DNA or signal cell death through apoptosis.

## II. METHODS USED TO IDENTIFY PLATINUM-DNA BINDING PROTEINS

The evaluation of cellular proteins that bind to platinated DNA dates back many years. Globally platinated as well as site-specifically platinated DNA constructs were synthesized.<sup>8</sup> The globally platinated fragments were radiolabeled and incubated with cytosolic and nuclear extracts from several cell lines, including HeLa cells. The mixtures were then analyzed by native PAGE, which allows protein-DNA interactions to remain intact. Any bound proteins will slow

the elution of the radiolabeled DNA down the gel. This type of assay is referred to as a gel retardation assay or electrophoretic mobility shift assay (EMSA, Figure 1.3). Increasing levels of platinum adducts on the DNA caused more of the DNA to be shifted to a large upper band comprising a DNA-protein complex. Complex formation was eliminated by proteinase K, which degrades the proteins, or by adding platinated competitor DNA that was not radiolabeled. Using site-specifically modified probes, the authors showed that protein complexation occurs readily for the 1,2-d(GpG) and 1,2-d(ApG) adducts, but not for the 1,3-d(GpTpG) adduct or the adducts of the inactive *trans*-diamminedichloroplatinum(II) compound. This work highlighted the importance of proteins with an affinity for platinum-modified DNA, although the proteins bound to the probe were not identified in this work.

EMSAs were used to show that a protein that binds to cisplatin-modified DNA is not present in the nuclear extracts of cells deficient in xeroderma pigmentosum complementation group E (XPE).<sup>9,10</sup> These types of cells have defects in DNA damage repair.<sup>11</sup> The authors named the protein XPE binding factor, which was later purified and characterized as the 125 kDa protein, DNA damage binding protein-1 (DDB1).<sup>12</sup> EMSAs have provided a mechanistic understanding of *in vivo* observations. For instance, after the discovery that *E. coli* cells lacking certain mismatch repair proteins were more resistant to cisplatin,<sup>13</sup> it was demonstrated that the mismatch repair protein, MutS $\alpha$  binds to cisplatin-modified DNA.<sup>14</sup> Cells expressing high levels of the protein YB-1 are resistant to several DNA-damaging agents,<sup>15,16</sup> which led to the discovery that YB-1 binds to cisplatin-damaged DNA using EMSAs.<sup>17</sup>

EMSAs can also be used to probe the platinum-damaged DNA-binding abilities of known DNA damage response proteins. Based on the discovery that the protein binds to bent DNA structures, the affinity of the methylated-DNA repair protein 3-methyladenine DNA glycosylase

(AAG) for cisplatin-modified DNA was demonstrated.<sup>18</sup> An interest in the interactions between transcription machinery and NER led to the finding that the transcription factor TATA-binding protein (TBP) has an affinity for cisplatin-modified DNA.<sup>19</sup> While EMSAs are useful for investigating known proteins, the methodology is not feasible for identifying every protein that binds to cisplatin-modified DNA, since it would be necessary to purify and test each nuclear protein individually.

In order to survey the entire proteome for proteins that bind to cisplatin-damaged DNA, different methodologies had to be used. One of these methods, southwestern blotting (Figure 1.3), necessitates resolving the nuclear proteins by SDS-PAGE. The proteins are then transferred to a membrane, which is incubated with radiolabeled DNA containing cisplatin adducts. The molecular weight of the bound proteins can be estimated based on the migration of the protein down the gel. Using this methodology, platinum-DNA-specific proteins of 28 and 100 kDa were characterized.<sup>20</sup> The same type of methodology was used to identify proteins of 25, 48 and 97 kDa that bind specifically to cisplatin-damaged DNA.<sup>21</sup> Southwestern blotting is able to characterize cisplatin-damaged DNA-binding proteins by molecular weight, but the identification of the protein is not achieved by this method.

Screening of cDNA libraries (Figure 1.3) is another method that was able to identify proteins with an affinity for platinum-modified DNA. In this type of assay, *E. coli* cells are transfected with a library of plasmids, each expressing a human protein. Each cell is able to take up only one plasmid and expresses a singular human protein. The contents of each cell are transferred onto a membrane that is then treated with radiolabeled DNA. The DNA will be immobilized on spots belonging to cells that express a relevant DNA-damage recognition protein. Using this methodology, recombinant phages of the platinum-DNA binding proteins were isolated<sup>20</sup> and an 80 kDa protein containing an HMG-domain, structure specific recognition

protein (SSRP1), was identified.<sup>22</sup> This protein is a subunit of the transcription elongation complex FACT.<sup>23</sup> The identification of SSRP1 led to the investigation of the cisplatin-modified DNA-binding properties of other HMG-domain proteins using EMSAs, including high mobility group protein-1 (HMGB1), upstream binding factor-1 (UBF1), mitochondrial transcription factor mtTFA, lymphoid enhancer binding factor (LEF-1) and sex-determining factor (SRY).<sup>24-27</sup>

Despite the successes of southwestern blotting and cDNA library screening methods in identifying proteins that bind to platinum-modified DNA, these methods do not allow for multiprotein complexes to remain intact. One example of this type of interaction is the FACT complex itself. The HMG-domain protein SSRP1 binds strongly to cisplatin-modified DNA only in the presence of the other subunit, SPT16.<sup>28</sup> EMSA methodology allows for proteins to bind in their native states, but does not afford a proteome-wide survey of isolable protein-DNA complexes. Southwestern blotting and cDNA library methods allow for better characterization of bound proteins, but require the proteins to be sequestered prior to DNA-binding.

In order to isolate proteins that bind to platinum-modified DNA as multiprotein complexes, unplatinated or cisplatin-modified DNA was immobilized on cellulose.<sup>29</sup> The cellulose was incubated with cell extracts and then washed to remove unbound proteins. The cellulose was then heated in denaturing buffer to dissociate the DNA-bound proteins and these proteins were analyzed by SDS-PAGE. This method was able to identify that HMGB1 and HMGB2 bind specifically to cisplatin-modified DNA. In a similar manner, platinated calf thymus DNA was immobilized onto a sepharose column and the column was incubated with HeLa cell-free extracts (Figure 1.3).<sup>30</sup> The column was washed with a low-salt buffer to remove free proteins and then washed with a buffer containing 0.75 M NaCl to dissociate proteins that bind with high affinity to the platinum-modified DNA. The collected protein fraction was then

subjected to EMSAs to confirm that the collected proteins bind to cisplatin-modified DNA. This method was able to identify HMGB1, DNA-PK, RPA and XPA. The roles of these proteins in the cellular response to cisplatin-damaged DNA will be discussed later in this review.

Another method that has been used to isolate cisplatin-modified DNA-binding proteins is chemical cross-linking. A cisplatin analogue containing a photoactive aryl azide moiety was synthesized to photo-cross-link platinum-damaged DNA binding proteins.<sup>31</sup> Control experiments from this work revealed that cisplatin itself can form DNA-platinum-protein complexes more efficiently with HMGB1 than the aryl azide analogues when irradiated at 254 and 302 nm. Irradiation at 365 nm was much less efficient. Irradiation using a laser at 325 or 350 nm could also activate the Pt-DNA bond and form DNA-platinum-protein complexes.<sup>32</sup> This type of photo-cross-linking requires an extremely close interaction between the platinum site and the protein, since a platinum-protein bond must be formed.

Benzophenone, with an activation wavelength of 360 nm, is an ideal photo-cross-linker for this application since this wavelength should not significantly activate the cisplatin-DNA bond.<sup>31,33</sup> A cisplatin analogue containing a benzophenone moiety connected by a six-carbon linker was synthesized.<sup>34</sup> This compound was reacted with biotinylated DNA containing a single 1,2-d(GpG) site. The platinated DNA was exposed to nuclear extracts from HeLa cells and irradiated at 365 nm. The biotinylated DNA-platinum-protein complexes could be isolated from unbound nuclear proteins using streptavidin-coated magnetic beads, which form a tight complex with the tethered biotin moiety. This method is superior to the cellulose- and sepharose-based assays described earlier because a covalent bond is formed between the platinated DNA and the protein, eliminating the need to attenuate the washing conditions to differentiate between weakly- and tightly-bound proteins. Once the unbound proteins were washed away, the

remaining proteins were resolved by SDS-PAGE, and several DNA-platinum-protein complexes were identified. Two of these proteins were characterized by mass spectrometry as HMGB1 and PARP-1.<sup>34</sup> This methodology allows for exposure of the platinated DNA to the entire nuclear milieu, followed by isolation and identification of the photo-cross-linked proteins. One major advantage of this method is that proteins can compete for binding to the platinum-modified DNA, providing a more realistic DNA-damage environment.

### III. HUMAN PROTEINS THAT BIND PLATINUM-MODIFIED DNA AND IMPLICATIONS IN DNA REPAIR

Many types of proteins have an affinity for platinum-modified DNA. Each of these proteins may contribute to the repair of the damaged DNA, or conversely, may lead to cellular death signaling. In the context of a cancer cell, identifying the proteins that lead to cell death could lead to improved therapeutic strategies. The section examines some of the proteins with an affinity for platinum-modified DNA (Table 1.1).

#### *Nucleotide excision repair (NER) proteins*

NER is the repair process implicated in the removal of cisplatin adducts from DNA.<sup>1</sup> This repair results in an excised DNA fragment of approximately 32 bases.<sup>35</sup> The resulting gap in the remaining DNA is subsequently filled in by DNA polymerases and ligases.<sup>36</sup> The DNA-damage sensing is carried out by two different mechanisms, global genome repair (GGR) or transcription-coupled repair (TC-NER). In GGR, the DNA damage is recognized by XPC-RAD23B or XPA-RPA,<sup>36</sup> while in TC-NER, damage recognition is initiated by the stalling of a polymerase at the damaged base.<sup>37</sup> The XPA-RPA complex has an affinity for cisplatin-damaged DNA.<sup>38</sup> The protein mentioned earlier that causes a mobility shift in cisplatin-modified DNA and

is not present in XPE cells<sup>9,10</sup> has been identified as DNA damage binding protein-1 (DDB1), a protein involved in NER.<sup>12,39</sup>

The 1,3-d(GpTpG) adduct is repaired more efficiently by NER than the 1,2-d(GpG) adduct.<sup>35</sup> The reason for this difference is most likely two-fold. EMSA studies using purified RPA1 indicate that the protein has a 1.5-2-fold stronger affinity for the 1,3-d(GpNpG) than the 1,2-d(GpG) cisplatin cross-link,<sup>40</sup> demonstrating that the 1,3-d(GpNpG) adduct is more readily recognized by the NER machinery. HMG-domain proteins will block DNA repair of cisplatin-damaged DNA by NER.<sup>35</sup> As mentioned previously in this chapter, HMG-domain proteins bind to the 1,2-d(GpG) but not the 1,3-d(GpNpG) adduct.<sup>26</sup> So repair of the 1,2-d(GpG) adduct will be shielded by these proteins, but repair of the 1,3-d(GpNpG) adduct will not.

#### *HMG-domain proteins*

*HMGB1 and HMGB2.* HMGB1 and HMGB2 are chromosomal proteins that bind to distorted DNA structures, such as four-way junctions, and induce further bending of the DNA.<sup>41</sup> Each protein consists of two HMG-box domains and an acidic C-terminus. Both HMG domains of HMGB1 bind to cisplatin-modified DNA, though HMGB1 domain A binds 100-fold more strongly to 1,2-d(ApGpGpA) cisplatin adducts than domain B.<sup>42</sup> HMGB1 binding to cisplatin-modified DNA will block repair by NER.<sup>35</sup> Supporting this model, analysis of the NCI library of cancer cell lines reveals a correlation between cells expressing high levels of HMGB1 and cisplatin sensitivity.<sup>43,44</sup> Also, treatment of breast cancer cells with estrogen, which causes the cells to overexpress HMGB1, sensitizes the cells to cisplatin.<sup>45</sup> The consequences of HMGB1 binding to cisplatin-modified DNA are discussed in a recent review.<sup>5</sup> HMGB2 also binds to cisplatin-modified DNA,<sup>29</sup> and is likely to have the same effects on cisplatin-damaged DNA processing as HMGB1.

*UBF1*. Upstream binding factor 1 (UBF1) is a transcription factor that exhibits sequence-specific binding to DNA and interacts with a number of cellular factors to induce the polymerase activity of RNA polymerase I (Pol I).<sup>46,47</sup> UBF is inactivated during mitosis when Pol I is dormant and then activated in late G<sub>1</sub>, correlating with the onset of Pol I activity.<sup>48</sup> UBF1 binds strongly to cDDP-damaged DNA but not *trans*-DDP damaged DNA.<sup>27</sup> This strong interaction of UBF1 to cisplatin-damaged DNA is a consequence of the presence of 6 HMG domains in the protein.<sup>49</sup> There are about 5 x 10<sup>5</sup> UBF1 molecules per cell, compared to between 10<sup>5</sup> and 10<sup>6</sup> cisplatin-DNA adducts in patients treated with the drug.<sup>49</sup> The possibility exists that cisplatin-DNA adducts act as decoy binding sites for UBF1, leading to hijacking of the protein from rDNA promoter regions. This idea is supported by the fact that cisplatin treatment will lower rRNA levels *in vivo*,<sup>50</sup> although this may be related to stalling of the polymerase at platinum lesions analogous to the behavior of RNA Polymerase II.<sup>6</sup>

UBF1 expression is correlated to cisplatin sensitivity in hepatocellular carcinoma cell lines.<sup>51</sup> Hepatocellular carcinoma cell lines expressing UBF1 are threefold more sensitive to cisplatin than cell lines lacking in UBF1 expression. If the hijacking hypothesis is correct, these results suggest that UBF1 hijacking by cisplatin lesions leads to cisplatin resistance. Lowered expression of UBF1, which makes cells more resistant to cisplatin, would make titration of the protein away from Pol I promoter regions easier. This model fits if UBF1 hijacking leads to cell cycle arrest, since cell cycle arrest is generally associated with increased repair of cisplatin adducts.<sup>52</sup> Another possibility is that UBF1 blocks DNA repair machinery in a similar fashion to other HMG-domain proteins, such as HMGB1. If this is the case, then high levels of UBF1 expression would lead to sensitization of cells to cisplatin, in accord with the behavior of the hepatocellular carcinoma cells in the described study.<sup>51</sup>



*Other HMG-domain-containing transcription factors.* As mentioned previously, the structure-specific recognition protein (SSRP1) subunit of the facilitates chromatin transcription (FACT) complex binds to cisplatin-modified DNA.<sup>28</sup> Binding of this protein complex to cisplatin-modified DNA may compromise its ability to remodel chromatin. The binding of the sequence-specific lymphoid enhancer-binding factor (LEF-1) to a native recognition site is about ten times stronger than binding to cisplatin-modified DNA,<sup>53</sup> so it is unlikely that cisplatin-modified DNA could sequester the transcription factor from native functions. The protein still may play a role in shielding the adducts from NER as demonstrated with other HMG-domain proteins.<sup>35</sup> Testis-specific cisplatin-damaged DNA-binding proteins are of particular interest due to the sensitivity of testicular cancer to cisplatin treatment.<sup>1</sup> Unlike LEF-1, the binding affinity of testis-specific sex-determining factor SRY to cisplatin-damaged DNA is strong enough to compete with a putative native recognition sequence.<sup>54</sup> The binding of SRY also blocks NER of the lesion.<sup>54</sup> Mitochondrial transcription factor mtTFA binds to cisplatin-modified DNA and also prevents the repair of the lesion by blocking NER.<sup>25,35</sup> The interaction of mtTFA with the tumor suppressor p53 may also play a role in the response to cisplatin-damaged DNA.<sup>55</sup> These results demonstrate that the binding of HMG-domain transcription factors to cisplatin-damaged DNA has several possible consequences, including hijacking of the transcription factor from native functions, shielding the adduct from repair and interactions with other DNA damage repair related proteins, such as p53.

#### *Transcription factors lacking an HMG-domain*

*TBP.* The TATA-binding protein (TBP) is the recognition element of TFIID, which binds the TATA box and initiates transcription of RNA polymerases I, II and III.<sup>56</sup> TBP will recognize cisplatin-damaged DNA,<sup>19</sup> and this affinity is enhanced if the platination site is located near a

TATA box.<sup>57</sup> This affinity is likely due to structural similarities between the TATA box bound by TBP and DNA containing a 1,2-d(GpG) intrastrand adduct of cisplatin.<sup>19</sup> Binding to damaged DNA may sequester the protein from transcription initiation sites, leading to a decrease in transcription characteristic of cells treated with cisplatin.<sup>58</sup> Alternatively, the affinity of TBP for cisplatin-damaged DNA near a TATA box could lead to increased turn-on of transcription at the cisplatin-flanked TATA box sites.<sup>57</sup> One role of TBP following exposure to cisplatin-damaged DNA may not be transcription-related, as TBP bound to cisplatin-modified DNA will block NER from repairing the lesion.<sup>59</sup>

*YB-1*. Y-box binding protein-1 (YB-1) is a nucleic acid binding protein containing a cold-shock domain (CSD). Under normal conditions, 90% of the protein is present in the cytoplasm, and translocation to the nucleus occurs when the cell is under stress.<sup>60</sup> YB-1 is involved in stress response, transcription, translation and is often correlated with cellular proliferation.<sup>60</sup> The protein will bind to cisplatin-modified DNA,<sup>17</sup> and several cell lines resistant to cisplatin showed an increase in expression of YB-1.<sup>15</sup> Knockdown of the protein using RNAi in these cell lines conferred a twofold sensitivity to cisplatin.<sup>15</sup> Although the role of YB-1 in DNA repair is not fully understood, YB-1 interacts with proliferating cell nuclear antigen (PCNA)<sup>17</sup> as well as tumor suppressor p53,<sup>61</sup> two proteins involved in DNA repair..

#### *Mismatch repair (MMR) proteins*

*Msh2*. MutS homolog 2 (Msh2) has an affinity for the 1,2-d(GpG) intrastrand cross-link of cisplatin.<sup>14,62</sup> Msh2 is a MMR protein that binds to the site of a mismatched base.<sup>63</sup> Cell lines deficient in MMR are generally more resistant to cisplatin damage;<sup>64-68</sup> however, the extent of resistance in MMR-deficient cells may be minimal.<sup>69</sup> This discrepancy may be due to certain MMR mutations that can disrupt repair of mismatches without disabling MMR-dependent

apoptosis signaling pathways.<sup>70</sup> This hypothesis is supported by a molecular modeling study demonstrating that different residues of Msh2 and Msh6 are involved in hydrogen bonding with mismatched DNA versus cisplatin-modified DNA.<sup>71</sup> MMR-deficient cells have an increased probability of DNA polymerases bypassing cisplatin adducts, and it is suggested that Msh2 may be responsible for blocking DNA polymerases from translesion synthesis that can lead to mutagenesis.<sup>64</sup> The blocking of DNA polymerases by Msh2-bound cisplatin adducts may result in the formation of double-strand breaks, which are present after cisplatin treatment.<sup>72</sup> This behavior would explain why cell lines deficient in recombination repair pathways are often more sensitive to cisplatin.<sup>72</sup>

Another possible explanation for the cytotoxicity of cisplatin lesions is that the MMR pathway treats cisplatin adducts as mismatched bases, which would lead to cycles of excision and resynthesis of the strand opposite the cisplatin adduct in an effort to find a base which confers normal duplex structure to the adduct. These futile cycles could lead to apoptosis.<sup>72</sup> The mechanism for the MMR-dependent response to cisplatin may also be related to cell cycle arrest and apoptosis signaling through the tyrosine kinase, c-Abl.<sup>73,74</sup> Cisplatin exposure activates the c-Abl MAPK pathway,<sup>75</sup> which can stabilize p73 and lead to cell death through apoptosis in an MMR-dependent manner.<sup>74</sup>

#### *DNA protein kinase (DNA-PK)*

DNA-PK is a heterotrimer of the proteins DNA-PK<sub>cs</sub>, Ku70 and Ku80 and is a component of the primary nonhomologous end-joining (NHEJ) double strand break repair pathway.<sup>76</sup> The Ku subunits of DNA-PK will recognize DNA double-strand breaks and recruit the catalytic subunit DNA-PK<sub>cs</sub>.<sup>76</sup> Ku proteins do bind to cisplatin-DNA adducts, although this binding will not activate DNA-PK.<sup>77</sup> The lack of activity may be due to the inhibition of Ku

translocation down the DNA because it can be stalled by the cisplatin adduct. This translocation is a necessary step in the activation of DNA-PK.<sup>78</sup> A 1,2-d(GpG) cisplatin cross-link six base pairs from a DNA terminus will inhibit NHEJ by 95%, and an adduct 15 bases pairs from the terminus will inhibit NHEJ by 60%.<sup>79</sup> In these examples, Ku binding was not affected, only DNA-PK activity. This process requires a cisplatin adduct to be located near a double-strand break. If double-strand breaks occur near a platination site, the inhibition of NHEJ by the cisplatin lesion could be a factor in cell-killing by cisplatin. Supporting this theory, treatment of cells with high levels of cisplatin prior to ionizing radiation will inhibit repair of the irradiation-induced double-strand breaks.<sup>80</sup> Treatment of the cells with lower levels of cisplatin prior to treatment resulted in the opposite effect,<sup>80</sup> most likely due to the induction of UV-damage response proteins following cisplatin-DNA adduct processing.<sup>81</sup>

#### *3-Methyladenine DNA glycosylase (AAG)*

The protein 3-methyladenine DNA glycosylase (AAG), which is responsible for repairing methylated DNA, will bind to cisplatin-modified DNA.<sup>18</sup> Although the protein has an affinity for both the 1,2-d(GpG) and 1,3-d(GpTpG) intrastrand cross-links of the compound, it is unable to excise the lesions.<sup>18</sup> AAG is a base excision repair (BER) protein, a repair process not active on cisplatin lesions. Recognition of lesions by the protein may signal the NER machinery to repair the damaged DNA.<sup>82</sup> If AAG recruits NER proteins to the damaged DNA, repair of cisplatin-DNA cross-links could be indirectly stimulated by this protein.

#### *Poly(ADP-ribose) polymerase 1 (PARP-1)*

PARP-1 belongs to a family of proteins with an enzymatic activity resulting in the addition of poly(ADP-ribose) (PAR) polymers onto itself and other proteins in a reaction that consumes nicotinamide.<sup>83</sup> The affinity of this protein for platinum-damaged DNA was recently

discovered<sup>34</sup> using methodologies described in detail in this thesis. The DNA damage-stimulated activity of PARP proteins can lead to DNA repair or cell death through apoptosis or necrosis, each involving an independent pathway.<sup>83</sup> A detailed discussion of the activity of PARP-1 following exposure to platinum-damaged DNA is presented in Chapter 5.

#### IV. SUMMARY OF CONSEQUENCES OF PROTEINS BINDING TO PLATINUM-MODIFIED DNA

*Potential of repair.* Cisplatin-damaged DNA is repaired by the nucleotide excision repair (NER) pathway and this repair is necessary for survival of the cell.<sup>1</sup> In global genome NER (GG-NER), the binding of proteins XPA and RPA to cisplatin-modified DNA signals the repair of these adducts.<sup>36,38</sup> Although the protein XPE-BF, now referred to as DDB1, is not necessary for NER to take place *in vitro*, the sensitivity of patients with mutated DDB1 to DNA damaging agents suggests that the protein plays a role in DNA repair.<sup>84</sup> HMG-domain proteins can counteract NER activity by shielding cisplatin-modified DNA from repair.<sup>1</sup> The significance of this interaction was demonstrated by inducing the expression of the HMG-domain protein tsHMG in HeLa cells, which sensitized the cells to cisplatin.<sup>85</sup> Whereas HMG-domain proteins have been specifically implicated, the binding of any protein to cisplatin-modified DNA may inhibit repair by blocking NER proteins from recognizing the lesion.

Proteins binding to cisplatin-damaged DNA can signal repair through interactions with other proteins involved in DNA repair pathways. The protein AAG recognizes cisplatin-damaged DNA, although it is involved in the base excision repair pathway and cannot excise the lesions.<sup>18</sup> AAG has a greater affinity for the 1,2-d(ApG) versus 1,2-d(GpG) intrastrand adduct of cisplatin. The 1,2-d(ApG) adduct is repaired more efficiently in crude extracts but the two adducts are

repaired to a similar extent in purified NER components, suggesting that a cisplatin-DNA binding protein, such as AAG, may recruit NER proteins to repair the lesion and account for the repair discrepancy.<sup>82</sup> Another example of these types of associations is YB-1, which interacts with the proliferating cell nuclear antigen (PCNA).<sup>17</sup> PCNA is required for NER,<sup>86</sup> because is involved in the resealing of single-stranded DNA gaps formed when damaged DNA is excised by NER.<sup>87</sup>

The cisplatin-damaged DNA-binding proteins HMGB1, YB-1 and mtTFA each interact with the tumor suppressor p53.<sup>55,61,88</sup> This protein serves a variety of roles following DNA damage.<sup>89</sup> Global genome NER (GG-NER) is dependent on BRCA1- and p53-dependent expression of the DNA damage recognition proteins DDB2 and XPC.<sup>90</sup> Following DNA damage, p53 localizes to sites of NER and its activity leads to chromatin loosening through histone acetylation, which makes the damaged DNA more accessible to repair proteins.<sup>91</sup> This work was performed using UV-irradiation as the DNA damaging agents, but the dependence of NER on p53 has recently been demonstrated for cisplatin-DNA adducts.<sup>92</sup> Paradoxically, p53 can also signal apoptosis, and p53-deficient cells, despite having more persistent DNA adducts, are *less* sensitive to DNA damaging agents such as cisplatin.<sup>93</sup> This result indicates that the p53-dependence of NER is outweighed by the ability of the protein to signal cell death.

*Hijacking proteins from native functions.* Another possibility is that proteins with an affinity for platinum-damaged DNA are hijacked from other responsibilities within the cell. The hijacking of transcription factors, such as UBF1, may lead to transcription inhibition as discussed earlier. Other proteins may also be hijacked. For instance, the sequestration of mismatch repair proteins could compromise the ability of the cell to repair actual DNA mismatches. This is

especially significant for mismatch repair proteins, since they are expressed at low levels in cells.<sup>94</sup>

*Death signaling.* Another possibility is that the proteins bound to cisplatin-damaged DNA lead to the induction of cell death mechanisms. The tumor suppressor p53, which interacts indirectly with these adducts, is a part of the apoptosis-signaling pathway.<sup>95</sup> As mentioned above, cells deficient in functional p53 protein are more resistant to DNA damaging agents such as cisplatin.<sup>93</sup> Mismatch repair (MMR) proteins bind to platinum-modified DNA, despite being unable to repair the adducts. Futile cycles of failed attempts to repair the DNA may lead to apoptosis signaling, a hypothesis supported by the observation that MMR-deficient cells are often more tolerant of cisplatin adducts.<sup>62</sup> MMR proteins may also signal apoptosis through the tyrosine kinase, c-ABL.<sup>73,74</sup> The protein PARP-1, which has recently been characterized as a platinum-damaged DNA-binding protein, can lead to apoptosis or necrosis through unique pathways.<sup>96</sup> The consequences of these signaling pathways are discussed in more detail in Chapter 5.

## V. NEW PLATINUM ANTICANCER COMPOUNDS

The search for new chemotherapeutics continues to face the challenge of selectively and efficiently killing cancer cells while allowing healthy cells to survive. Many new chemotherapeutics agents incorporate more efficient targeting and delivery of anticancer compounds into cancer cells. Recent work has shown the efficacy of nanotubes in the delivery of platinum compounds to cancer cells.<sup>97</sup> These transport mechanisms present the cell with a platinum(IV) compound, which will be reduced upon entry into the cellular medium, yielding *cis*-diamminedichloroplatinum(II), cisplatin.<sup>98</sup> Improved delivery mechanisms should increase

the number of cisplatin-DNA adducts in the cell, and these adducts will be recognized by the same proteins listed in this review. Other new strategies for improved anticancer therapeutics involve the synthesis of platinum compounds with different ammine ligands than cisplatin. These ligands may effect uptake of the compounds,<sup>3</sup> and will lead to differential recognition of the platinum-DNA adducts.

Oxaliplatin is an FDA-approved platinum anticancer drug that contains a diaminocyclohexane (DACH) ligand (Figure 1.4). The oxaliplatin-DNA adduct is repaired by NER with similar efficiency to the cisplatin-DNA adduct.<sup>99</sup> Mismatch repair proteins, however, do not bind oxaliplatin-DNA adducts as strongly as cisplatin-DNA adducts, and mismatch repair deficient cell lines are equally sensitive to oxaliplatin treatment.<sup>100</sup> Cisplatin is ineffective against colorectal cancers,<sup>3</sup> a cancer type that is commonly MMR-deficient.<sup>101</sup> The efficacy of oxaliplatin in colorectal cancer has recently been attributed to the expression of organic cation transporters (OCTs), which greatly increase the uptake of oxaliplatin compared to cisplatin in these cells.<sup>3</sup> These data together suggest that the benefit of oxaliplatin over cisplatin in colorectal cancer cells is due both to uptake and processing of the drugs.

Satraplatin is a platinum anticancer compound currently undergoing clinical trials for the treatment of hormone refractory prostate cancer (Figure 1.4). The DNA bound form of this compound is analogous to that of cisplatin with one ammine ligand replaced with a cyclohexylamine.<sup>102</sup> This type of DNA adduct is repaired by NER to a similar extent as cisplatin-DNA adducts.<sup>99</sup> The advantage of this compound is its oral availability.<sup>102</sup> Both oxaliplatin and satraplatin form similar types of DNA adducts to cisplatin. Platinum complexes with different DNA-binding properties are more likely to be processed differently.



Multinuclear platinum compounds connected by long alkyl linkers were designed such that they bind to DNA through long-range intra- and interstrand cross-links (Figure 1.4). These compounds are not affected by the mismatch repair status of the cell<sup>103</sup> and are effective in cell lines with both wild-type and mutant p53.<sup>104</sup> This result is especially important because p53 is mutated in most cancer cells.<sup>89</sup> The anticancer properties of these compounds may derive from their ability to form interstrand cross-links, which account for about 20% of DNA adducts formed.<sup>105</sup> Monofunctional platinum compounds are also under investigation for anticancer potential. The compound [Pt(NH<sub>3</sub>)<sub>2</sub>(pyridine)Cl]Cl binds DNA monofunctionally, and exhibits transcription inhibitory and anti-proliferative properties.<sup>106</sup> Unlike cisplatin-DNA adducts, these lesions do not bend or unwind DNA, indicating that their recognition by nuclear proteins will be significantly different than that of bifunctional platinum-DNA adducts.<sup>106</sup>

The identification of proteins that bind to platinum-modified DNA has yielded many hits, which may have clinical significance to the efficacy of platinum anticancer drugs. Some of these proteins are involved in the repair of these adducts, allowing cancer cells to survive, and other proteins block this repair or initiate signaling cascades that will lead to cell death. These discoveries have led to clinical trials of combination therapies, such as cisplatin with ionizing radiation or estrogen, which aim to improve the chemotherapeutic potential of the drug. The intrinsic or acquired resistance to cisplatin that is common in many types of tumors has also led to the development of new platinum constructs, including monofunctional and multinuclear compounds, which are recognized differently by DNA repair proteins. The continued search for proteins with an affinity for cisplatin-modified DNA, as well as DNA damaged with these new types of platinum lesions, will provide mechanistic information about DNA damage processing that will continue to foster improved strategies of chemotherapy.

## VI. ORGANIZATION AND SCOPE OF THESIS

Following the success of the serendipitously discovered platinum anticancer drug cisplatin, the mechanisms by which such a simple compound is able to selectively and effectively kill cancer cells has been studied thoroughly.<sup>1</sup> The intrinsic and acquired resistance of certain tumors to the drug has led to the development of new platinum constructs capable of treating resistant tumors.<sup>105</sup> Resistance to cisplatin derives from a dysfunction of certain mechanisms required for cisplatin to be effective. The uptake of cisplatin into cells can be compromised, or the cell can have an increased ability to efflux the drug.<sup>107</sup> Once aquated inside the cell, the platinum compound can be rendered less effective by an upregulation of “decoy” binding sites, such as glutathione.<sup>108</sup> This thesis focuses on another type of resistance, in which the processing of the platinum-DNA adducts enables the cancer cell to survive.<sup>108</sup> This resistance mechanism is probed by the identification of proteins with an affinity for platinum-modified DNA.

This thesis addresses the challenge of compiling a comprehensive index of nuclear proteins that bind to platinum-modified DNA. The identification of these proteins is accomplished by using a photoactive cisplatin analogue *cis*-[Pt(NH<sub>3</sub>)(*N*-(6-aminohexyl)-4-benzophenonamide)Cl<sub>2</sub>] (PtBP6). Photo-cross-linking is advantageous over other methods for protein identification since it allows the platinum-modified DNA to be exposed to the nuclear milieu. Proteins can compete for binding to the probe as they would in the nucleus. Multiprotein complexes that bind to damaged DNA can stay intact in these extracts. The presence of multiprotein complexes is important because some proteins bind more strongly in complex with other proteins, such as the FACT complex, comprising subunits SSRP1 and SPT16.<sup>28</sup> This

method allows for screening of nuclear extracts from different cancer cell lines to determine whether differences in protein binding result in differences in sensitivity to cisplatin.

Chapter 2 focuses on the optimization of photo-cross-linking conditions for identification of proteins with an affinity for a 25-bp duplex containing a 1,2-d(GpG) cross-link of the photoactive analogue of cisplatin, PtBP6. The 25-bp duplex allows for simpler synthesis than longer DNA probes, so that many conditions could be tested to optimize cross-linking. Once the conditions were optimized, photo-cross-linking experiments identified several proteins with an affinity for platinum-modified DNA, HMGB1, HMGB2, HMGB3, Ku70, Ku80, DNA-PKcs, UBF1, Msh2, DNA Ligase III, PARP-1. The cisplatin-damaged DNA-binding ability of many of the proteins identified has been characterized by other methods, such as EMSAs. The identification of PARP-1, and the PARP-1 associating protein DNA Ligase III, was novel to this type of photo-cross-linking experiment. In Chapter 3, these photo-cross-linking were extended to identify nuclear proteins that bind to various constructs of a 25-bp duplex containing a site-specific adduct of PtBP6. Preparative-scale photo-cross-linking experiments with a 25-bp duplex containing a 1,3-d(GpTpG) cross-link of PtBP6 indicated that this type of adduct does not bind strongly to HMG-domain proteins but does bind to the NER protein, RPA. A probe containing a compound lesion with both a mismatched base and a 1,2-d(GpG) intrastrand adduct of PtBP6 binds more strongly to the mismatch repair protein Msh2. This finding agrees with EMSA assays using purified Msh2 reported in the literature.<sup>109</sup> Photo-cross-linking experiments were also carried out using nuclear extracts from various cancer cell lines and reveal differences in protein expression between cell lines, but also suggest that DNA damage recognition is consistent between cells with different sensitivity to cisplatin.

In Chapter 4, photo-cross-linking studies were extended to a longer DNA dumbbell probe. This probe separates the platination site further from the DNA ends, making it less likely that end-binding proteins will be photo-cross-linked. Only the first four bases of the dumbbell ends should interact with the protein PARP-1,<sup>110</sup> allowing us to determine whether the protein is able to bind to platinum-damaged DNA. All of the proteins identified by the 25-bp duplex probe were also found using this probe. Several other proteins were also identified, Msh3, Msh6, DNA topoisomerase I, SPT16, YB-1, DDB1 as well as members of the SWI/SNF chromatin remodeling complex. The implications of these proteins binding to platinum-modified DNA are discussed.

The identification of PARP-1 using these photo-cross-linking methods was the first evidence that the protein binds to platinum-modified DNA.<sup>34</sup> PARP inhibitors have proven effective in the potentiation of cisplatin sensitivity, although some reports show little effect.<sup>111-113</sup> In Chapter 5, the ability of PARP inhibitors to sensitize four cell lines to cisplatin was investigated. The effect of one of these inhibitors on photo-cross-linking experiments was analyzed. These cells lines were then used for nuclear extract- and cell-based assays of PARP activity following exposure to cisplatin. It was determined by this work that the sensitization of cells to cisplatin using PARP inhibitors is cell-line dependent, however, a clear understanding of the activity of PARP proteins following treatment with cisplatin was not attained.

In order to evaluate the proteins that bind to different types of platinum-DNA adducts, a benzophenone-modified DNA probe was synthesized. This work, described in Appendix A, led to the design of the DNA probe 15G-BP, which is able to photo-cross-link proteins specific to cisplatin-damaged DNA. A longer PtBP6-modified probe was synthesized as well. The ability to photo-cross-link proteins using a long DNA probe is important for future experiments that will

photo-cross-link proteins with an affinity for platinum-damaged nucleosomes. As described in Appendix B, photo-cross-linking using a 157-bp duplex results in complications in resolving the protein-platinum-DNA complexes. The binding of asymmetric cisplatin analogues to DNA will result in orientational isomers of the lesions.<sup>114,115</sup> Preliminary NMR studies of the binding of PtBP6 to d(GpG) were carried out and are discussed in Appendix C.

## VII. REFERNCES

1. Jamieson, E. R.; Lippard, S. J., *Chem. Rev.* **1999**, 99, 2467-2498.
2. Wang, D.; Lippard, S. J., *Nat. Rev. Drug Discov.* **2005**, 4, 307-320.
3. Zhang, S.; Lovejoy, K. S.; Shima, J. E.; Lagpacan, L. L.; Shu, Y.; Lapuk, A.; Chen, Y.; Komori, T.; Gray, J. W.; Chen, X.; Lippard, S. J.; Giacomini, K. M., *Cancer Res.* **2006**, 66, 8847-8857.
4. Baik, M.-H.; Friesner, R. A.; Lippard, S. J., *J. Am. Chem. Soc.* **2003**, 125, 14082-14092.
5. Jung, Y.; Lippard, S. J., *Chem. Rev.* **2007**, 107, 1387-1407.
6. Jung, Y.; Lippard, S. J., *J. Biol. Chem.* **2006**, 281, 1361-1370.
7. Kartalou, M.; Essigmann, J. M., *Mutat. Res.* **2001**, 478, 23-43.
8. Donahue, B. A.; Augot, M.; Bellon, S. F.; Treiber, D. K.; Toney, J. H.; Lippard, S. J.; Essigmann, J. M., *Biochemistry* **1990**, 29, 5872-5880.
9. Chu, G.; Chang, E., *Science* **1988**, 242, 564-567.
10. Chu, G.; Chang, E., *Proc. Natl. Acad. Sci. U.S.A.* **1990**, 87, 3324-3327.
11. Cleaver, J. E., *Nature* **1968**, 218, 652-656.
12. Hwang, B. J.; Chu, G., *Biochemistry* **1993**, 32, 1657-1666.
13. Fram, R. J.; Cusick, P. S.; Wilson, J. M.; Marinus, M. G., *Mol. Pharmacol.* **1985**, 28, 51-55.
14. Duckett, D. R.; Drummond, J. T.; Murchie, A. I. H.; Reardon, J. T.; Sancar, A.; Lilley, D. M. J.; Modrich, P., *Proc. Natl. Acad. Sci. U.S.A.* **1996**, 93, 6443-6447.
15. Ohga, T.; Koike, K.; Ono, M.; Makino, Y.; Itagaki, Y.; Tanimoto, M.; Kuwano, M.; Kohno, K., *Cancer Res.* **1996**, 56, 4224-4228.
16. Shibahara, K.; Uchiumi, T.; Fukuda, T.; Kura, S.; Tominaga, Y.; Maehara, Y.; Kohno, K.; Nakabeppu, Y.; Tsuzuki, T.; Kuwano, M., *Cancer Sci.* **2004**, 95, 348-353.
17. Ise, T.; Nagatani, G.; Imamura, T.; Kato, K.; Takano, H.; Nomoto, M.; Izumi, H.; Ohmori, H.; Okamoto, T.; Ohga, T.; Uchiumi, T.; Kuwano, M.; Kohno, K., *Cancer Res.* **1999**, 59, 342-346.
18. Kartalou, M.; Samson, L. D.; Essigmann, J. M., *Biochemistry* **2000**, 39, 8032-8038.
19. Vichi, P.; Coin, F.; Renaud, J.-P.; Vermeulen, W.; Hoeijmakers, J. H. J.; Moras, D.; Egly, J.-M., *EMBO J.* **1997**, 16, 7444-7456.
20. Toney, J. H.; Donahue, B. A.; Kellett, P. J.; Bruhn, S. L.; Essigmann, J. M.; Lippard, S. J., *Proc. Natl. Acad. Sci. U.S.A.* **1989**, 86, 8328-8332.
21. Bissett, D.; McLaughlin, K.; Kelland, L. R.; Brown, R., *Br. J. Canc.* **1993**, 67, 742-748.
22. Bruhn, S. L.; Pil, P. M.; Essigmann, J. M.; Housman, D. E.; Lippard, S. J., *Proc. Natl. Acad. Sci. U.S.A.* **1992**, 89, 2307-2311.
23. Orphanides, G.; Wu, W.-H.; Lane, W. S.; Hampsey, M.; Reinberg, D., *Nature* **1999**, 400, 284-288.
24. Brown, S. J.; Kellett, P. J.; Lippard, S. J., *Science* **1993**, 261, 603-605.
25. Chow, C. S.; Whitehead, J. P.; Lippard, S. J., *Biochemistry* **1994**, 33, 15124-15130.
26. Pil, P. M.; Lippard, S. J., *Science* **1992**, 1992, 234-237.
27. Treiber, D. K.; Zhai, X.; Jantzen, H.-M.; Essigmann, J. M., *Proc. Natl. Acad. Sci. U.S.A.* **1994**, 91, 5672-5676.
28. Yarnell, A. T.; Oh, S.; Reinberg, D.; Lippard, S. J., *J. Biol. Chem.* **2001**, 278, 25736-25741.
29. Billings, P. C.; Engelsberg, B. N.; Hughes, E. N., *Cancer Invest.* **1994**, 12, 597-604.

30. Turchi, J. J.; Henkels, K. M.; Hermanson, I. L.; Patrick, S. M., *J. Inorg. Biochem.* **1999**, 77, 83-87.
31. Kane, S. A.; Lippard, S. J., *Biochemistry* **1996**, 35, 2180-2188.
32. Mikata, Y.; He, Q.; Lippard, S. J., *Biochemistry* **2001**, 40, 7533-7541.
33. Dormán, G.; Prestwich, G. D., *Biochemistry* **1994**, 33, 5661-5673.
34. Zhang, C. X.; Chang, P. V.; Lippard, S. J., *J. Am. Chem. Soc.* **2004**, 126, 6536-6537.
35. Huang, J.-C.; Zamble, D. B.; Reardon, J. T.; Lippard, S. J.; Sancar, A., *Proc. Natl. Acad. Sci. U.S.A.* **1994**, 91, 10394-10398.
36. Shuck, S. C.; Short, E. A.; Turchi, J. J., *Cell Res.* **2008**, 18, 64-72.
37. Fousteri, M.; Mullenders, L. H. F., *Cell Res.* **2008**, 18, 73-84.
38. Patrick, S. M.; Turchi, J. J., *J. Biol. Chem.* **2002**, 277, 16096-16101.
39. Wakasugi, M.; Kawashima, A.; Morioka, H.; Linn, S.; Sancar, A.; Mori, T.; Nikaido, O.; Matsunaga, T., *J. Biol. Chem.* **2002**, 277, 1637-1640.
40. Patrick, S. M.; Turchi, J. J., *J. Biol. Chem.* **1999**, 274, 14972-14978.
41. Thomas, J. O.; Travers, A. A., *Trends Biochem. Sci.* **2001**, 26, 167-174.
42. Dunham, S. U.; Lippard, S. J., *Biochemistry* **1997**, 36, 11428-11436.
43. Robert, J., 2007, *Personal Communication*.
44. Robert, J.; Laurand, A.; Meynard, D.; Le Morvan, V. In Platinum drugs and DNA repair. Lessons from the NCI-60 panel and clinical correlates, 10th International Symposium on Platinum Coordination Compounds in Cancer Chemotherapy, Verona, Italy; 2007.
45. He, Q.; Liang, C. H.; Lippard, S. J., *Proc. Natl. Acad. Sci. U.S.A.* **2000**, 97, 5768-5772.
46. Lin, C.-Y.; Navarro, S.; Reddy, S.; Comai, L., *Nucleic Acids Res.* **2006**, 34, 4752-4766.
47. White, R. J., *Nat. Rev. Mol. Cell Biol.* **2005**, 6, 69-78.
48. Klein, J.; Grummit, I., *Proc. Natl. Acad. Sci. U.S.A.* **1999**, 96, 6096-6101.
49. Zhai, X.; Beckmann, H.; Jantzen, H.-M.; Essigmann, J. M., *Biochemistry* **1998**, 37, 16307-16315.
50. Jordan, P.; Carmo-Fonseca, M., *Nucleic Acids Res.* **1998**, 26, 2831-2836.
51. Huang, R.; Wu, T.; Xu, L.; Liu, A.; Ji, Y.; Hu, G., *FASEB J.* **2002**, 16, 293-301.
52. Siddik, Z. H., *Oncogene* **2003**, 22, 7265-7279.
53. Chválová, K.; Sari, M.-A.; Bombard, S.; Kozelka, J., *J. Inorg. Biochem.* **2008**, 102, 242-250.
54. Trimmer, E. E.; Zamble, D. B.; Lippard, S. J.; Essigmann, J. M., *Biochemistry* **1998**, 37, 352-362.
55. Yoshida, M.; Izumi, H.; Torigoe, T.; Ishiguchi, H.; Itoh, H.; Kang, D.; Kohno, K., *Cancer Res.* **2003**, 63, 3729-3734.
56. Orphanides, G.; Lagrange, T.; Reinberg, D., *Genes Dev.* **1996**, 10, 2657-2683.
57. Cohen, S. M.; Jamieson, E. R.; Lippard, S. J., *Biochemistry* **2000**, 39, 8259-8265.
58. Coin, F.; Frit, P.; Viollet, B.; Salles, B.; Egly, J.-M., *Mol. Cell. Biol.* **1998**, 18, 3907-3914.
59. Jung, Y.; Mikata, Y.; Lippard, S. J., *J. Biol. Chem.* **2001**, 276, 43589-42596.
60. Kohno, K.; Izumi, H.; Uchiumi, T.; Ashizuka, M.; Kuwano, M., *BioEssays* **2003**, 25, 691-698.
61. Okamoto, T.; Izumi, H.; Imamura, T.; Takano, H.; Ise, T.; Uchiumi, T.; Kuwano, M.; Kohno, K., *Oncogene* **2000**, 19, 6194-6202.
62. Mello, J. A.; Acharya, S.; Fishel, R.; Essigmann, J. M., *Chem. Biol.* **1996**, 3, 579-589.
63. Schofield, M. J.; Hsieh, P., *Annu. Rev. Microbiol.* **2003**, 57, 579-608.

64. Lin, X.; Kim, H.-K.; Howell, S. B., *J. Inorg. Biochem.* **1999**, *77*, 89-93.
65. Clodfelter, J. E.; Gentry, M. B.; Drotschmann, K., *Nucleic Acids Res.* **2005**, *33*, 3323-3330.
66. Vaisman, A.; Varchenko, M.; Umar, A.; Kunkel, T. A.; Risinger, J. I.; Barret, J. C.; Hamilton, T. C.; Chaney, S. G., *Cancer Res.* **1998**, *58*, 3579-3585.
67. Fink, D.; Zheng, H.; Nebel, S.; Norris, P. S.; Aebi, S.; Lin, T.-P.; Nehme, A.; Christen, R. D.; Haas, M.; Macleod, C. L.; Howell, S. B., *Cancer Res.* **1997**, *57*, 1841-1845.
68. Drummond, J. T.; Anthoney, A.; Brown, R.; Modrich, P., *J. Biol. Chem.* **1996**, *271*, 19645-19648.
69. Branch, P.; Masson, M.; Aquilina, G.; Bignami, M.; Karran, P., *Oncogene* **2000**, *19*, 3138-3145.
70. Lin, D. P.; Wang, Y.; Scherer, S., J.; Clark, A. B.; Yang, K.; Avdievich, E.; Jin, B.; Werling, U.; Parris, T.; Kurihara, N.; Umar, A.; Kucherlapati, R.; Lipkin, M.; Kunkel, T. A.; Edelman, W., *Cancer Res.* **2004**, *64*, 517-522.
71. Salsbury Jr., F. R.; Clodfelter, J. E.; Gentry, M. B.; Hollis, T.; Scarpinato, K. D., *Nucleic Acids Res.* **2006**, *34*, 2173-2185.
72. Zdraveski, Z. Z.; Mello, J. A.; Marinus, M. G.; Essigmann, J. M., *Chem. Biol.* **2000**, *7*, 39-50.
73. Meyers, M.; Hwang, A.; Wagner, M. W.; Boothman, D. A., *Environ. Mol. Mutagen.* **2004**, *44*, 249-264.
74. O'Brien, V.; Brown, R., *Carcinogenesis* **2006**, *27*, 682-692.
75. Galan-Moya, E. M.; Herndandez-Losa, J.; Luquero, C. I. A.; de la Cruz-Morcillo, M. A.; Ramírez-Castillejo, C.; Callejas-Valera, J. L.; Arriaga, A.; Aramburo, A. F.; Cajal, S. R. y.; Gutkind, J. S.; Sánchez-Prieto, R., *Int. J. Cancer* **2008**, *122*, 289-297.
76. Collis, S. J.; DeWeese, T. L.; Jeggo, P. A.; Parker, A. R., *Oncogene* **2005**, *24*, 949-961.
77. Turchi, J. J.; Henkels, K., *J. Biol. Chem.* **1996**, *271*, 13861-13867.
78. Turchi, J. J.; Henkels, K. M.; Zhou, Y., *Nucleic Acids Res.* **2000**, *28*, 4634-4641.
79. Pawelczak, K. S.; Andrews, B. J.; Turchi, J. J., *Nucleic Acids Res.* **2005**, *33*, 152-161.
80. Dolling, J.-A.; Boreham, D. R.; Drown, D. L.; Mitchel, R. E. J.; Raaphorst, G. P., *Int. J. Radiat. Biol.* **1998**, *74*, 61-69.
81. Vaisman, A.; Chaney, S. G., *Biochemistry* **1995**, *34*, 105-114.
82. Kartalou, M.; Essigmann, J. M., *Mutat. Res.* **2001**, *478*, 1-21.
83. Kim, M. Y.; Zhang, T.; Kraus, W. L., *Genes Dev.* **2005**, *19*, 1951-1967.
84. de Laat, W. L.; Jaspers, N. G. J.; Hoeijmakers, J. H. J., *Genes Dev.* **1999**, *13*, 768-785.
85. Zamble, D. B.; Mikata, Y.; Eng, C. H.; Sandman, K. E.; Lippard, S. J., *J. Inorg. Biochem.* **2002**, *91*, 451-462.
86. Nichols, A. F.; Sancar, A., *Nucleic Acids Res.* **1992**, *20*, 2441-2446.
87. Gillet, L. C. J.; Schärer, O. D., *Chem. Rev.* **2006**, *106*, 253-276.
88. Imamura, T.; Izumi, H.; Nagatani, G.; Ise, T.; Nomoto, M.; Iwamoto, Y.; Kohno, K., *J. Biol. Chem.* **2001**, *276*, 7534-7540.
89. Vogelstein, B.; Lane, D.; Levine, A. J., *Nature* **2000**, *408*, 307-310.
90. Adimoolam, S.; Ford, J. M., *DNA Repair* **2003**, *2*, 947-954.
91. Rubbi, C. P.; Milner, J., *EMBO J.* **2003**, *22*, 975-986.
92. Bhana, S.; Hower, A.; Phillips, D. H.; Lloyd, D. R., *Mutagenesis* **2008**, *23*, 131-136.
93. Bhana, S.; Lloyd, D. R., *Mutagenesis* **2008**, *23*, 43-50.
94. Feng, G.; Tsui, H.-C. T.; Winkler, M. E., *J. Bacteriol.* **1996**, *178*, 2388-2396.



95. Moll, U. M.; Zaika, A., *FEBS Lett.* **2001**, 493, 65-69.
96. Schreiber, V.; Dantzer, F.; Amé, J.-C.; de Murcia, G., *Nat. Rev. Mol. Cell Biol.* **2006**, 7, 517-528.
97. Feazell, R. P.; Nakayama-Ratchford, N.; Dai, H.; Lippard, S. J., *J. Am. Chem. Soc.* **2007**, 129, 8438-8439.
98. Nemirovski, A.; Kasherman, Y.; Tzaraf, Y.; Gibson, D., *J. Med. Chem.* **2007**, 50, 5554-5556.
99. Reardon, J. T.; Vaisman, A.; Chaney, S. G.; Sancar, A., *Biochemistry* **1999**, 38, 3968-3971.
100. Zdraveski, Z. Z.; Mello, J. A.; Farinelli, C. K.; Essigmann, J. M.; Marinus, M. G., *J. Biol. Chem.* **2002**, 277, 1255-1260.
101. Chao, E. C.; Lipkin, S. M., *Nucleic Acids Res.* **2006**, 34, 840-852.
102. Samimi, G.; Kishimoto, S.; Manorek, G.; Breaux, J. K.; Howell, S. B., *Cancer Chemother. Pharmacol.* **2006**, 59, 301-312.
103. Perego, P.; Gatti, L.; Caserini, C.; Supino, R.; Colangelo, D.; Leone, R.; Spinelli, S.; Farrell, N.; Zunino, F., *J. Inorg. Biochem.* **1999**, 77, 59-64.
104. Kasparikova, J.; Fojta, M.; Farrell, N.; Brabec, V., *Nucleic Acids Res.* **2004**, 32, 5546-5552.
105. Zhang, C. X.; Lippard, S. J., *Curr. Opin. Chem. Biol.* **2003**, 7, 481-489.
106. Lovejoy, K. S.; Todd, R. C.; Zhang, S.; McCormick, M. S.; D'Aquino, J. A.; Reardon, J. T.; Sancar, A.; Giacomini, K. M.; Lippard, S. J., *Proc. Natl. Acad. Sci. U.S.A.* **2008**, accepted for publication.
107. Holzer, A. K.; Manorek, G. H.; Howell, S. B., *Mol. Pharmacol.* **2006**, 70, 1390-1394.
108. Kelland, L. R., *Drugs* **2000**, 59, 1-8.
109. Fourrier, L.; Brooks, P.; Malinge, J.-M., *J. Biol. Chem.* **2003**, 278, 21267-21275.
110. Potaman, V. N.; Shlyakhtenko, L. S.; Oussatcheva, E. A.; Lyubchenko, Y. L.; Soldatenkov, V. A., *J. Mol. Biol.* **2005**, 348, 609-615.
111. Donawho, C. K.; Luo, Y.; Luo, Y.; Penning, T. D.; Bauch, J. L.; Bouska, J. J.; Bontcheva-Diaz, V. D.; Cox, B. F.; DeWeese, T. L.; Dillehay, L. E.; Ferguson, D. C.; Ghoreishi-Haack, N. S.; Grimm, D. R.; Guan, R.; Han, E. K.; Holley-Shanks, R. R.; Hristov, B.; Idler, K. B.; Jarvis, K.; Johnson, E. F.; Kleinberg, L. R.; Klinghofer, V.; Lasko, L. M.; Liu, X.; Marsh, K. C.; McGonigal, T. P.; Meulbroek, J. A.; Olson, A. M.; Palma, J. P.; Rodriguez, L. E.; Shi, Y.; Stavropoulos, J. A.; Tsurutani, A. C.; Zhu, G.-D.; Rosenberg, S. H.; Giranda, V. L.; Frost, D. J., *Clin. Cancer Res.* **2007**, 13, 2728-2739.
112. Miknyoczki, S. J.; Jones-Bolin, S.; Pritchard, S.; Hunter, K.; Zhao, H.; Wan, W.; Ator, M.; Bihovsky, R.; Hudkins, R.; Chatterjee, S.; Klein-Szanto, A.; Dionne, C.; Ruggeri, B., *Mol. Cancer Ther.* **2003**, 2, 371-382.
113. Bernges, F.; Zeller, W. J., *J. Cancer Res. Clin. Oncol.* **1996**, 122, 665-670.
114. Hartwig, J. F.; Lippard, S. J., *J. Am. Chem. Soc.* **1992**, 114, 5646-5654.
115. Dunham, S. U.; Lippard, S. J., *J. Am. Chem. Soc.* **1995**, 117, 10702-10712.

## VIII. TABLES

Table 1.1: Proteins with an affinity for cisplatin-damaged DNA

Protein(s)	DNA-binding domain	Notable interactions	Comments	References
AAG	Glycosylase-DNA binding site	NER proteins?	Base excision repair protein	18, 82
DDB1	DNA damage recognition domain	NER proteins	Nucleotide excision repair protein	12, 39
DNA-PK	Ku70/Ku80 heterodimer	PARP-1	Nonhomologous end joining repair protein	76-81
HMGB1, HMGB2	HMG-domain	p53	Chromatin remodeling proteins	5, 35, 41, 42
LEF-1	HMG-domain		Transcription factor	53
Msh2	Mismatch binding domain	MMR proteins	Mismatch repair protein	14, 62-75
mtTFA	HMG-domain	p53	Transcription factor	25, 35, 55
PARP-1	Two zinc fingers	p53, histones	Involved in repair, death signaling, transcription regulation	83
SRY	HMG-domain		Transcription factor	54
SSRP1	HMG-domain	FACT subunit	Binding facilitated by FACT subunit	28
TBP	TATA-binding domain	RNA Pol II	Transcription factor	19, 57, 59
UBF1	HMG-domain	RNA Pol I	Transcription factor	27, 49, 51
XPA/RPA	XPA minimal DNA binding domain (MBD)	NER proteins	Nucleotide excision repair proteins	36, 38
YB-1	Cold shock domain	p53, PCNA	Transcription factor	15, 17, 61

## IX. FIGURES

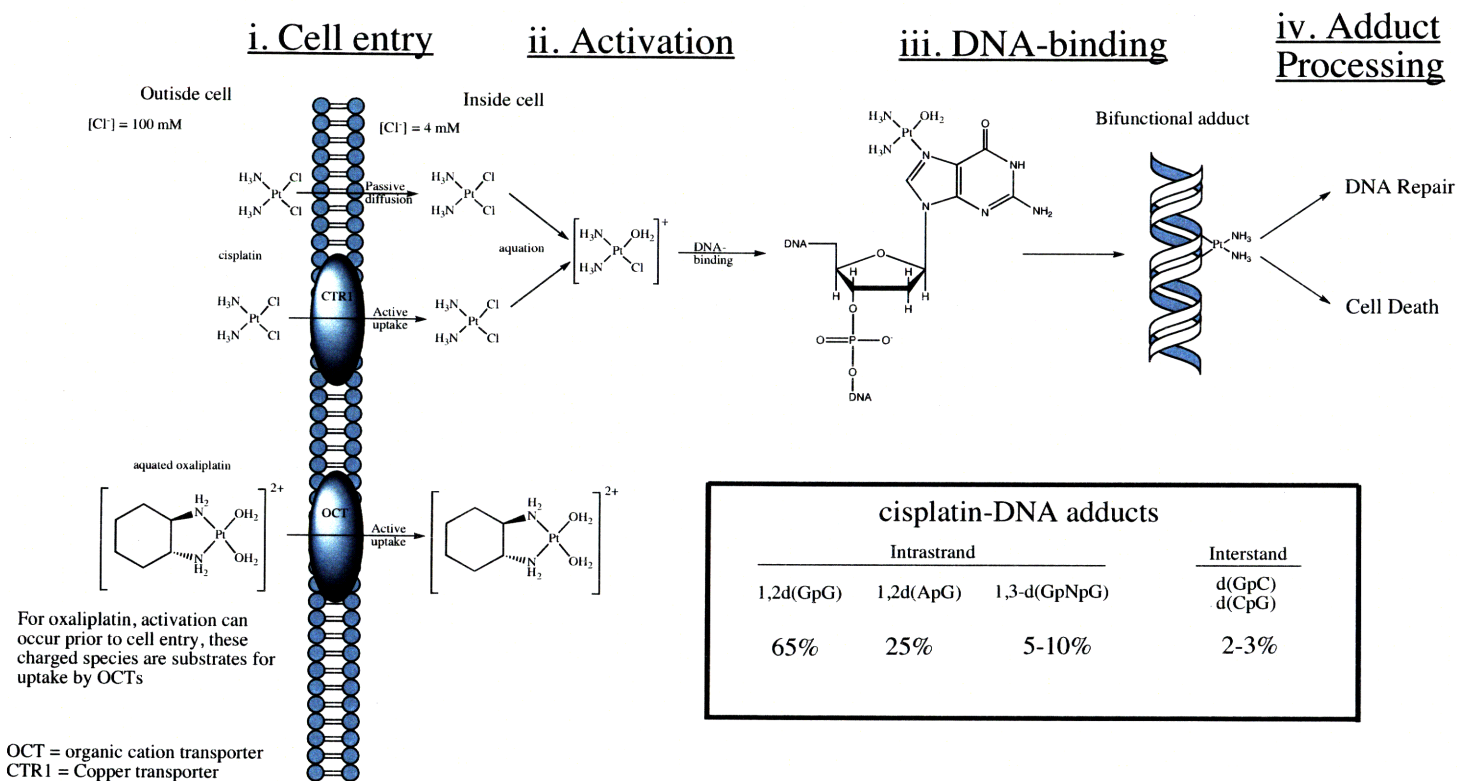
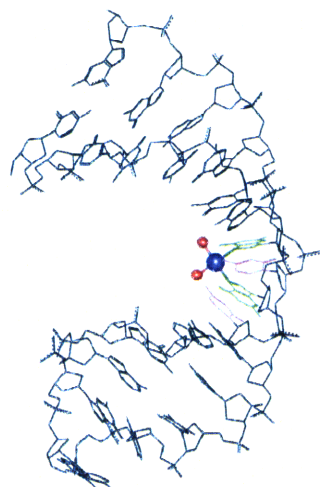
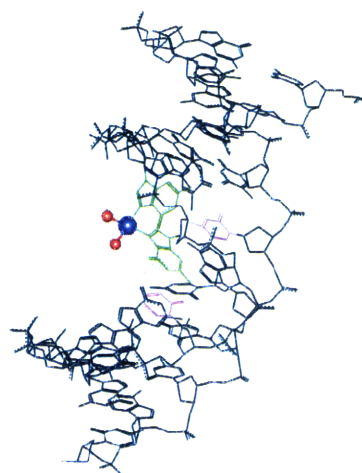


Figure 1.1. The four steps of cisplatin anticancer activity.

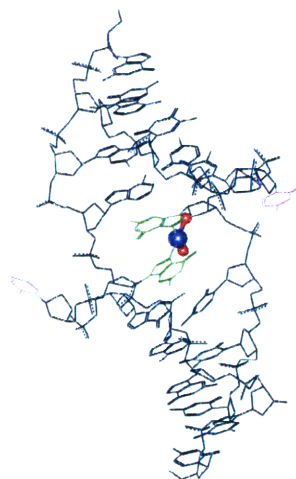
i) Cisplatin and analogous platinum complexes enter cells by passive and active diffusion mechanisms. ii) The platinum compound is aquated due to the low intracellular chloride concentration. iii) These positively charged compounds will bind to DNA and form several bifunctional DNA adducts. iv) The adducts must be repaired for the cell to survive, otherwise cell death mechanisms will be initiated.



1,2-d(GpG)  
intrastrand



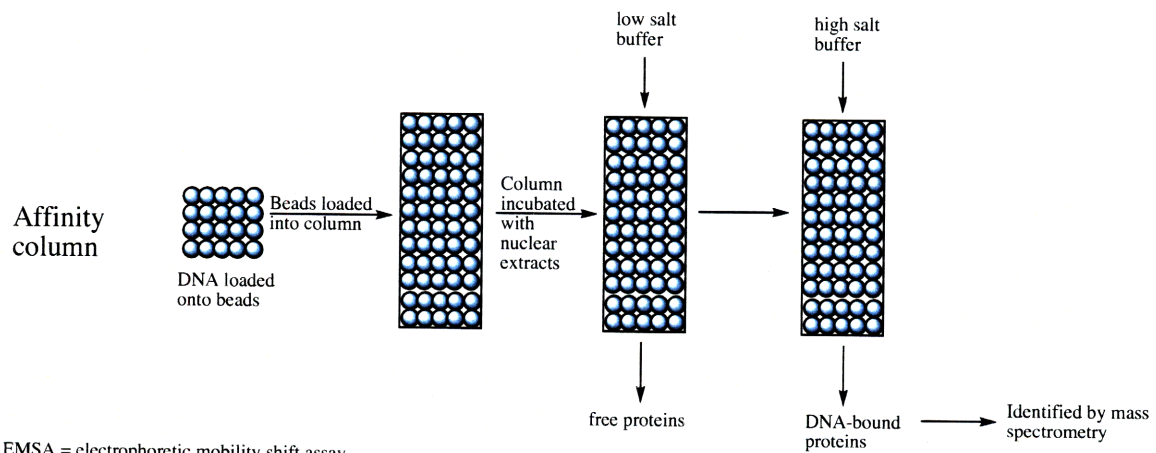
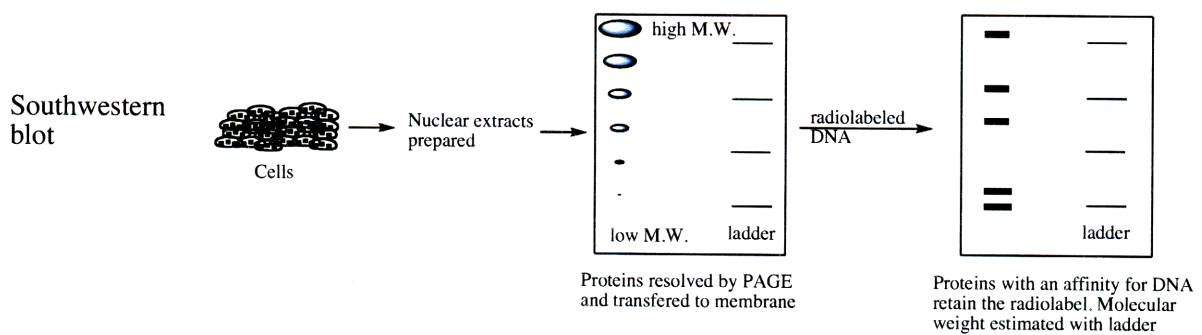
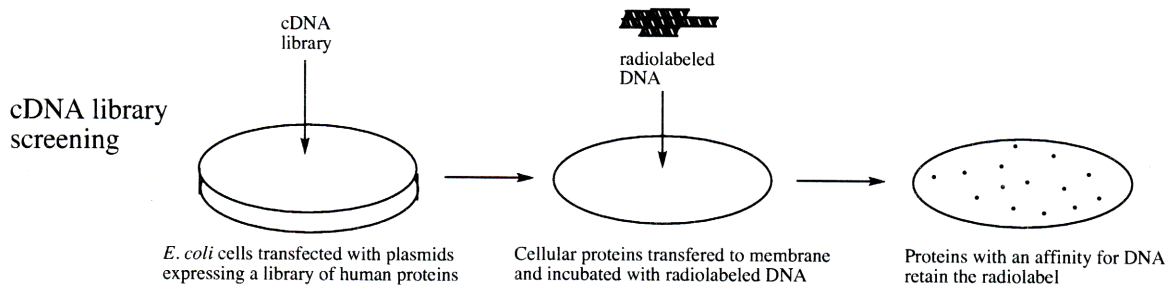
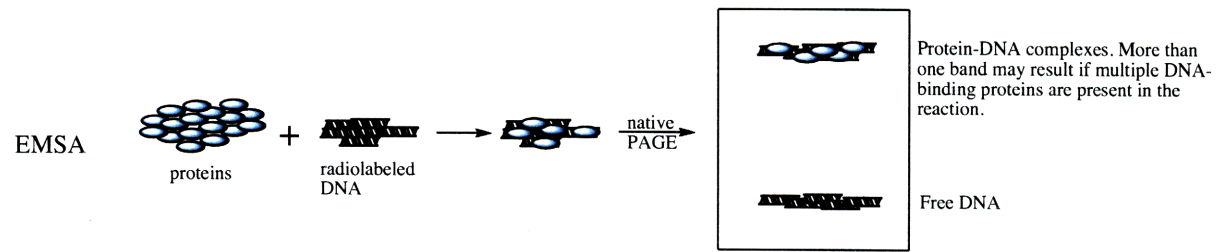
1,3-d(GpTpG)  
intrastrand



d(GpC)/d(CpG)  
interstrand

Figure 1.2. Structures of three adducts of cisplatin on DNA.

Structures from Kartalou and Essigmann.<sup>82</sup> The platinum atom is blue, the ammine ligands are red. The platinated guanine bases are green and the adenine bases opposite the platination are red.



EMSA = electrophoretic mobility shift assay  
PAGE = polyacrylamide gel electrophoresis

Figure 1.3. Methodologies developed for the characterization and identification of proteins with an affinity for damaged DNA.

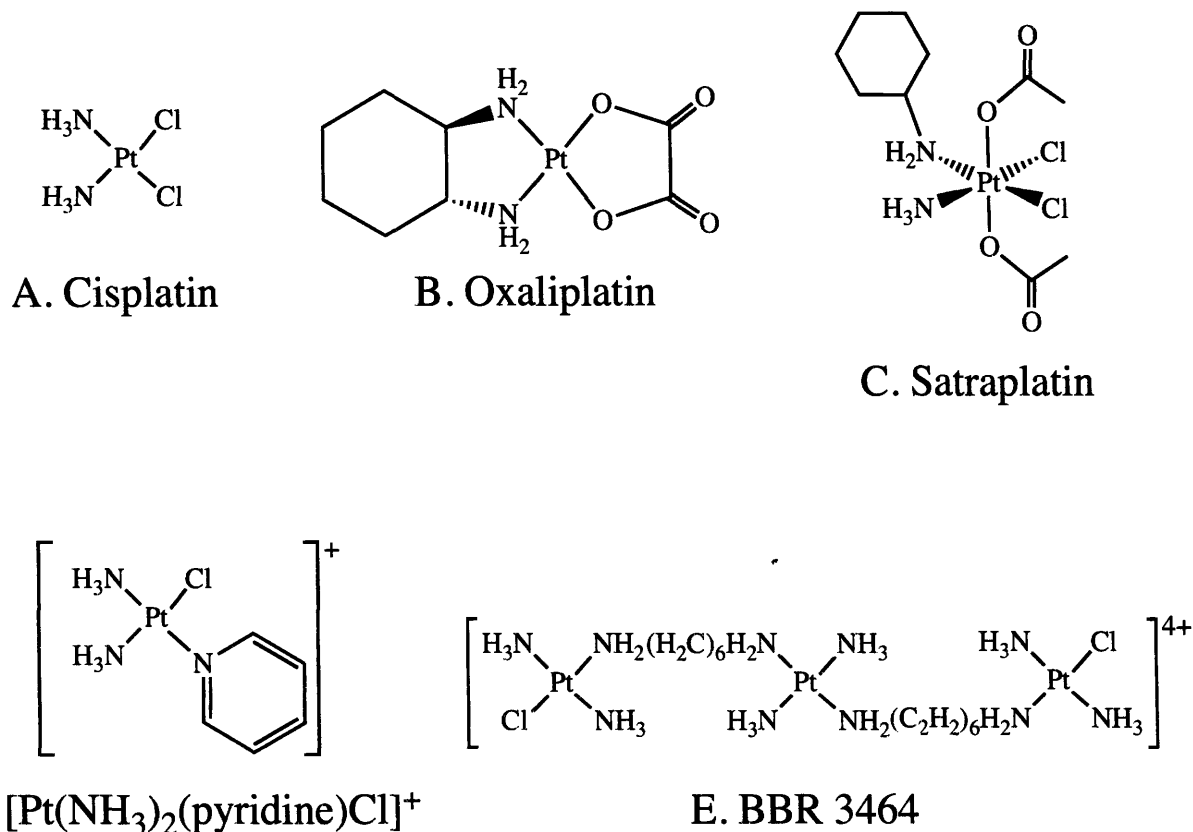


Figure 1.4. Platinum compounds with anticancer activity.

Cisplatin (**A**), oxaliplatin (**B**) and the reduced form of satraplatin (**C**) form the same types of bifunctional adducts with DNA, but contain different ammine ligands which may influence the recognition of the adduct. The platinum-pyridine compound (**D**), with only one chloride leaving group, forms monofunctional adducts with DNA. BBR 2464 (**E**), which has one chloride leaving group on each outer platinum atom, forms long-range bifunctional intrastrand and interstrand adducts.

**Chapter 2. Optimization of Photo-Cross-Linking Conditions for Identification of Proteins with an Affinity for a 25-bp Duplex DNA Containing a 1,2-d(GpG) Adduct of *cis*-[Pt(NH<sub>3</sub>)(*N*-(6-aminohexyl)-4-benzophenonamide)Cl<sub>2</sub>].**

\*Work from this chapter was submitted for publication; Guggenheim, E. R., Xu, D., Zhang, C. Z., Chang, P. V., Lippard, S. J., "Photo-Affinity Isolation and Identification of Proteins in Cancer Cell Extracts that Bind to Platinum-Modified DNA."

**Chapter 2: Optimization of Photo-Cross-Linking Conditions for Identification of Proteins with an Affinity for a 25-bp Duplex DNA Containing a 1,2-d(GpG) Adduct of *cis*-[Pt(NH<sub>3</sub>)(*N*-(6-aminohexyl)-4-benzophenamide)Cl<sub>2</sub>].**

\*Work from this chapter was submitted for publication; Guggenheim, E. R., Xu, D., Zhang, C. Z., Chang, P. V., Lippard, S. J., "Photo-Affinity Isolation and Identification of Proteins in Cancer Cell Extracts that Bind to Platinum-Modified DNA."



Following recognition of DNA damage, a series of cellular signaling pathways are activated. These damage-response pathways can result in DNA repair or cell death. Several repair processes have been implicated in response to platinum-damaged DNA. Chief among these is nucleotide excision repair (NER), which removes platinum adducts from DNA<sup>12</sup> and is correlated with cisplatin resistance.<sup>13</sup> In addition, *E. coli* and human cancer cells deficient in recombination repair pathways are sensitized to cisplatin damage.<sup>14,15</sup> Inhibition of the mismatch repair (MMR) pathway correlates with increased resistance to the drug<sup>16</sup>. Proteins involved in repair processes bind preferentially to cisplatin-DNA adducts, including the Ku70/80 subunits of the multiprotein complex DNA protein kinase (DNA-PK)<sup>17</sup>. The DNA-PK complex participates in non-homologous end-joining (NHEJ) repair of double-strand breaks (DSB).<sup>18</sup> These findings suggest that the identification of proteins that bind to platinum-modified DNA in cells with varying sensitivities to cisplatin may provide insight into processing of cisplatin adducts in these different contexts.<sup>19</sup>

Studies of the cellular proteins that interact with cisplatin-damaged DNA date back many years. Early work applied electrophoretic mobility shift assays (EMSAs) to demonstrate that xeroderma pigmentosum group E binding factor (XPE-BF) binds preferentially to cisplatin-modified versus unmodified DNA.<sup>20</sup> Using EMSAs to identify proteins with an affinity for platinum-modified DNA would require a separate experiment for each of numerous nuclear proteins. In another study, use of a cisplatin-modified DNA probe to screen a cDNA expression library identified the HMG-domain protein SSRP1.<sup>10,21</sup> Because SSRP1 contains an HMG domain that is homologous to domains in HMGB1 (formerly HMG1), it was hypothesized that the latter would also bind to cisplatin-modified DNA. Following isolation and purification of rat HMGB1, gel retardation assays revealed that the protein binds to the 1,2-d(G\*pG\*), but not the

1,3-d(G\*pG\*), intrastrand cross-link of cisplatin.<sup>8</sup> That HMGB1 and HMGB2 have an affinity for cisplatin-damaged DNA was also revealed by southwestern blotting methods.<sup>9,22</sup> Despite these successes, however, neither cDNA library screening nor southwestern blotting methods can gauge protein binding to platinated DNA in the context of multiprotein complexes.

Globally platinated DNA immobilized onto a column treated with nuclear extracts identified Pt–DNA-binding proteins DNA-PK, HMGB1, replication protein A (RPA), and xeroderma pigmentosum group A protein (XPA).<sup>23</sup> This method requires a sensitive adjustment of salt concentration to remove proteins with different affinities for the probe. Also, the use of globally platinated DNA does not distinguish which of many possible Pt–DNA adducts is being recognized.

A superior method for identifying proteins that bind to platinum-modified DNA utilizes a cisplatin analogue capable of forming a covalent bond to capture DNA-damage-response proteins following incubation with nuclear extracts. This method is sensitive to all nuclear proteins that bind to Pt-modified DNA, affording a more complete assessment. Photo-cross-linking provides a convenient way to bind the proteins covalently to the platinated DNA, which can then be isolated for identification.

To achieve this type of photo-cross-linking, we first synthesized a cisplatin analogue containing a photo-reactive azide moiety.<sup>24</sup> Control experiments performed during this study showed that *cis*-{Pt(NH<sub>3</sub>)<sub>2</sub>}<sup>2+</sup>-d(G\*pG\*) adduct itself was activated by the 302 nm irradiation required to convert the aryl azide to a nitrene. The aryl azide-modified analogue of cisplatin did not form photo-cross-links more effectively than the *cis*-{Pt(NH<sub>3</sub>)<sub>2</sub>}<sup>2+</sup> adduct alone.<sup>24</sup> We also showed that the *cis*-{Pt(NH<sub>3</sub>)<sub>2</sub>}<sup>2+</sup> could be more efficiently activated using a laser at 325 or 350 nm to irradiate the sample.<sup>25</sup> A limitation of experiments using *cis*-{Pt(NH<sub>3</sub>)<sub>2</sub>}<sup>2+</sup> as the cross-

linker is that the protein must come into close contact with the platinum atom in order to form a covalent DNA-Pt-protein linkage. This requirement make it difficult to capture DNA-damage recognition proteins that recognize the bulge created on the undamaged DNA strand,<sup>26</sup> where it is unlikely to be close enough to the *cis*-{Pt(NH<sub>3</sub>)<sub>2</sub>}<sup>2+</sup> adduct to be photo-cross-linked.

In order to cross-link proteins bound to Pt-DNA adducts more effectively, a photo-reactive benzophenone moiety was tethered to a platinum center. This compound, Pt-BP6, contains a six-carbon linker separating the platinum complex from the benzophenone (Figure 2.1), a hexamethylene chain proving to be optimal for efficient protein photo-cross-linking.<sup>27</sup> With an excitation wavelength of 365 nm, benzophenone is an excellent photo-activatable cross-linker for biological applications. The photophore excitation energy is low enough such that it does not cause significant damage to biological samples, and benzophenone moieties are not prohibitively sensitive to background light sources.<sup>28</sup>

In a preliminary study, we prepared a site-specifically platinated duplex containing a single 1,2-d(GpG) PtBP6 adduct, exposed it to HeLa nuclear extracts, and irradiated the solution to activate the benzophenone moiety (Figure 2.2). The protein-platinum-DNA complexes were isolated using streptavidin-coated magnetic beads (Figure 2.3). Several photo-cross-linked proteins were observed, two of which were identified as HMGB1 and poly(ADP-ribose) polymerase-1 (PARP-1).<sup>27</sup> Binding to HMGB1 was expected, given the results of work reported in the literature using EMSAs, but the photo-cross-linking of PARP-1 was the first evidence that the protein has an affinity for platinum-damaged DNA. In the present study, we have optimized the analytical and preparative photo-cross-linking conditions. We have also increased the scale of the preparative work, which has allowed us to identify all the proteins that photo-cross-link to

this probe. These experiments were able to identify a complete panalogy of proteins with an affinity for platinum-damaged DNA.

## II. MATERIALS AND METHODS

Solvents and chemical reagents were purchased from commercial sources. Potassium tetrachloroplatinate(II) was provided by Engelhard. DNA strands were synthesized on an Applied Biosystems ABI 392 DNA/RNA synthesizer using solvents and reagents supplied by Glen Research. Enzymes were purchased from New England BioLabs and Promega. UV-vis spectra were obtained on an HP 8453 UV-visible spectrometer. Platinum analyses were performed by flameless atomic absorption spectroscopy on a Perkin-Elmer AAnalyst 300 system. Analytical and preparative HPLC work was performed either on an HP Waters or an Agilent 1200 HPLC system. UV irradiation was conducted in a Stratagene Stratalinker UV Crosslinker. Protein digestion and analyses were performed by trypsin digestion-coupled LC-MS/MS analysis at the MIT Biopolymers facility. Antibodies used in western blot experiments were purchased from Axxora Life Sciences

### *Cell culture*

HeLa cells were grown in Dulbecco's Modified Eagle's Medium (DMEM) with 10% fetal bovine serum (FBS) and 1% penicillin-streptomycin at 37 °C under 5% CO<sub>2</sub>. Once growth reached ~80% confluence, cells were trypsinized and passed or collected. Cells between passages 4 and 18 were collected and used for preparing nuclear extracts.

### *Nuclear extraction*

In a typical extraction, a cell pellet from 5 x 175 cm<sup>2</sup> plates was used. Cells were collected and pelleted at 1000 rpm for 5 min. Cell pellets were washed with ice cold sterile PBS

(10 mM Na<sub>2</sub>HPO<sub>4</sub> pH 7.4, 137 mM NaCl, 2.7 mM KCl) twice at five times the pellet volume. Pellets were resuspended in five times the pellet volume of lysis buffer (10 mM HEPES pH 7.9, 10 mM KCl, 1.5 mM MgCl<sub>2</sub>, 1 mM DTT, 1 mM PMSF) and incubated for 15 min on ice. Pellets were centrifuged at 450 g for 5 min and resuspended in 2X volume of lysis buffer. The cells were lysed through a 26 3/8-gauge needle 10 times. The lysates were centrifuged at 11,000 g for 20 min and resuspended in two-thirds the cell pellet volume of extraction buffer (20 mM HEPES pH 7.9, 25% glycerol, 400 mM NaCl, 0.5 mM EDTA, 1.5 mM MgCl<sub>2</sub>, 1 mM DTT, 1 mM PMSF). The pellets were lysed again with a needle. The lysate was incubated at 4°C for 30 min with gentle mixing and centrifuged at 18,400 g for 10 min. The supernatant containing the nuclear extracts was removed and the protein content quantified by the BCA Assay. Nuclear extracts were stored at -80 °C. Between 0.5 – 1 mg of protein was obtained from each 175-cm<sup>2</sup> plate. For preparative scale photo-cross-linking experiments, 4 mg of nuclear extracts was required; nuclear extracts from 4-8 x 175 cm<sup>2</sup> plates were used.

#### *Synthesis of PtBP6*

The compound cis-[Pt(NH<sub>3</sub>)(N-(6-aminohexyl)-4-benzophenonamide)Cl<sub>2</sub>] (PtBP6) was synthesized as reported previously.<sup>27</sup> The synthesis was repeated in this work and reported here for completeness (Scheme 2.1).

#### *Synthesis of cis-Diamminediiodoplatinum(II) (1)*

To a stirring solution of K<sub>2</sub>PtCl<sub>4</sub> (4.00 g, 9.59 mmol) in 25 mL warm water was added KI (6.63 g, 39.7 mmol) in 2 mL of water. The solution was stirred and heated slowly to 60°C and NH<sub>4</sub>OH (4.0 mL, 31.0 mmol) was added slowly. A yellow precipitate formed almost immediately. The solution was filtered and dried under vacuum to give 91% yield of 1 (4.21 g, 8.72 mmol).

*Synthesis of cis-Diamminedichloroplatinum(II) (2)*

To a stirring suspension of **1** (2.01 g, 4.16 mmol) in 20 mL water was added AgNO<sub>3</sub> (1.42 g, 8.36 mmol). The solution was heated to 60 °C for 10 min with gentle stirring. Solid AgI was removed by filtration and KCl (0.70 g, 12.0 mmol) was added to the filtrate with gentle stirring. The solution was stirred for 10 min and **2** was removed by vacuum filtration. The yellow solid was washed with ice-cold water, ethanol and ether and dried in air to give a 72% yield of **2** (0.89 g, 3.0 mmol).

*Synthesis of (Ph<sub>4</sub>P)[PtCl<sub>3</sub>(NH<sub>3</sub>)] (3)*

A portion of **2** (0.52 g, 1.7 mmol) and tetraethylammonium chloride (0.29 g, 1.8 mmol) were dissolved in 120 mL dimethylacetamide. The solution was stirred and heated to 100°C with nitrogen bubbling through it for six h. Over this period, the solution evaporated to a volume of 20 mL. Then 360 mL of 1:1 ethyl acetate/hexanes was added and a yellow precipitate formed immediately. The solution was stored at -24°C overnight. The filtrate was decanted, and the remaining yellow solid was dissolved in 50 mL of water. Unreacted **2** was then removed by filtration and tetraphenylphosphonium chloride (0.65 g, 1.733 mmol) in 2 mL of water was added to the yellow filtrate. The solution was stirred for four h, followed by vacuum filtration to remove **3** (0.6898 g, 1.049 mmol) in a 61% yield.

*Synthesis p-Benzoylbenzoic acid N-hydroxysuccinimide ester (4)*

The synthesis of **4** has been previously established.<sup>29</sup> N-hydroxysuccinimide (0.86 g, 7.5 mmol), 4-benzoylbenzoic acid (1.68 g, 7.50 mmol) and 1,3-dicyclohexylcarbodiimide (1.64 g, 7.96 mmol) were combined in 80 mL of acetonitrile and stirred in the dark overnight. A white solid was filtered out and the solvent was removed by rotary evaporation. Compound **4** was collected in 51% yield and characterized by TLC (R<sub>f</sub> = 0.35 in 1:1 ethyl acetate/hexanes).

*Synthesis of [(4-Benzoyl-benzoylamino)-hexyl]-carbamic acid tert-butyl ester (5)*

*Tert*-butyl-*N*-(6-aminohexyl)carbamate hydrochloride (0.60 g, 2.4 mmol) was stirred in 25 mL of dichloromethane to which **4** (0.77 g, 2.4 mmol) in 10 mL of dichloromethane was added. Upon dissolution of these two reactants, triethylamine (1.50 mL, 10.7 mmol) was added. The solution was stirred overnight in the dark. The solvent was removed by rotary evaporation and the resulting white solid was purified by silica gel chromatography.  $R_f = 0.30$  (95:5 dichloromethane/methanol). The solvent of the eluate was removed by rotary evaporation to afford **5** in an 81% yield (0.82 g, 1.9 mmol). The product was characterized by  $^1\text{H}$  NMR spectroscopy; ( $\text{CDCl}_3$ ):  $\delta$ 7.93 (2H, d), 7.83 (4H, m), 7.60 (1H, m), 7.50 (2H, m), 6.59 (1H, t, br), 4.57 (1H, t, br), 3.47 (2H, m), 3.15 (2H, m), 1.78 – 1.25 (17H, m). The results agreed with published data for this compound.<sup>27</sup>

*Synthesis of N-Aminohexyl-4-benzoyl-benzamide (5b)*

To a solution of **5** (0.31 g, 0.72 mmol) in 5 mL chloroform was added trifluoroacetic acid (1.00 mL, 13.0 mmol). The solution was stirred overnight in the dark. The solvent was removed by rotary evaporation. The remaining solid was dissolved in 50 mL of ethyl acetate to which 75 mL 1M NaOH was added. The solution was shaken three times in a separatory funnel and the organic layer was removed with ethyl acetate. The solvent was removed by rotary evaporation and the remaining white solid was purified by silica gel chromatography.  $R_f$  (impurity) = 1.0,  $R_f$  (**5b**) = 0.20. The solvent was removed by rotary evaporation to give a 47% yield of product (0.5376g, 1.657 mmol). The white solid was characterized by  $^1\text{H}$  NMR; ( $\text{CDCl}_3$ ):  $\delta$ 7.90 – 7.75 (6H, m), 7.61 (1H, m), 7.50 (2H, m), 6.25 (1H, br), 3.49 (2H, m), 2.72 (2H, m), 1.79 – 1.20 (10H, m). This data agreed with previously published results.<sup>27</sup>

*Synthesis of [PtCl<sub>2</sub>(NH)<sub>2</sub>(BP6)] (6)*

Sodium tetraphenylborate (0.43 g, 1.3 mmol) and **3** (0.86 g, 1.3 mmol) were stirred in 100 mL of methanol for ten min. The compound (Ph<sub>4</sub>P)(BPh<sub>4</sub>) precipitated as a white solid and was removed by filtration. 10 mL of water was added to the yellow filtrate and the filtrate was slowly reduced to about 10 mL by rotary evaporation. A portion of **5b** (0.50 g, 1.5 mmol) was added in 5 mL of ethanol. The solution was stirred overnight in the dark. The solvent was decanted leaving a tan precipitate in the flask. The solid was dissolved in 5 mL dimethylformamide to which 35 mL of water was added and the solution was put on ice for 30 minutes. The solution was then centrifuged for 30 minutes at 4000 rpm and 4°C. The solvent was decanted and 35 mL of water was added. The suspension was then centrifuged again under the same conditions. The water was decanted and the tan solid was dried by lyophilization. The product (0.10 g, 0.17 mmol) was collected at 13% yield and characterized by <sup>1</sup>H NMR; (DMF-*d*<sub>7</sub>): δ8.70 (1H, t), 8.13 (2H, d), 7.84 (4H, m), 7.73 (1H, m), 7.61 (2H, m), 4.85 (2H, t, br), 4.25 (3H, t, br), 3.44 (2H, m, partially buried by H<sub>2</sub>O peak), 2.78 (2H, m, buried under DMF signal), 1.80 – 1.20 (8H, m). These data agree with previously published results.<sup>27</sup>

#### *DNA Synthesis*

5'-CCTCTCCTCTCAGGATCTTCTCTCC-3' and its complementary strand were synthesized on ABI DNA/RNA synthesizer on a 1 μmole scale. For preparative-scale photo-cross-linking experiments, DNA containing a 3'-biotin-TEG moiety was synthesized and platinated. The DNA was incubated overnight at 55°C in 30% ammonium hydroxide. DNA strands were purified by 12% urea denaturing PAGE and visualized by UV shadowing. The DNA was then isolated from the gel using the crush and soak method. DNA-containing gel pieces were broken up with a spatula and incubated overnight at 37°C with mixing in soaking buffer (10 mM Tris HCl pH 7.3, 50 mM NaCl, 1 mM EDTA). The gel was then filtered from



DNA and the solution was ethanol precipitated. The DNA pellet dissolved in water and dialyzed against water using dialysis tubing with a molecular weight cutoff of 3500.

*Preparation of a 25 base DNA containing a site-specific PtBP6 adduct*

To a solution of PtBP6 dissolved in 90  $\mu\text{L}$  of DMF was added 1.9 molar equivalents of  $\text{AgNO}_3$  dissolved in 10  $\mu\text{L}$  of water. The solution was protected from light and vortexed for 4 h at room temperature. The solution was then centrifuged to separate precipitated  $\text{AgCl}$  from the activated platinum complex. To a 10  $\mu\text{L}$  aliquot of the solution is added 1  $\mu\text{L}$  of 5 M  $\text{NaCl}$ . No precipitate formed, demonstrating that all of the silver had been removed from the solution. The 25-bp DNA was dissolved in 10 mM  $\text{Na}_2\text{HPO}_4$  pH 6.3. To this solution was added 2 molar equivalents of activated PtBP6. The solution was incubated overnight at 37  $^\circ\text{C}$  in the dark with mixing.

The PtBP6-modified 25 base DNA was purified by IE-HPLC. The eluant was a gradient of 40-50% B over 30 min at 45  $^\circ\text{C}$ , where solvent A was 90/10 water/acetonitrile, 0.025M TEAA, pH 6.8 and solvent B was A + 1 M  $\text{NaCl}$ . The 25 base DNA containing a 1,2-d(GpG) adduct of PtBP6 eluted at 25.4 min. The peak was collected and lyophilized. The product was resuspended in water and dialyzed against water, MWCO 3500. In a typical purification, 5 nmol of platinated DNA was collected, a 17% yield.

*Characterization of 25 base DNA containing a 1,2-d(GpG) adduct of PtBP6*

Each collected peak was characterized by UV-visible absorbance and atomic absorption spectroscopy to establish a 1:1 ratio of platinum per DNA strand. The collected peaks were characterized by ESI-MS to confirm that both chloride ligands were replaced by Pt-DNA bonds.

Platination of the guanine bases was verified by enzymatic digestion of the DNA. The digests consisted of 20  $\mu\text{L}$  100 mM  $\text{NaOAc}$  (pH 5.2), 1  $\mu\text{L}$  100 mM  $\text{ZnCl}_2$ , 10  $\mu\text{L}$  nuclease P1,

and 150 pmol DNA. The total reaction volumes were increased to 100  $\mu\text{L}$  with ddH<sub>2</sub>O. The solutions were mixed thoroughly and incubated at 37 °C overnight. Next, 5  $\mu\text{L}$  of 1.5 M Tris-HCl (pH 8.8) and 1  $\mu\text{L}$  of calf intestinal phosphatase (CIP) was added. After a 4-h incubation at 37 °C, the samples were centrifuged at 5000 rpm for 5 min. The supernatants were analyzed by RP-HPLC using a Supelcosil LC-18-S column. The eluant was a gradient of 5 – 15% B over 30 min, 15 – 80% B over 10 min, and 80% B for 5 min, where solvent A was 100 mM NaOAc, pH 5.2, and solvent B was methanol. PtBP6 was activated as described above and allowed to react with deoxyguanosine overnight, followed by analysis with this HPLC methodology. This experiment was carried out to determine the elution of the compound PtBP6-(dG)<sub>2</sub>, a likely product of the nuclease digestion of the platinated 25-base DNA, under these HPLC conditions.

The platination of the guanines was also verified by the four Maxam-Gilbert sequencing reactions.

G reaction: A 1.5  $\mu\text{L}$  portion of radiolabeled DNA was combined with 14.5  $\mu\text{L}$  of water and 200  $\mu\text{L}$  of DMS Buffer (50 mM sodium cacodylate pH 7.0, 1 mM EDTA pH 8.0). A 1  $\mu\text{L}$  aliquot of dimethyl sulfate was then added and the reaction was incubated at room temperature for 5 minutes. Then a 50  $\mu\text{L}$  portion of DMS stop solution (1.5 M sodium acetate, 1 M mercaptoethanol, 250  $\mu\text{g}/\text{mL}$  salmon sperm DNA) was added.

A+G reaction: A 3  $\mu\text{L}$  portion of DNA was combined with 13  $\mu\text{L}$  of water and 25  $\mu\text{L}$  of formic acid. The reaction was incubated at room temperature for 5 minutes. Then a 200  $\mu\text{L}$  aliquot of stop solution #2 (0.3 M sodium acetate pH 7.0, 0.1 mM EDTA pH 8.0, 100  $\mu\text{g}/\text{mL}$  salmon sperm DNA) was added.

C+T reaction: A 16  $\mu\text{L}$  aliquot of DNA was combined with 10  $\mu\text{L}$  of water and 30  $\mu\text{L}$  of hydrazine. The solution was incubated at room temperature for 15 minutes. Then a 200  $\mu\text{L}$  portion of stop solution #2 was added.

C reaction: A 9.5  $\mu\text{L}$  aliquot of DNA was combined with 6.5  $\mu\text{L}$  of 5 M NaCl and 10  $\mu\text{L}$  of water. This solution was then incubated with 30  $\mu\text{L}$  of hydrazine for 15 minutes followed by the addition of 200  $\mu\text{L}$  of stop solution #2.

All reactions: After each of these steps was completed, to each reaction was added 750  $\mu\text{L}$  of ice-cold ethanol, and each was cooled on dry ice for 30 minutes. Each was then centrifuged at 1350 rpm and  $-4^{\circ}\text{C}$  for 30 minutes. Each sample was then ethanol precipitated once more and dried in the vacufuge. To each reaction was then added 75  $\mu\text{L}$  of 1:9 piperidine/water and heated to  $90^{\circ}\text{C}$  for 30 min. The reactions were then dried in the vacufuge, washed with 45  $\mu\text{L}$  of water and dried again twice in the vacufuge. Platinated probes were then treated with 50  $\mu\text{L}$  of 0.2 M NaCN at  $37^{\circ}\text{C}$  overnight, followed by another ethanol precipitation. The reactions were then analyzed by 20% urea-denaturing PAGE.

#### *Radiolabeling of 25 base DNA*

In an eppendorf tube, 50 pmol of DNA was combined with 3  $\mu\text{L}$  of 10X PNK Buffer (700 mM Tris-HCl, 100 mM  $\text{MgCl}_2$ , 50 mM DTT, pH 7.6), 3  $\mu\text{L}$  of  $\gamma\text{-}^{32}\text{P}\text{-ATP}$  (Perkin-Elmer) and 1  $\mu\text{L}$  of T4 PNK (New England Biolabs). The solutions were diluted to 30  $\mu\text{L}$  and incubated at  $37^{\circ}\text{C}$  for 2 h. The solutions were then purified by Sephadex G-25 spin columns (GE Healthcare), ethanol precipitated, and dried by vacuum centrifugation.

#### *Synthesis of duplex probes*

Equimolar amounts of PtBP6-modified top strand and unmodified bottom strand were combined in 50  $\mu\text{L}$  of NEBuffer 3 (New England BioLabs, 50 mM Tris-HCl pH 7.9, 100 mM

NaCl, 10 mM MgCl<sub>2</sub>, 1 mM DTT). For preparative-scale photo-cross-linking, 500 pmol unradiolabeled DNA were used, and for analytical-scale photo-cross-linking, 50 pmol of radiolabeled DNA was used. The solutions were heated to 90 °C for 5 min, cooled to 16 °C over 3 h. The solution was then ethanol precipitated and dried by vacuum centrifugation. The DNA was then purified by 15% native PAGE and located using either autoradiography for radiolabeled DNA or UV shadowing for unlabeled DNA. The DNA was isolated by using the crush and soak method and the purity of the oligonucleotide was verified by 15% native PAGE.

*Optimization of analytical-scale photo-cross-linking with a 1,2-d(GpG)-PtBP6 probe*

In a typical analytical-scale photo-cross-linking reaction, 1 pmol of 1,2-d(GpG)-PtBP6-modified double-stranded radiolabeled DNA was combined with 20 µg of HeLa nuclear extracts in 20 µL of protein binding buffer (10 mM Tris pH 7.5, 10 mM KCl, 10 mM MgCl<sub>2</sub>, 1 mM EDTA, 0.05% NP-40, 0.2 µg/mL BSA). The solution was incubated on ice and then exposed to UV irradiation. Irradiation was performed by using NEC FL8BL 8W bulbs, which provide a maximum at 360 nm with minimal output at 300 nm (<http://www.nelt.co.jp/english/products/safl/>). The latter wavelength could potentially labilize the platinum-DNA bonds. The cross-linking was then analyzed by 10% SDS-PAGE with a 4% stacking gel. The irradiation time was varied between 0, 5, 30, 60, 90 and 120 min. The incubation time was varied between 0, 30, 60, 120, 240 and 360 min. The temperature was varied between 4°C, 25°C and 37°C.

*Optimization of preparative-scale photo-cross-linking of probes*

Into four eppendorf tubes were added 20 µg of HeLa nuclear extracts and 28.5 µL of binding buffer. This mixture was added to 0.5 mg of streptavidin-coated magnetic beads and the solution was vortexed thoroughly. The tubes were placed on a magnetic rack and the supernatant

was removed. The beads were then vortexed in 100  $\mu$ L of wash/binding buffer (5 mM Tris pH 7.5, 0.5 mM EDTA, 1 M NaCl) and put back on the magnetic rack to separate the supernatant from the beads again. This washing process was repeated 0, 2, 5 or 10 times for each eppendorf tube. After the final supernatant was removed, to each sample was added 50  $\mu$ L of gel-loading solution (125 mM Tris-HCl pH 6.8, 40% glycerol, 4% SDS, 10%  $\beta$ -mercaptoethanol). The solutions were heated to 90  $^{\circ}$ C for 10 min and then the supernatant was isolated immediately using the magnetic test tube stand. To denature the samples, they were heated to 90 $^{\circ}$  C for 5 min and then cooled immediately on ice. The cross-links were then separated by a 4-20% BioRad pre-cast SDS-PAGE gel. The gel was removed from the gel box and soaked for 1 h in destain solution (10% methanol, 7% acetic acid, 83% water by volume). The gel was soaked in Sypro Ruby Gel Stain (Cambrex) overnight and then soaked in destain solution for 1 h. The gel was then wrapped in plastic wrap and analyzed by a BioRad FluorS Multimager scanner exciting at 450 nm.

#### *Preparative scale photo-cross-linking*

To 100 pmol of unradiolabeled duplex in 100  $\mu$ L of binding buffer was added 2 mg of HeLa nuclear extract. The reaction mixtures were irradiated for 2 h on ice. To each reaction mixture was then added 5 mg of streptavidin-coated magnetic beads (Dynabeads, Invitrogen), and the solutions were incubated with mixing for 20 min at 4  $^{\circ}$ C. To the solution was then added 400  $\mu$ L of 2X elution buffer (50 mM Tris-HCl, 10 mM DTT, 1% SDS, pH 7.9) and the mixture was incubated with agitation for 20 min at 4  $^{\circ}$ C.

The supernatant was then removed from the beads using a magnet. The beads were washed four times with high salt buffer (5 mM Tris-HCl, 500  $\mu$ M EDTA, 1 M NaCl, pH 7.5), each time the supernatant was removed using the magnet. The beads were then washed five

times with 1X elution buffer, again each time removing the supernatant using the magnet. After the fifth elution buffer wash was removed, 40  $\mu$ L of 2X SDS-PAGE loading buffer (100 mM Tris-HCl, 20 mM DTT, 2% SDS, 30% glycerol, 0.1% bromophenol blue, pH 7.9) was added to the solution. The solution was heated to 90 °C for 10 min to dissociate the biotinylated DNA from the beads and the supernatant was quickly removed using the magnet. The samples were then resolved by 12% SDS-PAGE with a 4% stacking gel. Following electrophoresis, the gel was removed from the plates and the lanes containing the preparative scale photo-cross-linking products were separated from the rest of the gel using a blade. These lanes were then soaked in Coomassie Blue R-250 for 1 h and destained in 10% methanol, 7% glacial acetic acid, 83% ddH<sub>2</sub>O 2 times for 1 h each.

The bands were located using the results from the radioactive analytical scale cross-linking experiment as a guide. Molecular weight ladders were run on both gels, so that the locations of each band on the gel could be precisely estimated prior to excision. Bands were excised from lanes containing PtBP6-platinated DNA as well as unplatinated DNA. The excised bands were analyzed by trypsin digest-coupled LC-MS/MS. The peptide fragments were then processed by SEQUEST protein analysis software to identify the parent proteins.<sup>30</sup>

The proteins present in the lane containing the unplatinated DNA were eliminated from the list of those found in the lane with the PtBP6-platinated DNA. Proteins were scored as binding to the platinated probe only if they occurred in two repetitions of the photo-cross-linking experiments. In accordance with suggested guidelines for the identification of proteins by trypsin digest-coupled mass spectrometry,<sup>31</sup> the proteins identified were only accepted if they met the criteria of low probability of coincidental identification ( $P < 1.0 \times 10^{-3}$ ) and/or multiple unique matching peptides found. “Unique peptides” were defined as having entirely different sequences

from one another; two peptides differing only by a modified amino acid were scored as being identical.

### III. RESULTS

As described in a preliminary report,<sup>27</sup> a 25-bp duplex containing a 1,2-d(GpG) intrastrand cross-link of the photo-active cisplatin analogue PtBP6 was prepared and characterized. This probe was used to photo-cross-link proteins with an affinity for platinum-modified DNA (Figure 2.2). Most of the proteins that bind to this probe were previously unidentified, and cross-linking conditions were optimized here in order to characterize them.

#### *Synthesis and characterization of cis-[Pt(NH<sub>3</sub>)(N-(6-aminohexyl)-4-benzophenonamide)Cl<sub>2</sub>] (PtBP6)*

PtBP6 was synthesized in seven steps and characterized as previously reported.<sup>27</sup> <sup>1</sup>H NMR spectroscopic analysis of the final product indicated that the desired compound was pure (Figure 2.4).

#### *Synthesis and characterization of a 25 base 1,2-d(GpG) intrastrand probe*

A 25 base DNA containing a 1,2-d(GpG) intrastrand cross-link of PtBP6 was synthesized as reported previously.<sup>27</sup> The purification did not afford significant separation of the orientational isomers<sup>27,32</sup> of PtBP6-modified DNA by RP-HPLC (Figure 2.5), and a mixture of the two isomers was used for these studies. Following purification, the collected peak was dialyzed to remove salt using a molecular weight cutoff of 3500. In a typical purification, 5 nmol of platinated DNA was collected, a 17% yield. The ratio of bound platinum atoms per DNA fragment was determined to be  $0.99 \pm 0.10$ .

Nuclease digestion analyses of the platinated probe (Figure 2.6) confirm that the platinum atom is bound to both guanine bases. The expected ratio of C:G:T:A for the unplatinated 25 base DNA was 12:2:9:2, and the experimental ratio was 11.9:2.1:9.1:2.0 (Figure 2.6A). For the platinated probe, the experiment revealed 11.9:0.4:9.1:1.6 (Figure 2.6B). These data indicate that, following nuclease digestion of the platinated DNA, the signal for guanosine is muted. The signal for adenosine is also slightly less intense, suggesting the possibility of some d(ApG) platination. In the digestion of cisplatin-modified DNA, described in Appendix A, the digested platinum-nucleobase products elute during the HPLC gradient. PtBP6-nucleobase complexes may exhibit stronger retention on the column, because no new peaks are present in the trace (Figure 2.6B). To confirm that the platinum-containing products of this digestion should not elute during the run, activated PtBP6 and deoxyguanosine were allowed to react and the resulting complexes were analyzed using the same HPLC methodology (Figure 2.7). The products of the reaction elute at about 43 min (Figure 2.7B), during the washing sequence of the HPLC run. This is likely due to the benzophenone moiety and six-carbon chain on PtBP6 (Figure 2.1), which will interact favorably with the C18 column. The peak for guanosine was not completely depleted by the binding of PtBP6 to the base (Figure 2.6B), so it was necessary to ensure that the platinum was bound to the DNA in a bifunctional manner by mass spectrometric analysis.

The purified DNA is bound to the DNA in a bifunctional manner, as indicated by ESI-MS (Figure 2.8). The platinum-modified DNA has a calculated value of 7967.4 m/z, and ESI-MS revealed an experimental value of  $7967.2 \pm 1.64$  m/z. A monofunctional adduct would require another ligand to fulfill the coordination of the platinum, which would be evident by an increase in the molecular weight of the complex. Maxam-Gilbert analysis of the platinated DNA (Figure 2.9) confirms that the platinum is bound to the N7 of guanine, since it is able to block the



Maxam-Gilbert G reaction of dimethyl sulfate (Figure 2.9C). The ability of the Maxam-Gilbert AG reaction to access the guanosine bases was also compromised by platination. These three methods conclusively demonstrate that the product of the reaction is a 25-base DNA containing a 1,2-d(GpG) cross-link of PtBP6.

#### *Duplex 25-bp probes*

Radiolabeled 25-bp duplex probes were prepared in approximately 70% yield, an estimated value since UV-vis measurements were not taken on the radioactive material. The double-stranded constructs could be well separated from single-stranded material by native PAGE, and the ImageQuant gel analysis program was used to determine that their purity was approximately 100% (Figure 2.10). For preparative-scale photo-cross-linking experiments, unradiolabeled 25-bp duplex probes were prepared. Following purification, 455 pmol of the unplatinated 25-bp duplex and 379 pmol of the 25-bp duplex containing a 1,2-d(GpG) intrastrand adduct of PtBP6 were isolated. These values correspond to 91% and 76% yields, respectively.

#### *Analytical-scale photo-cross-linking of a 25-bp duplex containing a 1,2-d(GpG) adduct of PtBP6*

Analytical-scale photo-cross-linking afforded a number of bands corresponding to protein-platinum-DNA complexes containing different covalently-bound proteins. The parameters used for analytical-scale photo-cross-linking were analyzed. Varying the UV-irradiation time indicates that the maximum photo-cross-linking occurs at the full 120 min irradiation (Figure 2.11). By varying the pre-irradiation incubation time, we observed that little incubation time was required prior to UV-irradiation to achieve maximum photo-cross-linking (Figure 2.12). Incubation and photo-cross-linking at temperatures higher than 4°C revealed that the proteins are degraded significantly under these conditions (Figure 2.13).

*Analysis of protein retention on streptavidin-coated magnetic beads*

Incubation of the streptavidin-coated magnetic beads with nuclear extracts revealed significant retention of proteins onto the beads. Subsequent washing of the beads with high salt buffer was able to remove most of these proteins (Figure 2.14). These washing conditions were used for preparative-scale photo-cross-linking experiments. Some protein still remains even after 10 washes. These proteins are identified in the control experiments outlined below and are listed in Table 2.2.

*Preparative-scale photo-cross-linking of a 25-bp duplex containing a 1,2-d(GpG) intrastrand PtBP6 adduct with HeLa nuclear extracts*

The PtBP6-modified DNA was irradiated in the presence of HeLa nuclear extracts to generate covalent bonds between the benzophenone moiety of the platinum compound and any proteins in the vicinity of the damage site. The DNA-to-protein ratio was adjusted to be the same for both preparative-scale preparative and analytical-scale experiments. After immobilization of the biotinylated DNA-platinum-protein conjugates on streptavidin-coated magnetic beads, the complexes were washed thoroughly with high salt and SDS-containing buffers to remove any non-covalently bound proteins. SDS-PAGE analysis was performed on a slab gel to obtain better separation of proteins. An analytical-scale photo-cross-linking experiment was run in parallel to the preparative-scale experiment as a guide for excising DNA-platinum-protein complexes, as shown in Figure 2.15. Mass spectral analysis of the preparative-scale photo-cross-linking experiment identified a number of proteins in each of the six major bands on the analytical gel (Table 2.1), including the DNA repair proteins PARP-1, DNA ligase III, Msh2, and all three members of the DNA-PK heterotrimer, as well as HMG-domain proteins HMGB1, HMGB2, HMGB3 and UBF1.

A control lane containing unplatinated DNA was included in the preparative scale photo-cross-linking experiment. Proteins identified in this control lane (Table 2.2), as well as proteins for which the molecular weight was inconsistent with the band location, were excluded from the list in Table 2.1, which reports the results of three repeats of preparative-scale photo-cross-linking experiments. In the table, the “Band” column refers to the relative mobility of the protein-platinum-DNA complex through the gel, with 1 being the fastest migrating species. The “Unique Peptides” column reports the number of individual peptide fragments matching those expected from the known protein sequence. Peptides differing by only one amino acid were not considered to be unique. The “Probability” column assigns a number to each protein based on the likelihood of a coincidental match of the best unique peptide for each protein. For example, three unique peptides were found that correspond to the protein UBF1. One of these peptides, RQLQEERPELSESELTRL, produced MS/MS data with a probability of  $7.96 \times 10^{-7}$ , meaning there is a 0.0000796% probability that this identification is an artifact due to background. Peptides with probabilities of  $1.0 \times 10^{-3}$  or higher were not accepted.

#### IV. DISCUSSION

Since the discovery that cisplatin targets DNA, much effort has been expended to identify proteins with an affinity for the platinated duplex. In the present study, we prepared and characterized a site-specifically modified 25-bp duplex containing a 1,2-d(GpG) intrastrand cross-link bearing a pendent photo-activatable benzophenone. Upon irradiation, these probes form covalent bonds between the platinated DNA and any proteins in a nuclear extract with an affinity for the adduct. Isolation of the DNA-platinum-protein complexes followed by trypsin digestion and mass spectrometric analysis allowed the proteins to be identified. Unlike

southwestern blotting and other techniques, the present approach exposes the platinated DNA to multiprotein complexes. The method requires proteins to compete for binding to the probe, thus providing a more realistic assessment of the cellular milieu. Although cisplatin itself can cross-link proteins, in order to form such a covalent bond a protein would have to be in very close proximity to the adduct.<sup>24,33</sup> PtBP6 probes utilize a photo-reactive moiety with a six-carbon atom linker chain, allowing for a larger number of DNA-bound proteins to be captured. Our probes also can carry site-specific platinum adducts such that proteins having an affinity for a specific cross-link can be analyzed.

#### *Optimization of photo-cross-linking experiments*

The parameters for photo-cross-linking were optimized. UV-irradiation time-dependent experiments (Figures 2.10) revealed that the samples should be irradiated for 2 h prior to resolving them by SDS-PAGE. Incubation time-dependent experiments (Figure 2.12) indicated that a pre-irradiation incubation is unnecessary, and samples can be irradiated immediately after the DNA and proteins are combined. Temperature-dependent experiments (Figure 2.13) emphasized the need to keep the samples on ice throughout processing, otherwise the proteins will degrade significantly.

Preparative-scale experiments were optimized to ensure the removal of non-covalently bound proteins from the streptavidin-coated magnetic beads. This was achieved by washing the beads with high salt (Figure 2.14) and SDS-containing buffers prior to resolution by SDS-PAGE. Control experiments using unplatinated DNA are able to identify many proteins (Table 2.2). These proteins are present because of binding to the streptavidin-coated magnetic beads that is not compromised using our washing methods, or as background signal from the LTQ mass spectrometry instrument. This could be due to a phenomenon known as carryover, described

below. The protein-to-DNA ratio was kept constant between the analytical and preparative-scale experiments to ensure the same protein-platinum-DNA complexes that can be visualized in analytical-scale experiments (Figures 2.14) were formed in both types of experiment.

#### *Protein carryover*

Many of the proteins identified in the photo-cross-linking experiments conducted in this study (Table 2.1) appear in more than one band. This phenomenon occurs for a number of reasons. During photo-cross-linking and subsequent work-up steps, the samples were kept at low temperatures whenever possible. Despite these efforts, some protein degradation is inevitable. Degraded proteins travel down the gel more rapidly and the fragments appear in faster eluting bands. The nature of trypsin-digest coupled mass spectrometric analysis does not distinguish between full-length proteins and protein fragments. For example, a small amount of DNA-PK<sub>cs</sub>, a protein that is clearly identified in the slowest eluting band (Figure 2.15, Band 6), also occurs to a lesser degree in the three bands just below. Another common problem with trypsin-digest coupled mass spectrometry is a phenomenon known as carry-over. The instrumentation is extremely sensitive, able to detect attamole quantities of peptides, and very small amounts of protein from one run can be carried over into the next.

Even with 2 mg of nuclear extracts used for photo-cross-linking, only the band containing DNA-PK<sub>cs</sub> is distinctly visible by Coomassie staining. Since the analytical-scale photo-cross-linking must be used as a guide to excise bands that run extremely close together on the gel, some overlap of excised bands is inevitable. The methodology was able to isolate and identify a band containing DNA-PK<sub>cs</sub> and one containing HMGB1, HMGB2, and HMGB3. The other bands were labeled based on molecular weight and experiments carried out on Chapter 3.

#### *Detection limits of photo-cross-linking*

The instrument used to detect proteins is a Thermo Electron Model LTQ Ion Trap mass spectrometer connected to an Agilent Model 1100 Nanoflow HPLC system. This type of instrument should be able to detect peptides at an attamole range. One attamole is  $6.022 \times 10^5$  molecules. Each reaction in these experiments contains 2 mg of nuclear extracts. This amount of extracts are prepared from approximately  $6 \times 10^7$  HeLa cells. Even if a protein is expressed at one copy per cell, there would be 100 times the detection limit present in the reaction. The binding of proteins to DNA is an equilibrium, however, the equilibrium is disturbed by photo-cross-linking, since a covalently bound protein will no longer be able to dissociate from the probe. Any protein bound to the DNA, no matter what the abundance, will be permanently photo-cross-linked. Even a protein with very low abundance should be above the detection limit of the instrument. These calculations indicate that this method is able to detect the complete panoply of proteins that bind to platinum-modified DNA.

#### *Consideration of the end effect*

One concern of this present study is that proteins that recognize the ends of the 25-bp duplex may be photo-cross-linked together with those that bind specifically to the platinum lesion. The DNA-PK heterotrimer, for example, is involved in the repair of DNA double strand breaks through the nonhomologous end-joining pathway.<sup>34</sup> Although the Ku proteins, which comprise two thirds of the DNA-PK heterotrimer, have previously been associated with cisplatin adducts,<sup>17</sup> Ku-binding to DNA ends would probably extend far enough down the duplex to reach the platination site.<sup>35</sup> Another photo-cross-linked protein that may be involved in double-strand break repair is PARP-1. Evidence that this protein is bound to the platinum adduct and not the DNA ends is discussed in Chapters 3 and 4.

#### *PtBP6 versus cisplatin adducts*

All of the proteins cross-linked, with the exceptions of PARP-1, DNA ligase III, and HMGB3, have been previously associated with cisplatin-damaged DNA. This finding is consistent with the notion that *cis*-{Pt(NH<sub>3</sub>)(*N*-(6-aminohexyl)-4-benzophenonamide)}<sup>2+</sup>-DNA cross-links are being processed in a manner identical to that of the *cis*-[Pt(NH<sub>3</sub>)<sub>2</sub>]<sup>2+</sup>-DNA adducts. HMGB3 contains two tandem HMG domains,<sup>36</sup> similar to HMGB1 and HMGB2, and its affinity for platinum-modified DNA was not unexpected. The fact that the ammine/alkyl amine platinum complex PtBP6 behaves like cisplatin is relevant to the mechanism of the orally available platinum(IV) compound *cis,trans,cis*-[Pt(NH<sub>3</sub>)(cyclohexylamine)(acetato)<sub>2</sub>Cl<sub>2</sub>], satraplatin, which is undergoing clinical trials for hormone resistant prostate cancer. Satraplatin is reduced to platinum(II) in blood, and in cells the *cis*-{Pt(NH<sub>3</sub>)(cyclohexylamine)}<sup>2+</sup> cation is expected to be the DNA-binding moiety.<sup>32,37</sup> DNA adducts made by satraplatin are apparently not recognized by mismatch repair proteins.<sup>38</sup> Our present results suggest that its adducts, containing a pendent cyclohexylamine similar to the BP6 ligand, may be processed by the cell in a manner comparable to that of cisplatin.

#### *DNA repair proteins*

Proteins involved in DNA repair processes were identified by these photo-cross-linking experiments. Included are the nonhomologous end-joining heterotrimer DNA-PK, mismatch repair protein Msh2, PARP-1, and DNA Ligase III, which have been implicated in base excision repair and nonhomologous end-joining. The DNA-PK heterotrimer and Msh2 have been previously reported to bind to cisplatin-modified DNA and the significance of this affinity has been discussed in the literature and in Chapter 1.<sup>17,39,40</sup> The affinity of PARP-1 for platinum-modified DNA was not established prior to these experiments,<sup>27</sup> and the importance of this

interaction will be discussed further in Chapter 5. DNA Ligase III was most likely photo-cross-linked in these experiments due to a close association with PARP-1.<sup>41</sup>

#### *HMG-domain proteins*

HMG-domain proteins HMGB1, HMGB2, HMGB3, and UBF1 were also identified using this methodology. The interaction of UBF1 with platinated DNA has been reported<sup>11</sup> and is discussed in Chapter 1. Detailed studies of the binding of HMGB1 to cisplatin-modified DNA are available in the literature<sup>42</sup> and are discussed in greater detail in Chapter 1. HMGB3, originally named HMG4, contains two HMG domains and an acidic C-terminal tail shorter than those of HMGB1 and HMGB2.<sup>36</sup> The platinated DNA-binding properties of HMGB3 have not been investigated previously. Due to its homology with HMGB1 and 2, the affinity of HMGB3 for platinum-damaged DNA is not surprising. HMGB3 is expressed at high levels during embryonic development, and adult tissues often have little or no expressed protein.<sup>36</sup> HMGB3 is differentially expressed, though not to a significant degree, in platinum-resistant versus sensitive ovarian tumors.<sup>43</sup> Based on these data and the results of the photo-cross-linking experiment, HMGB3 most likely plays a very small role, if any, in cisplatin cytotoxicity since its structure and activity is nearly identical to the more abundant HMGB1 and HMGB2 proteins.

## V. CONCLUSIONS

Methodology for the photo-cross-linking and identification of proteins with an affinity for platinum-modified DNA has been established. These studies were able to identify several nuclear proteins. The binding of the nuclear protein PARP-1 to platinum-modified DNA had not been previously established and has led to more detailed research into the mechanism of this protein as a mediator of cisplatin cytotoxicity, detailed in Chapter 5. This research also provides



a basis for using this photo-active cisplatin analogue to study other types of platinum-DNA adducts, detailed in Chapter 3.

## VI. REFERENCES

1. Horwich, A.; Shipley, J.; Huddart, R., *Lancet* **2006**, 367, 754-765.
2. Jamieson, E. R.; Lippard, S. J., *Chem. Rev.* **1999**, 99, 2467-2498.
3. Cohen, G. L.; Ledner, J. A.; Bauer, W. R.; Ushay, H. M.; Caravana, C.; Lippard, S. J., *J. Am. Chem. Soc.* **1980**, 102, 2487-2488.
4. Fichtinger-Schepman, A. M. J.; van der Veer, J. L.; den Hartog, J. H. J.; Lohman, P. H. M.; Reedijk, J., *Biochemistry* **1985**, 24, 707-713.
5. Rice, J. A.; Crothers, D. M.; Pinto, A. L.; Lippard, S. J., *Proc. Natl. Acad. Sci. U.S.A.* **1988**, 85, 4158-4161.
6. Jung, Y.; Lippard, S. J., *Chem. Rev.* **2007**, 107, 1387-1407.
7. Zlatanova, J.; Yaneva, J.; Leuba, S. H., *FASEB J.* **1998**, 12, 791-799.
8. Pil, P. M.; Lippard, S. J., *Science* **1992**, 256, 234-237.
9. Hughes, E. N.; Engelsberg, B. N.; Billings, P. C., *J. Biol. Chem.* **1992**, 267, 13520-13527.
10. Toney, J. H.; Donahue, B. A.; Kellett, P. J.; Bruhn, S. L.; Essigmann, J. M.; Lippard, S. J., *Proc. Natl. Acad. Sci. U.S.A.* **1989**, 86, 8328-8332.
11. Treiber, D. K.; Zhai, X.; Jantzen, H.-M.; Essigmann, J. M., *Proc. Natl. Acad. Sci. U.S.A.* **1994**, 91, 5672-5676.
12. Chu, G., *J. Biol. Chem.* **1994**, 269, 787-790.
13. Saldivar, J. S.; Wu, X.; Follen, M.; Gershenson, D., *Gynecol. Oncol.* **2007**, 107, S56-S71.
14. Zdraveski, Z. Z.; Mello, J. A.; Marinus, M. G.; Essigmann, J. M., *Chem. Biol.* **2000**, 7, 39-50.
15. Chan, N.; Koritzinsky, M.; Zhao, H.; Bindra, R.; Glazer, P. M.; Powell, S.; Belmaaza, A.; Wouters, B.; Bristow, R. G., *Cancer Res.* **2008**, 68, 605-614.
16. Lin, X.; Kim, H.-K.; Howell, S. B., *J. Inorg. Biochem.* **1999**, 77, 89-93.
17. Turchi, J. J.; Henkels, K., *J. Biol. Chem.* **1996**, 271, 13861-13867.
18. Jackson, S. P.; Jeggo, P. A., *Trends Biochem. Sci.* **1995**, 20, 412-415.
19. Chaney, S. G.; Sancar, A., *J. Natl. Cancer Inst.* **1996**, 88, 1346-1360.
20. Chu, G.; Chang, E., *Science* **1988**, 242, 564-567.
21. Bruhn, S. L.; Pil, P. M.; Essigmann, J. M.; Housman, D. E.; Lippard, S. J., *Proc. Natl. Acad. Sci. U.S.A.* **1992**, 89, 2307-2311.
22. Chao, C. C.-K., *Mutat. Res.* **1991**, 264, 59-66.
23. Turchi, J. J.; Henkels, K. M.; Hermanson, I. L.; Patrick, S. M., *J. Inorg. Biochem.* **1999**, 77, 83-87.
24. Kane, S. A.; Lippard, S. J., *Biochemistry* **1996**, 35, 2180-2188.
25. Mikata, Y.; He, Q.; Lippard, S. J., *Biochemistry* **2001**, 40, 7533-7541.
26. Buterin, T.; Meyer, C.; Giese, B.; Naegeli, H., *Chem. Biol.* **2005**, 12, 913-922.
27. Zhang, C. X.; Chang, P. V.; Lippard, S. J., *J. Am. Chem. Soc.* **2004**, 126, 6536-6537.
28. Dormán, G.; Prestwich, G. D., *Biochemistry* **1994**, 33, 5661-5673.
29. Thiele, C.; Fahrenholz, F., *Biochemistry* **1993**, 32, 2741-2746.
30. MacCoss, M. J.; Wu, C. C.; Yates, J. R. I., *Anal. Chem.* **2002**, 74, 5593-5599.
31. Carr, S.; Aebersold, R.; Baldwin, M.; Burlingame, A.; Clauser, K.; Nesvizhskii, A., *Mol. Cell. Proteomics* **2004**, 3, 531-533.
32. Hartwig, J. F.; Lippard, S. J., *J. Am. Chem. Soc.* **1992**, 114, 5646-5654.

33. Ciccarelli, R. B.; Solomon, M. J.; Varshavsky, A.; Lippard, S. J., *Biochemistry* **1985**, 24, 7533-7540.
34. Collis, S. J.; DeWeese, T. L.; Jeggo, P. A.; Parker, A. R., *Oncogene* **2005**, 24, 949-961.
35. Walker, J. R.; Corpina, R. A.; Goldberg, J., *Nature* **2001**, 412, 607-614.
36. Vaccari, T.; Beltrame, M.; Ferrari, S.; Bianchi, M. E., *Genomics* **1998**, 49, 247-252.
37. Carr, J. L.; Tingle, M. D.; McKeage, M. J., *Cancer Chemother. Pharmacol.* **2002**, 50, 9-15.
38. Fink, D.; Nebel, S.; Aebi, S.; Zheng, H.; Cenni, B.; Nehmé, A.; Christen, R. D.; Howell, S. B., *Cancer Res.* **1996**, 56, 4881-4886.
39. Mello, J. A.; Acharya, S.; Fishel, R.; Essigmann, J. M., *Chem. Biol.* **1996**, 3, 579-589.
40. Duckett, D. R.; Drummond, J. T.; Murchie, A. I. H.; Reardon, J. T.; Sancar, A.; Lilley, D. M. J.; Modrich, P., *Proc. Natl. Acad. Sci. U.S.A.* **1996**, 93, 6443-6447.
41. Bouchard, V. J.; Rouleau, M.; Poirier, G. G., *Exp. Hematol.* **2003**, 31, 446-454.
42. Dunham, S. U.; Lippard, S. J., *Biochemistry* **1997**, 36, 11428-11436.
43. Helleman, J.; Jansen, M. P. H. M.; Span, P. N.; van Staveren, I. L.; Massuger, L. F. A. G.; Meijer-van Gelder, M. E.; Sweep, F. C. G. J.; Ewing, P. C.; van der Burg, M. E. L.; Stoter, G.; Nooter, K.; Berns, E. M. J. J., *Int. J. Cancer* **2006**, 118, 1963-1971.
44. Huang, J.-C.; Zamble, D. B.; Reardon, J. T.; Lippard, S. J.; Sancar, A., *Proc. Natl. Acad. Sci. U.S.A.* **1994**, 91, 10394-10398.
45. Robert, J., 2007, *Personal Communication*.
46. Robert, J.; Laurand, A.; Meynard, D.; Le Morvan, V. In Platinum drugs and DNA repair. Lessons from the NCI-60 panel and clinical correlates, 10th International Symposium on Platinum Coordination Compounds in Cancer Chemotherapy, Verona, Italy; 2007.
47. Thomas, J. O.; Travers, A. A., *Trends Biochem. Sci.* **2001**, 26, 167-174.
48. Schofield, M. J.; Hsieh, P., *Annu. Rev. Microbiol.* **2003**, 57, 579-608.

## VII. TABLES

Table 2.1: Proteins identified by preparative scale photo-cross-linking of a 25-bp duplex containing a 1,2-d(GpG) intrastrand PtBP6 adduct.

Band <sup>a</sup>	Protein <sup>b</sup>	Probability <sup>c</sup>	MW (Da)	Unique Peptides <sup>d</sup>	Protein Function
1	HMGB1	3.50E-10	24977.3	5	HMGB1 shields cisplatin-DNA adducts from excision repair <sup>44</sup>
	HMGB2	3.12E-07	24018.7	5	Analysis of the NCI library of cancer cell lines reveals a correlation between cells expressing high levels of HMGB1 and cisplatin sensitivity <sup>45,46</sup>
	HMGB3	4.14E-08	22849	3	HMGB1, HMGB2 and HMGB3 are chromatin architectural proteins <sup>47</sup>
2	Ku70	4.47E-11	69829.2	17	Ku70 and Ku80 are members of the DNA-PK complex involved in nonhomologous end-joining repair of double-strand breaks <sup>34</sup>
	Ku80	2.50E-09	82652.4	5	
	PARP-1	7.01E-11	113012.4	4	See Chapter 5 for more information.
3	Ku80	4.44E-15	82652.4	37	
	Ku70	1.11E-15	69829.2	22	
	PARP-1	1.35E-10	113012.4	9	
4	Ku80	2.22E-15	82652.4	30	
	Ku70	1.26E-12	69829.2	27	
	UBF1	7.96E-07	89350	3	HMG-domain protein responsible for initiation of RNA polymerase I <sup>11</sup>
	PARP-1	9.88E-10	113012.4	14	
	DNA-PKcs	4.01E-11	468786.9	13	
	DNA ligase III	3.91E-08	112834.9	6	See text
	Msh2	8.53E-06	104676.8	4	Protein involved in the recognition of base pair mismatches <sup>48</sup>
5	PARP-1	2.63E-13	113012.4	42	
	DNA-PKcs	4.26E-11	468786.9	29	Member of the DNA-PK complex involved in nonhomologous end-joining repair of double-strand breaks <sup>34</sup>

	DNA ligase III	8.10E-14	112834.9	11
	Msh2	7.57E-12	104676.8	5
6	DNA-PKcs	8.73E-15	468786.9	146

---

<sup>a</sup>The LC-MS/MS analysis was carried out on six gel slices corresponding to the bands from the analytical-scale experiment (Figure 2.15). The proteins found in each band are listed here. <sup>b</sup>Proteins identified as described in the Materials and Methods section. <sup>c</sup>Probability of the peptide identification being an artifact of background signal from the LC-MS/MS instrument. For example, a probability of 1.0E-4 indicates that there is a 0.01% chance that the identified peptide is not actually present in the sample. The values listed correspond to the peptide most likely to be present for each protein. <sup>d</sup>The number of peptides identified for each protein. Peptides differing by only one amino acid were not considered to be unique.

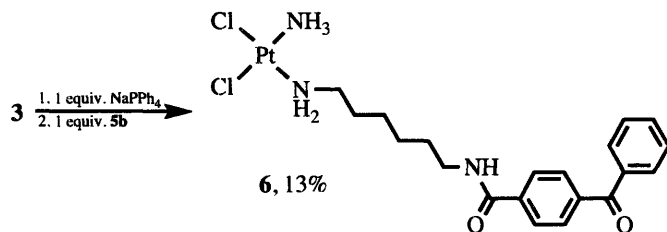
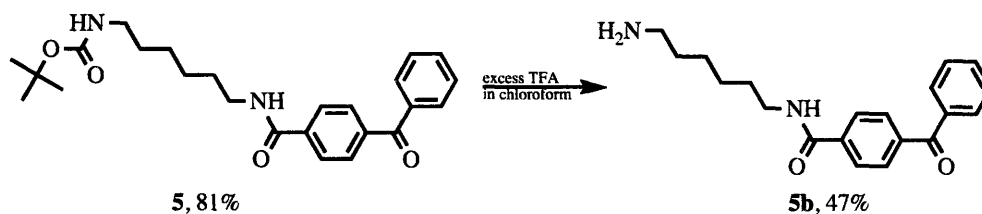
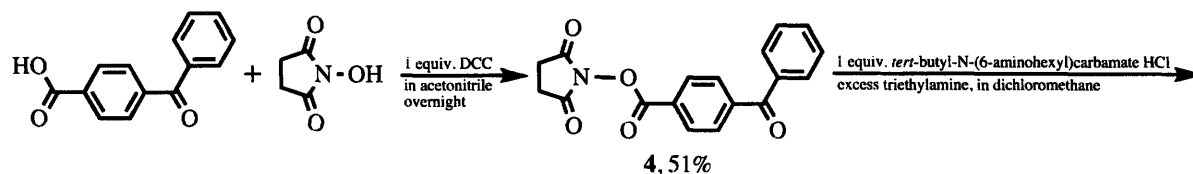
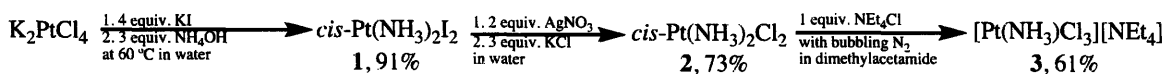
Table 2.2: Proteins identified by preparative-scale photo-cross-linking of an unplatinated 25-bp duplex.

Band <sup>a</sup>	Protein <sup>a</sup>	Probability <sup>a</sup>	MW (Da)	Unique Peptides <sup>a</sup>
1	60 kDa heat shock protein, mitochondrial precursor	8.65E-13	61016.5	6
	Transmembrane emp24 domain-containing protein 9 precursor	8.10E-12	25088.9	1
	L-lactate dehydrogenase A chain	7.38E-10	36665.4	3
	Tubulin alpha-1A chain	9.29E-09	50103.7	5
	Heterogeneous nuclear ribonucleoprotein K	1.01E-08	47527.7	2
	Hornerin	1.17E-08	282225.7	2
	Creatine kinase, ubiquitous mitochondrial precursor	1.91E-08	47007.3	1
	Alpha-enolase	2.29E-08	47139.4	1
	Pyruvate kinase isozymes M1/M2	2.50E-08	57900.2	1
	Nucleolin	3.40E-08	76568.5	4
	Protein disulfide-isomerase A3 precursor	5.04E-08	56746.8	1
	Heterogeneous nuclear ribonucleoprotein A1	7.06E-08	38822.1	2
	Tubulin, beta, 4	7.87E-08	88324.5	3
	14-3-3 protein epsilon	2.19E-07	29155.4	1
	60S ribosomal protein L10a	3.28E-07	24815.5	1
	Transmembrane emp24 domain-containing protein 7 precursor	7.66E-07	25155.6	1
	TUBB protein	4.23E-06	14407.6	1
	TUBB6 protein	5.17E-05	50058.2	1
	UMP-CMP kinase	7.76E-05	22208.3	1
	Caspase-14 precursor	6.25E-07	27662.0	2
Protein S100-A8	5.99E-06	10827.7	1	
Hypothetical protein DKFZp686P03159	3.52E-04	40327.7	1	
Uncharacterized protein C7orf24	8.25E-04	20994.3	1	
2	60 kDa heat shock protein, mitochondrial precursor	8.29E-13	61016.5	3

	Complement component 1 Q subcomponent-binding protein, mitochondrial precursor	1.22E-12	31342.6	1
	L-lactate dehydrogenase A chain	3.21E-09	36665.4	2
	Trypsin-3 precursor	2.85E-07	32478.0	1
	Heterogeneous nuclear ribonucleoproteins A2/B1	3.61E-07	37406.7	1
	Nucleolin	2.69E-06	76568.5	1
	FASN variant protein	5.96E-06	277192.9	1
	Heterogeneous nuclear ribonucleoprotein A1	1.79E-05	38822.1	1
	Transmembrane emp24 domain-containing protein 9 precursor	3.02E-05	25088.9	1
	Tubulin, beta, 4	4.16E-05	88324.5	1
	Alpha-enolase	5.82E-05	47139.4	1
	Pyruvate carboxylase, mitochondrial precursor	6.06E-07	129551.6	2
	Serum albumin precursor	1.48E-06	69321.6	1
3	Pyruvate carboxylase, mitochondrial precursor	7.98E-09	129551.6	10
	Serum albumin precursor	3.73E-06	69321.6	2
	G-protein signalling modulator 2	2.26E-04	76614.3	1
	UTP--glucose-1-phosphate uridylyltransferase	6.97E-04	56904.8	1
	60 kDa heat shock protein, mitochondrial precursor	1.05E-09	61016.5	1
	Pyruvate carboxylase, mitochondrial precursor	4.92E-09	129551.6	8
	Heterogeneous nuclear ribonucleoprotein K	9.35E-06	47527.7	1
	RRP1-like protein B	6.10E-05	84359.2	1
4	Serum albumin precursor	1.24E-08	69321.6	2
	RRP1-like protein B	1.71E-06	84359.2	4
	Propionyl Coenzyme A carboxylase, alpha polypeptide	1.60E-04	11872.0	1
5	Methylcrotonoyl-CoA carboxylase subunit alpha, mitochondrial precursor	2.26E-07	80422.0	3
	HSPA5 protein	2.39E-07	72377.6	1
6	Serum albumin precursor	2.73E-05	69321.6	1

<sup>a</sup>Headings discussed in Table 2.1.

## VIII. SCHEMES



DCC = 1,3-dicyclohexylcarbodiimide  
TFA = trifluoroacetic acid

Scheme 2.1. Synthesis of *cis*-[Pt(NH<sub>3</sub>)(*N*-(6-aminohexyl)-4-benzophenonamide)Cl<sub>2</sub>], PtBP6 (**6**).

Products are numbered and yields are reported.



IX. FIGURES

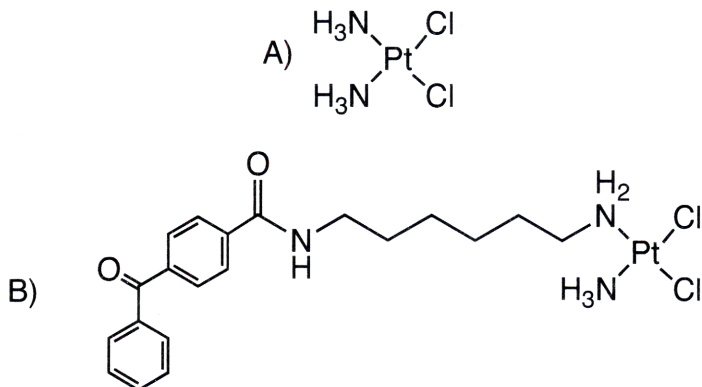


Figure 2.1. Chemical structures of cisplatin and PtBP6.

The structure of *cis*-diamminedichloroplatinum (A), cisplatin and the photoactive analogue *cis*-[Pt(NH<sub>3</sub>)(N-(6-aminohexyl)-4-benzophenonamide)Cl<sub>2</sub>], PtBP6 (B).

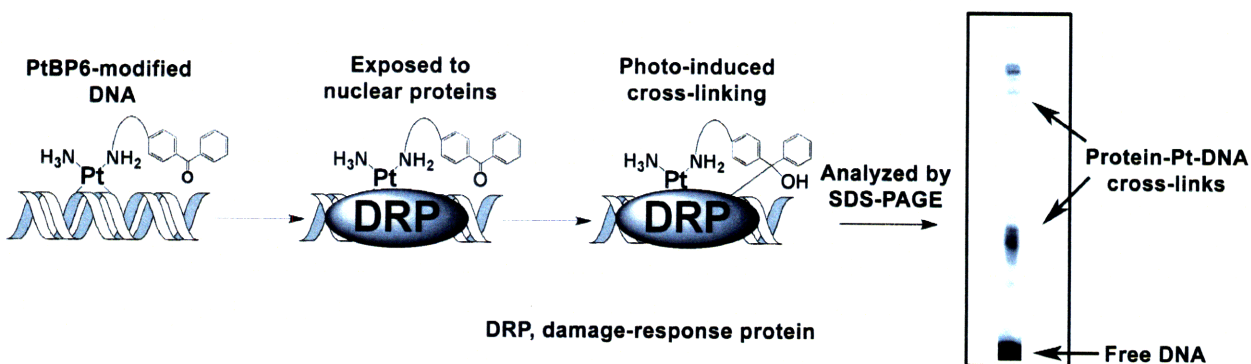


Figure 2.2. Photo-cross-linking with a PtBP6-modified DNA probe.

Radiolabeled duplex DNA that is site-specifically platinated with PtBP6 is incubated with nuclear extracts, allowing nuclear proteins to bind to the damaged DNA. The mixture is then UV irradiated, creating protein-platinum-DNA complexes that can be resolved by SDS-PAGE. DRP = damage response protein.

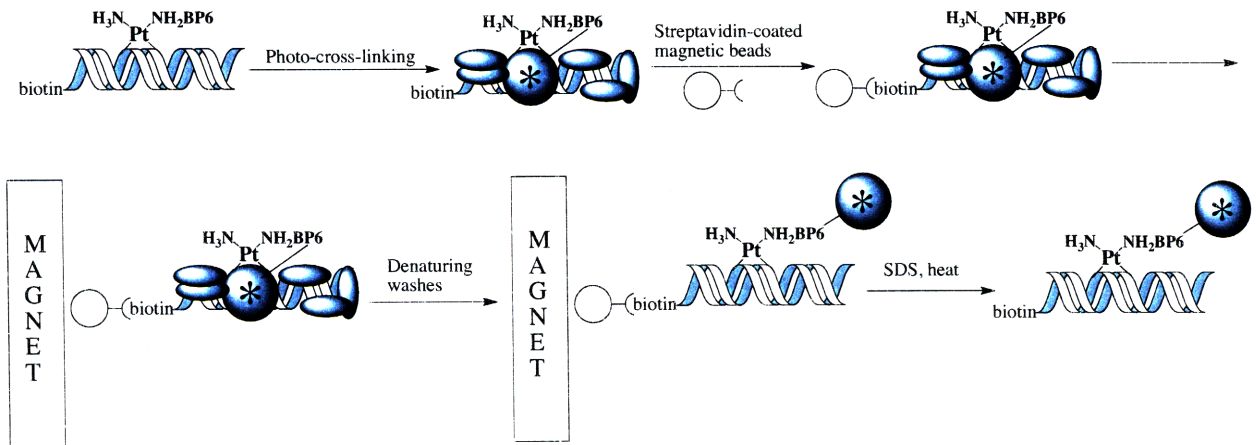


Figure 2.3. Isolation of photo-cross-linked proteins using streptavidin-coated magnetic beads.

After photo-cross-linking, many nuclear proteins will be bound to the DNA that are not the protein of interest (marked with an \*). The protein-DNA complexes are incubated with streptavidin-coated magnetic beads. The strong affinity of biotin for streptavidin holds the protein-DNA complex to the bead. The beads are then held in place using a magnetic test tube stand. The complex is subjected to several denaturing washes to disrupt protein-DNA interactions. The only protein that will remain is the photo-cross-linked protein. The complex is then heated in sodium dodecyl sulfate (SDS) to dissociate the biotin from the streptavidin and the purified DNA-platinum-protein complex can be analyzed by SDS-PAGE.

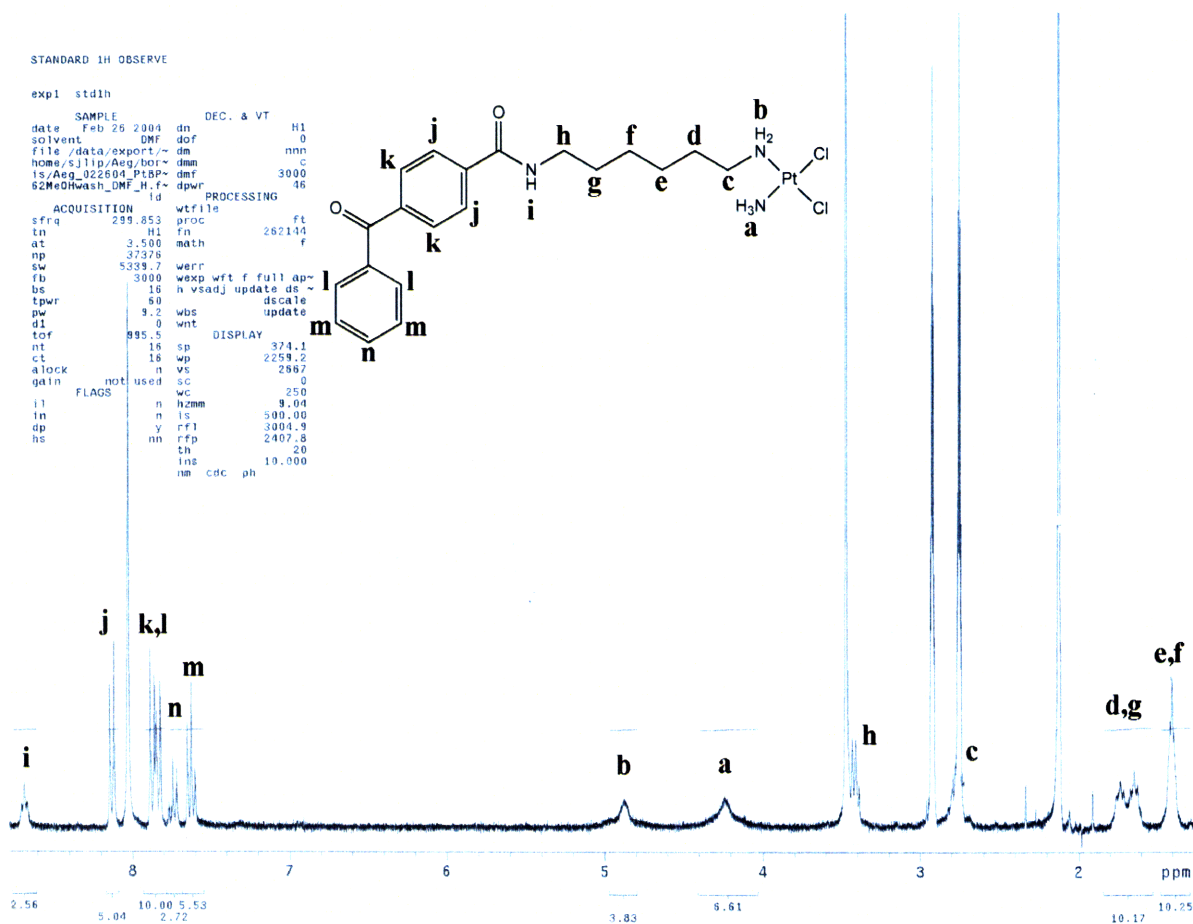


Figure 2.4. <sup>1</sup>H NMR spectroscopic analysis of *cis*-[Pt(NH<sub>3</sub>)(N-(6-aminohexyl)-4-benzophenamide)Cl<sub>2</sub>] (PtBP6) in DMF.

The compound *cis*-[Pt(NH<sub>3</sub>)(N-(6-aminohexyl)-4-benzophenamide)Cl<sub>2</sub>] was synthesized as indicated in Scheme 2.1 in 13% yield.

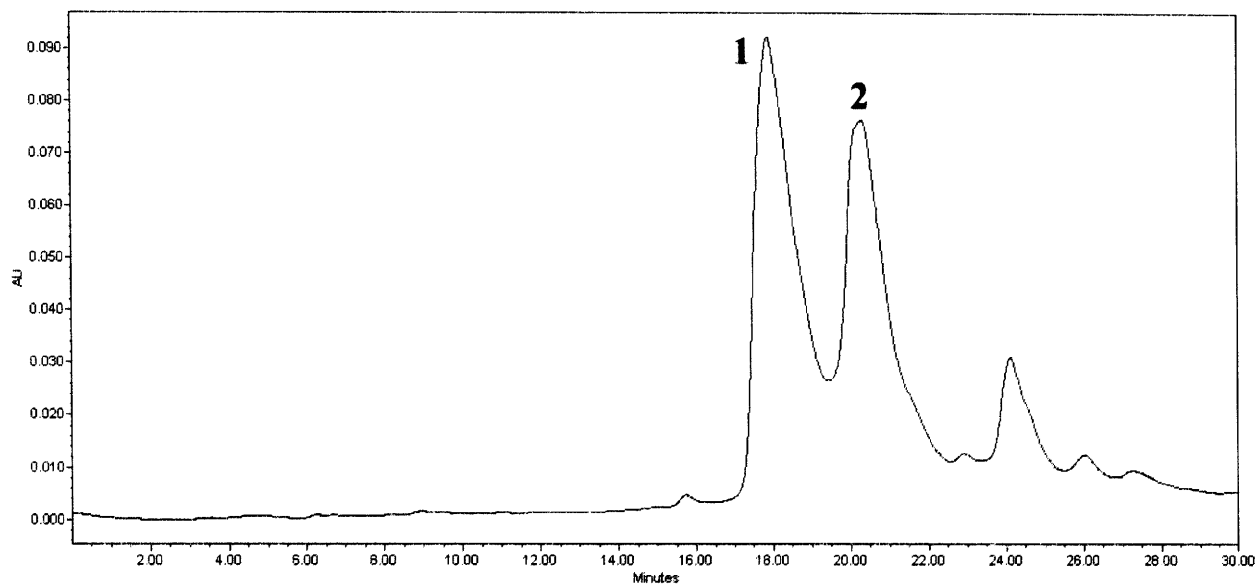


Figure 2.5. RP-HPLC purification of platinated 25 base DNA.

This method was able to separate unplatinated DNA (1) from PtBP6-modified DNA (2).

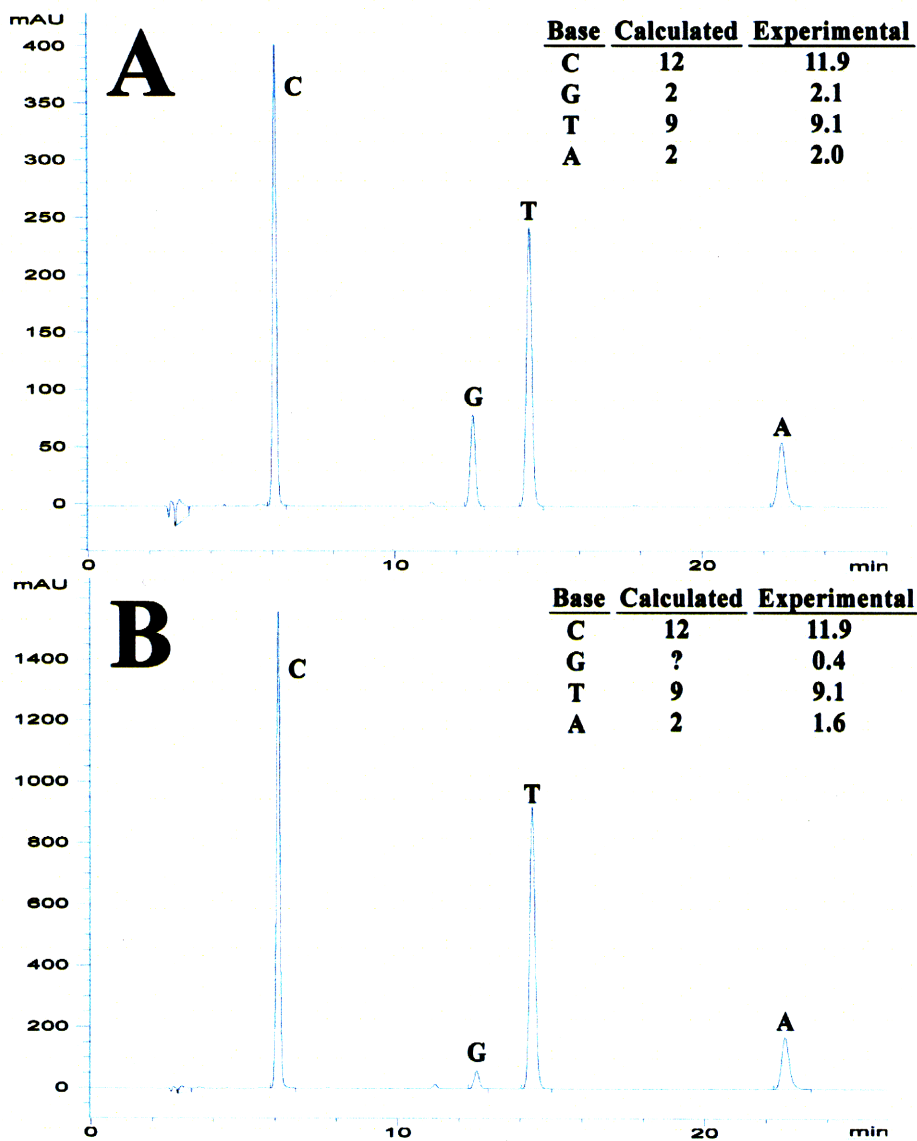


Figure 2.6. Nuclease digestion of 25 base DNA.

Unplatinated 25 base DNA (A) and 25 base DNA containing a 1,2-d(GpG) adduct of PtBP6 (B). The signal for the guanosine peak is decreased due to platination of the base.

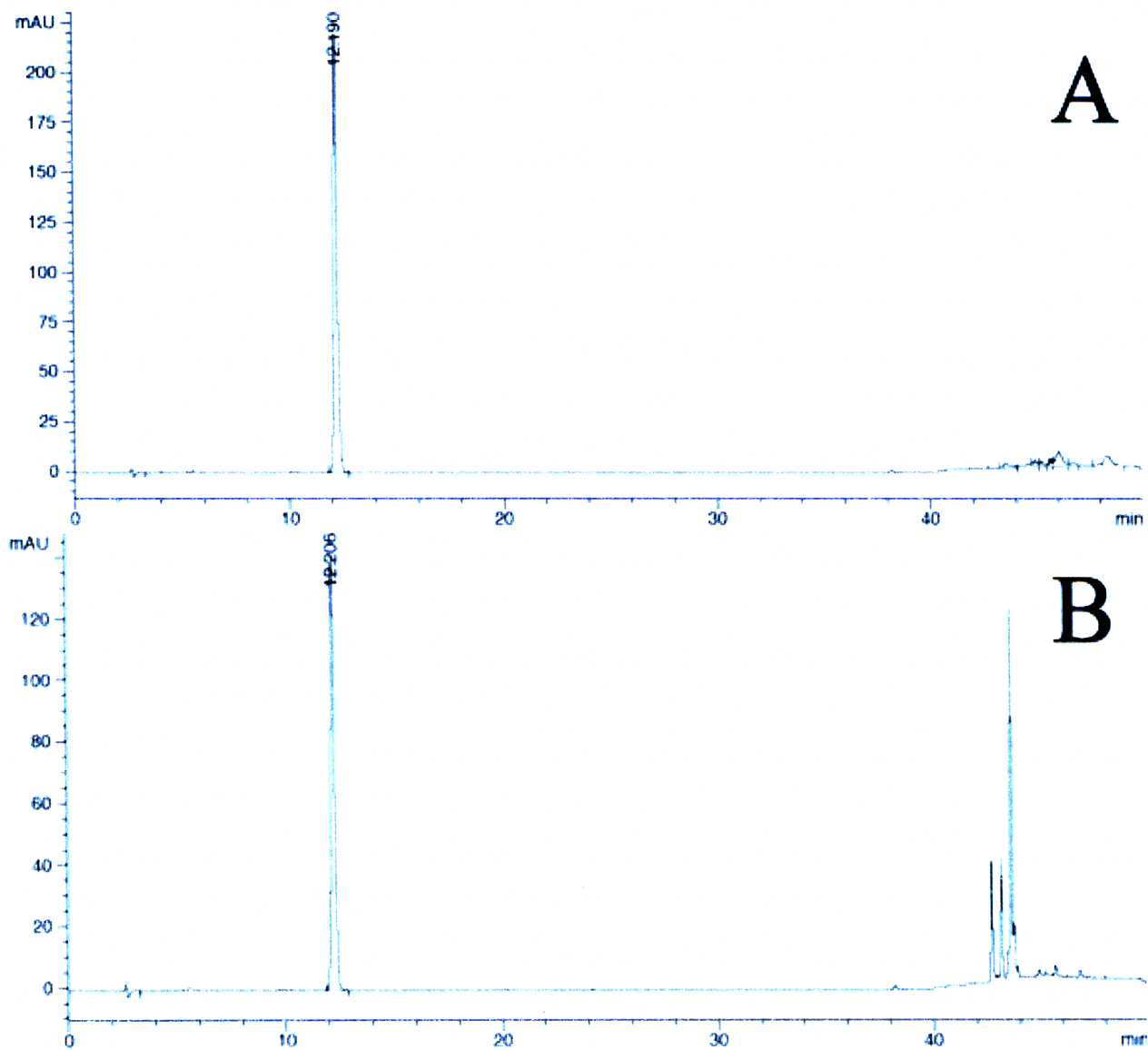


Figure 2.7. Analysis of the reaction between activated PtBP6 and deoxyguanosine.

Deoxyguanosine (A) and the reaction between deoxyguanosine and activated PtBP6 (B) were analyzed by RP-HPLC under the same conditions as the analysis of a nuclease digestion. The deoxyguanosine elutes at 12.2 min, and the reaction products elute at about 43 min.

Info for pane 1: E4233-2 (Peak 2: ~5.4pmol/μl in 50% ACN, 2% TEA infused @ 5μl/min after Amberlite desalting)

Period 1, Expt. 1; Mass range: 500.0 to 1600.0 by 0.1 amu, Dwell: 0.7 ms; Pause: 5.0 ms

Acq. Time: Thu, Aug 12, 2004 at 10:51:16 AM; Exp. Comment: ROUTINE Q1 SCAN

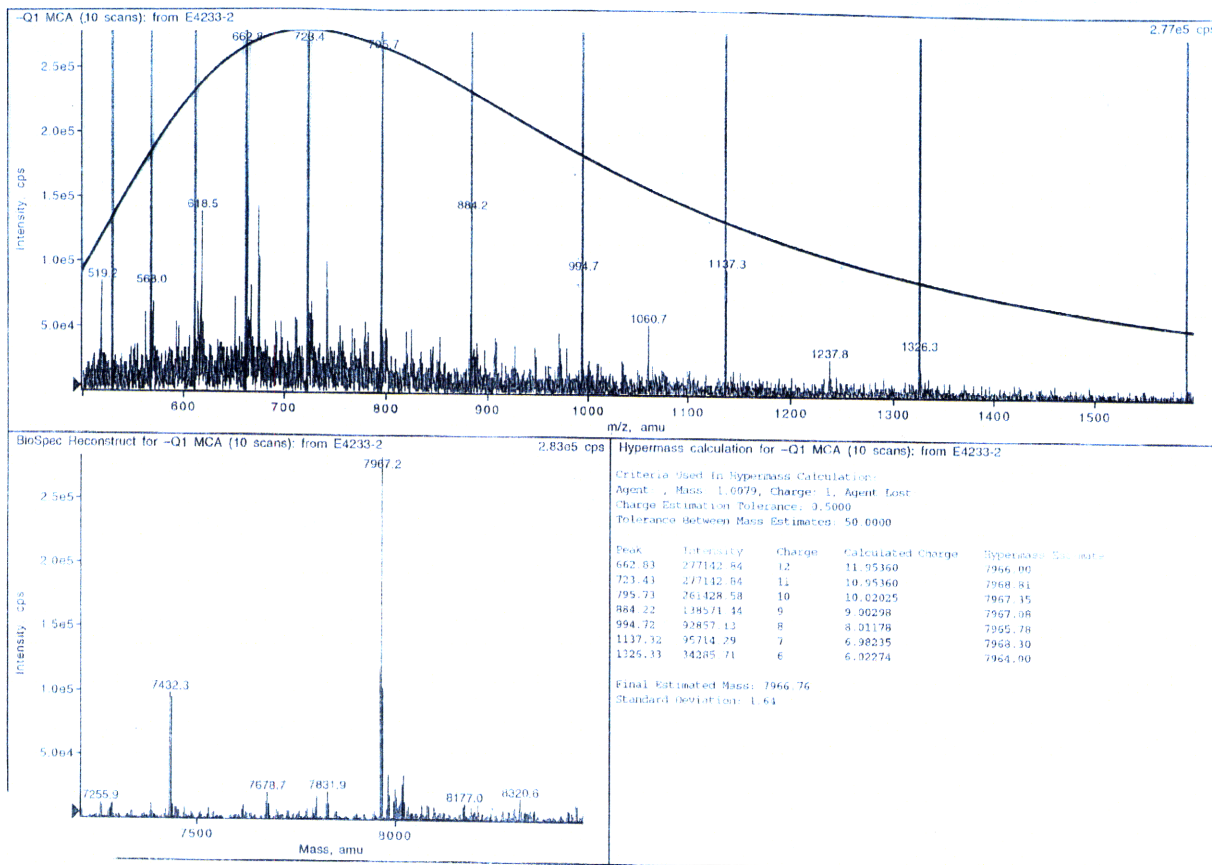


Figure 2.8. ESI-MS analysis of 25-base DNA containing a 1,2-d(GpG) adduct of PtBP6.

The PtBP6-modified DNA has a calculated value of 7967.4 m/z, and an experimental value of  $7967.2 \pm 1.64$  m/z. This spectrum indicates that some unplatinated DNA is present, and the platinated DNA contains PtBP6 bound in a bifunctional manner. A monofunctional adduct would require another ligand to satisfy the coordination environment of the platinum, and the mass of the complex would be increased. The analysis was performed by the staff of the MIT Biopolymers facility.

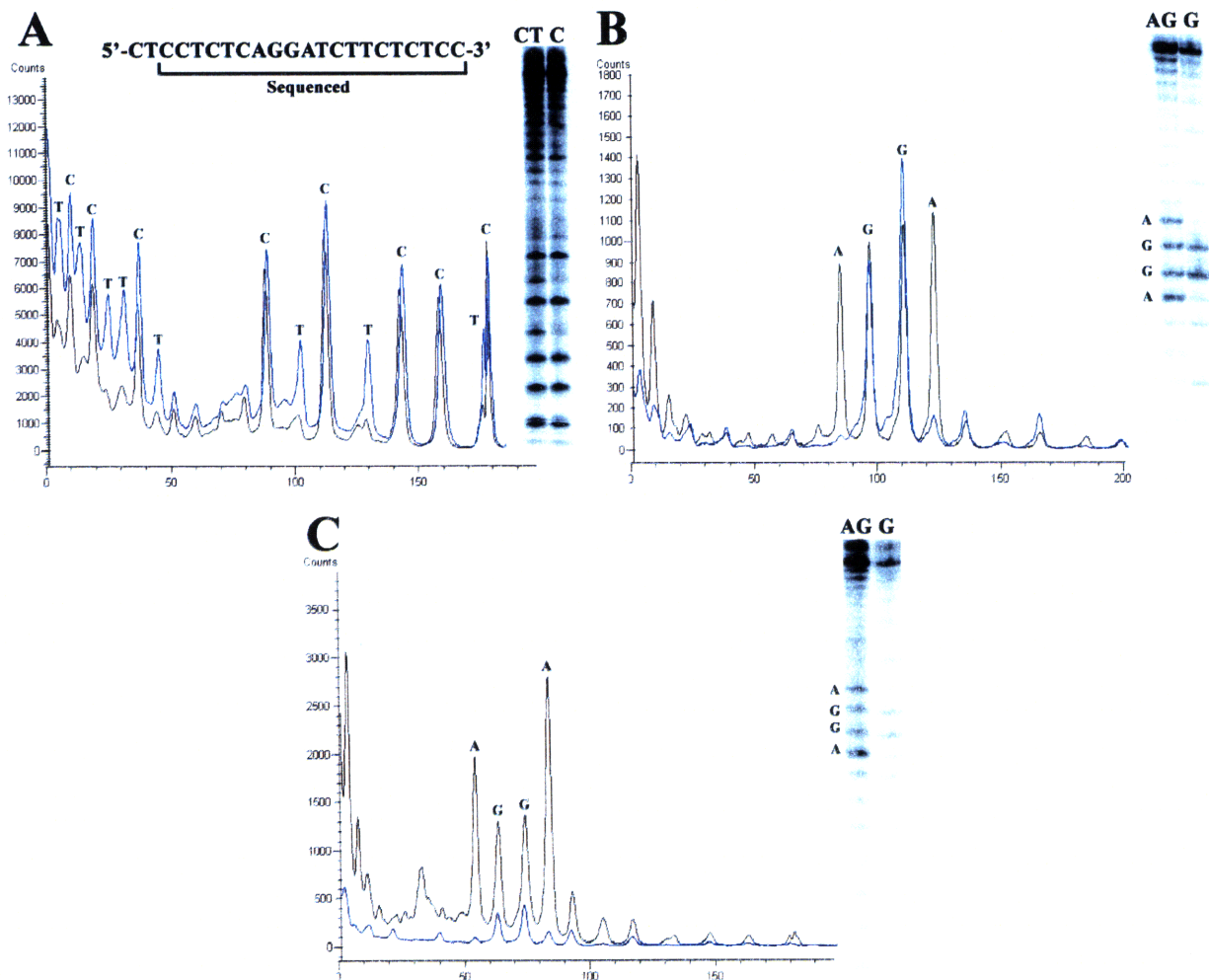


Figure 2.9. Maxam-Gilbert analysis of 25 base probe.

Each gel and a graphical representation of the bands are presented. (A) C+T reaction of unplatinated DNA. All bases except for the two bases on the 5'-end of the DNA were sequenced using this method. (B) A+G reaction of unplatinated DNA. (C) A+G reaction of platinated DNA. The platination reaction significantly decreases the intensity of the bands for the G reaction, and decreases the intensity of the G bands in the A+G reaction as well.



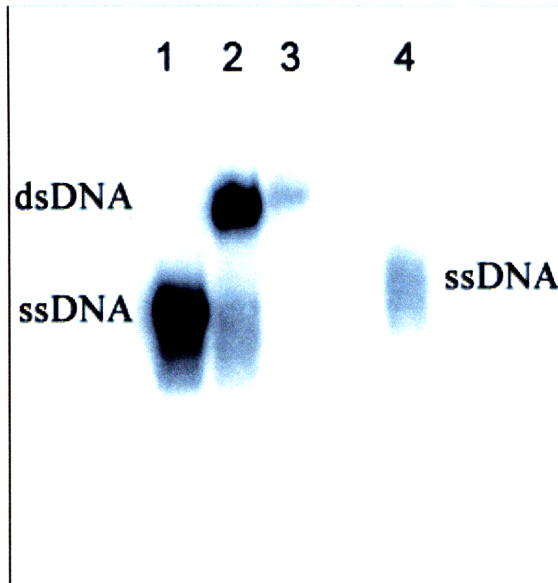


Figure 2.10. Native PAGE analysis of 25-bp duplexes.

Lane 1: 25 base ssDNA. Lane 2: 25-bp duplex. Lane 3: PtBP6-modified 25-bp duplex. Lane 4: PtBP6-modified 25 base ssDNA. The single-stranded (ss) DNA migrates faster down the gel than the duplex (ds) DNA.

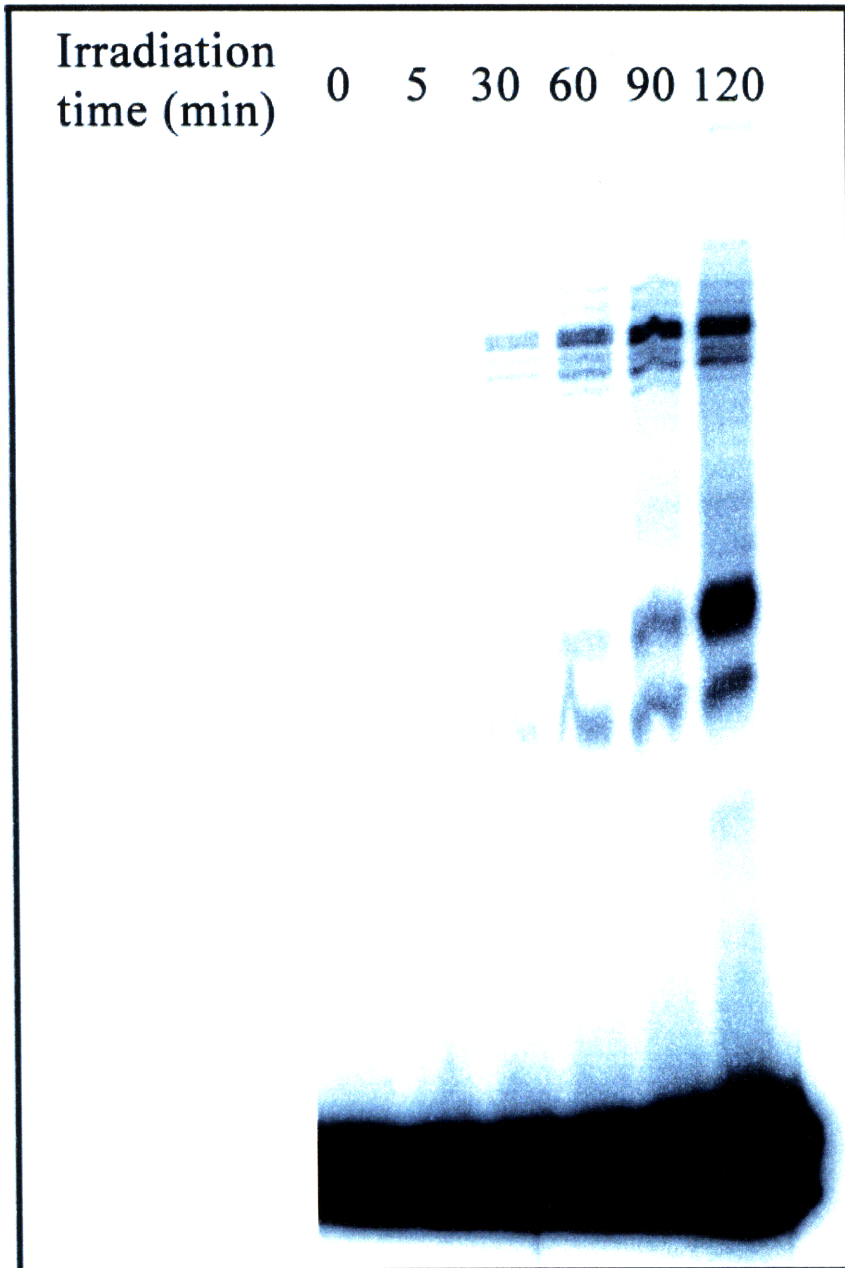


Figure 2.11. Effect of varying the UV irradiation time on photo-cross-linking of PtBP6-modified 25-bp duplex.

The photo-cross-linking is maximized at 2 h.

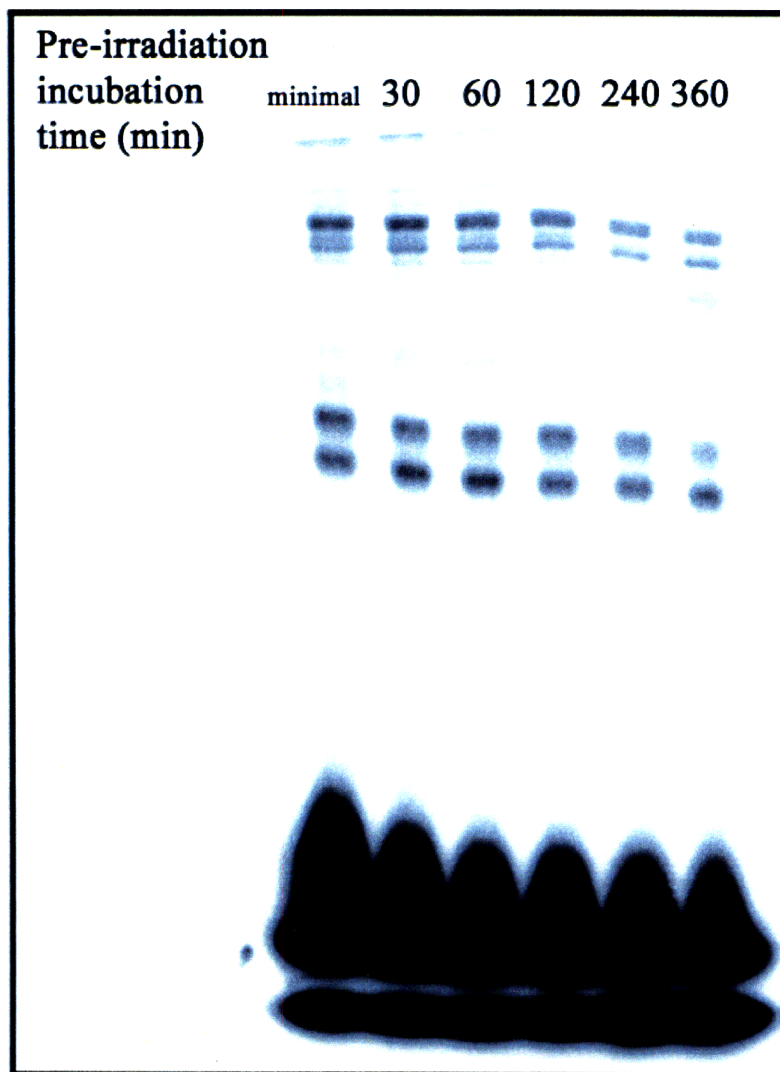


Figure 2.12. Effect of varying the pre-irradiation incubation time on photo-cross-linking of PtBP6-modified 25-bp duplex.

No incubation is necessary for maximum photo-cross-linking, and an incubation of longer than 60 minutes results in less photo-cross-linking, most likely due to degradation of the proteins.

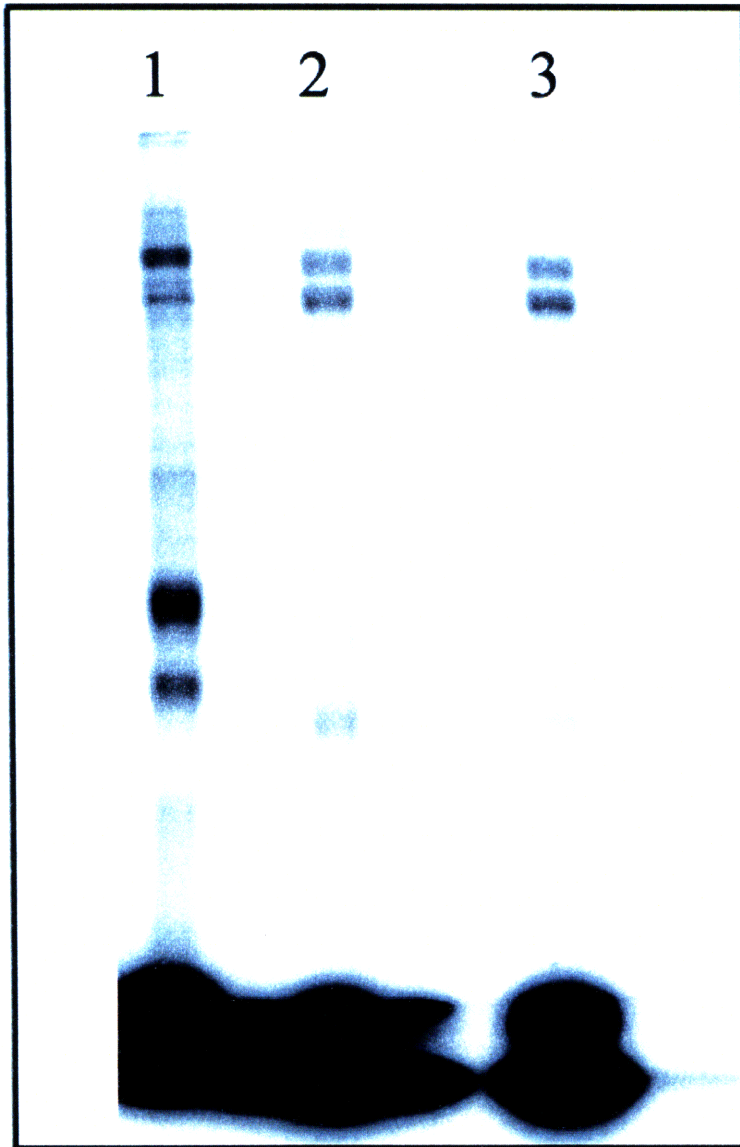


Figure 2.13. Effect of temperature on photo-cross-linking.

Lane 1: Reaction kept on ice. Lane 2: Reaction kept at room temperature. Lane 3: Reaction incubated at 37°C and irradiated at room temperature. Elevated temperatures lead to protein degradation.

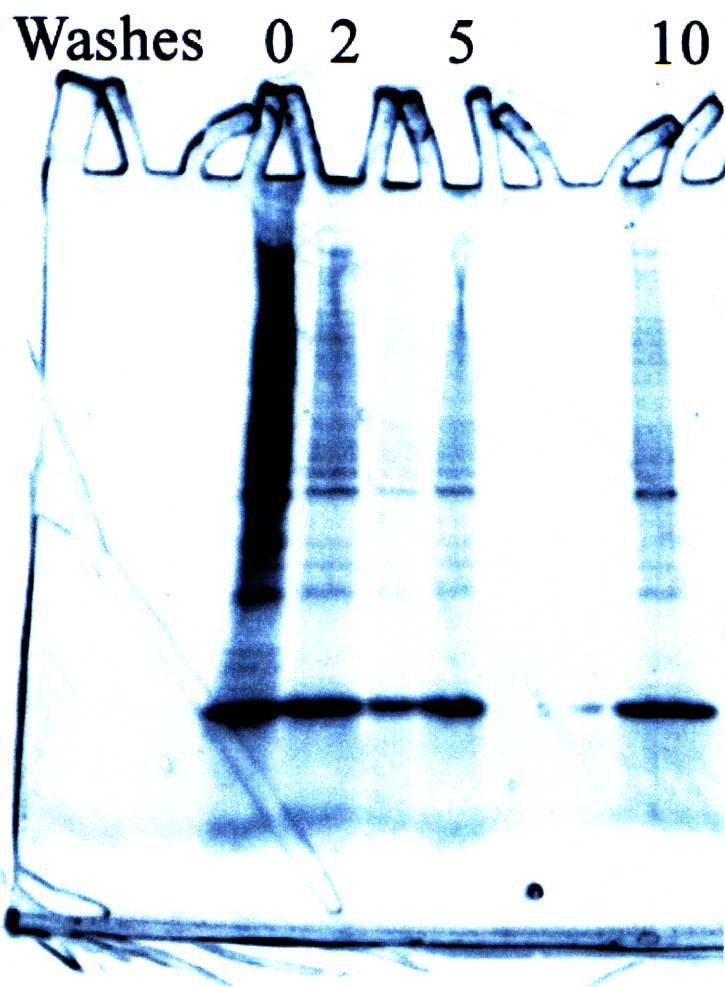


Figure 2.14. Analysis of washing conditions of the streptavidin-coated magnetic beads.

The beads were incubated with nuclear proteins and washed using a high salt containing buffer. The gel was stained using Sypro Ruby protein stain. The well containing the “5 washes” sample leaked into the lane to the left. The beads retain proteins which need to be washed 5 times to sufficiently remove background for the photo-cross-linking experiments.

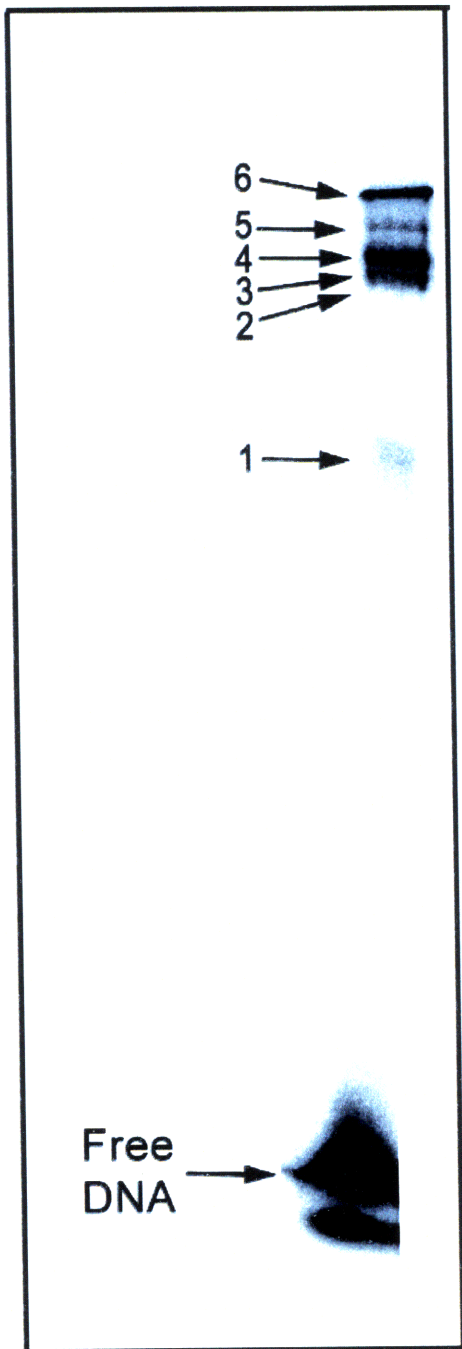


Figure 2.15. Analytical-scale photo-cross-linking of 25-bp duplex containing a 1,2-d(GpG) adduct of PtBP6.

The bands indicated were used as a guide to excise protein-platinum-DNA adducts from the preparative-scale experiments.

**Chapter 3: Photo-cross-linking and identification of nuclear proteins that bind to constructs of a 25-bp probe containing a site-specific adduct of PtBP6.**

\*Work from this chapter was submitted for publication; Guggenheim, E. R., Xu, D., Zhang, C. Z., Chang, P. V., Lippard, S. J., "Photo-Affinity Isolation and Identification of Proteins in Cancer Cell Extracts that Bind to Platinum-Modified DNA."

## I. INTRODUCTION

Results from Chapter 2 indicate that we have developed a powerful tool to analyze proteins that bind to platinum-damaged DNA. The methodology was used to address several other questions regarding platinum-damaged DNA. Beside the 1,2-d(GpG) intrastrand adduct, cisplatin also forms 1,3-d(GpNpG) intrastrand adducts on DNA.<sup>1</sup> Photo-cross-linking experiments were therefore extended to include a DNA duplex probe containing a PtBP6 1,3-d(GpTpG) intrastrand adduct to identify proteins with an affinity for this type of adduct. Bypass of cisplatin adducts by polymerases could result in a compound lesion containing a d(G\*pG\*)/d(CpT) mismatched intrastrand cisplatin adduct, where G\* denotes the platinated guanine.<sup>2</sup> These compound lesions bind more strongly to the mismatch repair (MMR) protein Msh2.<sup>3</sup> A probe containing a mismatched 1,2-d(GpG)/d(CpT) adduct of PtBP6 was synthesized to determine whether this behavior extended to nuclear extracts, where all nuclear proteins can compete for binding to the damaged DNA. We also applied the methodology to investigate nuclear proteins from cancer cells with varying degrees of sensitivity to cisplatin. Photo-cross-linking experiments were carried out using nuclear extracts from testicular, cervical, bone and pancreatic cancer cells. The results provide a comprehensive knowledge of nuclear proteins that contact the major cisplatin adducts in cancer cells.

## II. MATERIALS AND METHODS

All solvents and most chemical reagents were purchased from commercial sources. DNA strands were synthesized on an Applied Biosystems ABI 392 DNA/RNA synthesizer using solvents and reagents supplied by Glen Research. Enzymes were purchased from New England BioLabs and Promega. UV-vis spectra were obtained on an HP 8453 UV-visible spectrometer.



Platinum analyses were performed by flameless atomic absorption spectroscopy on a Perkin-Elmer AAnalyst 300 system. ESI-MS was performed by staff at the MIT Biopolymers instrumentation facility on a Sciex Model API 365 triple stage mass spectrometer. Analytical and preparative HPLC work was performed either on an HP Waters or an Agilent 1200 HPLC system. UV irradiation was conducted in a Stratagene Stratalinker UV Crosslinker. Protein digestion and analyses were performed by trypsin digestion-coupled LC-MS/MS analysis at the MIT Biopolymers facility.

#### *Cell culture*

Cells were grown in Dulbecco's Modified Eagle's Medium (DMEM) with 10% fetal bovine serum (FBS) and 1% penicillin-streptomycin at 37 °C under 5% CO<sub>2</sub>. Once growth reached ~80% confluence, cells were trypsinized and passed or collected. Cells between passages 4 and 18 were collected and used for preparing nuclear extracts. Testicular (NTera2), cervical (HeLa), bone (U2OS), pancreatic (BxPC3), and HeLa cells in which PARP-1 was silenced by RNAi were used for these experiments.

#### *Short hairpin RNA (shRNA)-induced RNAi on PARP-1 in HeLa cells*

The silencing of PARP-1 in HeLa cells was performed by Dong Xu. He designed several DNA sequences that transcribe to shRNAs for silencing PARP-1 in HeLa cells. These DNA constructs were cloned into the plasmid vector pcDNA3.1-Zeo (-) -U6. This plasmid, derived from the Invitrogen pcDNA3.1-Zeo (-), has the human U6 promoter inserted upstream of the cloning site to drive shRNA transcription. The transfected HeLa cells were selected in DMEM with 100 µg/ml Zeocin. After the Zeocin selection, cells were collected by trypsin digestion and their nuclear extracts were prepared as previously reported.<sup>4</sup> The total protein concentrations of the extracts were estimated by bicinchoninic acid solution (BCA) assay. For each sample,

extracts with 20 µg of total protein were analyzed by western blot. With the use of a MoFlo high-performance cell sorter (DakoCytomation), HeLa cells transfected with the plasmid were sorted into wells of two 96-well plates. The instrument set up allows only 0.1 µl of diluted culture with no more than one cell being added to each well. The single clones were incubated at 37 °C for two weeks. During this time, the medium was changed every four d. These cells were collected by trypsin digestion and grown in 6-well plates. The nuclear extracts of surviving clones were analyzed by western blot to evaluate the expression level of PARP-1.

#### *Nuclear extraction*

Nuclear extracts were prepared as described in Chapter 2.

#### *Cytotoxicity assays*

Cells were plated at 500 – 1000 cells/well in a 96-well plate. On day 2, the cells were treated with varying concentrations of cisplatin. On day 6, cellular survival was measured by the MTT assay. Cells were treated with 1 mg/mL of 3-(4,5-dimethylthiazol-2-yl)-2,5-diphenyltetrazolium bromide (MTT) for 4 h. The media was removed from each well and replaced with 100 µL of DMSO. The absorbance of each cell at 562 nm was measured using a plate reader.

#### *Synthesis of a 25-base single stranded DNA containing a 1,3-d(GpTpG) intrastrand*

#### *PtBP6 cross-link*

In a method similar to that used to prepare a DNA strand containing the 1,2-d(GpG) adduct, *cis*-ammine(BP6)dichloroplatinum(II) was activated with AgNO<sub>3</sub>. To a solution of 35 nmol of a 25-base DNA containing one d(GpTpG) site, 5'-CCTCTCCTCTCGTGATCTTCTCTCC-desthiobiotin-TEG-3', in 10 mM NaH<sub>2</sub>PO<sub>4</sub> (pH 6.3) was added 70 nmol of activated PtBP6. The reaction was incubated overnight at 37 °C with

mixing. The singly-platinated 25-base DNA was then isolated by reverse-phase HPLC on an Agilent C18 300-SB column. The method used was 0 – 12% B over 5 min, followed by 12-25% over 25 min, where solvent A contained 95:5 water:acetonitrile, 0.1% trifluoroacetic acid, and solvent B contained 90:10 acetonitrile:water, 0.1% trifluoroacetic acid. The collected fractions were neutralized and lyophilized. The samples were then reconstituted in water and dialyzed to remove salt.

*Characterization of 1,3-d(GpTpG) intrastrand PtBP6-modified 25-base DNA probes*

Each collected peak was characterized by UV-visible absorbance and atomic absorption spectroscopy to establish a 1:1 ratio of platinum per DNA. The collected peaks were characterized by ESI-MS to confirm that both chloride ligands were replaced by Pt–DNA bonds.

Platination of the guanine bases was verified by enzymatic digestion of the DNA. The digests consisted of 20  $\mu$ L 100 mM NaOAc (pH 5.2), 1  $\mu$ L 100 mM ZnCl<sub>2</sub>, 10  $\mu$ L nuclease P1, and 150 pmol DNA. The total reaction volumes were increased to 100  $\mu$ L with ddH<sub>2</sub>O. The solutions were mixed thoroughly and incubated at 37 °C overnight. Next, 5  $\mu$ L of 1.5 M Tris-HCl (pH 8.8) and 1  $\mu$ L of calf intestinal phosphatase (CIP) was added. After a 4-h incubation at 37 °C, the samples were centrifuged at 5000 rpm for 5 min. The supernatants were analyzed by RP-HPLC using a Supelcosil LC-18-S column. The method was 5 – 15% B over 30 min, 15 – 80% B over 10 min, and 80% B for 5 min, where solvent A was 100 mM NaOAc, pH 5.2 and solvent B was methanol.

*Synthesis of duplex DNA*

A single-stranded 25-base DNA of the sequence 5'-GGAGAGAAGATCTTGAGAGG-AGAGG-3' was prepared on a DNA synthesizer using standard phosphoramidite methods. The

DNA was heated to 55 °C for 14 h and then purified by 12% denaturing PAGE. The DNA was located using UV shadowing and then extracted from the gel and dialyzed as described above.

The 25-base DNA containing a 1,2-d(GpG) adduct were prepared and characterized as described in Chapter 1. For analytical-scale experiments, 50 pmol of each DNA was annealed in NEBuffer 3 (New England BioLabs, 50 mM Tris-HCl pH 7.9, 100 mM NaCl, 10 mM MgCl<sub>2</sub>, 1 mM DTT). Three types of DNA were prepared, a 25-base DNA containing a 1,3-d(GpTpG) adduct of PtBP6 and the complementary bottom strand a 25-base DNA containing a 1,2-d(GpG) adduct of PtBP6 and the complementary bottom strand, and a 25-base DNA containing a 1,2-d(GpG) adduct of PtBP6 and the mismatched bottom strand.

In an eppendorf tube, 50 pmol of duplex DNA was combined with 3 μL of 10X PNK Buffer (700 mM Tris-HCl, 100 mM MgCl<sub>2</sub>, 50 mM dithiothreitol, pH 7.6), 3 μL γ-<sup>32</sup>P-ATP (Perkin-Elmer) and 1 μL polynucleotide kinase (New England Biolabs). The solutions were diluted to 30 μL and incubated at 37 °C for 2 h. The solutions were then purified by Sephadex G-25 spin columns (GE Healthcare), ethanol precipitated, and dried by vacuum centrifugation. The purity of the DNA was evaluated by 15% native PAGE.

For preparative-scale experiments, 500 pmol of each DNA was annealed in NEBuffer 3 (New England BioLabs, 50 mM Tris-HCl pH 7.9, 100 mM NaCl, 10 mM MgCl<sub>2</sub>, 1 mM DTT). Duplex DNA was synthesized containing a 1,3-d(GpTpG) adduct or an unplatinated top strand. The DNA was purified by 15% native PAGE. The duplexes were visualized by UV shadowing and isolated from the gel using the crush and soak method. The absorbance of the solutions at 260 nm was measured by UV-vis spectroscopy and the DNA concentration was determined.

#### *Analytical-scale photo-cross-linking*

Analytical-scale photo-cross-linking experiments were carried out using a methodology identical to that for the analytical-scale photo-cross-linking of the 25-bp duplex containing a 1,2-d(GpG) adduct of PtBP6, as described in Chapter 2. These experiments were carried out for the 25-bp duplex containing a 1,3-d(GpTpG) adduct of PtBP6 and 25-bp duplex containing a mismatched 1,2-d(GpG) adduct of PtBP6. Analytical-scale photo-cross-linking experiments were also performed for the 25-bp duplex containing a 1,3-d(GpTpG) or a 1,2-d(GpG) intrastrand adduct of PtBP6 with nuclear extracts from HeLa, NTERA2, U2OS, BxPC3 and HeLa cells in which PARP-1 was silenced (HeLa YS).

*Preparative-scale photo-cross-linking of 25-bp duplex containing a 1,3-d(GpTpG) adduct of PtBP6*

The photo-cross-linking was carried out using identical methodology to that applied in the preparative-scale photo-cross-linking of the 25-bp duplex containing a 1,2-d(GpG) adduct of PtBP6, as described in Chapter 2.

*Western blot for PARP-1 in HeLa and NTERA2 nuclear extracts*

For each cell line, 50 µg of nuclear extracts were resolved by 10% SDS-PAGE. The proteins were then transferred to PVDF using a BioRad Semi Dry Transfer Cell. The membrane was cut at 80 kDa to isolate PARP-1 from β-actin. Each membrane was soaked in t-PBS (10 mM Na<sub>2</sub>HPO<sub>4</sub> pH 7.4, 137 mM NaCl, 2.7 mM KCl, 0.1% Tween-20) with 5% milk for one h. The membranes were washed with t-PBS and incubated in t-PBS with 1/1000X dilution of mouse anti-PARP-1 or rabbit anti-β-actin antibodies for two h. The membranes were again washed with t-PBS and incubated in t-PBS with 1/2000X dilution of HRP anti-mouse or anti-rabbit for one h. The membranes were washed thoroughly with t-PBS and exposed to luminol-containing imaging

reagent (Pierce) for one min. Each membrane was then exposed to Kodak MR autoradiography film, which was developed.

### III. RESULTS

Photo-cross-linking experiments detailed in Chapter 1 were carried out using two new probes. A 25-bp duplex containing a 1,3-d(GpTpG) intrastrand adduct of PtBP6 was synthesized and characterized. This type of adduct is the second most common in patients treated with cisplatin.<sup>1</sup> Several proteins were photo-cross-linked to this probe, with some differences from the set obtained with the probe containing a 1,2-d(GpG) intrastrand adduct Chapter 2. The other new probe contained a mismatched 1,2-d(GpG)-d(CpT) adduct, such that there was both a mismatch and a platinum lesion. The 1,2-d(GpG) and 1,3-d(GpTpG) probes were employed in analytical-scale photo-cross-linking experiments with nuclear extracts from cell lines having varying sensitivities to cisplatin. In one cell line from HeLa, PARP-1 was silenced by RNAi technology.

#### *Preparation of nuclear extracts*

Nuclear extracts were prepared from HeLa, NTera2, BxPC3, U2OS and HeLa YS cells at concentrations between 6 and 12 mg/mL. These extracts were frozen in liquid nitrogen stored at -80 °C.

#### *Cytotoxicity assays*

The cytotoxicity of cisplatin toward each cell line was determined by the MTT assay. Figure 3.1 contains graphical representations of cellular survival versus cisplatin concentration for each cell line. The calculated IC<sub>50</sub> values for HeLa, NTera2, BxPC3, U2OS and HeLa YS cells were 0.80, 0.040, 1.5, 3.3 and 0.35 μM, respectively.

*Preparation and characterization of 25-base DNA containing a 1,3-d(GpTpG) adduct of PtBP6*

Platinated and unplatinated DNA were separated using RP-HPLC (Figure 3.2). Three peaks were collected and dialyzed. In a typical 60 nmol synthesis, 5 nmol of platinated DNA was isolated, a 17% yield. It was determined by UV-vis and atomic absorption spectroscopy that the collected peak 1 did not contain platinum and peaks 2 and 3 contained  $0.90 \pm 0.16$  and  $0.96 \pm 0.09$  Pt atoms per DNA strand, respectively.

Nuclease digestion analysis was able to cut the DNA into individual nucleosides, which were resolved by RP-HPLC (Figure 3.3). The expected ratio C:G:T:A was 12:2:10:1 for the 25-base DNA used in these experiments. For unplatinated DNA the ratio was 12.0:1.9:9.9:1.0. For peak 2 the ratio was 12.0:0.8:9.8:0.9 and for peak 3 the ratio was 12.0:0.6:10.0:0.9. This confirms that the platinum was bound to the guanine residues, since the guanosine peak was the only one muted in these experiments. The guanosine peaks do not completely disappear in these analyses, similar to results from Chapter 2. This suggests that the platinum may be bound to the DNA in a monofunctional manner. This possibility was investigated by ESI-MS. For DNA containing a bifunctional adduct of PtBP6, the expected mass would be 7956.3 m/z. For peaks 2 and 3, the experimental values were  $7955.7 \pm 0.6$  m/z and  $7955.8 \pm 0.7$  m/z, respectively (Figure 3.4). From these data, it is evident that both of these peaks contain a 25-base DNA with PtBP6 bound in a bifunctional manner.

*Synthesis of duplex DNA*

The platinated and unplatinated DNA was annealed to the complementary strand and the duplexes were purified by 15% native PAGE. For analytical-scale experiments, the radiolabeled DNA was analyzed by 15% native PAGE, demonstrating that both the 25-bp duplex containing

a 1,3-d(GpTpG) adduct and mismatched 1,2-d(GpG) adduct of PtBP6 were 100% pure (Figure 3.5).

*Silencing of PARP-1 in HeLa cells*

The silencing of PARP-1 in HeLa cells, carried out by Dong Xu, successfully eliminated the desired protein, as determined by western blotting (Figure 3.6).

*Photo-cross-linking of 25-bp duplex containing a 1,3-d(GpTpG) adduct of PtBP6*

The 25-bp duplex containing a 1,3-d(GpTpG) adduct of PtBP6 photo-cross-linked to several proteins. In analytical-scale photo-cross-linking experiments, several proteins appear to be identical to those of the 1,2-d(GpG) adduct, although there are differences (Figure 3.7A). The cross-linking experiments identified several proteins that bind to this probe (Table 3.1). Unlike the probe containing a 1,2-d(GpG) PtBP6 adduct, this probe exhibited only weak affinity for HMGB1 and HMGB3, and no affinity at all for HMGB2 or UBF1. The probe formed photo-cross-links to DNA repair proteins PARP-1, DNA ligase III, Msh2, all three members of the DNA-PK heterotrimer, and RPA1, which was not photo-cross-linked by the 1,2-d(GpG) adduct.

*Analytical-scale photo-cross-linking using nuclear extracts from HeLa cells in which PARP-1 was silenced by RNAi*

Nuclear extracts from HeLa cells in which PARP-1 was silenced by RNAi were used in photo-cross-linking experiments with the probe containing a 1,2-d(GpG) intrastrand PtBP6 adduct (Figure 3.7B). The band identified as PARP-1 by preparative-scale photo-cross-linking was completely abolished when using nuclear extracts from the PARP-1 silenced cells.

*Analytical-scale photo-cross-linking of a 25-bp duplex containing a mismatched 1,2-d(GpG) intrastrand adduct*



A 25-bp duplex containing a mismatched 1,2-d(GpG) intrastrand cross-link was synthesized and purified. The duplex was constructed such that the platinated guanine on the 3'-side of the top strand was mismatched against a thymine residue on the bottom strand. Photo-cross-linking experiments using this probe and Ntera2 nuclear extracts were performed (Figure 3.7C). The main result was formation of a band containing the protein Msh2 that appears with much greater intensity in lane 2. The increase in affinity of Msh2 for the compound lesion competes other proteins that bind to the platinum adduct (Table 3.2). In particular, the HMG-domain proteins and PARP-1 are photo-cross-linked less effectively, and proteins that comprise the DNA-PK heterotrimer are also somewhat less competed.

*Analytical-scale photo-cross-linking using nuclear extracts from different cancer cell lines*

Nuclear extracts from cervical (HeLa), bone (U2OS), testicular (Ntera2) and pancreatic (BxPC3) cancer cells were used in photo-cross-linking experiments with both the 1,2-d(GpG) and 1,3-d(GpTpG) adducts of PtBP6 (Figure 3.8). The proteins cross-linked to each probe appear to be the same for nuclear extracts from the four different cell lines, but with varying quantities. The most dramatic difference occurs for PARP-1, the band for which is strong using nuclear extracts from Ntera2 cells, but very weak for nuclear extracts from BxPC3 cells.

*Western blot of analysis PARP-1 in HeLa and Ntera2 cells*

Western blot analyses of HeLa and Ntera2 nuclear extracts reveal that PARP-1 expression is significantly higher in the latter (Figure 3.9). This result indicates that the greater amount of photo-cross-linking to PARP-1 in Ntera2 nuclear extracts is a consequence of its higher expression level.

## IV. DISCUSSION

Since the discovery that cisplatin targets DNA, much effort has been expended to identify proteins with an affinity for the platinated duplex. In the present study, we prepared and characterized site-specifically modified 25-bp duplex containing a 1,3-d(GpTpG) intrastrand cross-link bearing a pendent photo-activatable benzophenone. Upon irradiation, this probe forms covalent bonds between the platinated DNA and any proteins in a nuclear extract with an affinity for the adduct. Isolation of the DNA-platinum-protein complexes followed by trypsin digestion and mass spectrometric analysis allowed the proteins to be identified. Photo-cross-linking using a probe containing a mismatched 1,2-d(GpG) PtBP6 adduct was also performed. Analytical-scale photo-cross-linking experiments were conducted using both the 1,2-d(GpG) and 1,3-d(GpTpG) adducts in nuclear extracts from various cancer cell lines with different sensitivity to cisplatin.

### *Protein identification*

Many of the proteins identified in the photo-cross-linking experiments conducted in this study (Table 3.1) appear in more than one band. This phenomenon is discussed in detail in Chapter 2. The work in this chapter confirmed the identity of the bands containing PARP-1 and Msh2. As described below, the band containing PARP-1 was identified by photo-cross-linking using nuclear extracts from HeLa cells in which PARP-1 was silenced with RNAi (Figure 3.7B). Also, the band that contains Msh2 was identified by photo-cross-linking with a DNA duplex containing a combination of a platinum adduct and a mismatched base (Figure 3.7C). The identification of the remaining bands is in accord with the molecular weights of the individual proteins, Ku70, Ku80, and UBF1.

### *Consideration of the end effect*

One concern of this present study is that proteins that recognize the ends of the 25-bp duplex may be photo-cross-linked together with those that bind specifically to the platinum lesion. The DNA-PK heterotrimer, for example, is involved in the repair of DNA double strand breaks through the nonhomologous end-joining pathway.<sup>5</sup> Although the Ku proteins, which comprise two thirds of the DNA-PK heterotrimer, have previously been associated with cisplatin adducts,<sup>6</sup> Ku-binding to DNA ends would probably extend far enough down the duplex to reach the platination site.<sup>7</sup> Another photo-cross-linked protein that may be involved in double-strand break repair is PARP-1. Evidence that this protein is bound to the platinum adduct and not the DNA ends is presented below.

*Photo-cross-linking with nuclear extracts from different cancer cell lines*

The photo-cross-linking experiments were extended to include nuclear extracts from a variety of cancer cell lines with varying sensitivity to cisplatin (Figures 3.1 and 3.8). The proteins photo-cross-linked by the platinated probe are generally consistent among all cell lines tested, although their relative amounts differ. The fact that extracts from a variety of cells exhibit an identical array of platinated DNA-binding proteins is consistent with recent work indicating that the success of oxaliplatin, by comparison to cisplatin or carboplatin, to treat colorectal cancer is a consequence of increased cellular uptake<sup>8</sup> and not differential processing of the Pt-DNA adducts. The photo-cross-linking of PARP-1 between the different extracts varies greatly, with the greatest levels appearing in extracts from NTera2 testicular cancer cells (Figure 3.8). The significance of PARP-1 as a DNA-damage sensor is discussed below.

*HMG-domain proteins and the 1,3-d(GpTpG) adduct*

A difference between the 1,2-d(GpG) and 1,3-d(GpTpG)-intrastrand Pt cross-links is that the former are recognized by HMG-domain proteins.<sup>9</sup> These chromosomal proteins bind to

distorted DNA structures such as four-way junctions and induce further bending of the DNA.<sup>10</sup> The present results indicate that, in cell extracts, HMGB1 and HMGB3 bind weakly to the 1,3-d(GpG) adduct (Table 3.1), whereas HMGB1, HMGB2, HMGB3, and UBF1 all bind strongly to the 1,2-d(GpG) cross-link (Figure 3.7A), as described in Chapter 2. This finding supports previous work utilizing electrophoretic mobility shift assays (EMSAs) and isolated HMGB1, revealing that the protein binds to the 1,2-d(GpG) but not the 1,3-d(GpTpG) adduct.<sup>9</sup> Here we provide conclusive evidence that this behavior occurs in a nuclear milieu, where many other proteins can compete for binding to the platinum adduct, supporting the conclusion that *cis*-{Pt(NH<sub>3</sub>)(*N*-(6-aminohexyl)-4-benzophenonamide)}<sup>2+</sup> and *cis*-{Pt(NH<sub>3</sub>)<sub>2</sub>}<sup>2+</sup> DNA cross-links are processed in an identical manner.

*Nucleotide excision repair protein, RPA1*

Replication protein A1 (RPA1) is a component of the nucleotide excision repair apparatus, the major machinery for removing cisplatin adducts from DNA.<sup>1</sup> We observe this protein to be photo-cross-linked only to the 1,3-d(GpTpG) intrastrand adduct of PtBP6. EMSA studies using purified RPA1 indicate that the protein has a 1.5-2-fold stronger affinity for the 1,3-d(GpTpG) than the 1,2-d(GpG) cisplatin cross-link.<sup>11</sup> The 1,3-d(GpTpG) adduct is repaired more efficiently by NER than the 1,2-d(GpG) adduct, and the repair is further inhibited, exclusively for the 1,2-d(GpG) cross-link, by the binding of HMG-domain proteins.<sup>12</sup> The affinity of HMG-domain proteins for the 1,2-d(GpG) intrastrand adduct has been confirmed in the present experiments, as discussed earlier. Our results indicate that RPA1 binds with greater affinity to the 1,3-d(GpTpG) intrastrand cross-link of PtBP6 in the nuclear milieu, where other proteins such as HMGB1 are available to compete for binding. That RPA1 does not bind to the

1,2-d(GpG) intrastrand adduct of PtBP6 most likely reflects lower affinity for the lesion in addition to competition for binding from HMG-domain proteins.

Nucleotide excision repair of cisplatin adducts results in excised DNA fragments of approximately 28-32 base pairs,<sup>12</sup> only 3-7 bp longer than the probe used in these experiments. Use of a longer DNA probe modified with PtBP6 will most likely increase the ability of nucleotide excision repair proteins to bind and become activated, possibly providing a more complete account of proteins that compete for binding with platinated DNA. Given the present results using a 25-bp duplex, work with longer platinated photo-cross-linkable DNA duplexes is clearly warranted.

#### *Platinum-modified DNA containing a mismatch*

Previous work using EMSAs indicates that the mismatch repair protein, Msh2, has a greater affinity for a 1,2-d(GpG) cisplatin cross-link in which the unplatinated DNA strand contains a mismatched thymine opposite the 3'-guanosine.<sup>3</sup> This result nicely correlates with the finding in the present study that the cross-linking efficiency is enhanced in the mismatched probe (Figure 3.7C). The increased affinity of Msh2 for DNA containing the mismatched Pt adduct is accompanied by diminished photo-cross-linking to the other proteins (Table 3.2). If a DNA polymerase were able to bypass a cisplatin adduct, the resulting duplex could incorporate a mismatched base<sup>2</sup> and become a better binding site for mismatch repair proteins, inducing futile attempts to repair the compound lesion and eventually signaling apoptosis.<sup>13</sup>

#### *PARP-1 and DNA ligase III*

Photo-cross-linking experiments identified PARP-1 binding to both the 1,2-d(GpG) and 1,3-d(GpTpG) intrastrand PtBP6 cross-links. Using nuclear extracts from HeLa cells in which PARP-1 was silenced by RNAi, the identification of the band containing the protein could be

confirmed (Figure 3.7B). PARP-1 has been associated with base excision repair<sup>14</sup> and a backup system of nonhomologous end joining (NHEJ); this process repairs double strand breaks when the DNA-PK heterotrimer is compromised.<sup>15,16</sup> In both of these processes, PARP-1 recruits DNA ligase III to the damage site,<sup>14</sup> which we propose to be the reason for DNA ligase III photo-cross-linking by our probes. Since PARP-1 recognizes double strand breaks, we considered the possibility that the protein binds to the ends of our probe and not to the platinum cross-links. The present work provides three strong pieces of evidence that PARP-1 binds to DNA at the platinum adduct and not the duplex ends.

The first line of evidence stems from the fact that PARP-1 and the Ku proteins of the DNA-PK heterotrimer compete for binding to DNA double-strand breaks.<sup>15-19</sup> Photo-cross-linking experiments using nuclear extracts from NTERA2 cells, which express high levels of PARP-1 (Figure 3.9), reveal much greater PARP-1 cross-linking compared to extracts from HeLa cells (Figure 3.8). Using ImageQuant data analysis software, we determined the photo-cross-linking of PARP-1 to be 3.1-fold higher in NTERA2 extracts, whereas the relative photo-cross-linking of the Ku proteins and DNA-PK<sub>cs</sub> was almost unchanged, being 1.1-fold and 0.9-fold, respectively.

The second piece of evidence stems from photo-cross-linking using HeLa nuclear extracts from cells in which PARP-1 had been silenced, which revealed comparable photo-cross-linking to the DNA-PK heterotrimer (Figure 3.7B). Despite the absence of PARP-1, the Ku proteins and DNA-PK<sub>cs</sub> were photo-cross-linked 0.9-fold and 1.1-fold as efficiently, respectively, in PARP-1 silenced HeLa nuclear extracts compared to normal HeLa nuclear extracts. These results indicate that the binding of PARP-1 to this probe is independent of the DNA ends and requires the platinum lesion itself. If PARP-1 were competing with the DNA-PK heterotrimer for

binding to the DNA ends, differences in expression of the protein should affect the binding of the DNA-PK heterotrimer.

The third line of evidence derives from photo-cross-linking experiments using the mismatched DNA probe. Table 3.2 lists the relative photo-cross-linking efficiency of each protein for the mismatched versus correctly matched probes. Since the mismatched repair protein Msh2 has a greater affinity for the mismatched probe, photo-cross-linking of other proteins is decreased. The photo-cross-linking of HMG-domain proteins, which bind to the platination site, is competed efficiently, being 18% for HMGB1, HMGB2 and HMGB3 and 38% for UBF1 compared to the matched probe. Photo-cross-linking of DNA end-binding proteins Ku70, Ku80 and DNA-PKcs is less efficiently competed, being 82%, 65% and 55%, respectively. The photo-cross-linking of PARP-1 and DNA ligase III is competed to 33%, suggesting that the proteins are bound in a similar fashion as the HMG-domain proteins and not the DNA-PK heterotrimer.

Given the sensitivity of NTERa2 cells to cisplatin, the high levels of PARP-1 expression in this context (Figure 3.9) suggest a role of this protein in mediating the anticancer activity of the drug. The catalytic domain of PARP-1 is commonly mutated in germ cells,<sup>20</sup> which may account for the increase in expression of the protein necessary for the cells to function. PARP proteins can lead to DNA repair or conversely, cell death signaling through distinct pathways.<sup>21</sup> It is possible that the binding of PARP-1 to platinum-damaged DNA has different consequences depending on the cell line. A number of studies indicate that PARP-1 inhibition by 3-aminobenzamide in ovarian and cervical cell lines leads to cisplatin sensitization,<sup>22-25</sup> although there are conflicting results indicating no effect.<sup>26</sup> A newly developed inhibitor for PARP-1 and PARP-2 revealed that PARP inhibition sensitizes a non-small cell lung carcinoma line to cisplatin.<sup>27</sup> These data suggest that PARP-1 may facilitate repair of Pt-DNA adducts, since its

inhibition sensitizes cells to cisplatin. PARP inhibitors are currently being evaluated in several clinical trials, including those applied in combination with carboplatin.<sup>28</sup> The present work demonstrates that the activity of PARP-1 following exposure to cisplatin most likely arises from an enhanced ability of the protein to bind to platinated DNA. The role of PARPs following cisplatin exposure in cancer cells is investigated further in Chapter 5.

## V. CONCLUSIONS

A platinated 25-bp DNA duplex containing a cisplatin analog with an amino ligand bearing a pendent photo-activatable moiety, PtBP6, was prepared to photo-cross-link proteins with an affinity for Pt-modified DNA. Differences in photo-cross-linking between 1,2-d(GpG) and 1,3d(GpTpG) intrastrand cross-linked probes reflected preferences previously reported for DNA adducts of cisplatin studied in isolation. For example, HMG-domain proteins strongly favor the 1,2-d(GpG) intrastrand cross-link whereas the nucleotide excision repair protein RPA1 prefers the 1,3-d(GpTpG) adduct. Similarly, a duplex containing the 1,2-d(GpG) adduct of PtBP6 carrying a mismatched base opposite the platination site has a greater affinity for the mismatch repair protein, Msh2. These results indicate that the PtBP6-DNA lesion is processed in manner analogous to cisplatin-DNA lesions. The PtBP6-DNA probe allowed us to identify PARP-1 binding specificity to Pt-modified DNA. This protein is currently a subject of much scrutiny by cancer biologists, and the discovery that it binds to platinum-modified DNA warrants further attention. This protein is differentially expressed among the sampling of cancer cell lines routinely investigated in our laboratory and high levels of expression in testicular cancer cells lead to greater photo-cross-linking. The significance of PARP-1 binding to platinated DNA remains under investigation.



## VI. REFERENCES

1. Jamieson, E. R.; Lippard, S. J., *Chem. Rev.* **1999**, 99, 2467-2498.
2. Hoffmann, J.-S.; Pillaire, M.-J.; Garcia-Estefania, D.; Lapalu, S.; Villani, G., *J. Biol. Chem.* **1996**, 271, 15386-15392.
3. Fourrier, L.; Brooks, P.; Malinge, J.-M., *J. Biol. Chem.* **2003**, 278, 21267-21275.
4. Zhang, C. X.; Chang, P. V.; Lippard, S. J., *J. Am. Chem. Soc.* **2004**, 126, 6536-6537.
5. Collis, S. J.; DeWeese, T. L.; Jeggo, P. A.; Parker, A. R., *Oncogene* **2005**, 24, 949-961.
6. Turchi, J. J.; Henkels, K., *J. Biol. Chem.* **1996**, 271, 13861-13867.
7. Walker, J. R.; Corpina, R. A.; Goldberg, J., *Nature* **2001**, 412, 607-614.
8. Zhang, S.; Lovejoy, K. S.; Shima, J. E.; Lagpacan, L. L.; Shu, Y.; Lapuk, A.; Chen, Y.; Komori, T.; Gray, J. W.; Chen, X.; Lippard, S. J.; Giacomini, K. M., *Cancer Res.* **2006**, 66, 8847-8857.
9. Pil, P. M.; Lippard, S. J., *Science* **1992**, 1992, 234-237.
10. Thomas, J. O.; Travers, A. A., *Trends Biochem. Sci.* **2001**, 26, 167-174.
11. Patrick, S. M.; Turchi, J. J., *J. Biol. Chem.* **1999**, 274, 14972-14978.
12. Huang, J.-C.; Zamble, D. B.; Reardon, J. T.; Lippard, S. J.; Sancar, A., *Proc. Natl. Acad. Sci. U.S.A.* **1994**, 91, 10394-10398.
13. Zdraveski, Z. Z.; Mello, J. A.; Marinus, M. G.; Essigmann, J. M., *Chem. Biol.* **2000**, 7, 39-50.
14. Bouchard, V. J.; Rouleau, M.; Poirier, G. G., *Exp. Hematol.* **2003**, 31, 446-454.
15. Audebert, M.; Salles, B.; Calsou, P., *J. Biol. Chem.* **2004**, 279, 55117-55126.
16. Wang, M.; Wu, W.; Wu, W.; Rosidi, B.; Zhang, L.; Wang, H.; Iliakis, G., *Nucleic Acids Res.* **2006**, 34, 6170-6182.
17. Hochegger, H.; Dejsuphong, D.; Fukushima, T.; Morrison, C.; Sonoda, E.; Schreiber, V.; Zhao, G. Y.; Saberi, A.; Masutani, M.; Adachi, N.; Koyama, H.; de Murcia, G.; Takeda, S., *EMBO J.* **2006**, 25, 1305-1314.
18. D'Silva, I.; Pelletier, J. D.; Lagueux, J.; D'Amours, D.; Chaudhry, M. A.; Weinfeld, M.; Lees-Miller, S. P.; Poirier, G. G., *Biochim. Biophys. Acta* **1999**, 1430, 119-126.
19. Ariumi, Y.; Masutani, M.; Copeland, T. D.; Mimori, T.; Sugimura, T.; Shimotohno, K.; Ueda, K.; Hatanaka, M.; Noda, M., *Oncogene* **1999**, 18, 4616-4625.
20. Shiokawa, M.; Masutani, M.; Fujihara, H.; Ueki, K.; Nishikawa, R.; Sugimura, T.; Kubo, H.; Nakagama, H., *Jpn. J. Clin. Oncol.* **2005**, 35, 97-102.
21. Nguewa, P. A.; Fuertes, M. A.; Alonso, C.; Perez, J. M., *Mol. Pharmacol.* **2003**, 64, 1007-1014.
22. Boike, G. M.; Petru, E.; Sevin, B.-U.; Averette, H. E.; Chou, T.-C.; Penalver, M.; Donato, D.; Schiano, M.; Hilsenbeck, S. G.; Perras, J., *Gynecol. Oncol.* **1990**, 38, 315-322.
23. Chen, G.; Pan, Q.-C., *Cancer Chemother. Pharmacol.* **1988**, 22, 303-207.
24. Chen, G.; Zeller, W. J., *Cancer Chemother. Pharmacol.* **1990**, 26, 37-41.
25. Nguewa, P. A.; Fuertes, M. A.; Cepeda, V.; Alonso, C.; Quevedo, C.; Soto, M.; Pérez, J. M., *Med. Chem.* **2006**, 2, 47-53.
26. Bernges, F.; Zeller, W. J., *J. Cancer Res. Clin. Oncol.* **1996**, 122, 665-670.

27. Miknyoczki, S. J.; Jones-Bolin, S.; Pritchard, S.; Hunter, K.; Zhao, H.; Wan, W.; Ator, M.; Bihovsky, R.; Hudkins, R.; Chatterjee, S.; Klein-Szanto, A.; Dionne, C.; Ruggeri, B., *Mol. Cancer. Ther.* **2003**, *2*, 371-382.
28. Helleday, T.; Petermann, E.; Lundin, C.; Hodgson, B.; Sharma, R. A., *Nat. Rev. Cancer* **2008**, *8*, 193-204.
29. Robert, J., 2007, *Personal Communication*.
30. Robert, J.; Laurand, A.; Meynard, D.; Le Morvan, V. In Platinum drugs and DNA repair. Lessons from the NCI-60 panel and clinical correlates, 10th International Symposium on Platinum Coordination Compounds in Cancer Chemotherapy, Verona, Italy; 2007.
31. Schofield, M. J.; Hsieh, P., *Annu. Rev. Microbiol.* **2003**, *57*, 579-608.

TABLES

Table 3.1: Proteins identified by preparative scale photo-cross-linking of a 25-bp duplex containing a 1,3-d(GpTpG) intrastrand PtBP6 adduct.

Protein <sup>b</sup>	Probability <sup>c</sup>	MW (Da)	Unique Peptides <sup>d</sup>	Protein Function
HMGB1	2.57E-04	24878.2	1	Analysis of the NCI library of cancer cell lines reveals a correlation between expressing high levels of HMGB1 and cisplatin sensitivity <sup>29,30</sup>
HMGB3	4.97E-04	14597.2	1	HMGB1 and HMGB3 are chromatin architectural proteins HMGB1 shields cisplatin-DNA adducts from excision repair <sup>12</sup>
PARP-1	1.61E-07	113012.4	2	See Chapter 5 for more information.
RPA1	2.13E-06	68095.4	1	
Ku70	1.30E-05	69799.2	1	Member of the DNA-PK complex (Ku70, Ku80 and DNA-PKcs) involved in nonhomologous end-joining repair of double-strand breaks <sup>5</sup>
Ku80	7.72E-13	82652.4	13	
PARP-1	1.20E-08	113012.4	5	
RPA1	8.47E-07	68095.4	1	RPA1 is involved in DNA-damage recognition of NER. It has a 2-fold greater affinity for cisplatin 1,3-d(GpNpG) vs 1,2-d(GpG) intrastrand adducts <sup>11</sup> .
DNA ligase III	1.36E-06	112834.9	4	
Msh2	1.51E-05	104676.8	3	Protein involved in the recognition of base pair mismatches <sup>31</sup>
Ku70	2.21E-05	69799.2	3	
PARP-1	8.47E-10	113012.4	14	
DNA ligase III	8.51E-07	112834.9	6	See Chapter 5 for more information.
PARP-1	2.44E-07	113012.4	7	
DNA ligase III	4.46E-07	112834.9	3	
DNA-PKcs	4.94E-09	468786.9	8	

LC-MS/MS analysis was carried out on six gel slices corresponding to the bands from the analytical-scale photo-cross-linking experiment. The proteins identified in each band are listed here. <sup>b</sup>Proteins identified as described in the Materials and Methods section. <sup>c</sup>Probability of the peptide identification being due to background signal from the LC-MS/MS instrument. For example, a probability of 1.0E-4 indicates that there is a 0.01% chance that the identified protein is not actually present in the sample. The values listed correspond to the peptide most likely to be present for each protein. <sup>d</sup>The number of peptides identified for each protein. Peptides differing by only one amino acid were not considered to be unique.

Table 3.2: Ratios of normalized<sup>a</sup> intensities of photo-cross-linking using a mismatched 1,2-d(GpG) intrastrand adduct of PtBP6 to a correctly matched 1,2-d(GpG) intrastrand adduct of PtBP6.

Protein	Mismatched/ Matched
DNA-PK <sub>cs</sub>	0.55
PARP-1/DNA ligase III	0.33
Msh2	1.32
UBF1	0.38
Ku80	0.65
Ku70	0.82
HMGB1, HMGB2, HMGB3	0.18

<sup>a</sup>The intensity of each band was normalized to total signal in the lane.

## VIII. FIGURES

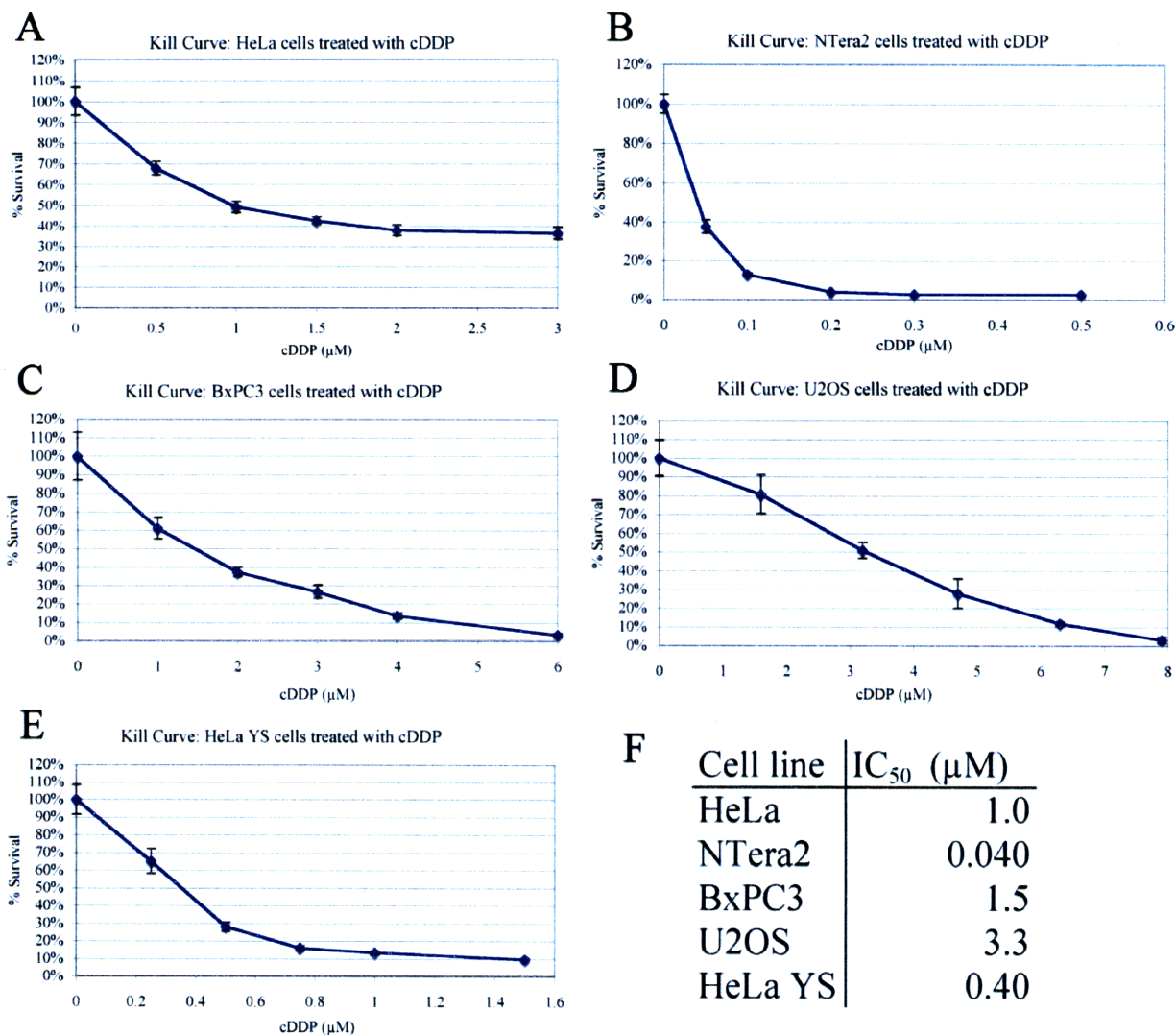


Figure 3.1. Cytotoxicity assays of HeLa, NTERA2, BxPC3, U2OS and HeLa YS cancer cell lines with increasing concentrations of cisplatin.

Various cancer cell lines were treated with cisplatin and the survival was measured using the MTT assay. Error bars represent one standard deviation. The cell lines tested were (A) HeLa, (B) NTERA2, (C) BxPC3, (D) U2OS and (E) HeLa YS in which PARP-1 was silenced by RNAi. The  $\text{IC}_{50}$  for each cell line is tabulated (F).

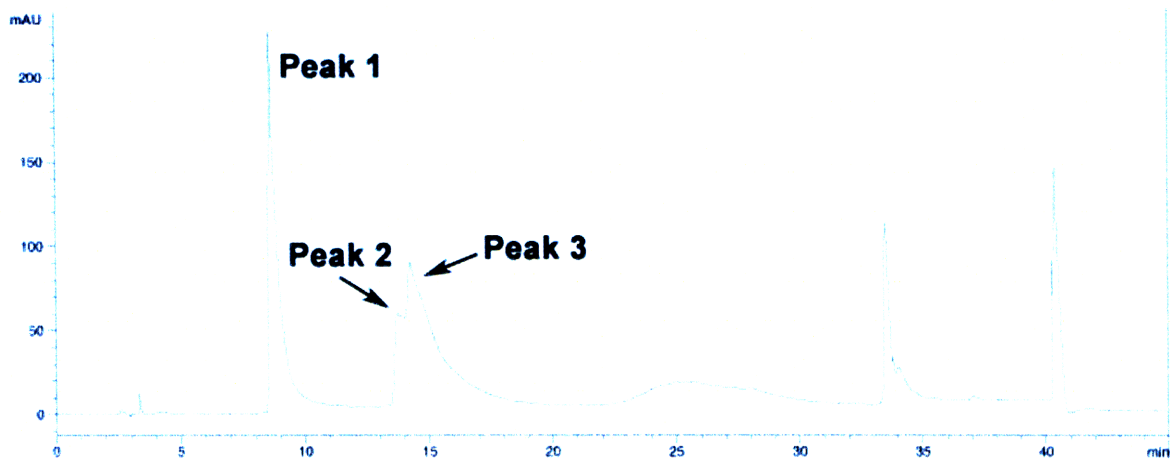


Figure 3.2. RP-HPLC purification of the reaction between a 25-base DNA fragment and the activated form of PtBP6.

This reaction yields three major peaks. Peak 1 is the starting material, and peaks 2 and 3 are platinated DNA.

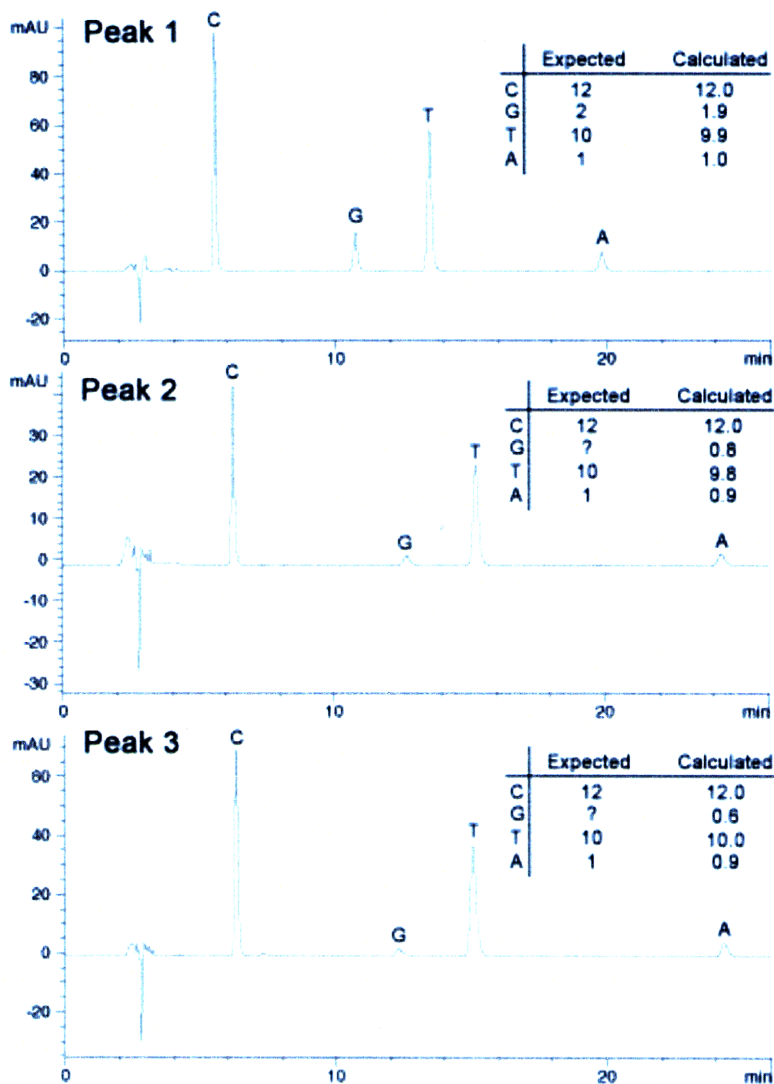


Figure 3.3. Nuclease digestion analysis of products from the reaction of PtBP6 with DNA containing a 1,3-d(GpTpG) site.

The analysis indicates that the platinum atom is bound to guanosine. The signal for this base is muted after the platination reaction (Peaks 2 and 3) compared to starting material (Peak 1).

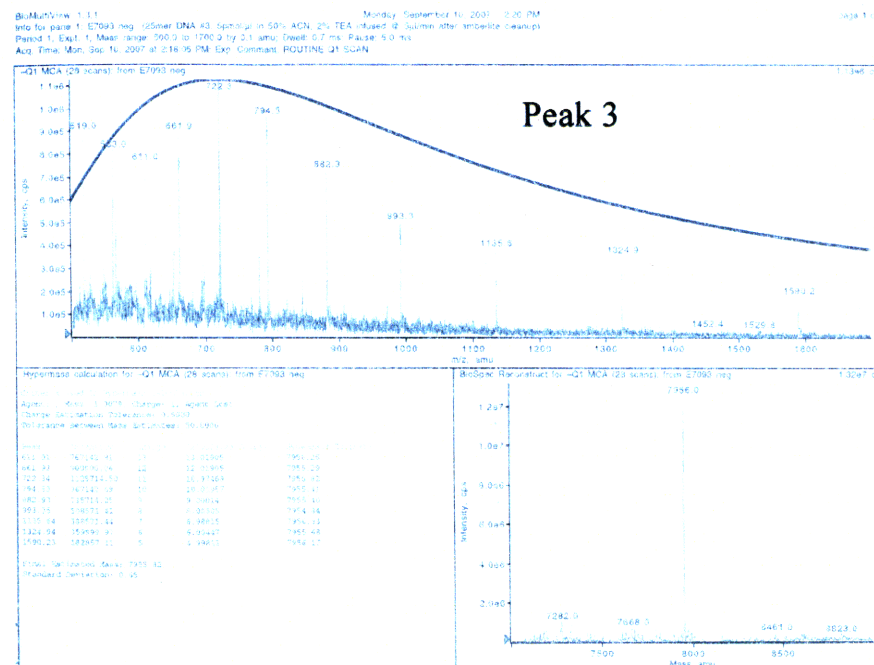
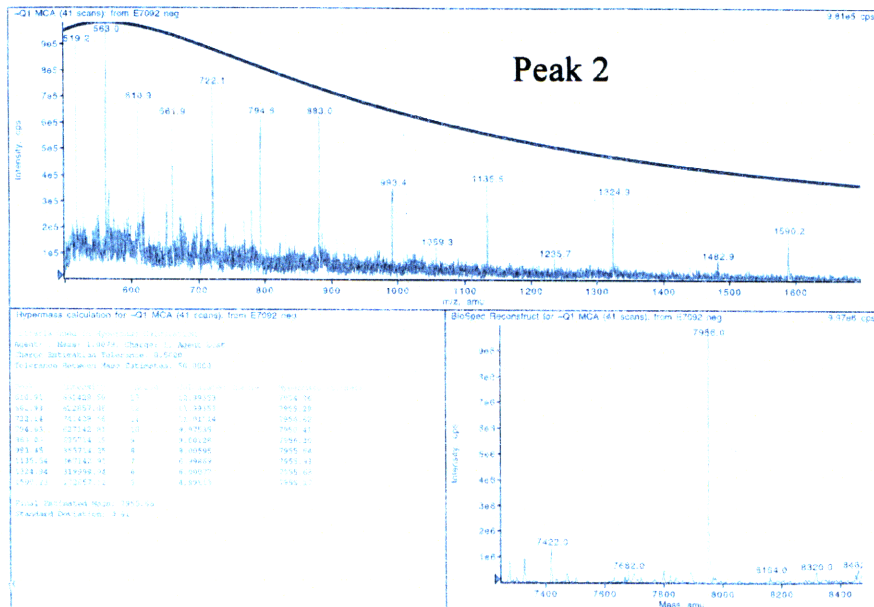


Figure 3.4. ESI-MS analysis of 25-base DNA containing a 1,2-d(GpTpG) adduct of PtBP6.

The PtBP6-modified DNA has a calculated value of 7956.3 m/z. For peaks 2 and 3, the experimental values were  $7955.7 \pm 0.6$  m/z and  $7955.8 \pm 0.7$  m/z. This spectrum indicates that the platinated DNA contains PtBP6 bound in a bifunctional manner. A monofunctional adduct would require another ligand to satisfy the coordination environment of the platinum, and the mass of the complex would be increased. No unplatinated DNA is detected. The analysis was performed by the staff of the MIT Biopolymers facility.



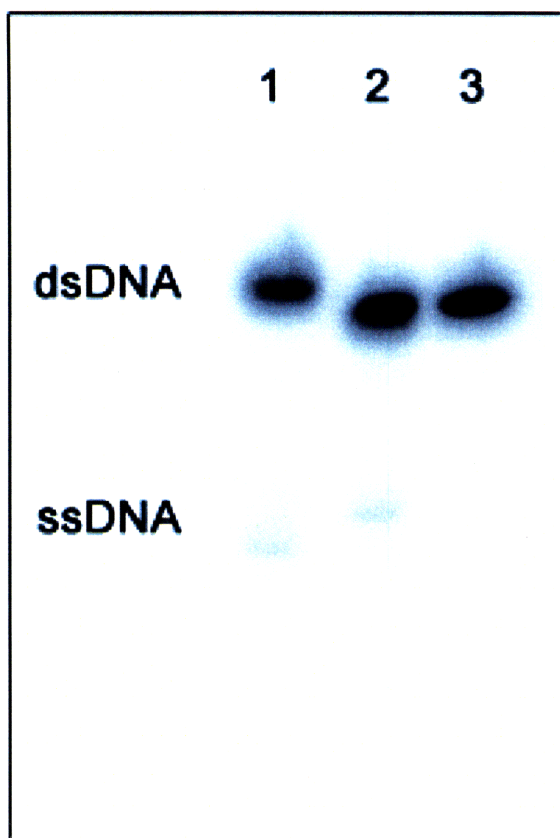


Figure 3.5. Native PAGE analysis of 25-bp duplexes.

Lane 1: duplex containing a 1,3-d(GpTpG) adduct of PtBP6. Lane 2: duplex containing a 1,2-d(GpG) adduct of PtBP6. Lane 3: duplex containing a mismatched 1,2-d(GpG) adduct of PtBP6.

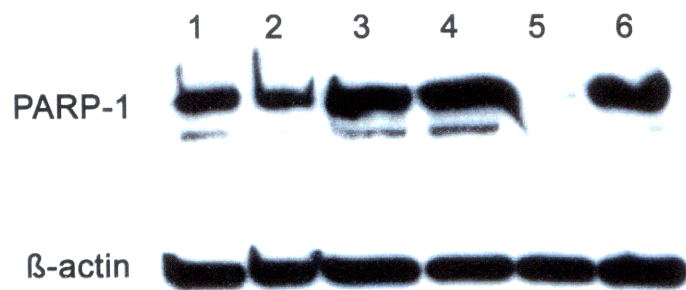


Figure 3.6. Western blot analysis of single clones of HeLa cells transfected with the plasmid for RNAi of PARP-1.

The nuclear extracts of clones #4, #5, #11 and #13 were loaded in lanes 3 to 6, respectively. Untransfected HeLa cells (lane 1) and transfected but unsorted cells (lane 2) were used as controls. The cells from lane 5 were used for subsequent experiments.

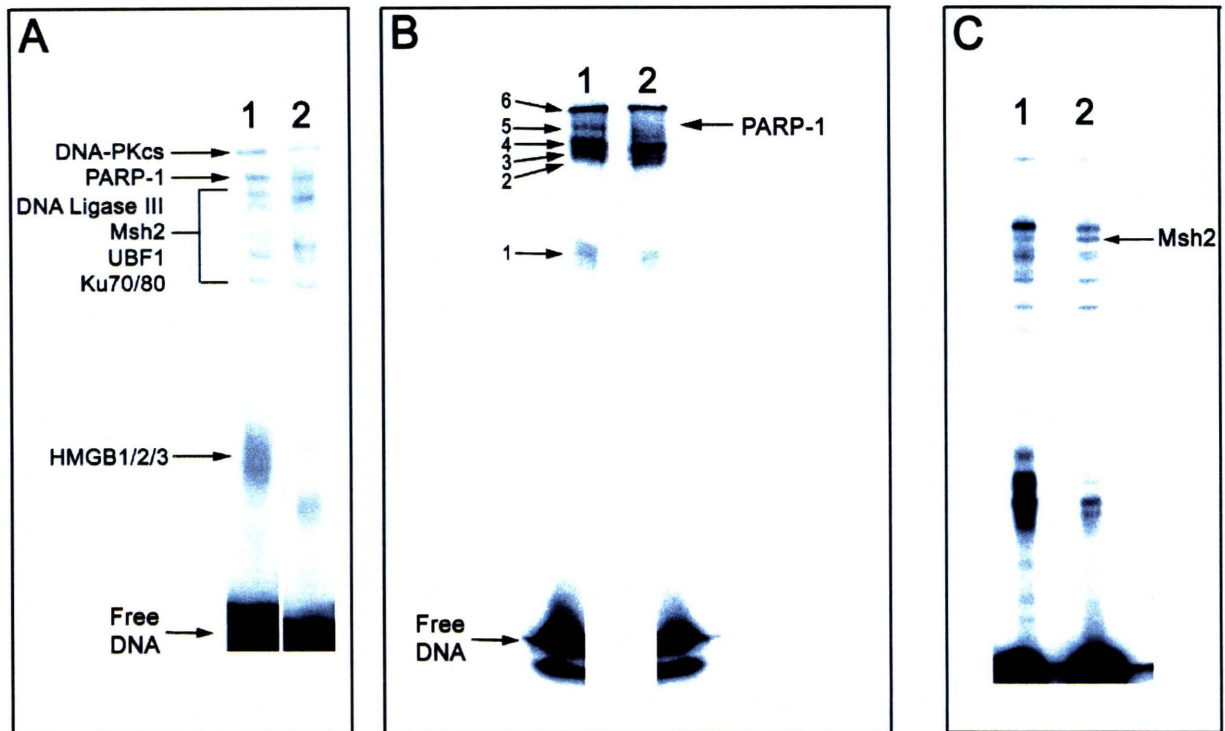


Figure 3.7. Analytical-scale photo-cross-linking results of the 1,2-d(GpG), 1,3-d(GpTpG) and mismatched 1,2-d(GpG) intrastrand adduct-containing probes, and photo-cross-linking using nuclear extracts from HeLa YS cells.

(A) 10% SDS-PAGE analysis of photo-cross-linking of HeLa nuclear extracts using a 25-bp duplex containing a 1,2-d(GpG) (lane 1) or 1,3-d(GpTpG) (lane 2) cross-link of PtBP6. (B) 12% SDS-PAGE analysis of photo-cross-linking using a 25-bp duplex containing a 1,2-d(GpG) cross-link of PtBP6 incubated with HeLa nuclear extracts (lane 1) or nuclear extracts from HeLa cells in which PARP-1 has been silenced using RNAi (lane 2). Lane 1 was used as a guide to excise six bands from preparative scale photo-cross-linking experiments for analysis by LC-MS/MS. (C) 10% SDS-PAGE analysis of photo-cross-linking of Ntera2 nuclear extracts using a 25-bp duplex containing a 1,2-d(GpG) cross-link of PtBP6 (lane 1) or a 25-bp duplex containing a mismatched 1,2-d(GpG)/d(CpT) cross-link of PtBP6 (lane 2).

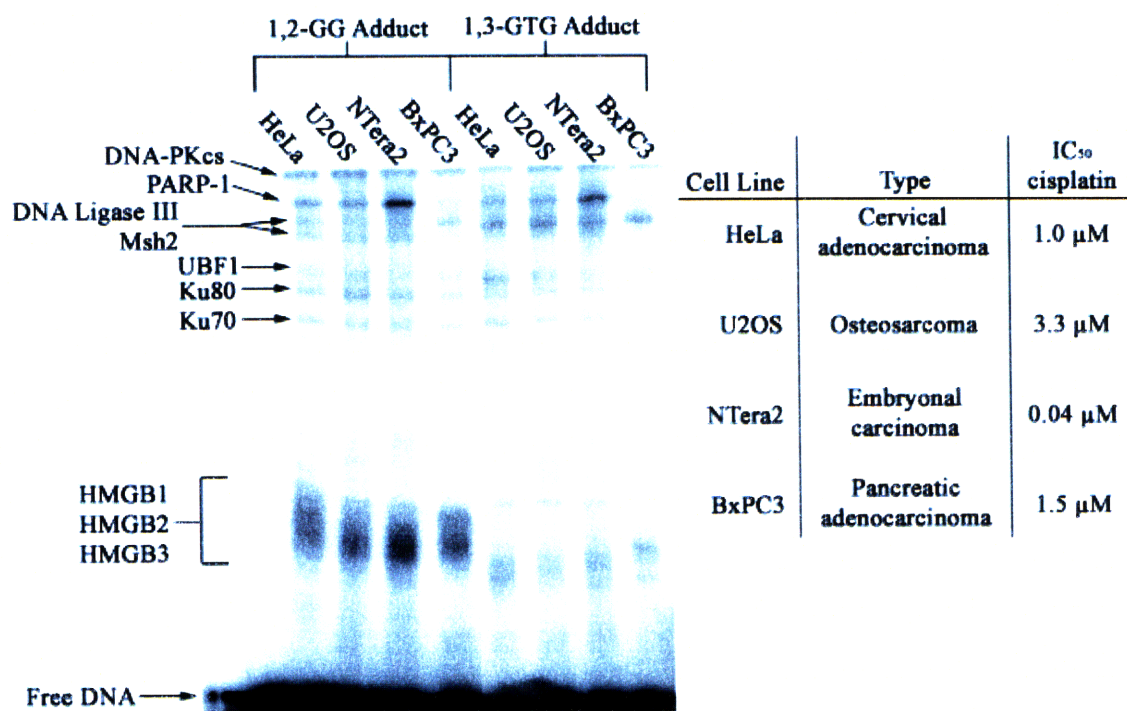


Figure 3.8. Photo-cross-linking of 25-bp PtBP6 probes with nuclear extracts from various cell lines.

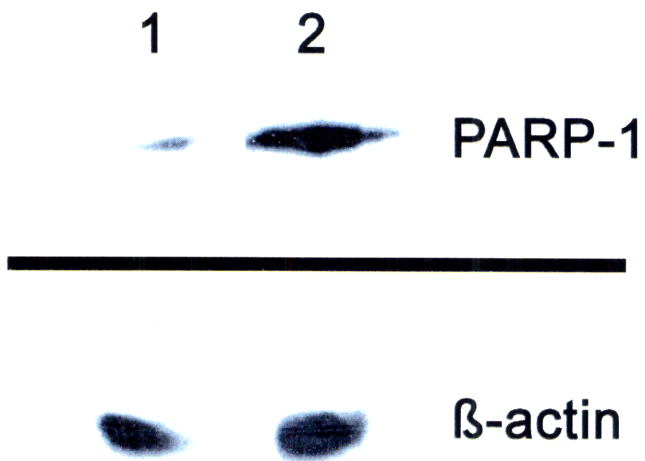


Figure 3.9. Western blot analysis of PARP-1 expression using HeLa and NTERA2 nuclear extracts.

NTERA2 cells (lane 2) express much higher levels of PARP-1 than HeLa cells (lane 1).

## **Chapter 4: Photo-Cross-Linking and Identification of Nuclear Proteins that Bind to a PtBP6-Modified 90-base DNA Dumbbell Probe.**

**\*Work from this chapter was submitted for publication; Guggenheim, E. R., Xu, D., Zhang, C. Z., Chang, P. V., Lippard, S. J., “Photo-Affinity Isolation and Identification of Proteins in Cancer Cell Extracts that Bind to Platinum-Modified DNA.”**

## I. INTRODUCTION

In Chapters 2 and 3, a photoactive analogue of cisplatin, *cis*-[Pt(NH<sub>3</sub>)(*N*-(6-aminohexyl)-4-benzophenonamide)Cl<sub>2</sub>] (PtBP6), was used to photo-cross-link proteins with an affinity for platinum-damaged. In the work, PtBP6-modified 25-bp duplexes containing a site-specific adducts were synthesized. This DNA was used to photo-cross-link and identify a number of proteins with an affinity for platinum-modified DNA. The proteins identified for the 1,2-d(GpG) intrastrand adduct were HMGB1, HMGB2, HMGB3, Ku70, Ku80, UBF1, Msh2, DNA Ligase III, PARP-1 and DNA-PK<sub>cs</sub>. These photo-cross-linking studies provide several advantages over previous methodologies. Since nuclear extracts are used for these experiments, the entire proteome can be surveyed in each experiment. These assays also identify the proteins that will bind to platinum-modified DNA in the context of the nuclear milieu, in which all nuclear proteins are able to compete for binding to the lesion.

In this chapter, a longer 90-base dumbbell DNA probe is used in these photo-cross-linking studies. This probe is superior to the 25-bp duplex because the platination site is further from the DNA ends (Figure 4.1). DNA end-binding proteins that make contacts deep into the DNA, such as the Ku proteins,<sup>1</sup> could potentially be photo-cross-linked without binding to the platinum lesion. Eliminating this possibility is important because the protein poly(ADP-ribose) polymerase-1 (PARP-1), which binds to DNA ends,<sup>2</sup> was photo-cross-linked by the 25-bp probe. This type of study was the first evidence that PARP-1 has an affinity for platinum-modified DNA.<sup>3,4</sup> The 90-base dumbbell probe contains two loops instead of blunt ends (Figure 4.1). PARP-1 will bind to these loops, but only come in contact with the first four base pairs of the DNA.<sup>5</sup> In this manner, proteins with an affinity for the loops are isolated from the platination site. The proteins with an affinity for the PtBP6-modified 90-base dumbbell probe were

identified, and photo-cross-linking studies were carried out using nuclear extracts from several cancer cell lines with different sensitivities to cisplatin.

## II. MATERIALS AND METHODS

Solvents and chemical reagents were purchased from commercial sources. DNA strands were synthesized on an Applied Biosystems ABI 392 DNA/RNA synthesizer using solvents and reagents supplied by Glen Research. Enzymes were purchased from New England BioLabs and Promega. UV-vis spectra were obtained on an HP 8453 UV-visible spectrometer. Platinum analyses were performed by flameless atomic absorption spectroscopy on a Perkin-Elmer Analyst 300 system. Analytical and preparative HPLC work was performed on an Agilent 1200 HPLC system. UV irradiation was conducted in a Stratagene Stratalinker UV Crosslinker. Protein digestion and analyses were performed by trypsin digestion-coupled LC-MS/MS analysis at the MIT Biopolymers facility.

### *Cell culture*

Cells were grown and nuclear extracts prepared as described in Chapters 2 and 3. Testicular (NTera2), cervical (HeLa), bone (U2OS), pancreatic (BxPC3), and HeLa cells in which PARP-1 was silenced by RNAi (HeLa YS) were used for these experiments.

### *Synthesis and characterization of a site-specifically platinated 25-base DNA*

Synthesis and characterization of a 25-base DNA containing a 1,2-d(GpG) adduct of PtBP6 was carried out as described in Chapter 2.

### *Synthesis of a biotinylated 65-base DNA*

DNA having the sequence 5'-CCACACCCTTTTGGGTGTGGGGAGAGAAGATCCT-GAGAGGAGAGGGCCGAGTT(biotin-T)TTTAACTCGGC-3' (see also Figure 4.1) was



prepared at a 1  $\mu$ mol scale. Biotin-T represents a commercially available biotin-modified thymine phosphoramidite (Glen Research). The DNA was purified by 6% urea-PAGE and visualized by UV shadowing and excised. The DNA was extracted from the gel using the crush and soak method, and dialyzed versus water using dialysis tubing with a molecular weight cutoff of 3500 (Pierce).

*Synthesis of site-specifically modified 90-base probe*

For analytical-scale experiments, 100 pmol each of 25-PtBP6 and 65-biotin were radiolabeled using T4 PNK (New England Biolabs) and a mixture of unlabeled and  $\gamma$ - $^{32}$ P-ATP. The radiolabeled DNA was annealed in 100  $\mu$ L of NEBuffer 3 (New England BioLabs, 50 mM Tris-HCl pH 7.9, 100 mM NaCl, 10 mM MgCl<sub>2</sub>, 1 mM DTT) from 90 °C to 16 °C over 4 h. The DNA was ligated by the addition of 100  $\mu$ L of T4 DNA ligase reaction buffer (50 mM Tris-HCl, 10 mM MgCl<sub>2</sub>, 1 mM ATP, 10 mM DTT pH 7.5, 400 units T4 DNA ligase) and incubated at 16 °C overnight. The ligated DNA was analyzed and then purified by 6% urea-PAGE. The bands were isolated by autoradiography, followed by DNA extraction by the crush and soak method. The DNA was then re-annealed and ethanol precipitated.

For preparative-scale experiments, 2 nmol 65-biotin and 1 nmol each of platinated and unplatinated 25-base DNA were phosphorylated using T4 PNK and 10 mM ATP. The DNA was annealed and ligated in a method analogous to that used for the analytical-scale probes. The ligated DNA was purified by 6% urea-PAGE and the band was isolated by UV shadowing. The DNA was extracted from the gel using the crush and soak method. The 90-base DNA was then reannealed and ethanol precipitated.

*Characterization of site-specifically modified 90-base probe*

To ensure that the collected product contained one 65-base DNA and one 25-base DNA, the preparative-scale probe was analyzed by nuclease digestion. Each digestion used 75 pmol of purified DNA. The DNA was digested with exonuclease III, T7 exonuclease and mung bean nuclease for 1 h at 30 °C in 60 µL of NEBuffer 4 (50 mM potassium acetate, 20 mM tris-acetate, 10 mM magnesium acetate, 1 mM DTT pH 7.9). To the solution was then added 10 µL of 10X S1 nuclease buffer (500 mM sodium acetate pH 4.5, 2.8 M NaCl, 45 mM ZnSO<sub>4</sub>) and 10 µL of nuclease S1 (Promega). The solutions were mixed thoroughly and incubated at 37 °C overnight. Next, 5 µL of 1.5 M Tris-HCl (pH 8.8) and 1 µL of calf intestinal phosphatase (CIP) were added. After a 4-h incubation at 37 °C, the samples were centrifuged at 5000 rpm for 5 min. The supernatants were analyzed by RP-HPLC using a Supelcosil LC-18-S column. The eluant was a gradient of 5 – 15% B over 30 min, 15 – 80% B over 10 min, and 80% B for 5 min, where solvent A was 100 mM NaOAc, pH 5.2 and solvent B was methanol.

To examine whether the DNA was fully ligated, the analytical-scale probe was determined by digestion with mung bean nuclease, which cleaves the looped ends. The purity of the DNA was first analyzed by 6% urea-PAGE. As a control, a singly ligated 90-base probe was synthesized on the DNA synthesizer, purified, and radiolabeled as above. In an eppendorf tube, 1 pmol of DNA was incubated in MBN reaction buffer (50 mM sodium acetate, 150 mM NaCl, 1 mM ZnSO<sub>4</sub>, 5 units mung bean nuclease, pH 5.0) for 30 min at room temperature. The reactions were analyzed by 8% or 12% urea-PAGE.

*Analytical-scale photo-cross-linking of 90-base probe*

A 1 pmol quantity of DNA was incubated in 20 µL of binding buffer (10 mM Tris pH 7.5, 10 mM KCl, 10 mM MgCl<sub>2</sub>, 1 mM EDTA, 0.05% NP-40, 0.2 µg/mL BSA) with 20 µg of nuclear extracts from HeLa, NTera2, BxPC3, U2OS, and HeLa YS cells. The reactions were UV

irradiated for 2 h on ice and the photo-cross-links were resolved by 7.5% SDS-PAGE with a 4% stacking gel.

#### *90-base probe repair assay*

A 1 pmol quantity of DNA was incubated in 20  $\mu$ L of binding buffer with 20  $\mu$ g of nuclear extracts from HeLa, NTera2, BxPC3 U2OS, and HeLa YS cells. The reactions were incubated on ice for 2 h. A sample containing U2OS nuclear extracts was exposed to UV irradiation for 2 h to assess whether irradiation effects the stability of the DNA. The samples were phenol extracted and ethanol precipitated to remove proteins and concentrate the DNA. The samples were analyzed by 8% urea-PAGE.

#### *Preparative-scale photo-cross-linking of 90-base probe*

Preparative-scale experiments were carried out using methodology analogous to preparative-scale photo-cross-linking of 25-bp probe described in Chapter 2, except using 7.5% SDS-PAGE with a 4% stacking gel.

### III. RESULTS

A 90-base dumbbell probe containing a site-specific 1,2-d(GpG) intrastrand adduct of *cis*-[Pt(NH<sub>3</sub>)(*N*-(6-aminohexyl)-4-benzophenonamide)Cl<sub>2</sub>] (PtBP6) was synthesized and characterized. This probe was used in photo-cross-linking experiments to identify proteins with an affinity for the platinum-modified DNA.

#### *Synthesis of a site-specifically platinated 90-base probe*

Biotinylated 65-base DNA was synthesized on the DNA synthesizer and purified by 6% urea-PAGE. A total of 12.4 nmol was collected. The 65-base DNA and a PtBP6-modified 25-base DNA were phosphorylated, annealed, and ligated to make a 90-base dumbbell probe

(Figure 4.1). Formation of the 90-base probe was confirmed by 6% urea-PAGE analysis (Figure 4.2). The 90-base probe was isolated by 6% urea-PAGE and visualized by autoradiography. For the preparative-scale probe, the DNA was visualized by UV shadowing. UV shadowing detected a band migrating the same distance through the gel as the radiolabeled 90-base DNA product. The DNA was excised from the gel and isolated by the crush and soak method. Following extraction of the DNA from the gel, 630 pmol of preparative-scale 90-base probe was obtained.

#### *Characterization of the site-specifically platinated 90-base probe*

To determine whether the excised DNA contained the desired 90-base probe, the preparative-scale sample was analyzed by nuclease digestion. The digestion was altered from that in Chapters 2 and 3 by addition of an initial step with exonuclease III, T7 exonuclease, and mung bean nuclease. This step is necessary to digest the dumbbell and duplex DNA prior to incubation with the single-stranded exonuclease S1. An additional peak outside of the four base peaks is visible at 19.5 minutes (Figure 4.3). The ratios of optical bands, at 280 nm:260 nm for cytosine, thymine, guanine and adenine are expected to be 1.03, 0.66, 0.78 and 0.16, respectively.<sup>6</sup> Experimentally, these ratios were 1.06, 0.66, 0.79 and 0.20, in very good agreement with theoretical values. For the peak at 19.5 min, this ratio was 2.14, indicating that this peak is unlikely to contain a DNA base. RP-HPLC analysis of the buffers and enzymes alone (without DNA) indicates that this peak is an artifact and not the 90-base DNA (Figure 4.3A).

If the probe contained only 65-base DNA, the C:G:T:A ratio would be 13:23:15:14; for 25-base DNA, 12:2:9:2; and for 90-base DNA, 25:25:24:16. For the unplatinated probe (Figure 4.3B), the experimental ratio was 23.1:26.5:23.7:15.7 and for the platinated probe (Figure 4.3C) it was 24.1:25.9:23.6:15.4. These ratios compare well to the expected ratios of a 90-base probe, indicating that the DNA contains one of each 25- and 65-base DNA. The presence of a 90-base

DNA was demonstrated using these experiments; the structure of the 90-base DNA was investigated using mung bean nuclease digestion.

To determine whether the DNA was in the completely ligated dumbbell form, a radiolabeled sample was analyzed by digestion with mung bean nuclease (MBN, Figure 4.4). The purity of the DNA was first determined as 100% by 6% urea-PAGE analysis (Figure 4.5A). MBN digestion of 90-base dumbbell probes produced a radiolabeled DNA fragment of 41 bases (Figure 4.5B). MBN digestion of a 90-base DNA that is only singly ligated produces a radiolabeled DNA fragment of 33 bases (Figure 4.5C).

#### *90-base probe repair assay*

The 90-base probe remains intact following exposure to nuclear extracts from various cell lines or after UV irradiation (Figure 4.6). DNA exposed to nuclear extracts shows no difference from untreated DNA. The lane labeled “U2OS + UV” indicates that exposure to UV light also does effect the probe. If the dumbbell ends were severed from the probe, as was demonstrated by incubation with mung bean nuclease (Figure 4.5), a digestion product of 41 bases would be present. If the platinum adduct were excised by NER proteins, a DNA fragment of 28-32 bases would be seen on the gel.<sup>7</sup>

#### *Analytical-scale photo-cross-linking of 90-base probe*

Photo-cross-linking using a radiolabeled 90-base probe containing a site-specific 1,2-d(GpG) adduct of PtBP6 and nuclear extracts from various cancer cell lines yielded several protein-platinum-DNA complexes (Figure 4.7). The complexes appear to be consistent between nuclear extracts from cell lines with different sensitivities to cisplatin.

#### *Preparative-scale photo-cross-linking of 90-base probe*

Preparative-scale photo-cross-linking experiments using the 90-base dumbbell probe and HeLa nuclear extracts led to the identification of many nuclear proteins with an affinity for this DNA (Table 4.1). All of the proteins identified using the 25-bp probe in chapter 2 were detected with the 90-base probe. The transcription factor YB-1, mismatch repair proteins Msh3 and Msh6, excision repair proteins DDB1, RFC1 and RFC2, and the chromatin remodeling proteins SMARCA3, DNA topoisomerase I, protein polybromo-1 (PB-1), SMARCA4, SMARCC2 and FACT subunit SPT16 were also photo-cross-linked.

#### IV. DISCUSSION

Proteins photo-cross-linked by a 25-bp probe containing a site-specific 1,2-d(GpG) intrastrand adduct of PtBP6 also bind a PtBP6-modified 90-base dumbbell probe. This result assures that photo-cross-linking is not simply a consequence of affinity of certain proteins for DNA ends. Several other proteins were also photo-cross-linked by this probe.

##### *Mung bean nuclease analysis of 90-base dumbbell probe*

A radiolabeled 90-base DNA was synthesized from a PtBP6-modified 25-base DNA and a biotin-modified 65-base DNA (Figure 4.1). Purified DNA was analyzed by digestion with mung bean nuclease (MBN). Completely and partially ligated DNA result in different digestion products, so the assay is able to distinguish the product obtained in our synthesis (Figure 4.4). MBN can also slowly digest double-stranded DNA ends, resulting in a pattern of digested DNA demonstrated in Figure 4.5B and 4.5C. A singly-ligated 90-base probe was used as a control; the resulting digested DNA migrates as a 33-base DNA (Figure 4.5C). This assay was able to determine that the 90-base probe synthesized for photo-cross-linking experiments was fully ligated.

*The photo-cross-linking of PARP-1 is not due to an affinity for DNA ends*

The affinity of PARP-1 for platinum-damaged DNA was first established by photo-cross-linking experiments using PtBP6.<sup>3</sup> PARP-1 has an affinity for DNA ends,<sup>2</sup> and protein binding to the ends of the 25-bp probe could allow it to be photo-cross-linked. PARP-1 will also bind to DNA loops, but it only interacts with the four base pairs adjacent to the loop,<sup>5</sup> making it unlikely to be photo-cross-linked by the 90-base probe if bound in this manner. The photo-cross-linking of PARP-1 by the 90-base DNA probe demonstrates that the protein has an affinity for platinum-damaged DNA.

PARP-1 contains two zinc finger DNA-binding domains, a catalytic domain and a BRCT domain responsible for mediating protein-protein interactions.<sup>2</sup> Although the zinc fingers of certain proteins, such the Wilms tumor suppressor protein (WT1), bind in the major groove of DNA,<sup>8</sup> such is not the case for PARP-1. A solution structure of the zinc finger of DNA ligase III $\alpha$ , which is homologous to those in PARP-1, indicates that major groove-binding of these zinc fingers would not be possible due to steric interactions.<sup>9</sup> In cisplatin-modified DNA, the platinum adduct causes the DNA to bend toward the major groove, resulting in a wide shallow minor groove.<sup>10</sup> A zinc finger is unlikely to bind to the distorted major groove of platinum-modified DNA, suggesting that the distorted helical structure of damaged DNA creates a recognition site for zinc fingers of PARP-1.<sup>9,11</sup>

The DNA-end binding proteins Ku70 and Ku80 were photo-cross-linked by the 90-base probe. These proteins bind to DNA double-strand breaks as well as loops,<sup>12</sup> and they form a complex that translocates along the DNA duplex.<sup>13</sup> The DNA-bound Ku proteins recruit DNA-PK<sub>cs</sub>.<sup>14</sup> Due to this activity, photo-cross-linking of these proteins to the 90-base probe was expected. Investigating the specificity of the Ku proteins for cisplatin-modified DNA remains a

challenge due to the affinity of these proteins for various DNA structures, such as loops and blunt ends.

*Mismatch repair recognition complexes Msh2/Msh3 and Msh2/Msh6 both bind to platinum-modified DNA*

The binding of mismatch proteins to cisplatin-damaged DNA is relevant to the anti-proliferative effects of the drug and is discussed in detail in the literature.<sup>15-21</sup> The affinity of MMR protein Msh2 for various constructs of cisplatin-modified DNA has been demonstrated.<sup>15,22</sup> Msh2 forms a complex with either Msh3 or Msh6 when it binds to mismatched DNA. These two distinct mismatch repair recognition complexes have different affinities for certain types of mismatched bases and nucleotide insertions or deletions.<sup>23</sup> The current study establishes that both protein complexes Msh2/Msh3 and Msh2/Msh6 will bind to platinum-modified DNA.

*The photo-cross-linking of SPT16 gives structural information about the binding of the FACT complex to platinum-modified DNA*

Facilitates chromatin transcription (FACT) complex subunit SPT16 increases the affinity of the other subunit of FACT, the HMG-domain protein SSRP1, for cisplatin-modified DNA.<sup>4</sup> Structural analysis of the HMG-domains of HMGB1 indicate that these domains bind to the widened minor groove of cisplatin-modified DNA, opposite the lesion itself.<sup>24,25</sup> The photo-cross-linking of the SPT16 subunit but not SSRP1 suggests that SSRP1 binds to the opposite side of the DNA with SPT16 directed toward the platinum adduct. The photo-cross-linking of this protein demonstrates that the protein will bind to platinum-modified DNA in the context of the nuclear milieu and is relevant to the processing of these adducts.

*Proteins implicated in nucleotide excision repair bind to PtBP6-modified DNA*



The DNA damage binding protein-1 (DDB-1), which is the 142 kDa subunit of the complex DDB, originally known as xeroderma pigmentosum complementation group E protein binding factor (XPE-BF), was photo-cross-linked by the 90-base probe. The cisplatin-modified DNA-binding ability of this protein was demonstrated by using electrophoretic mobility shift assays (EMSAs) with extracts from XPE cells, which contain mutated DDB-1.<sup>26,27</sup> This protein stimulates nucleotide excision repair (NER) of UV-damaged DNA,<sup>28</sup> although it is not necessary for the repair of the 1,3-d(GpTpG) intrastrand adduct of cisplatin.<sup>29</sup> The role of this protein in cisplatin-damaged DNA repair is not well understood; it may be one of the first NER proteins to bind to damaged DNA.<sup>30</sup>

The transcription factor YB-1, which was photo-cross-linked by the 90-base probe, binds to cisplatin-modified DNA.<sup>31</sup> The consequences of this binding may derive from the interaction of YB-1 with proliferating cell nuclear antigen (PCNA), a protein necessary for NER.<sup>10,32</sup> Another PCNA-interacting protein photo-cross-linked by our probe is replication factor C (RFC).<sup>30</sup> Five RFC proteins are involved in DNA replication and repair.<sup>33</sup> RFC1 binds to double-stranded DNA and interacts with PCNA to initiate transcription.<sup>33</sup> A role for RFC1 in DNA repair is supported by experiments demonstrating that the protein is necessary to promote cell survival following cisplatin or UV exposure.<sup>34</sup> The protein RFC2 was also photo-cross-linked. RFC2 binds to damaged DNA downstream of damage recognition in the nucleotide excision repair pathway following excision of the damaged bases.<sup>35,36</sup> It may be responsible for keeping the damage response activated until repair is completed.<sup>37</sup>

Since RFC2 binds to damaged DNA following excision of the lesion, the nature of the 90-base probe following incubation with nuclear extracts was investigated. After incubation with nuclear extracts, the DNA was analyzed by PAGE, which indicated that the platinum lesion was

not excised during the incubation period (Figure 4.6). This result indicates that RFC2 can bind to platinum-damaged DNA prior to excision of the lesion. The experiment also demonstrates that the dumbbell DNA structure is stable in nuclear extracts, consistent with other studies of this type of DNA.<sup>38</sup> The stability of dumbbell DNA structures in biological media has led to an investigation of their therapeutic potential as decoys for transcription factors.<sup>39</sup>

#### *Chromatin remodeling proteins bind to platinum-modified dumbbell DNA*

The binding of DNA topoisomerase I (topo I) to closed circular DNA and DNA-histone complexes containing cisplatin adducts indicates that this protein may be important in processing the adducts.<sup>40,41</sup> Topo I relaxes superhelical DNA by severing one strand, crossing the unbroken strand through the break, and then re-ligating the broken strand. This function is necessary for transcription.<sup>42</sup> The stalling of topo I at DNA damage sites can interfere with repair, an effect blocked by poly(ADP-ribosyl)ation of topo I by PARP-1 and PARP-2, which dissociates the protein from DNA.<sup>43</sup> The combination of cisplatin and topo I poisons, such as camptothecin, has showed improved response in clinical trials.<sup>44</sup> The synergistic cell-killing by these two drugs is not well understood, but the effect only occurs in cells with a functional homologous recombination repair pathway.<sup>45</sup> The ability of topo I to bind non-nucleosomal platinum-modified DNA has not been established, but the current study demonstrates that the interaction will occur in nuclear extracts.

The SWI/SNF family proteins SMARCA3, SMARCA4, SMARCC2 and protein polybromo-1 (PB-1) were photo-cross-linked by the 90-base dumbbell probe. The acronym SMARC stands for SWI/SNF-related matrix-associated actin-dependent regulators of chromatin. These proteins are responsible for chromatin remodeling, which allows the transcription machinery to process DNA that is tightly wrapped around histones.<sup>46</sup> One member of this

family, PB-1, contains an HMG-domain,<sup>47</sup> which may bind to the platinum site and recruit the other SWI/SNF proteins. The affinity of PB-1 and the SWI/SNF family of proteins for platinum-modified DNA has not been demonstrated prior to the present work. The ability of these proteins to bind to platinum-modified DNA may inhibit excision of the adduct by NER proteins or hijack the proteins from their native functions.

*PtBP6-modified DNA is able to photo-cross-link proteins with low cellular abundance*

The binding of proteins to DNA is an equilibrium process, but photo-cross-linking creates a covalent bond, which prevents proteins from dissociation. Due to this covalent linkage, any protein with an affinity for platinum-modified DNA will be photo-cross-linked by the probe. As few as 500 zeptomoles of trypsin-digested peptides can be detected by the Thermo Electron Model LTQ Ion Trap mass spectrometer used in our experiments.<sup>48</sup> In practice, the instrument used in these studies will detect sub-femtomolar amounts of peptide in complex mixtures,<sup>49</sup> corresponding to fewer than  $6.02 \times 10^8$  molecules. We used 2 mg of nuclear extracts for each experiment, obtained from approximately  $6 \times 10^7$  cells. These considerations indicate that proteins expressed at a level as low as ten copies per cell should be detectable by our methods.

Several highly abundant proteins present at upwards of  $10^5$  molecules per cell were identified using Pt-BP6-modified DNA, including PARP-1<sup>50</sup> and the Ku proteins.<sup>51</sup> Other proteins identified are not nearly as abundant, such as the MMR proteins Msh2, Msh3, and Msh6, as well as the SWI/SNF family proteins, for which there are only 100-200 molecules per cell,<sup>52,53</sup> and DDB1, which is present at 8,000 molecules per cell.<sup>54</sup> The expression of HMGB3 in adult tissues was undetectable by RT-PCR,<sup>55</sup> but was identified using our methodology. The identification of these proteins demonstrates that these photo-cross-linking experiments provide a very sensitive method for detection of platinum-damaged DNA-binding proteins. It is likely that

most if not all of the cisplatin-DNA binding proteins expressed in the cancer cells investigated have been identified in this study.

*Recognition of platinum-modified DNA is consistent between cancer cell lines*

Analytical-scale photo-cross-linking using nuclear extracts from various cell lines indicated that, similar to the results with the 25-bp probe described in Chapter 3, the same proteins are photo-cross-linked in each extract (Figure 4.7). Photo-cross-linking with nuclear extracts from PARP-1 silenced HeLa cells (Figure 4.7, lane 5) demonstrates that the band consisting of a PARP-1-platinum-DNA complex overlaps with other complexes and was not resolved. These data suggest that recognition of the damaged DNA is not responsible for the varying sensitivities of these cell lines to cisplatin.

## V. CONCLUSIONS

Using a 90-base dumbbell probe, proteins binding to a 1,2-d(GpG) intrastrand platinum lesion were identified. This probe is superior to previous work using a 25-bp probe, discussed in Chapters 2 and 3, because a longer DNA was used that does not contain blunt ends. The proteins identified by the 25-bp probe were also photo-cross-linked by the 90-base dumbbell probe. Additional proteins were identified as well, including members of the SWI/SNF family, such as the HMG-domain protein PB-1. The affinity of these proteins, and the protein DNA topoisomerase I, for platinum-damaged DNA could provide new insight into the processing of platinum-DNA adducts. The 90-base probe also photo-cross-linked to the proteins FACT, DDB1 and YB-1, which have an affinity for cisplatin-modified DNA. Although the affinity of the mismatch repair protein Msh2 for cisplatin-damaged DNA has been studied extensively, this work was able to demonstrate that both mismatch repair recognition complexes Msh2/Msh3 and

Msh2/Msh6 bind to platinum-modified DNA. Given the number of proteins that bind to this longer probe, it is remarkable that the same families of proteins that have been implicated binding to cisplatin-modified DNA for years are identified by this photo-cross-linking method.

## VI. REFERENCES

1. Walker, J. R.; Corpina, R. A.; Goldberg, J., *Nature* **2001**, 412, 607-614.
2. Kim, M. Y.; Zhang, T.; Kraus, W. L., *Genes Dev.* **2005**, 19, 1951-1967.
3. Zhang, C. X.; Chang, P. V.; Lippard, S. J., *J. Am. Chem. Soc.* **2004**, 126, 6536-6537.
4. Yarnell, A. T.; Oh, S.; Reinberg, D.; Lippard, S. J., *J. Biol. Chem.* **2001**, 278, 25736-25741.
5. Potaman, V. N.; Shlyakhtenko, L. S.; Oussatcheva, E. A.; Lyubchenko, Y. L.; Soldatenkov, V. A., *J. Mol. Biol.* **2005**, 348, 609-615.
6. Andrus, A.; Kuimelis, R. G., Unit 10.3: Overview of Purification and Analysis of Synthetic Nucleic Acids. In *Current Protocols in Nucleic Acid Chemistry*, Beaucage, S. L., Ed. John Wiley & Sons: New York City, 2000; pp 10.3.1-10.3.6.
7. Reardon, J. T.; Vaisman, A.; Chaney, S. G.; Sancar, A., *Biochemistry* **1999**, 39, 3968-3971.
8. Stoll, R.; Lee, B. M.; Debler, E. W.; Laity, J. H.; Wilson, I. A.; Dyson, H. J.; Wright, P. E., *J. Mol. Biol.* **2007**, 372, 1227-1245.
9. Kulczyk, A. W.; Yang, J.-C.; Neuhaus, D., *J. Mol. Biol.* **2004**, 341, 723-738.
10. Jamieson, E. R.; Lippard, S. J., *Chem. Rev.* **1999**, 99, 2467-2498.
11. Petrucco, S.; Percudani, R., *FEBS Journal* **2008**, 275, 883-893.
12. Arosio, D.; Cui, S.; Ortega, C.; Chovanec, M.; Marco, S. D.; Baldini, G.; Falaschi, A.; Vindigni, A., *J. Biol. Chem.* **2002**, 277, 9741-9748.
13. Turchi, J. J.; Henkels, K. M.; Zhou, Y., *Nucleic Acids Res.* **2000**, 28, 4634-4641.
14. Pawelczak, K. S.; Andrews, B. J.; Turchi, J. J., *Nucleic Acids Res.* **2005**, 33, 152-161.
15. Fourrier, L.; Brooks, P.; Malinge, J.-M., *J. Biol. Chem.* **2003**, 278, 21267-21275.
16. Lin, X.; Kim, H.-K.; Howell, S. B., *J. Inorg. Biochem.* **1999**, 77, 89-93.
17. Schofield, M. J.; Hsieh, P., *Annu. Rev. Microbiol.* **2003**, 57, 579-608.
18. Fink, D.; Zheng, H.; Nebel, S.; Norris, P. S.; Aebi, S.; Lin, T.-P.; Nehme, A.; Christen, R. D.; Haas, M.; Macleod, C. L.; Howell, S. B., *Cancer Res.* **1997**, 57, 1841-1845.
19. Fink, D.; Nebel, S.; Aebi, S.; Zheng, H.; Cenni, B.; Nehmé, A.; Christen, R. D.; Howell, S. B., *Cancer Res.* **1996**, 56, 4881-4886.
20. Meyers, M.; Hwang, A.; Wagner, M. W.; Boothman, D. A., *Environ. Mol. Mutagen.* **2004**, 44, 249-264.
21. Chao, E. C.; Lipkin, S. M., *Nucleic Acids Res.* **2006**, 34, 840-852.
22. Duckett, D. R.; Drummond, J. T.; Murchie, A. I. H.; Reardon, J. T.; Sancar, A.; Lilley, D. M. J.; Modrich, P., *Proc. Natl. Acad. Sci. U.S.A.* **1996**, 93, 6443-6447.
23. Acharya, S.; Wilson, T.; Gradia, S.; Kane, M. F.; Guerrette, S.; Marsischky, G. T.; Kolodner, R.; Fishel, R., *Biochemistry* **1996**, 35, 13629-13624.
24. He, Q.; Ohndorf, U.-M.; Lippard, S. J., *Biochemistry* **2000**, 39, 14426-14435.
25. Takahara, P. M.; Rosenzweig, A. C.; Frederick, C. A.; Lippard, S. J., *Nature* **1995**, 377, 649-652.
26. Chu, G.; Chang, E., *Science* **1988**, 242, 564-567.
27. Chu, G.; Chang, E., *Proc. Natl. Acad. Sci. U.S.A.* **1990**, 87, 3324-3327.
28. Wakasugi, M.; Kawashima, A.; Morioka, H.; Linn, S.; Sancar, A.; Mori, T.; Nikaido, O.; Matsunaga, T., *J. Biol. Chem.* **2002**, 277, 1637-1640.

29. Moggs, J. G.; Yarema, K. J.; Essigmann, J. M.; Wood, R. D., *J. Biol. Chem.* **1996**, 271, 7177-7186.
30. Gillet, L. C. J.; Schärer, O. D., *Chem. Rev.* **2006**, 106, 253-276.
31. Ise, T.; Nagatani, G.; Imamura, T.; Kato, K.; Takano, H.; Nomoto, M.; Izumi, H.; Ohmori, H.; Okamoto, T.; Ohga, T.; Uchiumi, T.; Kuwano, M.; Kohno, K., *Cancer Res.* **1999**, 59, 342-346.
32. Kartalou, M.; Essigmann, J. M., *Mutat. Res.* **2001**, 478, 23-43.
33. Mossi, R.; Hübscher, U., *Eur. J. Biochem.* **1998**, 254, 209-216.
34. Pennaneach, V.; Salles-Passador, I.; Munshi, A.; Brickner, H.; Regazzoni, K.; Dick, F.; Dyson, N.; Chen, T.-T.; Wang, J. Y. J.; Fotedar, R.; Fotedar, A., *Mol. Cell* **2001**, 7, 715-727.
35. Rechkunova, N. I.; Maltseva, E. A.; Lavrik, O. I., *Mol. Biol.* **2008**, 42, 20-26.
36. Friedberg, E. C., *Nat. Rev. Cancer* **2001**, 1, 22-33.
37. Zhou, B.-B. S.; Elledge, S., *Nature* **2000**, 408, 433-439.
38. Chu, B. C. F.; Orgel, L. E., *Nucleic Acids Res.* **1992**, 20, 5857-5858.
39. Hosoya, T.; Takeuchi, H.; Kanesaka, Y.; Yamakawa, H.; Miyano-Kurosaki, N.; Takai, K.; Yamamoto, N.; Takaku, H., *FEBS Lett.* **1999**, 461, 136-140.
40. Kobayashi, S.; Furukawa, M.; Dohi, C.; Hamashima, H.; Arai, T.; Tanaka, A., *Chem. Pharm. Bull.* **1999**, 47, 783-790.
41. Kobayashi, S.; Nakagawa, S.; Uehara, N.; Hamashima, H.; Tanaka, A., *Nucleic Acids Symp. Ser.* **2002**, 2, 283-284.
42. Wang, J. C., *Ann. Rev. Biochem.* **1996**, 65, 635-692.
43. Malanga, M.; Althaus, F. R., *J. Biol. Chem.* **2004**, 279, 5244-5248.
44. Gelderblom, H. A. J.; de Jonge, M. J. A.; Sparreboom, A.; Verweij, J., *Invest. New Drugs* **1999**, 17, 401-415.
45. van Waardenburg, R. C. A. M.; de Jong, L. A.; van Delft, F.; van Eijndhoven, M. A. J.; Bohlander, M.; Bjornsti, M.-A.; Brouwer, J.; Schellens, J. H. M., *Mol. Cancer Ther.* **2004**, 3, 393-402.
46. Saha, A.; Wittmeyer, J.; Cairns, B. R., *Nat. Rev. Mol. Cell Biol.* **2006**, 7, 437-447.
47. Štros, M.; Launholt, D.; Grasser, K. D., *Cell Mol. Life Sci.* **2007**, 64, 2590-2606.
48. Mayya, V.; Rezaul, K.; Cong, Y.-S.; Han, D., *Mol. Cell. Proteomics* **2005**, 4, 214-223.
49. Papayannopoulos, I. A., *Personal Communication*.
50. D'Amours, D.; Desnoyers, S.; D'Silva, I.; Poirier, G. G., *Biochem. J.* **1999**, 342, 249-268.
51. Lieber, M. R.; Ma, Y.; Pannicke, U.; Schwarz, K., *Nat. Rev. Mol. Cell Biol.* **2003**, 4, 712-720.
52. Feng, G.; Tsui, H.-C. T.; Winkler, M. E., *J. Bacteriol.* **1996**, 178, 2388-2396.
53. Cairns, B. R.; Lorch, Y.; Li, Y.; Zhang, M.; Lacomis, L.; Erdjument-Bromage, H.; Tempst, P.; Du, J.; Laurent, B.; Kornberg, R. D., *Cell* **1996**, 87, 1249-1260.
54. Precious, B. L.; Carlos, T. S.; Goodbourn, S.; Randall, R. E., *Virology* **2007**, 368, 114-121.
55. Vaccari, T.; Beltrame, M.; Ferrari, S.; Bianchi, M. E., *Genomics* **1998**, 49, 247-252.
56. Huang, J.-C.; Zamble, D. B.; Reardon, J. T.; Lippard, S. J.; Sancar, A., *Proc. Natl. Acad. Sci. U.S.A.* **1994**, 91, 10394-10398.
57. Robert, J., 2007, *Personal Communication*.

58. Robert, J.; Laurand, A.; Meynard, D.; Le Morvan, V. In Platinum drugs and DNA repair. Lessons from the NCI-60 panel and clinical correlates, 10th International Symposium on Platinum Coordination Compounds in Cancer Chemotherapy, Verona, Italy; 2007.
59. Thomas, J. O.; Travers, A. A., *Trends Biochem. Sci.* **2001**, 26, 167-174.
60. Collis, S. J.; DeWeese, T. L.; Jeggo, P. A.; Parker, A. R., *Oncogene* **2005**, 24, 949-961.
61. Treiber, D. K.; Zhai, X.; Jantzen, H.-M.; Essigmann, J. M., *Proc. Natl. Acad. Sci. U.S.A.* **1994**, 91, 5672-5676.
62. Schreiber, V.; Dantzer, F.; Amé, J.-C.; de Murcia, G., *Nat. Rev. Mol. Cell Biol.* **2006**, 7, 517-528.
63. Bouchard, V. J.; Rouleau, M.; Poirier, G. G., *Exp. Hematol.* **2003**, 31, 446-454.



## VII. TABLES

Table 4.1. Proteins identified by preparative scale photo-cross-linking of a 90-base DNA containing a 1,2-d(GpG) intrastrand PtBP6 adduct.

Band <sup>a</sup>	Protein <sup>b</sup>	Probability <sup>c</sup>	Unique Peptides <sup>d</sup>	M.W. (Da)	Comments
1	HMGB1	2.36E-05	1	24878.2	HMGB1 shields cisplatin-DNA adducts from excision repair <sup>56</sup>
	HMGB2	3.80E-08	1	24018.7	Analysis of the NCI library of cancer cell lines reveals a correlation between cells expressing high levels of HMGB1 and cisplatin sensitivity <sup>57,58</sup>
	HMGB3	8.64E-08	1	22980.0	HMGB1, HMGB2 and HMGB3 are chromatin architectural proteins <sup>59</sup>
2	YB-1	8.32E-07	1	35902.7	Y-box binding protein-1 (YB-1) is a transcription factor containing a cold-shock domain (CSD) that binds to cisplatin-modified DNA <sup>31</sup>
	RFC2	3.31E-05	2	39132.1	Involved in intermediate steps of nucleotide excision repair <sup>33</sup>
3	Ku70	7.29E-08	11	69799.2	Ku70 and Ku80 are members of the DNA-PK complex (Ku70, Ku80, DNA-PK <sub>cs</sub> ) involved in nonhomologous end-joining repair of double-strand breaks <sup>60</sup>
4	Msh2	1.70E-07	9	112834.9	Protein involved in the recognition of base pair mismatches <sup>17</sup>
	Ku70	3.72E-07	8	69799.2	
	Ku80	3.89E-07	3	82652.4	
	UBF1	7.21E-07	1	89350	HMG-domain protein responsible for initiation of RNA polymerase I <sup>61</sup>
	Msh3	5.72E-06	2	127376.1	Protein involved in the recognition of base pair mismatches <sup>17</sup>
	DNA topo I	1.05E-05	3	90668.9	Chromatin remodeling protein involved in relaxing superhelical DNA <sup>42</sup>
5	PARP-1	1.61E-11	13	113012.4	DNA damage-binding protein involved in repair and apoptosis signaling <sup>62</sup>
	RFC1	2.67E-10	4	128175	Binds to double-stranded DNA and interacts with PCNA to initiate transcription. <sup>33</sup>
	PB-1	2.02E-09	5	192823.9	SWI/SNF chromatin remodeling protein containing an HMG-domain <sup>47</sup>
	Msh3	4.04E-06	3	127376.1	
	SMARCA4	2.14E-09	4	184529.4	SWI/SNF chromatin remodeling protein <sup>46</sup>
	SMARCA3	1.31E-08	2	113856.7	SWI/SNF chromatin remodeling protein <sup>46</sup>
	DNA Ligase III	1.91E-08	10	112834.9	DNA repair protein that associates with PARP-1 <sup>63</sup>
	DDB1	7.71E-05	2	126887.4	Nucleotide excision repair protein that binds to cisplatin-modified DNA. <sup>10,26,27,32</sup>
6	PARP-1	6.32E-08	7	113012.4	
	SMARCC2	2.69E-06	2	132796.8	SWI/SNF chromatin remodeling protein <sup>46</sup>
	DNA Ligase III	7.68E-07	5	112834.9	

Msh6	2.44E-07	1	152688.4	Protein involved in the recognition of base pair mismatches <sup>17</sup>
Msh2	2.75E-06	3	104676.8	
SPT16	4.93E-05	2	119838.3	FACT complex subunit that increases the affinity of the HMG-domain protein SSRP1 for cisplatin-modified DNA. <sup>4</sup>
7 DNA-PKcs	1.48E-08	15	468786.9	

<sup>a</sup>The LC-MS/MS analysis was carried out on six gel slices corresponding to the bands indicated in Figure 4.7. The proteins found in each band are listed here. <sup>b</sup>Proteins identified as described in the Materials and Methods section. <sup>c</sup>Probability of the peptide identification being an artifact of background signal from the LC-MS/MS instrument. For example, a probability of 1.0E-4 indicates that there is a 0.01% chance that the identified peptide is not actually present in the sample. The values listed correspond to the peptide most likely to be present for each protein. <sup>d</sup>The number of peptides identified for each protein. Peptides differing by only one amino acid were not considered to be unique.

VIII. FIGURES

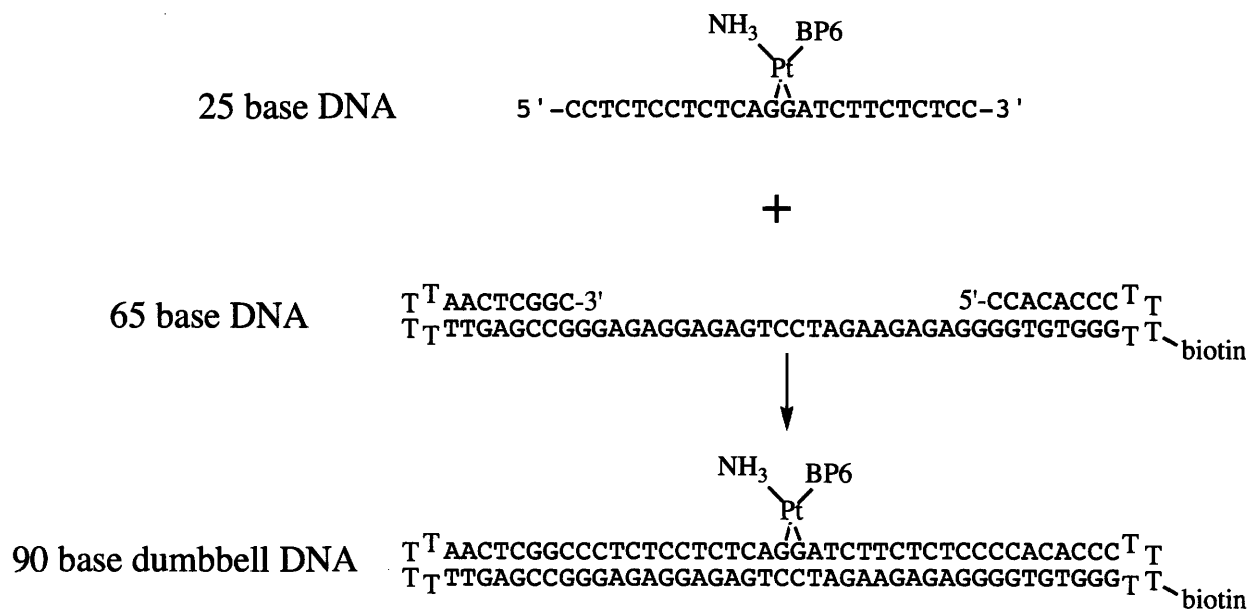


Figure 4.1. Synthesis of 90-base dumbbell DNA from a PtBP6-modified 25-base DNA and biotinylated 65-base DNA.

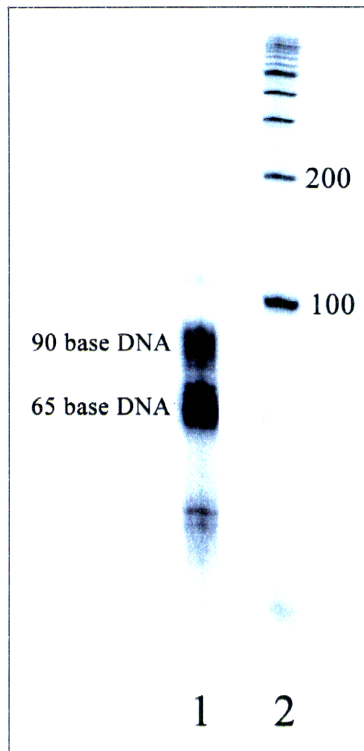


Figure 4.2. 6% urea-PAGE analysis of synthesis of 90-base DNA.

Lane 1: 90-base DNA reaction. Lane 2: 100 base DNA ladder.

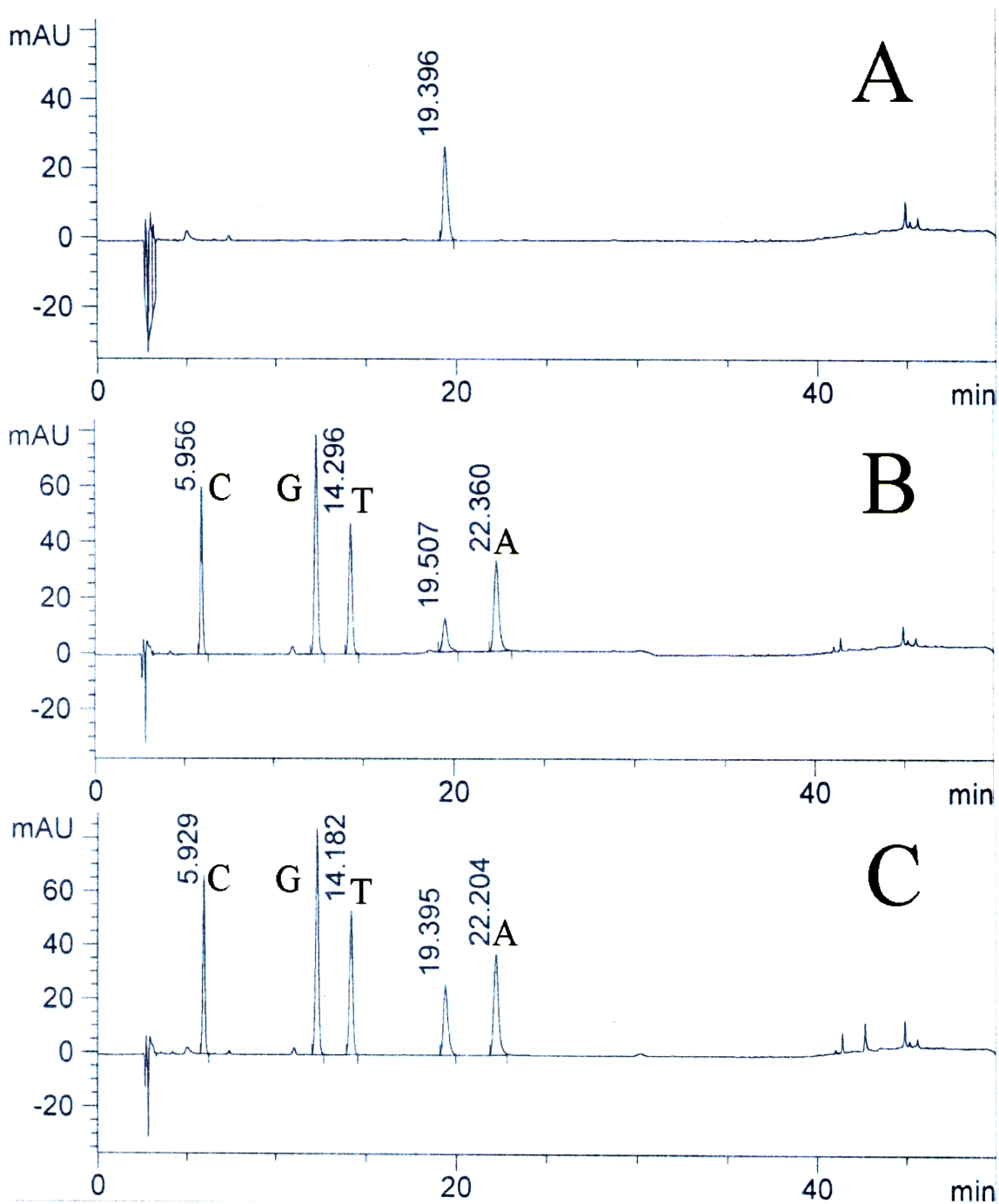


Figure 4.3. Nuclease digestion of the 90-base DNA probe.

(A) No DNA. (B) 90-base probe. (C) PtBP6-modified 90-base probe.

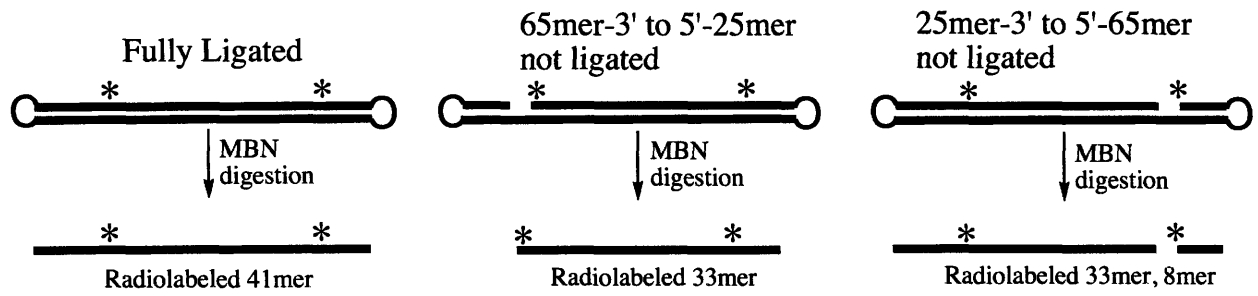


Figure 4.4. Mung bean nuclease digestion of 90-base DNA.

Digestion with this nuclease can differentiate fully and partially ligated 90-base DNA strands.

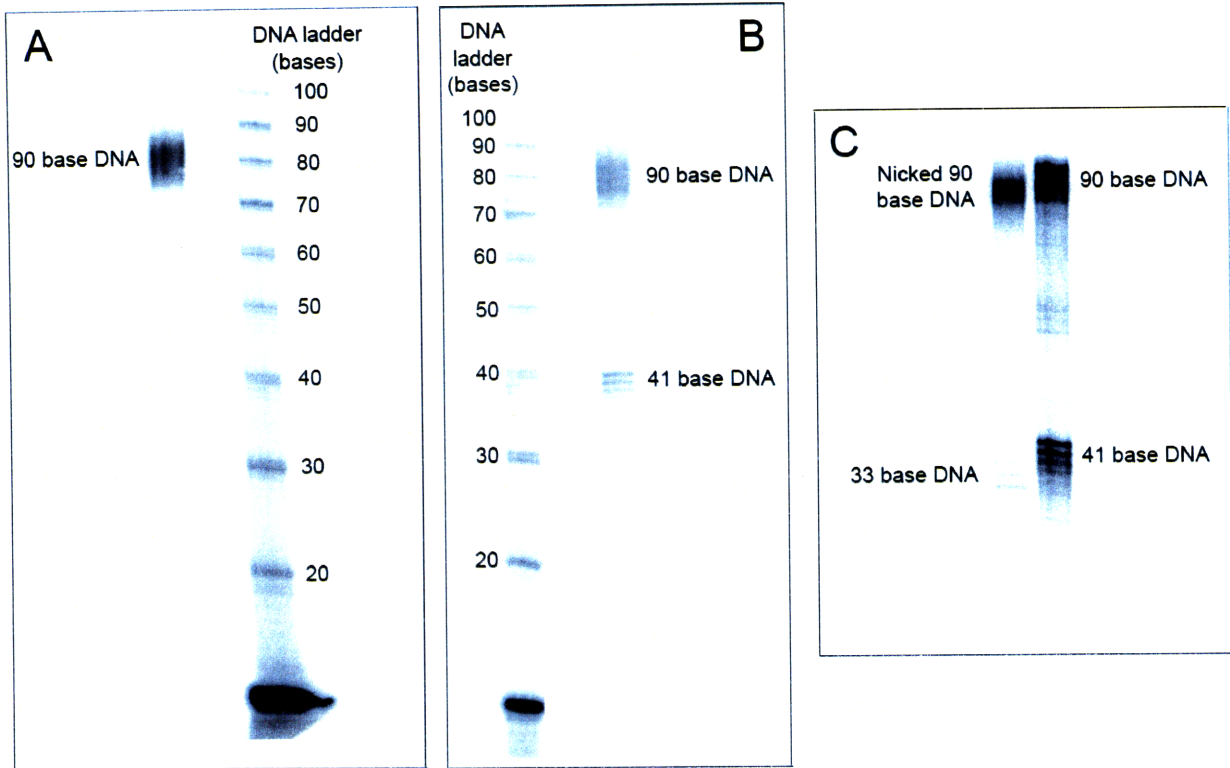


Figure 4.5. Analysis of purified 90-base DNA probe.

(A) 6% urea-PAGE analysis of purified 90-base DNA. (B) 8% urea-PAGE analysis of MBN-digested 90-base DNA probe. (C) 8% urea-PAGE analysis of MBN-digested 90-base DNA probe and control with nicked 90-base DNA. The 41 bases DNA digestion product indicates that the 90-base DNA is doubly ligated, and the 33-base DNA digestion product indicates that the 90-base DNA contains a nick. This is illustrated in figure 3.

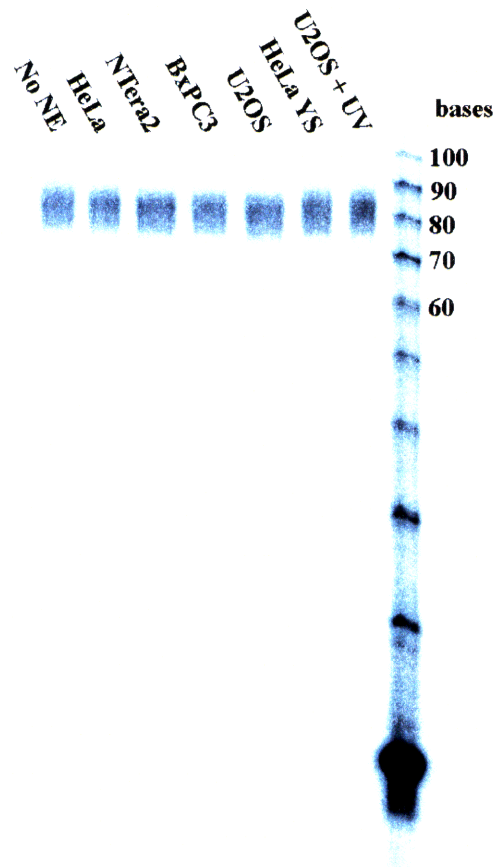


Figure 4.6. 90-base probe repair assay.

90-base dumbbell probe was incubated with nuclear extracts for 2 h and analyzed by 6% urea-PAGE. The DNA was stable in all nuclear extracts, even after UV irradiation.



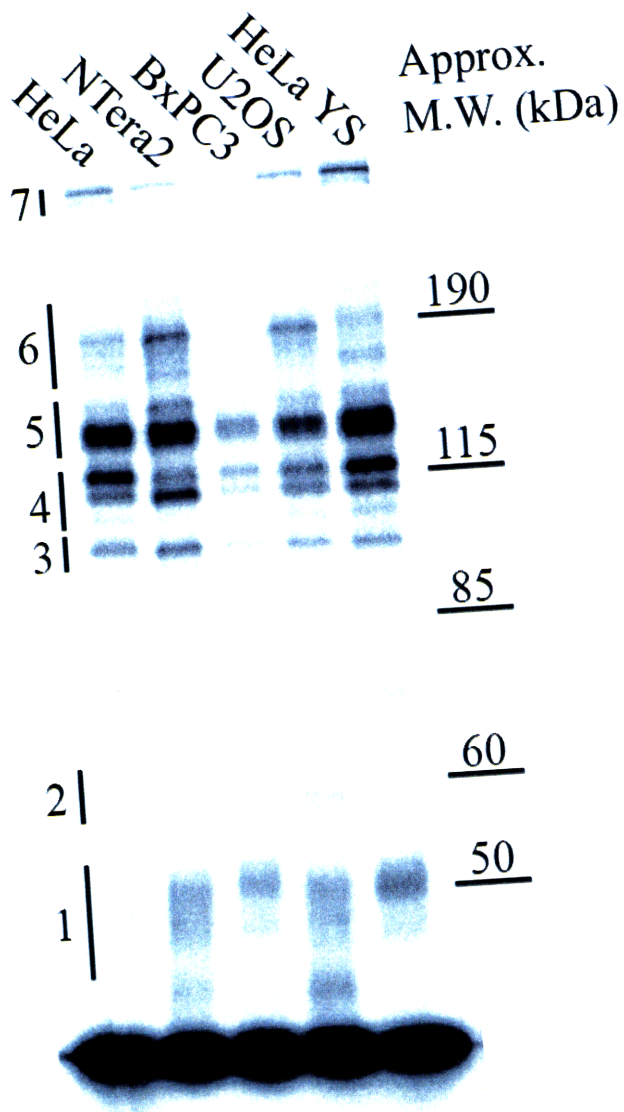


Figure 4.7. Photo-cross-linking with 90-base DNA probe using nuclear extracts from various cancer cell lines.

The numbers represent the bands from Table 4.1. The proteins photo-cross-linked between different nuclear extracts are consistent. The proteins in Table 4.1 match well to the approximate molecular weight marker; each protein is tethered to a 29 kDa platinated DNA.

**Chapter 5: The activity of PARP proteins following cisplatin exposure  
in cancer cells is cell line-dependent.**

\* Work from this chapter was submitted for publication; Guggenheim, E. R., Ondrus, A. E., Movassaghi, M., Lippard, S. J., "Poly(ADP-ribose) Polymerase-1 Activity Facilitates the Dissociation of Nuclear Proteins from Platinum-Damaged DNA."

## I. INTRODUCTION

In Chapters 3 and 4, the protein poly(ADP-ribose) polymerase-1 (PARP-1) was identified as a possible mediator of cisplatin cytotoxicity in NTERA2 cells, a testicular cancer cell line with an exceptional sensitivity to cisplatin. These cells express high levels of PARP-1, which binds to platinum-modified DNA. PARP-1 is a 113 kDa DNA-binding protein that catalyzes the addition of poly(ADP-ribose) (PAR) chains onto acceptor proteins (Figure 5.1), including PARP-1 itself. The activity of the PARP family of proteins has been implicated in DNA repair, chromatin remodeling, transcriptional control, and inflammation.<sup>1</sup> PARP-1 has a DNA-binding domain with two zinc fingers, an automodification domain, and a catalytic domain. The catalytic domain binds nicotinamide adenine dinucleotide (NAD<sup>+</sup>) and creates long, branched PAR chains in which each unit contains two negatively charged phosphate linkers (Figure 5.1A). These polymers can be digested by poly(ADP-ribose) glycohydrolase (PARG) which can restore proteins to their unmodified form.<sup>1</sup>

Upon exposure of cells to DNA-damaging agents, PARP proteins are strongly activated. PARP can activate three different pathways (Figure 5.2).<sup>2</sup> Under mild conditions, PARP proteins mediate DNA damage repair. PARP-1 is involved in base excision repair (BER)<sup>3</sup> and a backup pathway for nonhomologous end-joining (NHEJ) repair of double-strand breaks.<sup>4,5</sup> When DNA damage is too severe to be repaired efficiently, the PAR polymers created by PARP proteins signal the release of apoptosis-inducing factor (AIF) from mitochondria, which initiates apoptosis.<sup>6</sup> Apoptosis induced by cisplatin is due to both caspase- and AIF-dependent signaling mechanisms.<sup>7</sup> Under severe DNA damage conditions, the activity of PARP proteins depletes cellular reservoirs

of NAD<sup>+</sup>. The depletion of NAD<sup>+</sup> leads to shutdown of glycolysis, and since cancer cells rely on glycolysis for ATP production, the cells die by necrosis.<sup>8</sup>

The attachment of PAR polymers to proteins is an important biochemical mechanism. Automodified PARP-1 interacts with XRCC1, which may be responsible for the initiation of the base excision repair pathway.<sup>1</sup> A PAR-binding motif has been identified in DNA repair proteins, and this type of domain is present in core histones, p53, DNA topoisomerase I, Ku70, XPA, Msh6, DNA Ligase III, and XRCC1.<sup>9-11</sup> Negatively charged PAR polymers create an electrostatic repulsion between modified proteins and polyanionic DNA (Figure 5.1B). For example, the poly(ADP-ribosyl)ation of histones contributes to chromatin relaxation, making damaged DNA more accessible to repair proteins.<sup>1</sup> The C-terminal domain of the chromatin remodeling protein HMGB1 is poly(ADP-ribosyl)ated by PARP-1, causing it to dissociate from chromatin and translocate to the cytosol.<sup>12,13</sup> PARP inhibitors show promise for treating tumors with mutations in BRCA1 and BRCA2 genes, a feature of certain types of breast cancer. Inhibition of PARPs may lead to the inability of the cells to repair single-strand breaks at replication forks, causing the formation of double-strand breaks (DSBs). These DSBs cannot be repaired efficiently in BRCA-defective cells, which are intrinsically defective in homologous recombination (HR).<sup>14</sup>

Detailed studies to understand PARP activity following DNA damage have focused on DNA methylating agents, such as *N*-methyl-*N*-nitro-*N*-nitrosoguanidine (MNNG).<sup>6,15-17</sup> The activity of PARP proteins following cisplatin exposure is less well understood. One study revealed increased levels of PAR polymers following cisplatin treatment in rat and monkey tumor cells.<sup>18</sup> Another report demonstrated that PARP

activity is strongly upregulated following exposure of renal tubular cells to cisplatin, and ATP levels within these cells decreased significantly.<sup>19</sup> In this work, extremely high concentrations of cisplatin (500  $\mu$ M) were required to induce PARP activity. Recently, HT29 colon carcinoma cells were used to show a mild increase in PARP activity 24 h after a four h treatment with 10  $\mu$ M cDDP.<sup>20</sup> Only one cell line was tested using the assay, however, providing little information about the importance of PARP activity in cisplatin sensitivity. HeLa cervical cancer cells were also studied in the work, but PARP activity following cisplatin treatment was not reported.<sup>20</sup> Further investigations using cisplatin concentrations more relevant to human cancer are clearly warranted.

Although the activity of PARP proteins following cisplatin treatment is not well characterized, PARP inhibitors have been used to sensitize cells to cisplatin. Cotreatment of cisplatin and the NAD<sup>+</sup> analogue 6-aminonicotinamide sensitizes cells to cisplatin.<sup>21</sup> The increased cytotoxicity was due to greater uptake of cisplatin, however, and not a decrease in repair of platinum-DNA adducts or PARP-dependent cell death signaling. More recent work indicates that a potent PARP inhibitor, CEP-6800 (Figure 5.3), sensitizes non-small cell lung carcinoma cells to cisplatin in both culture and in xenografts.<sup>22</sup> Another newly developed PARP inhibitor, ABT-888, substantially improves tumor response to cisplatin and carboplatin.<sup>23</sup> The anticancer potential of PARP inhibitors and platinum drugs in combination therapies is currently being investigated in phase I and II clinical trials.<sup>24</sup>

In the present work, the role of PARP proteins in mediating cisplatin cytotoxicity has been investigated in a number of cell lines with varying sensitivity to cisplatin, namely, cervical (HeLa), testicular (NTera2), pancreatic (BxPC3) and osteosarcoma

(U2OS). The potentiation of cisplatin cytotoxicity by PARP inhibitors was investigated in these cancer cell lines. Photo-cross-linking studies, outlined in Chapters 2 and 3, were carried out in the presence of a PARP inhibitor to determine its effect on the binding of nuclear proteins to platinum-damaged DNA. In order to assess PARP activity, cells were treated with cisplatin and the PAR-modification of proteins was analyzed. To achieve a good signal in this type of assay, confluent cells were treated with cisplatin for one hour prior to analysis. In most of our previous cytotoxicity assays, cells at low confluence are treated with cisplatin for 96 h to assess the effect on growth. Here we report a new cytotoxicity assay designed to be compatible with the conditions of the PARP activity measurements. In this assay, confluent cells are treated with cisplatin for one hour and then re-plated at low confluence to allow for cell proliferation analysis. The cytotoxicity of cisplatin can be enhanced in cells at high versus low density due to intercellular signaling.<sup>25</sup> Following determination of  $IC_{50}$  values, PARP activity assays were performed. Cells were treated with cisplatin and nuclear extracts were then analyzed for PAR-modified proteins. The assay was repeated using a dounce homogenizer instead of nuclear extraction methods to limit the processing time of the cells following cisplatin exposure. A quick extraction method is necessary due to the transient nature of PAR polymers.<sup>26</sup>

## II. MATERIALS AND METHODS

Solvents and most chemical reagents were purchased from commercial sources. Enzymes were obtained from New England BioLabs and Promega. Antibodies were purchased from Axxora Life Sciences. NMR spectroscopy and high-resolution mass

spectrometry were performed at the MIT department of chemistry instrumentation facility (DCIF).

#### *Synthesis of CEP-A and CEP-6800*

CEP-A and CEP-6800 were prepared by co-author Alison Ondrus of the Movassaghi Lab, adapted from published synthetic strategies.<sup>27-29</sup>

#### *Cell culture*

HeLa, Ntera2, BxPC3, and U2OS cells were grown in DMEM with 10% FBS at 37 °C in an atmosphere of 5% CO<sub>2</sub>. HeLa YS and HeLa pcDNA cells were prepared as described in Chapter 3 and were grown in DMEM with 10% FBS supplemented with 100 µg/mL zeocin selection reagent (Invitrogen).

#### *MTT assays*

MTT assays carried out as described in Chapter 3. Cells were treated with varying concentrations of PARP inhibitors CEP-A, CEP-6800, and 4-amino-1,8-naphthalimide (4-ANI) to determine the maximum tolerated dose of inhibitor in each cell line. The cytotoxicity assays were then repeated with the maximum tolerated dose of PARP inhibitor plus varying concentrations of cisplatin.

#### *Density-dependent cytotoxicity assay*

Cells were plated at either  $1.0 \times 10^5$  or  $1.0 \times 10^4$  cells/well in six-well plates. On day two, cells were treated with varying concentrations of cisplatin and incubated for one h. The cells were then trypsinized and replated at 1000 cells/well in a 96-well plates. On day six, the cells were treated with one mg/mL 3-(4,5-dimethylthiazol-2-yl)-2,5-diphenyltetrazolium bromide (MTT) for four h. The medium was removed from each

well and replaced with 100  $\mu$ L of DMSO. The absorbance of each well at 562 nm was measured using a plate reader.

*Photo-cross-linking in the presence of PARP inhibitors*

Analytical-scale photo-cross-linking experiments were carried out as described in Chapters 2 and 3 for a 25-bp DNA containing a site-specific 1,2-d(GpG) or 1,3-d(GpTpG) adduct of PtBP6 and HeLa nuclear extracts in the presence of 0, 0.01, 0.05, 0.1, 0.3, or 1.0  $\mu$ M CEP-A. The inhibitor was dissolved in DMF and diluted to the desired concentration with the final solution containing 0.02% DMF. Photo-cross-linking was also performed without DMF as a control. Photo-cross-linking experiments were then repeated using nuclear extracts from Ntera2, BxPC3, U2OS, and HeLa YS cell lines, with or without 1.0  $\mu$ M CEP-A, for both types of PtBP6 cross-link.

*Preparation of nuclear extracts from cisplatin-treated cells*

Cells were treated with a concentration of cisplatin equal to the IC<sub>50</sub> value of the cell line as determined by the MTT assay for 0, 1, 4, 8, or 24 h. Nuclear extracts of these cells were prepared as described in Chapter 2.

*Preparation of cisplatin-treated cell lysates*

Cells were treated for one h with a concentration of cisplatin equal to their IC<sub>50</sub> value as determined by the density-dependent cytotoxicity assay. Cells were pelleted by centrifugation at 450 x g for five min. Each pellet was resuspended in 750  $\mu$ L of ice cold 20% trichloroacetic acid (TCA) and lysed using a Dounce homogenizer. The homogenate was centrifuged at 3000 x g for 10 min, and the supernatant was removed. The pellet was resuspended in 750  $\mu$ L 20% of TCA and centrifuged again three times. The pellet was



then resuspended in 750  $\mu$ L of ice-cold ethanol and pelleted by centrifugation. The pellets were dried briefly by vacuum centrifugation and stored at -80 °C.

*Nuclear extract-based PARP activity assay*

For each experiment, 100  $\mu$ g of nuclear extracts were resolved by 10% SDS-PAGE. The gel was transferred to PVDF membrane using a BioRad semi dry transfer cell and subjected to western blot analysis for PAR polymers as described below.

*Lysed cell-based PARP activity assay*

The cell lysate was dissolved in 100  $\mu$ L of 2X SDS-PAGE loading buffer (100 mM Tris-HCl, 20 mM DTT, 2% SDS, 30% glycerol, and 0.1% bromophenol blue, pH 7.9) to solubilize the proteins and resolved by 10% SDS-PAGE with a 4% stacking gel. The proteins on the gel were transferred to a PVDF membrane and subjected to western blot analysis for  $\beta$ -actin as described in Chapter 2. The images were analyzed using ImageJ software (NIH) and the relative intensities of the  $\beta$ -actin loading control were determined. These values were used to load equal amounts of each lysate onto a second gel. The proteins on the gel were then transferred to a PVDF membrane and subjected to western blot analysis for poly(ADP-ribose) (PAR) polymers described below.

*Western blot for PAR*

The PVDF membrane was soaked in t-PBS (10 mM Na<sub>2</sub>HPO<sub>4</sub> pH 7.4, 137 mM NaCl, 2.7 mM KCl, 0.1% Tween-20) with 5% milk for one h. The membrane was then washed with t-PBS and incubated in t-PBS with 1/1000X dilution of rabbit anti-PAR antibodies for two h. Next, the membrane was washed with t-PBS and incubated in t-PBS with 1/2000X dilution of HRP anti-rabbit for one h. The membrane was washed thoroughly with t-PBS and treated with luminol-containing imaging reagent (Pierce) for

one min. The blots were then exposed to Kodak MR autoradiography film, which was developed.

### III. RESULTS

#### *Synthesis of CEP-A and CEP-6800*

PARP inhibitors CEP-A and CEP-6800 (Figure 5.3) were synthesized by Alison Ondrus of the Movassaghi lab. CEP-A was analyzed by  $^1\text{H}$  NMR spectroscopy (Figure 5.4) and CEP-6800 was analyzed by  $^1\text{H}$  NMR (Figure 5.5) and high resolution mass spectrometry. The theoretical  $[\text{M}+\text{Na}]^+$  was 328.1056 m/z, and the experimental value, 328.1050 m/z.

#### *Cytotoxicity assays*

The toxicity of PARP inhibitors was investigated for each cell line to determine the maximum tolerated dose. These MTT assays are presented in Figure 5.6 and the results are summarized in Table 5.1. Cells were treated with the maximum tolerated dose of each PARP inhibitor and varying concentrations of cisplatin. The MTT assays are presented in Figure 5.7 and the results are summarized in Table 5.2. The sensitivity of HeLa and Ntera2 cells to cisplatin was unchanged by addition of PARP inhibitors, but BxPC3 and U2OS cells were sensitized to cisplatin by factors of 1.6 and 2.3, respectively.

Cells were treated with varying concentrations of cisplatin at high and low density in six-well plates. The cells were then transferred to 96-well plates for analysis by the MTT assay. There were some differences in  $\text{IC}_{50}$  values between the high and low-density cells (Table 5.3), but the curves (Figure 5.8) indicate little effect, if any, on cell

density in these cytotoxicity assays. The  $IC_{50}$  values at high density of HeLa cells in which PARP-1 has been silenced by RNAi (HeLa YS), as well as HeLa cells transfected with a control plasmid (HeLa pcDNA), were determined using this assay (Figure 5.9). The  $IC_{50}$  values for HeLa YS and HeLa pcDNA cells were 12 and 36  $\mu$ M, respectively. These cells must be grown in 100  $\mu$ g/mL zeocin selection reagent, so a control cell line was evaluated to determine the effect of zeocin on these cytotoxicity assays. The HeLa pcDNA cells are more resistant to cisplatin than untransfected HeLa cells, indicating that the presence of zeocin in the media interferes with the antiproliferative effects of cisplatin. This interference is possibly due to the direct interaction of cisplatin with zeocin, a large molecule containing several nitrogen atoms that may coordinate to cisplatin (Figure 5.10).

*Photo-cross-linking in the presence of the PARP inhibitor CEP-A*

For the 25-bp DNA duplex containing a 1,2-d(GpG) adduct of PtBP6, increasing amounts of CEP-A in the photo-cross-linking experiment resulted in a decrease in intensity of high-molecular weight band 2, and band 1 directly below increases in intensity (Figure 5.11A). The intensities of these bands were quantitated (Figure 5.11B), indicating that the overall photo-cross-linking of these two bands increases by a factor of 1.6 with the addition of CEP-A. For the 25-bp DNA containing a PtBP6 1,3-d(GpTpG) cross-link, there was no effect by PARP inhibition on these bands (Figure 5.11A).

These experiments were repeated with 1  $\mu$ M CEP-A using nuclear extracts from HeLa, NTera2, BxPC3, U2OS, and HeLa YS cells (Figures 5.11 and 5.12). The behavior of the high-molecular weight band for the duplex containing a 1,2-d(GpG) intrastrand cross-link with HeLa nuclear extracts was consistent with the foregoing results (Figures

5.10 and 5.11), but not for nuclear extracts from any other cell line (Figure 5.12). For duplexes containing the 1,2-d(GpG) intrastrand cross-link, the total amount of photo-cross-linking was increased with the addition of the PARP inhibitor for all cell lines tested by 20 to 100% of the original intensity. Consistent with the experiment using HeLa nuclear extracts presented in Figure 5.11, addition of CEP-A did not significantly affect the photo-cross-linking of the duplex containing a 1,3-d(GpTpG) intrastrand cross-link in nuclear extracts from any of the cell lines tested (Figure 5.13). The total amount of photo-cross-linking by the 1,3-d(GpTpG) probe increased only slightly upon addition of the PARP inhibitor for all cell lines tested except BxPC3, which was increased by almost 50%. These results are presented graphically in Figure 5.14.

#### *PARP activity assay with nuclear extracts*

HeLa and NTERA2 cells were treated with cisplatin for various time points and nuclear extracts were prepared. The extracts were resolved by SDS-PAGE and analyzed for the presence of PAR-modified proteins using an antibody for the polymer. These experiments indicated that several proteins are modified both with and without cisplatin exposure (Figure 5.15). In NTERA2 cells, there is a slight increase in poly(ADP-ribosyl)ation after one and four h of platinum treatment. After eight h, the amount of PAR-modified proteins decreases significantly (Figure 5.15A). In HeLa cells, there is no increase in poly(ADP-ribosyl)ation after cisplatin exposure (Figure 5.15B).

#### *Cell-based PARP activity assay*

Due to the nature of the nuclear extraction process, which can activate PARP proteins upon cellular fragmentation or allow degradation of PAR polymers by PARG, a quicker lysis method is required. Cells were therefore homogenized in 20%

trichloroacetic acid, a process that preserves these modifications.<sup>26</sup> Cells were treated with their IC<sub>50</sub> concentration of cisplatin for one h. Using the lysis method, no significant increase in poly(ADP-ribosyl)ation following cisplatin treatment was evident for any cell line (Figure 5.16).

#### IV. DISCUSSION

Poly(ADP-ribose) polymerase-1 (PARP-1) and the PARP family catalyze the addition of poly(ADP-ribose) (PAR) polymers onto acceptor proteins in a reaction that consumes NAD<sup>+</sup> (Figure 5.1A).<sup>9</sup> Each unit of the polymer contains two negatively charged phosphate moieties, which electrostatically repel DNA molecules from the PAR-modified protein (Figure 5.1B).<sup>1</sup> PARP-1 automodification leads to dissociation of the enzyme from DNA. PARP-1 can also modify other proteins, including histones, which relaxes histone-DNA interactions.<sup>9</sup> The activity of PARP proteins in the presence of DNA damage may lead to repair, or conversely, signal cell death (Figure 5.2).

##### *The cell lines tested do not show density-dependent cytotoxicity*

In order to develop an assay for the analysis of PARP activity following exposure to cisplatin, it was necessary to determine the IC<sub>50</sub> values for cells at high confluence treated for a short exposure time. Cells were plated at high density to ensure that enough nuclear extracts are collected to get a strong signal from western blot analysis of the isolated proteins, as discussed below. The MTT assay requires that cells be treated at low confluence, however, so that their subsequent differences in growth can be assessed. To achieve both objectives, cells were first treated with various cisplatin concentrations for one hour at high confluence, and then re-plated into 96-well plates at lower density to

monitor their growth. With this modified procedure, we tested HeLa, NTERA2, BXP3, and U2OS cell lines for density-dependent sensitivity to cisplatin.

Our assay was adapted from a paper demonstrating density-dependent sensitivity to cisplatin of cells with functional gap junctions and the DNA-PK heterotrimer.<sup>25</sup> Mouse fibroblast cell lines MEF and SCID, as well as Chinese hamster ovary (CHO) cells were used. Knocking down Ku80 in these lines eliminated the density-dependent effect. Human breast adenocarcinoma (MCF-7) cells only showed density-dependent sensitivity when supplemented with a vector expressing connexin43, a protein necessary to form gap junctions. The cell lines tested in the present study were not significantly more sensitive at high density (Table 5.3, Figure 5.8). This result suggests that these cells may not form gap junctions at high density, because photo-cross-linking experiments from Chapter 3 indicate that they express all three components of the DNA-PK heterotrimer.

The IC<sub>50</sub> values are much higher for this assay than the continuous MTT assay, described in Chapter 3, where the cells are exposed to cisplatin for 96 h. Here the cisplatin treatment was only one h. Under these conditions, the BXP3 cells are the most cisplatin-resistant of the lines tested (Table 5.3).

#### *NTERA2 cells are sensitive to PARP inhibition*

The toxicity of three PARP inhibitors (Figure 5.3) was determined for the cell lines tested to obtain the maximum tolerated dose that could be used to potentiate the cell-killing ability of cisplatin (Table 5.1, Figure 5.6). NTERA2 cells are extremely sensitive to PARP inhibitors, which hampers our ability to assess their capacity to enhance cisplatin sensitivity. This result is perplexing given that NTERA2 cells express high levels of PARP-1, as demonstrated in Chapter 3. PARP-1 is commonly mutated in

germ cells, specific variants being Val762Ala and Lys940Arg, two residues in the catalytic domain of the protein.<sup>30</sup> Compromised activity of the protein by these mutations may render it especially sensitive to PARP inhibitors. The reliance of NTERA2 cells on PARP activity, even without the addition of DNA-damaging agents, warrants further investigation.

*PARP inhibitors potentiate the cytotoxicity of cisplatin in certain cancer cell lines*

The potentiation of cisplatin sensitivity by PARP inhibitors was assessed in four cancer cell lines. Testicular (NTERA2) and cervical (HeLa) cancer cells were unaffected, but pancreatic (BxPC3) and osteosarcoma (U2OS) cancer cells are sensitized to cisplatin by PARP inhibition (Table 5.2, Figure 5.7). This finding is consistent with reports in the literature demonstrating that certain cell lines are unaffected by the presence of PARP inhibitors, whereas others are sensitized to cisplatin. For example, PARP inhibitors were unable to sensitize human ovarian tumor cell lines SK-OV-3, OAW-42, and the rat ovarian tumor cell line O-342 to cisplatin,<sup>31</sup> but could sensitize B16F10 murine melanoma, 9L rat glioma, HCT-116 human colon carcinoma, DOHH-2 human B-cell lymphoma, MX-1 human breast carcinoma, and Calu-6 human non-small cell lung carcinoma cells to the drug.<sup>22,23</sup> The use of new PARP inhibitors CEP-6800 and ABT-888 (Figure 5.3C and 5.3D) for experiments involving the B16F10, 9L, HCT-116, DOHH-2, MX-1, and Calu-6 cell lines is one reason for this discrepancy, because these compounds are more water soluble and are able to enter cells and inhibit PARP proteins more efficiently.<sup>22,23</sup> The present work demonstrates that there is also a cell line dependence to this effect. The sensitization of certain cell lines to cisplatin by PARP inhibitors may be caused by differences in the processing of platinum-DNA adducts in the absence of

PARP activity. This possibility was investigated by performing photo-cross-linking studies in the presence of the PARP inhibitor, CEP-A, as described in the next section.

*PARP-1 activity dissociates proteins from platinum-modified DNA in nuclear extracts*

The activity of poly(ADP-ribose) polymerase (PARP) proteins in the presence of DNA damage can lead to repair or, conversely, signal cell death (Figure 5.2). It was recently discovered that PARP-1 binds to platinum-modified DNA.<sup>32,33</sup> PARP-1 and the PARP family catalyze the addition of poly(ADP-ribose) (PAR) polymers onto acceptor proteins in a reaction that consumes NAD<sup>+</sup> (Figure 5.1A).<sup>9</sup> Each unit of the polymer contains two negatively charged phosphate moieties, which can electrostatically repel DNA molecules from PAR-modified proteins (Figure 5.1B).<sup>1</sup> PARP-1 automodification leads to dissociation of the enzyme from DNA, and the protein can also catalyze the modification other proteins, including histones, which relaxes histone-DNA interactions.<sup>9</sup> In the present work, we studied the consequences of PARP activity upon exposure of nuclear proteins to platinum-modified DNA using photo-cross-linking experiments.

The method utilizes DNA containing a site-specific adduct of a benzophenone-modified cisplatin analogue Pt-BP6. Photo-cross-linking with such probes enables the study of nuclear proteins that bind to platinum-modified DNA. Several platinum-modified DNA-binding proteins have been identified in this manner, as discussed elsewhere.<sup>32,33</sup> Here we performed photo-cross-linking experiments in the presence of the PARP inhibitor CEP-A (Figure 5.3B). The addition of CEP-A to nuclear extracts prior to photo-cross-linking generally increased the amount of proteins photo-cross-linked to Pt-BP6-modified DNA (Figures 5.12-14). This result is consistent with a model in which



PARP activity stimulated by platinum-DNA cross-links results in the PAR-modification of DNA-binding proteins, causing them to dissociate from the duplex (Figure 5.1B).<sup>1</sup> Inhibition of PARP activity by CEP-A eliminates this effect, resulting in more stable protein-DNA interactions and, consequently, increased amounts of photo-cross-linking.

Our experiments indicate that the addition of PARP inhibitor significantly increases the photo-cross-linking of proteins to the platinum-modified DNA containing a 1,2-d(GpG) intrastrand adduct of Pt-BP6 in each type of nuclear extract examined except for HeLa (Figures 5.12-14). Nuclear extracts from HeLa cells exhibited only a modest increase in photo-cross-linking following addition of the PARP inhibitor (Figures 5.11, 5.12, 5.14). In these nuclear extracts exclusively, a high molecular weight band decreases in intensity with the addition of PARP inhibitor (Figure 5.11, band 7). This result indicates that PARP-1 activity in HeLa extracts following exposure to platinum-damaged DNA is unique.

Photo-cross-linking was more significantly affected for the 1,2-d(GpG) than the 1,3-d(GpTpG) intrastrand cross-link (Figures 5.12-14). This effect was consistent across all cell lines tested, although to a lesser degree for BxPC3 extracts, indicating that the 1,2-d(GpG) intrastrand cross-link more efficiently activates the protein. Experiments using extracts from HeLa cells in which PARP-1 has been silenced with RNAi (HeLa YS) reveal an increase in photo-cross-linking, similar to the behavior of NTera2, BxPC3 and U2OS cellular extracts. This result most likely indicates that, in the PARP-1-silenced cell line, other PARP isoforms are present having the same activity as PARP-1.

*There is no significant change in poly(ADP-ribosyl)ation following cisplatin treatment of the cell lines tested*

Two methods were used to monitor poly(ADP-ribosyl)ation following exposure to cisplatin. Using nuclear extracts from cisplatin-treated cells, a small increase in PAR modification was evident in NTERA2 but not in HeLa cells (Figure 5.15). Several distinctly modified proteins are present in treated as well as untreated extracts. PAR-modification of proteins can be effected by the nuclear extraction process, so a rapid cell lysis procedure was employed.<sup>26</sup> Using this methodology, we observed no significant change in poly(ADP-ribosyl)ation (Figure 5.16). There were fewer distinct bands by this method, however, a large diffuse higher molecular weight signal was present. This feature is characteristic of proteins containing various degrees of PAR modification, as demonstrated by a similar assay for EM9 cells treated with a methylating agent.<sup>15</sup> This type of assay was also used to show a mild increase in PAR-modified proteins in HT29 colon cancer cells treated with 10  $\mu$ M cisplatin, but only 24 h after exposure.<sup>20</sup> If PARP proteins are activated upon binding to cisplatin-DNA adducts, this response would occur more quickly. Only HT29 cells were used in that experiment, so the importance of PARP activity in cisplatin sensitivity cannot be determined. Although HeLa cells were used for part of the study, the authors did not present PARP activity assays for the cell line.<sup>20</sup> The present results indicate either that PARP proteins are not significantly activated immediately following cisplatin exposure in the four cell lines tested, or that such modification is not revealed by our assay.

## V. CONCLUSIONS

Several studies in the literature report varying degrees of sensitization of cancer cells to cisplatin by PARP inhibitors. It has thus far been difficult to determine whether

these inconsistencies are due to the cell lines or the inhibitors used, since both are varied. We present here the finding that PARP inhibitors sensitize cells to cisplatin in a manner that is cell line dependent. In our work, PARP inhibition resulted in the greatest increase in cisplatin sensitivity for U2OS osteosarcoma cells. NTera2 testicular carcinoma cells do not show this effect, but are very sensitive to PARP inhibitor themselves. This effect may be due to PARP-1 mutations, which are common in germ cells. Photo-cross-linking studies in the presence of a PARP inhibitor indicate that the activity of PARP proteins bound to platinum-damaged DNA leads to dissociation of PARP-1 itself, as well as other proteins, from the damaged duplex. We also discovered that PARPs are more activated in nuclear extracts by a 1,2-d(GpG) than a 1,3-d(GpTpG) PtBP6 cross-link. Upon treating cells with cisplatin, we found no increase in PAR-modified proteins. Our assay was unable to resolve the activation of PARP proteins following cisplatin treatment even in U2OS cells, for which PARP inhibitors sensitized the cells to cisplatin by a factor of 3.6.

## VI. REFERENCES

1. Schreiber, V.; Dantzer, F.; Amé, J.-C.; de Murcia, G., *Nat. Rev. Mol. Cell Biol.* **2006**, 7, 517-528.
2. Nguewa, P. A.; Fuertes, M. A.; Alonso, C.; Perez, J. M., *Mol. Pharmacol.* **2003**, 64, 1007-1014.
3. Bouchard, V. J.; Rouleau, M.; Poirier, G. G., *Exp. Hematol.* **2003**, 31, 446-454.
4. Audebert, M.; Salles, B.; Calsou, P., *J. Biol. Chem.* **2004**, 279, 55117-55126.
5. Wang, M.; Wu, W.; Wu, W.; Rosidi, B.; Zhang, L.; Wang, H.; Iliakis, G., *Nucleic Acids Res.* **2006**, 34, 6170-6182.
6. Yu, S.-W.; Andrabi, S. A.; Wang, H.; Kim, N. S.; Poirier, G. G.; Dawson, T. M.; Dawson, V. L., *Proc. Natl. Acad. Sci. U.S.A.* **2006**, 103, 18314-18319.
7. Zhang, W.; Zhang, C.; Narayani, N.; Du, C.; Balaji, K. C., *Cancer Lett.* **2007**, 255, 127-134.
8. Amaravadi, R. K.; Thompson, C. B., *Clin. Cancer Res.* **2007**, 13, 7271-7279.
9. Kim, M. Y.; Zhang, T.; Kraus, W. L., *Genes Dev.* **2005**, 19, 1951-1967.
10. Fahrer, J.; Kranaster, R.; Altmeyer, M.; Marx, A.; Bürkle, A., *Nucleic Acids Res.* **2007**, 35, e143.
11. Pleschke, J. M.; Kleczkowska, H. E.; Strohm, M.; Althaus, F. R., *J. Biol. Chem.* **2000**, 275, 40974-40980.
12. Ditsworth, D.; Zong, W.-X.; Thompson, C. B., *J. Biol. Chem.* **2007**, 282, 17845-17854.
13. Tanuma, S.; Johnson, G. S., *J. Biol. Chem.* **1983**, 258, 4067-4070.
14. De Soto, J. A.; Deng, C.-X., *Int. J. Med. Sci.* **2006**, 3, 117-123.
15. Keil, C.; Gröbe, T.; Oei, S. L., *J. Biol. Chem.* **2006**, 281, 34394-34405.
16. Horton, J. K.; Stefanick, D. F.; Naron, J. M.; Kedar, P. S.; Wilson, S. H., *J. Biol. Chem.* **2005**, 280, 15773-15785.
17. Zong, W.-X.; Ditsworth, D.; Bauer, D. E.; Wang, Z.-Q.; Thompson, C. B., *Genes Dev.* **2004**, 18, 1272-1282.
18. Bürkle, A.; Chen, G.; Küpper, J. H.; Grube, K.; Zeller, W. J., *Carcinogenesis* **1993**, 14, 559-561.
19. Shino, Y.; Itoh, Y.; Kubota, T.; Yano, T.; Sendo, T.; Oishi, R., *Free Radic. Biol. Med.* **2003**, 35, 966-977.
20. Gambi, N.; Tramontano, F.; Quesada, P., *Biochem. Pharmacol.* **2008**, 75, 2356-2363.
21. Budihardjo, I. I.; Walker, D. L.; Svingen, P. A.; Buchwalter, C. A.; Desnoyers, S.; Eckdahl, S.; Shah, G. M.; Poirier, G. G.; Ried, J. M.; Ames, M. M.; Kaufmann, S. H., *Clin. Cancer Res.* **1998**, 4, 117-130.
22. Miknyoczki, S. J.; Jones-Bolin, S.; Pritchard, S.; Hunter, K.; Zhao, H.; Wan, W.; Ator, M.; Bihovsky, R.; Hudkins, R.; Chatterjee, S.; Klein-Szanto, A.; Dionne, C.; Ruggeri, B., *Mol. Cancer Ther.* **2003**, 2, 371-382.
23. Donawho, C. K.; Luo, Y.; Luo, Y.; Penning, T. D.; Bauch, J. L.; Bouska, J. J.; Bontcheva-Diaz, V. D.; Cox, B. F.; DeWeese, T. L.; Dillehay, L. E.; Ferguson, D. C.; Ghoreishi-Haack, N. S.; Grimm, D. R.; Guan, R.; Han, E. K.; Holley-Shanks, R. R.; Hristov, B.; Idler, K. B.; Jarvis, K.; Johnson, E. F.; Kleinberg, L. R.;

- Klinghofer, V.; Lasko, L. M.; Liu, X.; Marsh, K. C.; McGonigal, T. P.; Meulbroek, J. A.; Olson, A. M.; Palma, J. P.; Rodriguez, L. E.; Shi, Y.; Stavropoulos, J. A.; Tsurutani, A. C.; Zhu, G.-D.; Rosenberg, S. H.; Giranda, V. L.; Frost, D. J., *Clin. Cancer Res.* **2007**, *13*, 2728-2739.
24. Helleday, T.; Petermann, E.; Lundin, C.; Hodgson, B.; Sharma, R. A., *Nat. Rev. Cancer* **2008**, *8*, 193-204.
25. Jensen, R.; Glazer, P. M., *Proc. Natl. Acad. Sci. U.S.A.* **2004**, *101*, 6134-6139.
26. Adamietz, P.; Hilz, H., *Methods Enzymol.* **1984**, *106*, 461-471.
27. Ator, M. A.; Bihovsky, R.; Chatterjee, S.; Dunn, D.; Hudkins, R.; (Cephalon, I., USA) Preparation of novel multicyclic compounds and their amino acid derivatives as inhibitors of enzymes such as poly(ADP-ribose) polymerase. 2001.
28. Chatterjee, S.; Diebold, J. L.; Dunn, D.; Hudkins, R. L.; Dandu, R.; Wells, G. J.; Zulli, A. L.; (Cephalon Inc.) Preparation of novel multicyclic compounds and their amino acid derivatives as inhibitors of enzymes such as poly(ADP-ribose) polymerase. U.S. Patent Appl. No. 11/455,356, 2006.
29. Palmer, B. D.; Thompson, A. M.; Booth, R. J.; Dobrusin, E. M.; Kraker, A. J.; Lee, H. H.; Lunney, E. A.; Mitchell, L. H.; Ortwine, D. F.; Smaill, J. B.; Swan, L. M.; Denny, W. A., *J. Med. Chem.* **2006**, *49*, 4896-4911.
30. Shiokawa, M.; Masutani, M.; Fujihara, H.; Ueki, K.; Nishikawa, R.; Sugimura, T.; Kubo, H.; Nakagama, H., *Jpn. J. Clin. Oncol.* **2005**, *35*, 97-102.
31. Bernges, F.; Zeller, W. J., *J. Cancer Res. Clin. Oncol.* **1996**, *122*, 665-670.
32. Guggenheim, E. R.; Xu, D.; Zhang, C. X.; Chang, P. V.; Lippard, S. J., *submitted* **2008**.
33. Zhang, C. X.; Chang, P. V.; Lippard, S. J., *J. Am. Chem. Soc.* **2004**, *126*, 6536-6537.

## VII. TABLES

Table 5.1: Maximum tolerated dose of three PARP inhibitors in four cancer cell lines

Cell line	4-ANI ( $\mu\text{M}$ )	CEP-A ( $\mu\text{M}$ )	CEP-6800 ( $\mu\text{M}$ )
HeLa	2.0	0.1	3.0
NTera2	0.1	0.1	0.1
BxPC3	2.0	0.1	3.0
U2OS	1.0	0.1	1.0

Table 5.2:  $\text{IC}_{50}$  values for cDDP co-treated with maximum tolerated dose of three PARP inhibitors in four cancer cell lines

Cell line	cDDP alone ( $\mu\text{M}$ )	+ 4-ANI ( $\mu\text{M}$ )	+ CEP-A ( $\mu\text{M}$ )	+ CEP-6800 ( $\mu\text{M}$ )	Sensitization
HeLa	1.0	1.1	0.8	1.1	none
NTera2	0.04	0.04	0.04	0.04	none
BxPC3	1.5	0.9	1.0	1.0	1.6-fold
U2OS	3.3	1.4	1.4	1.6	2.3-fold

Table 5.3: Density-dependent  $\text{IC}_{50}$  values for cDDP in four cancer cell lines

Cell line	High density ( $\mu\text{M}$ )	Low density ( $\mu\text{M}$ )
HeLa	16	11
NTera2	0.94	1.70
BxPC3	24	24
U2OS	20	18

## VIII. FIGURES

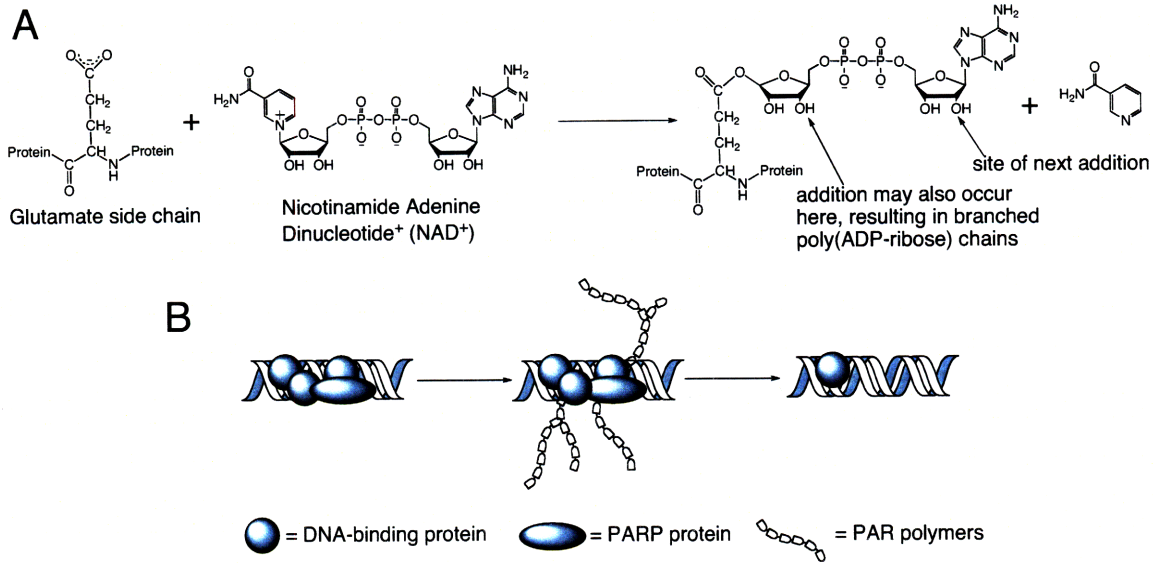


Figure 5.1. The catalytic activity of PARP proteins.

PARP proteins catalyze the addition of negatively charged poly(ADP-ribose) polymers to acceptor proteins using NAD<sup>+</sup> as a substrate (**A**). This modification is important for DNA repair because the modified proteins will be electrostatically repelled from the DNA (**B**). This activity can be eliminated by the addition of PARP inhibitors.

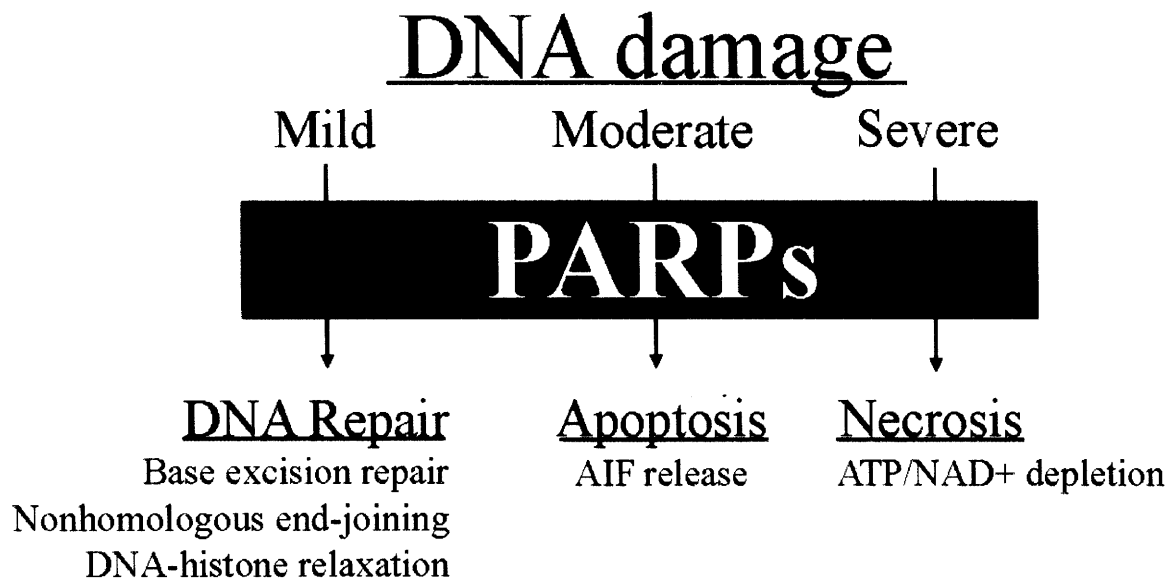
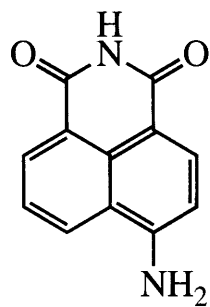


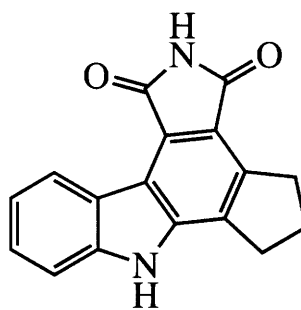
Figure 5.2. Three pathways of PARP activity.

The activity of PARP proteins following DNA damage can lead to DNA repair, apoptosis or necrosis through independent mechanisms.

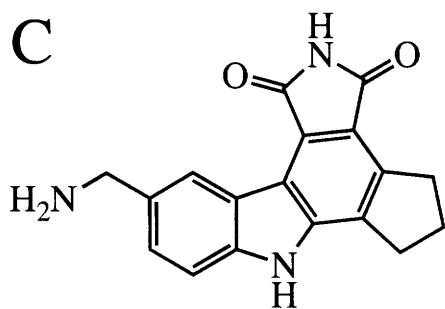


**A**

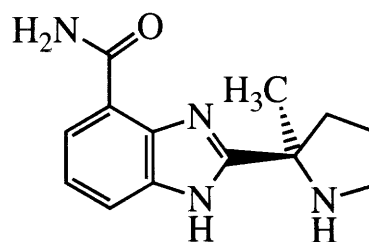
4-amino-1,8-naphthalimide  
(4-ANI)

**B**

CEP-6800 analogue  
(CEP-A)

**C**

CEP-6800

**D**

ABT-888

Figure 5.3. Chemical structures of four PARP inhibitors.

```

AD-IV-242/247
expl s2pu1
SAMPLE          DEC. & VT
data  Jan 14 2007  dfrq  125.673
solvent  DMSO  dn  C13
file  /data/export/~ dpwr  30
home/movassag/Mao/~ dcf  0
bullwinkle/Mao_011~ dm  nnn
407_AOIV242244_1H~ dmm  w
                               wft  10000
ACQUISITION  fid  dmf
sfrq  499.748  dseq  1.0
tn  H1  homo  n
qt  3.001  PROCESSING
np  63050  wtfile
sw  10504.2  proc  ft
fb  not used  fn  131072
bs  1  math  f
tpwr  56
pw  8.9  werr
d1  2.000  wexp
tof  1519.5  wbs
nt  100000  wnt  wft
ct  29
alock  n
gain  not used
FLAGS
fl  n
fn  n
dp  y
hs  nn
DISPLAY
sp  -0.1
wb  6246.6
vs  40
sc  0
wc  250
h2mm  4.17
is  33.57
rf1  1233.8
rfp  0
th  36
ins  2.000
nm  cdc  ph

```

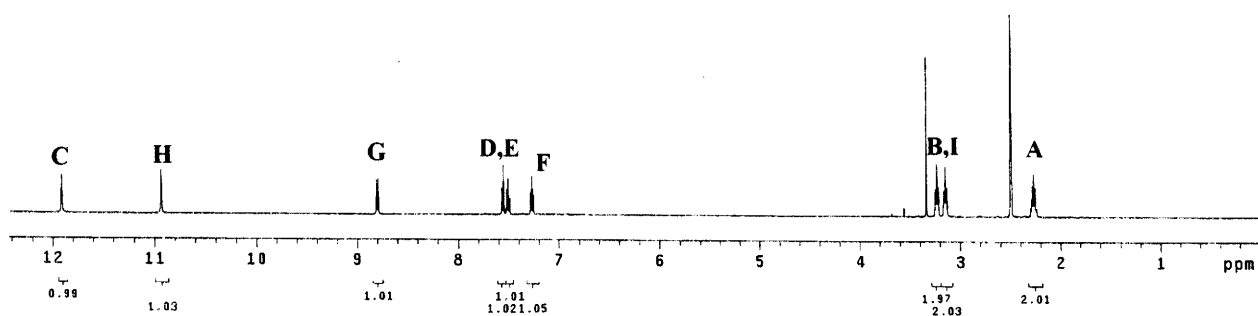
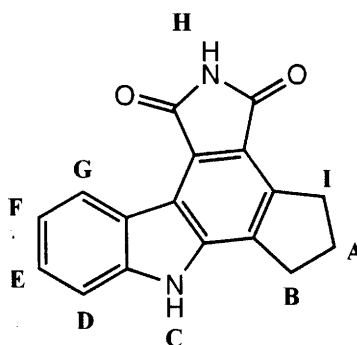


Figure 5.4. <sup>1</sup>H NMR of PARP inhibitor CEP-A.

This compound was synthesized and characterized by Alison Ondrus of the Movassaghi lab.

```

A0-IV-278_lyophilized HCl salt
exp3 s2pu1
SAMPLE
date Feb 15 2007 dfrq DEC. & VT 125.673
solvent DMSO dn C13
file /data/export/~ dpwr 30
home/movassag/Mao/~ dof 0
bullwinkle/Mao_021~ dm nnn
507_A0IV278_1H.fid dmm w
ACQUISITION
sfrq 499.748 dseq 10000
tn H1 dres 1.0
at 3.001 homo n
np 63050
sw 10504.2 wtfle PROCESSING
fb not used proc ft
bs 1 fn 131072
tpwr 56 math f
pw 8.9
d1 2.000 warr
tof 1519.5 wexp
nt 100000 wbs
ct 37 wnt wft
a1ock n
gain not used
ll FLAGS n
in n
dp y
hs nn
DISPLAY
sp 249.8
wp 8246.6
vs 63
sc 0
wc 250
hznm 4.73
ls 0.01
rf1 1233.8
rfp 0
th 7
ins 2.000
nm cdc ph

```

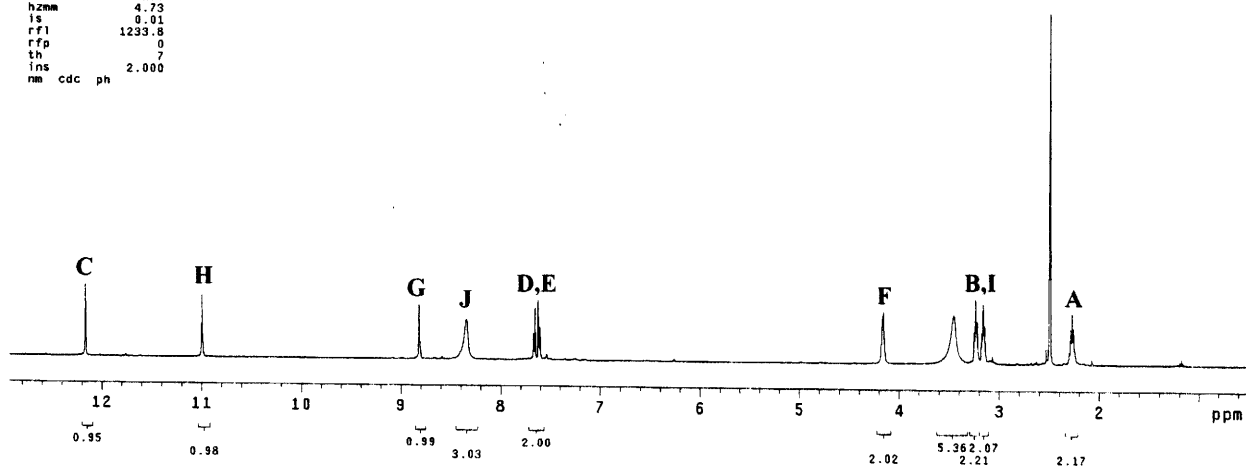
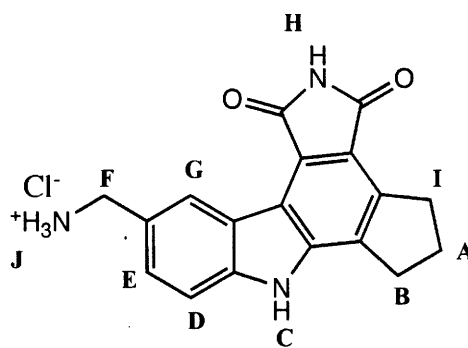


Figure 5.5. <sup>1</sup>H NMR of PARP inhibitor CEP-6800.

This compound was synthesized and characterized by Alison Ondrus of the Movassaghi lab.

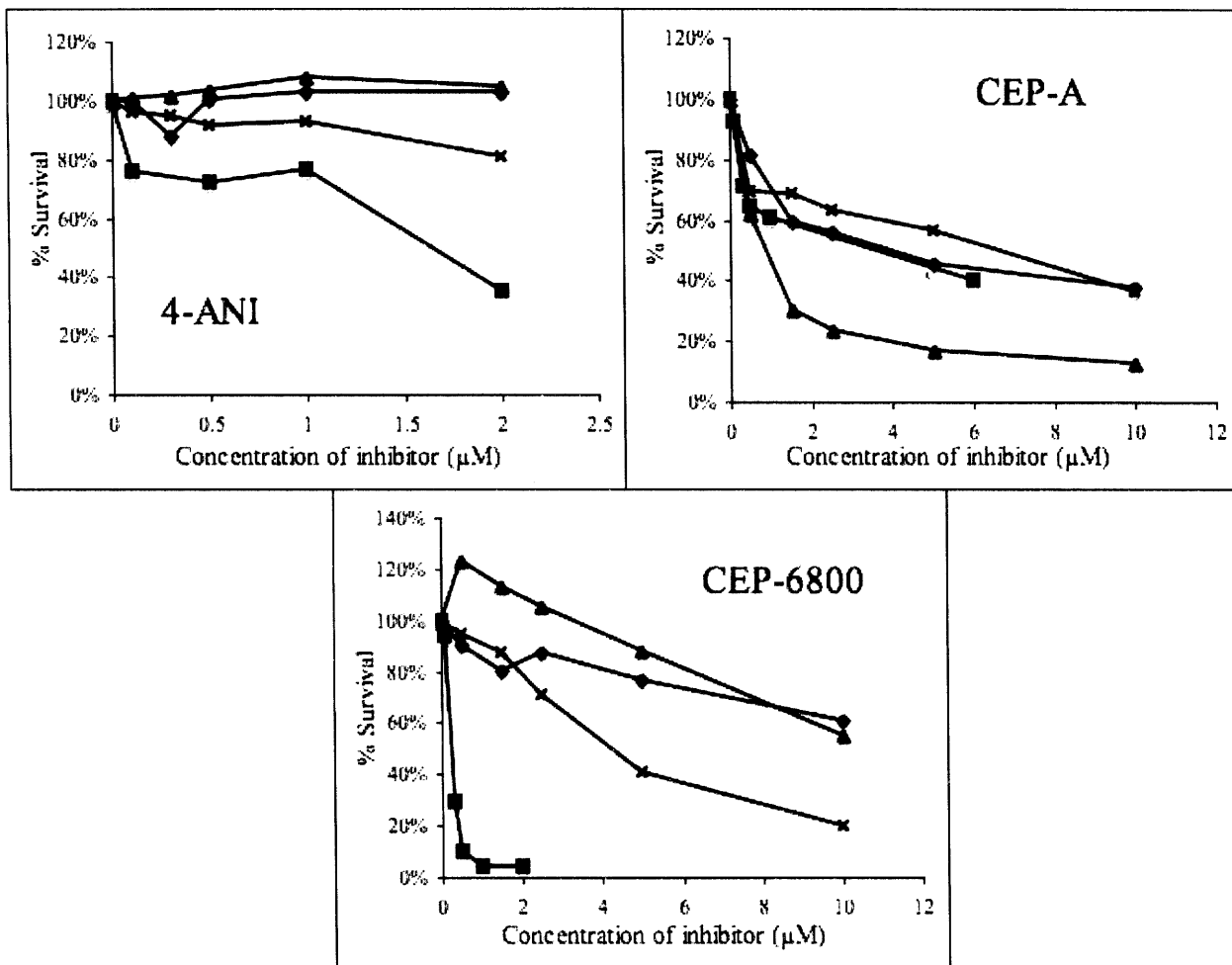


Figure 5.6. Cytotoxicity assays of PARP inhibitors in HeLa, NTERA2, BXP3 and U2OS cancer cell lines.

HeLa (◆), NTERA2 (■), BXP3 (▲), and U2OS (×) cells are evaluated. The PARP inhibitors used are 4-ANI, CEP-A and CEP-6800. These results are summarized in Table 5.1.

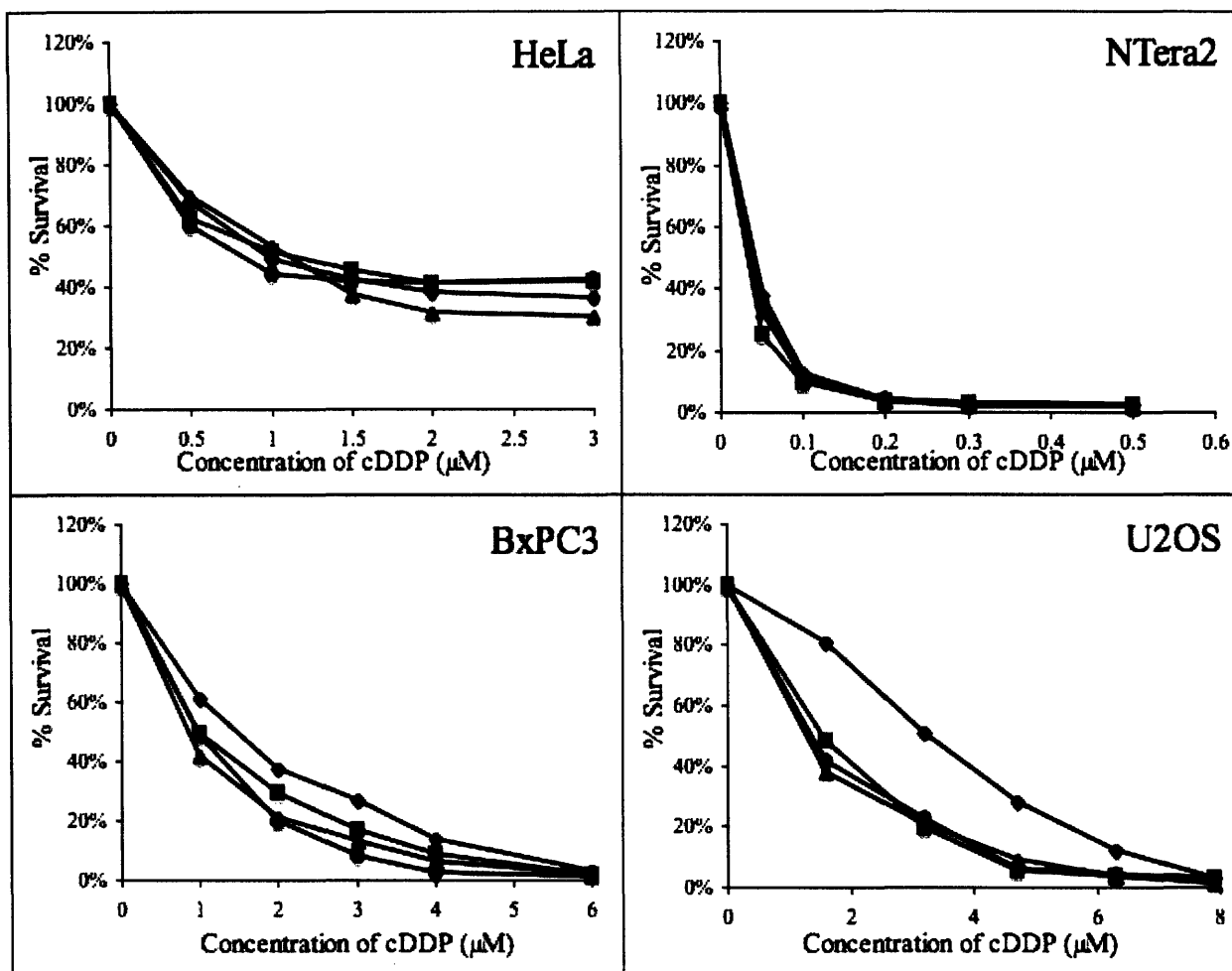


Figure 5.7. Cytotoxicity assays of cisplatin co-treated with PARP inhibitors in HeLa, NTERa2, BxPC3, and U2OS cells.

Cells were treated with cisplatin alone (◆) or co-treated with maximum tolerated dose of 4-ANI (■), CEP-A (▲) or CEP-6800 (●). These results are summarized in Table 5.2.

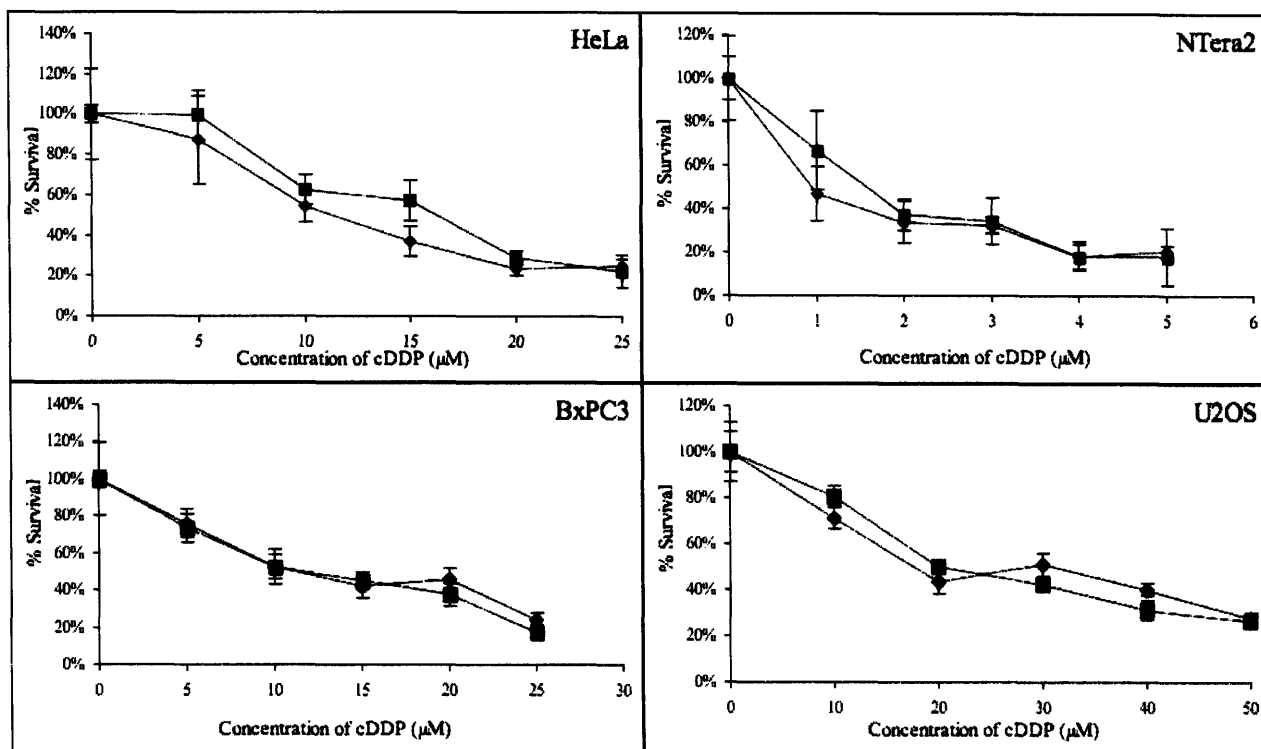


Figure 5.8. Density-dependent cytotoxicity assays for cisplatin in four cell lines.

Each cell line was tested against increasing concentrations of cisplatin. Cells were treated at high (■) or low (◆) density with cisplatin for one h and replated into a 96-well plate suitable for the MTT assay. These results are summarized in Table 5.3.

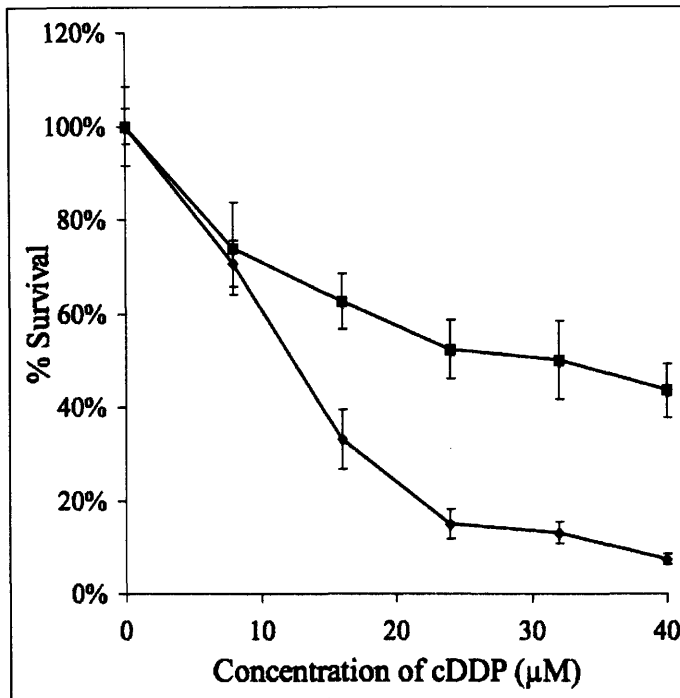


Figure 5.9. High density cytotoxicity assays for cisplatin in HeLa YS and HeLa pcDNA cell lines.

HeLa cells with PARP-1 silenced (◆) cells are significantly more sensitive to cisplatin than HeLa cells transfected with a control plasmid (■) using the high density cytotoxicity assay.

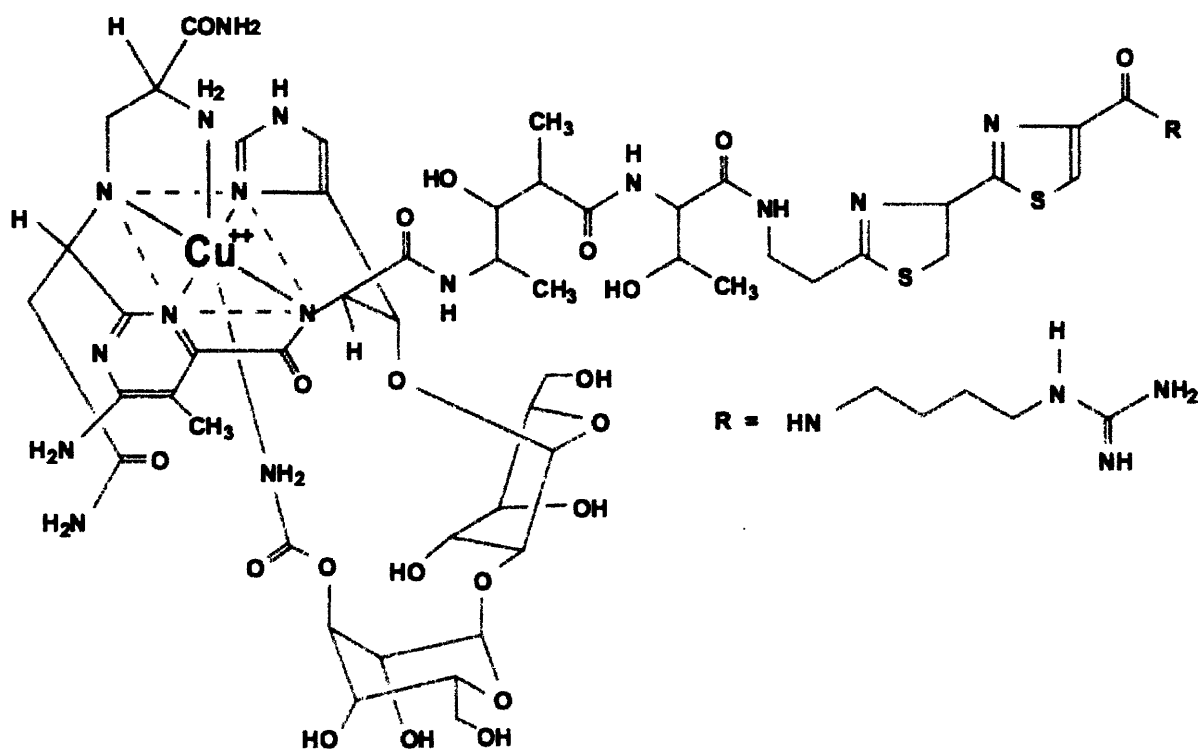


Figure 5.10. Structure of zeocin selection reagent.

This image was taken from [http://tools.invitrogen.com/content/sfs/manuals/zeocin\\_man.pdf](http://tools.invitrogen.com/content/sfs/manuals/zeocin_man.pdf).



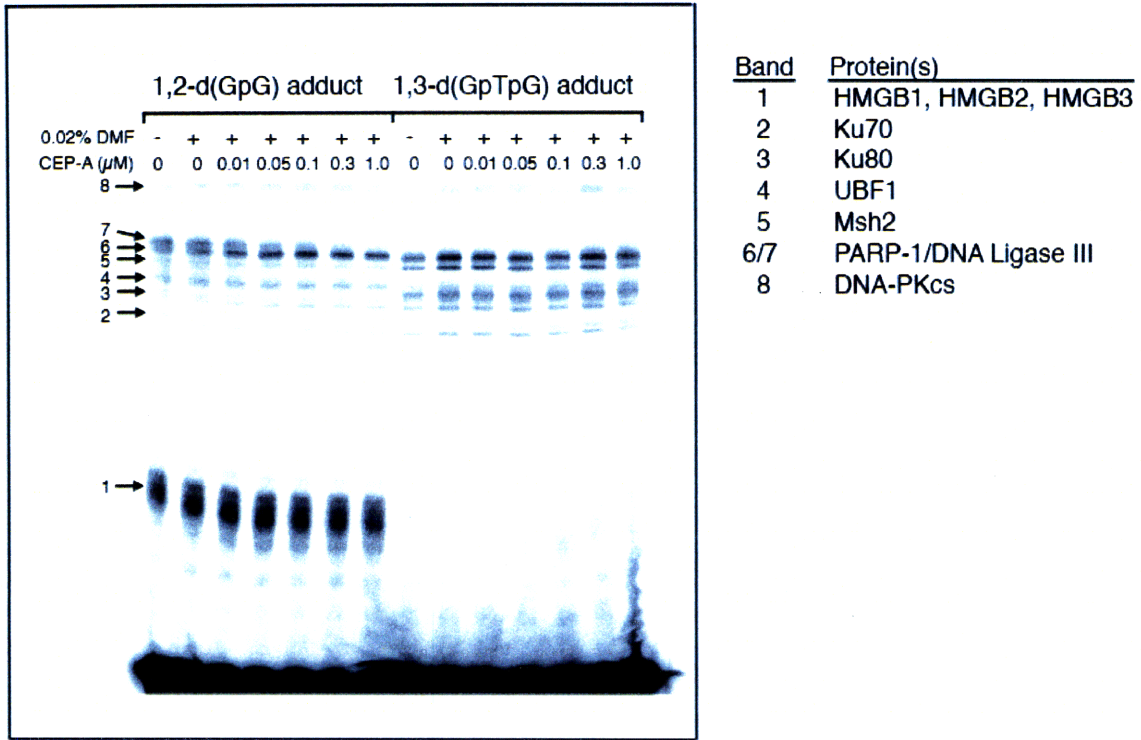


Figure 5.11. Photo-cross-linking of PtBP6-modified 25-bp duplexes with increasing concentrations of the PARP inhibitor, CEP-A.

For the 1,2-d(GpG) adduct, the intensity of Band 1 increases and the intensity of Band 2 decreases at increasing concentrations of CEP-A. The photo-cross-linking of the 1,3-d(GpTpG) is unaffected by the inhibitor.

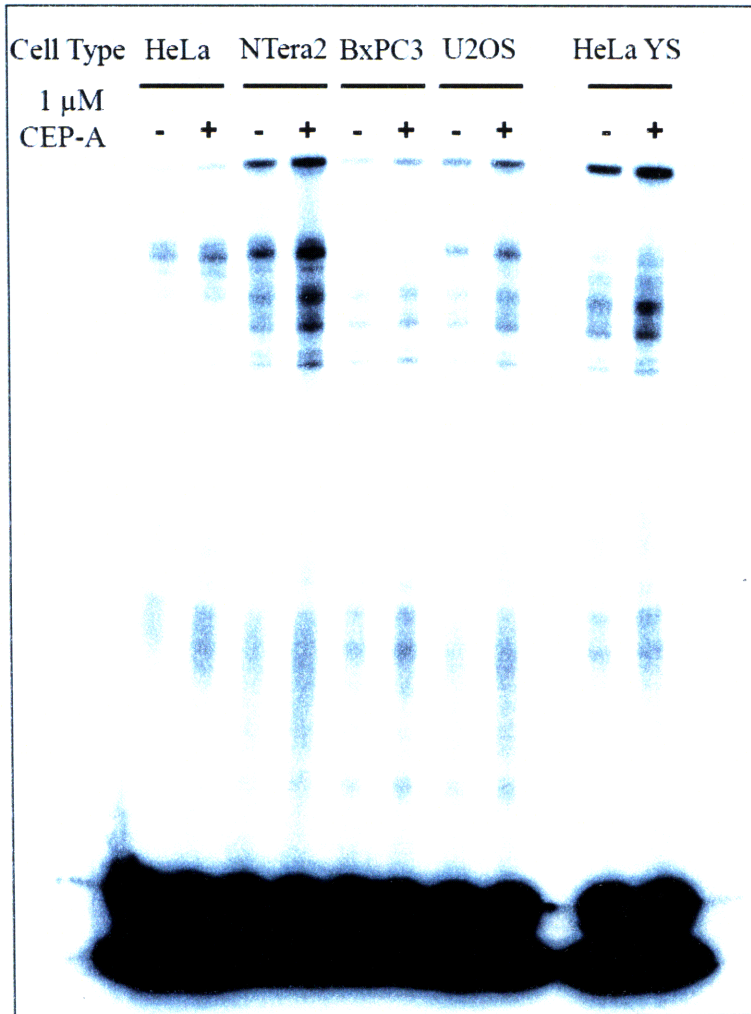


Figure 5.12. Photo-cross-linking of 25-bp duplex containing a 1,2-d(GpG) adduct of PtBP6 in various cancer cell extracts in the presence of the PARP inhibitor, CEP-A.

The inhibitor increases the intensity of photo-cross-linking in each cell line.

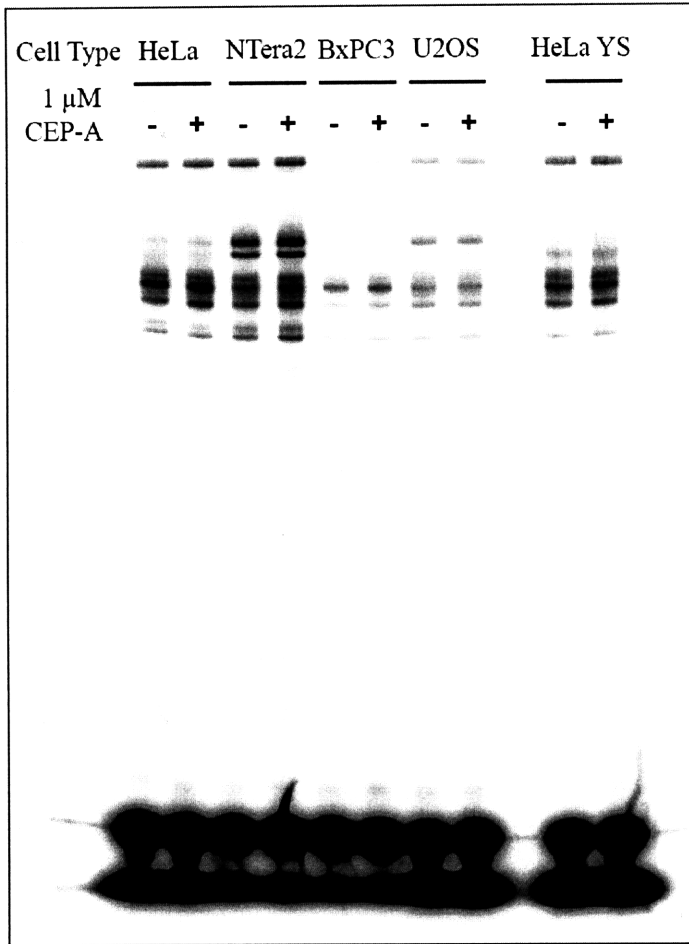


Figure 5.13. Photo-cross-linking of 25-bp duplex containing a 1,3-d(GpTpG) adduct of PtBP6 in various cancer cell extracts in the presence of the PARP inhibitor, CEP-A.

The inhibitor does not have a significant effect in any of the cell lines.

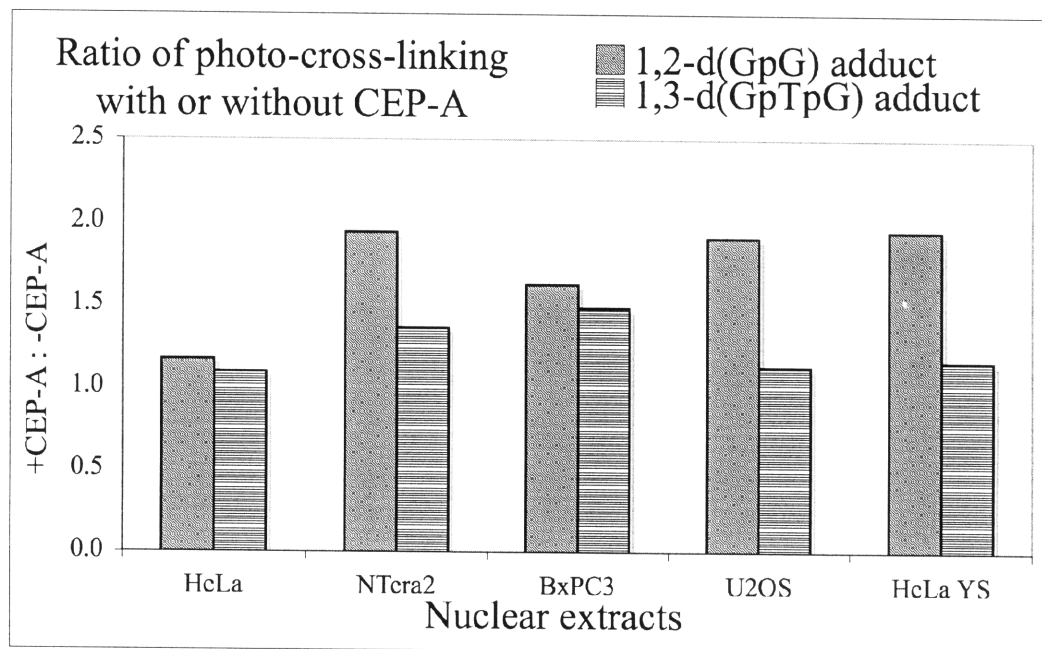


Figure 5.14. Intensity of total photo-cross-linking for site-specifically platinated DNA, with or without addition of the PARP inhibitor CEP-A.

The effect of PARP inhibitor CEP-A in photo-cross-linking experiments, revealing an increase in total intensity of photo-cross-linking. The effect is greater for the 1,2-d(GpG) than the 1,3-d(GpTpG) intrastrand cross-link. The effect is also cell-line dependent, with HeLa cells exhibiting the smallest increase.

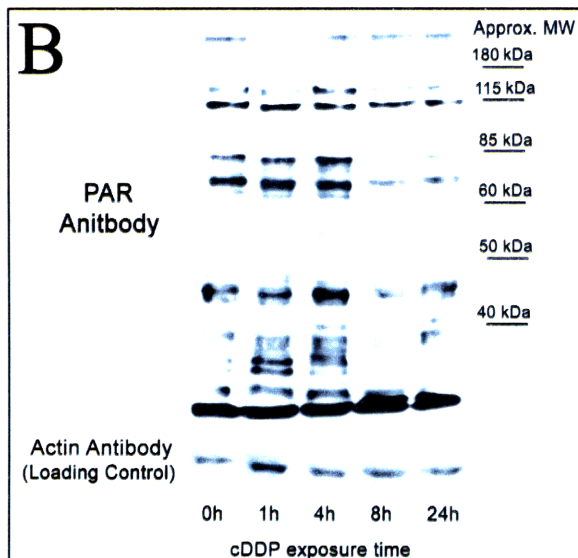
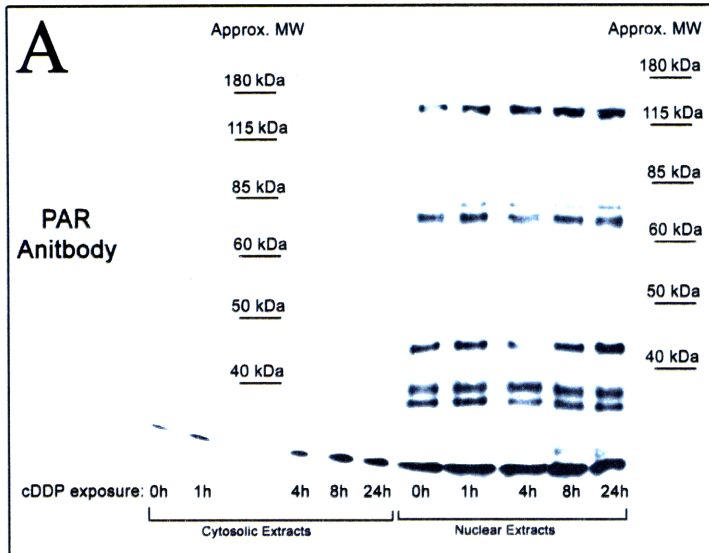


Figure 5.15. Nuclear extract-based PARP activity assay for HeLa and Ntera2 cells.

Nuclear extracts from HeLa (**A**) and Ntera2 (**B**) cells were prepared from cells treated with the  $IC_{50}$  value of cisplatin for various time points. The extracts were used in a western blot for PAR polymers. Cytosolic extracts from Ntera2 cells were also used, but yielded no signal. The membrane was blotted for  $\beta$ -actin as a loading control.

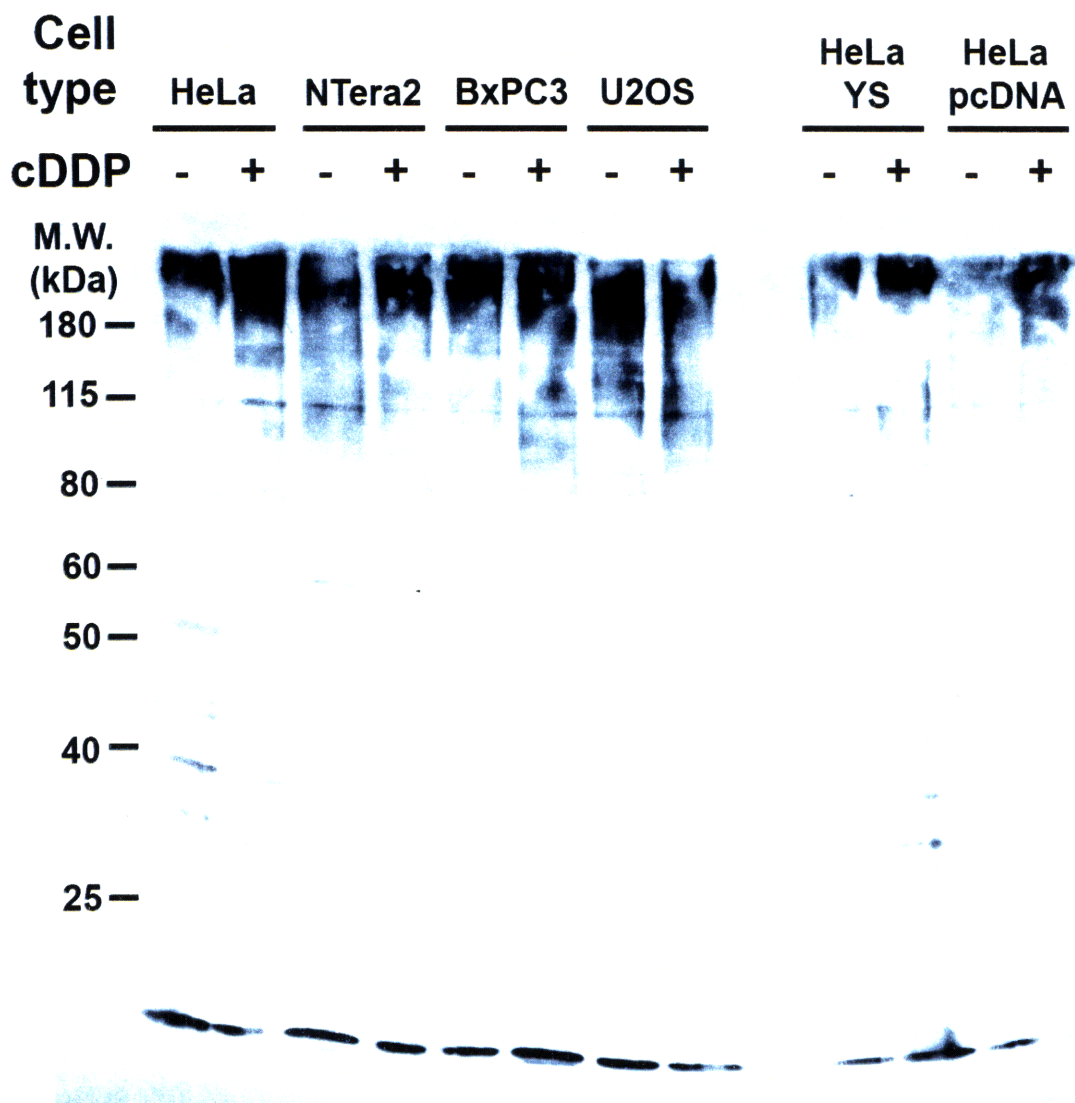


Figure 5.16. Cell lysis-based PARP activity assay.

Cells were treated with the  $IC_{50}$  concentration of cisplatin for 1 h, and then collected and lysed. The lysates were analyzed by western blot for the product of PARP activity, PAR polymers. No major differences exist between cisplatin treated and untreated cells or between the various cancer cell lines tested.

**Appendix A: Synthesis and characterization of a benzophenone-  
modified DNA probe.**

\*Some of the work discussed in this chapter was conducted by UROP students Cindy Yuan and Noel Lee.

## I. INTRODUCTION

Chapters 2-4 describe the synthesis of DNA containing site-specific adducts of a photo-activatable analogue of cisplatin, PtBP6. Photo-cross-linking experiments using PtBP6-modified DNA are limited to identifying proteins that bind to this type of platinum adduct. By tethering the benzophenone moiety directly to the DNA, photo-cross-linking experiments can be carried out using other DNA-damaging agents, as well as undamaged DNA (Figure A.1). As described in Chapter 2, PtBP6-modified DNA photo-cross-links the mismatch repair protein Msh2. This protein does not have an affinity for oxaliplatin-modified DNA,<sup>1</sup> demonstrating that there may be important differences in the recognition of these types of adducts. In Chapter 1, some new types of platinum compounds that display anticancer activity are discussed. Using a probe containing benzophenone-modified DNA, it would be possible to determine the proteins that bind to DNA lesions of these new complexes. The bulge created on the DNA strand opposite an intrastrand adduct is important for DNA damage recognition.<sup>2</sup> Placing a photo-cross-linking moiety on this strand may uncover new damage recognition proteins that are not positioned favorably to photo-cross-link to the PtBP6-modified probe.

Using commercially available amino-modified phosphoramidites (Figure A.2), benzophenone-modified DNA can be accessed in a one-step reaction (Scheme A.1). Three different probes were synthesized to optimize the location of the benzophenone unit along the DNA (Figure A.3). Analytical-scale photo-cross-linking experiments using one of these probes yielded unique protein-DNA complexes for cisplatin-modified versus unmodified DNA.



## II. MATERIALS AND METHODS

Solvents and chemical reagents were purchased from commercial sources. DNA strands were prepared on an Applied Biosystems ABI 392 DNA/RNA synthesizer using solvents and reagents supplied by Glen Research. Enzymes were purchased from New England BioLabs and Promega. UV-vis spectra were obtained on an HP 8453 UV-visible spectrometer. Platinum analyses were performed by flameless atomic absorption spectroscopy on a Perkin-Elmer AAnalyst 300 system. Analytical and preparative HPLC work was performed on an Agilent 1200 HPLC system. UV irradiation was conducted in a Stratagene Stratalinker UV Crosslinker.

### *Synthesis of amino-modified DNA*

Three 25-base DNA fragments were synthesized on the DNA synthesizer.

- a. 16A: 5'-GGAGAGAAG(A-am)TCCTGAGAGGAGAGG-3', in which (A-am) is an amino-modifier C6 dA phosphoramidite (Glen Research)
- b. 11T: 5'-GGAGAGAAGATCC(T-am)GAGAGGAGAGG-3', in which (T-am) is an amino-modifier C6 dT phosphoramidite (Glen Research)
- c. 15G: 5'-GGAGAGAA(G-am)ATCCTGAGAGGAGAGG-3', in which (G-am) is an amino-modifier C6 dT phosphoramidite (Glen Research)

The DNA was incubated overnight at 37 °C in 2 mL of 30% ammonium hydroxide. DNA strands were purified by 12% urea denaturing PAGE and visualized by UV shadowing. The DNA was then excised from the gel and isolated using the crush and soak method. The crushed gel was filtered and the purified DNA was ethanol

precipitated. The DNA pellet was then dissolved in water and dialyzed against water, using dialysis tubing with a MWCO of 3500.

#### *Synthesis of a benzophenone-modified DNA strand*

The synthesis of benzophenone-modified DNA was adapted from similar work with DNA modifications (Scheme A.1).<sup>3,4</sup> Amino-modified DNA was allowed to react with 200 molar equivalents of the N-hydroxysuccinimidyl ester of p-benzoylbenzoic acid (Invitrogen). The NHS ester of p-benzoylbenzoic acid was dissolved in 200  $\mu$ L of DMF, and a 50  $\mu$ L aliquot was added to the amino-modified DNA every 30 min for two h. The reaction was stirred overnight in the dark. The solution was filtered and the product was purified by RP-HPLC. The RP-HPLC method employed a gradient of 5-50% B over 30 min on an Agilent 300SB-C18 column where solvent A was 0.1 M ammonium acetate and solvent B was 0.1 M ammonium acetate in 50% water and 50% acetonitrile. Peaks were collected and lyophilized. The lyophilized DNA was dissolved in water and dialyzed against water, using dialysis tubing with a MWCO of 3500.

#### *Characterization of benzophenone-modified DNA*

The 25-base 16A-BP DNA was analyzed by ESI-TOF mass spectrometry, performed by Jim Delaney of the Essigmann lab. The 25-base 11T-BP DNA was analyzed by the Maxam-Gilbert sequencing reactions following the protocol outlined in Chapter 2. Enzymatic DNA digestion was used to characterize all three benzophenone-modified probes following the protocol outlined in Chapter 2.

#### *Synthesis of cisplatin-modified 25-base top strand*

A 25-base DNA of the sequence 5'-CCTCTCCTCTCAGGATCTTCTCTCC-3' was synthesized and purified as described previously for the amino-modified DNA. The

DNA was then incubated with cisplatin, which had been activated using the same methodology as reported for PtBP6 in Chapter 2. The reaction was purified by IE-HPLC using a gradient of 40-60% B over 30 min on an Agilent Zorbax Oligo column, where solvent A was 25 mM TEAA in 90% water and 10% acetonitrile and solvent B was solvent A with 1 M NaCl. The peak eluting at 16.3 min was collected and lyophilized. The lyophilized DNA was dissolved in water and dialyzed against water to remove salts, using dialysis tubing with a MWCO of 3500.

#### *Characterization of cisplatin-modified 25-base top strand*

The collected peak was characterized by UV-visible absorbance and atomic absorption spectroscopy to establish a 1:1 ratio of platinum per DNA. The DNA was also characterized by nuclease digestion analysis as described in Chapter 2.

#### *Preparation of double-stranded probes*

Each benzophenone-modified DNA fragment was radiolabeled as described in Chapter 2 and then combined with an equimolar amount of the complementary platinum-modified or unmodified strand in annealing buffer (50 mM Tris-HCl pH 7.9, 100 mM NaCl, 10 mM MgCl<sub>2</sub>, 1 mM DTT). The solution was heated to 90 °C for 5 min and cooled to 16 °C over 3 h. The DNA was then ethanol precipitated, dried by vacuum centrifugation, purified by 15% native PAGE, and located using autoradiography. The DNA was extracted using the crush and soak method and the purity of the duplex was verified by 15% native PAGE.

#### *Analytical-scale photo-cross-linking experiments*

In an eppendorf tube, 1 pmol of benzophenone-modified double-stranded radiolabeled DNA was combined with 20 µg of HeLa nuclear extracts in 20 µL of protein

binding buffer (10 mM Tris pH 7.5, 10 mM KCl, 10 mM MgCl<sub>2</sub>, 1 mM EDTA, 0.05% NP-40, 0.2 μg/mL BSA). The solution was exposed to UV irradiation for two h on ice. The cross-linked products were then analyzed by 10% SDS-PAGE with a 4% stacking gel.

### III. RESULTS

#### *Synthesis and characterization of benzophenone-modified DNA*

Commercially available amino-modified bases (Figure A.2) were incorporated into 25-base DNA strands. Three 25-base DNA probes (Figure A.3) containing benzophenone modifications were purified by RP-HPLC (Figure A.4). The analysis described below indicates that peak 1 for each reaction contains the amino-modified starting material, and peak 2 contains the benzophenone-modified product. Following dialysis at a MWCO of 3500, no UV-vis signal was present for peaks 3 and 4, indicating that they contain reaction byproducts of low molecular weight.

DNA strands 16A-BP, 11T-BP and 15G-BP were purified with 22%, 30% and 8% yields, respectively. ESI-TOF analysis of the 16A-BP DNA displayed a peak at 1642.0270 m/z corresponding to the -5 charged species, computed to have m/z = 1642.3 for a 25-base DNA with a benzophenone-modified adenine. Nuclease digestion of unmodified 25-base DNA, with theoretical values of 2:12:2:9 for C:G:T:A, indicated an experimental ratio of 1.9:12.0:2.0:9.1 (Figure A.5A). The 11T-BP DNA, which is expected to have one fewer thymine than the unmodified DNA, was 2.1:12.4:0.9:8.7 (Figure A.5B). The 15G-BP DNA was 2.2:10.7:2.0:9.0 (Figure A.5C) and the 16A-BP DNA, 2.1:11.8:2.0:8.1 (Figure A.5D). All of these ratios are consistent with a

modification at the expected base. Maxam-Gilbert analysis of the 11T-BP DNA indicates that the modified base is the expected thymine (Figure A.6). Digested DNA containing this base is slightly retarded in the gel compared to DNA containing the amino-modified base (Figure A.6).

#### *Synthesis and characterization of cisplatin-modified DNA*

A 25-base DNA fragment containing a 1,2-d(GpG) adduct of cisplatin was purified by IE-HPLC. The purification yielded 1.7 nmol of platinated DNA, a 2.4% yield. UV-vis and AAS analysis showed that the collected DNA had a  $1.04 \pm 0.16$  platinum atoms per 25-base DNA. Nuclease digestion of the unplatinated DNA, with a theoretical C:G:T:A ratio of 12:2:9:2, provided values of 12.0:2.1:9.0:2.0 (Figure A.7A). The platinated DNA returned a 12.0:0.2:9.0:1.8 ratio, indicating that the guanine bases were platinated (Figure A.7B). Peaks at 15.0 and 19.5 min appear in the nuclease digestion of the cisplatin-modified DNA (Figure A.7B). These peaks likely contain digestion products  $[cis-Pt(NH_3)_2\{d(GpG)\}]^+$ ,  $[cis-Pt(NH_3)_2\{d(pGpG)\}]$ ,  $[cis-Pt(NH_3)_2(d(G))_2]^{2+}$ , or  $[cis-Pt(NH_3)_2(d(G))(d(pG))]^+$ .

#### *Synthesis of 25-bp duplexes*

Each of the benzophenone-modified DNA probes was annealed to cisplatin-modified and unmodified DNA. The duplexes were purified by 15% native PAGE.

#### *Analytical-scale photo-cross-linking of benzophenone-modified DNA*

Analytical-scale photo-cross-linking indicated that all three probes were able to photo-cross-link to proteins (Figure A.8). Only photo-cross-linking using the 15G-BP probe yielded unique proteins for platinated versus unplatinated DNA (Figure A.8C).

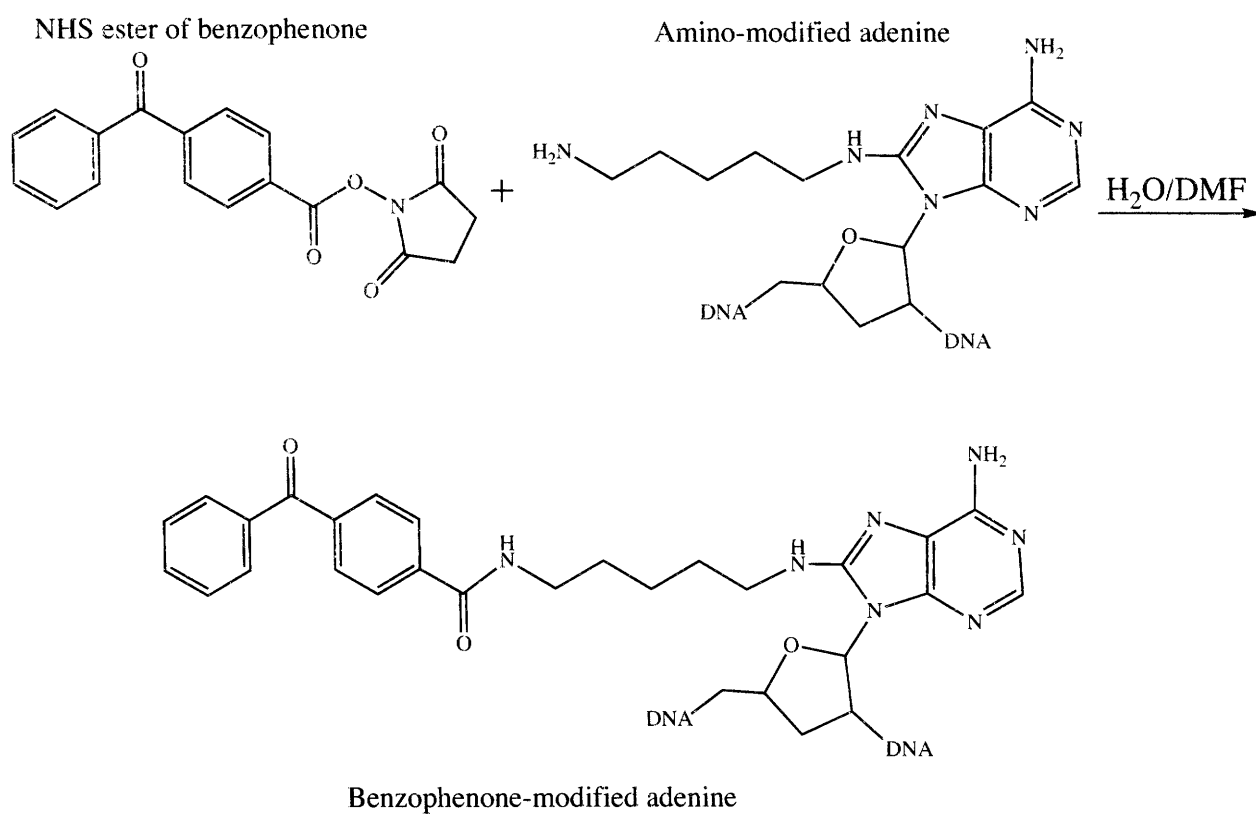
#### IV. DISCUSSION

The success of PtBP6-modified DNA in identifying proteins that bind to platinum-modified DNA, described in Chapters 2-4, had stimulated interest in photo-cross-linking methodologies that can identify proteins that bind to other types of platinum adducts and DNA-damaging agents. In this work, the benzophenone modification has been moved from the platinum atom to the DNA. Three benzophenone-modified DNA strands were synthesized. These strands were then annealed to cisplatin-modified and unmodified complementary DNA. The 11T-BP and 16A-BP (Figure A.3) probes photo-cross-linked to proteins, but the results from the undamaged or cisplatin-modified were identical (Figures A.8A and A.8B). Only the 15G-BP probe (Figure A.3) yielded cisplatin-specific photo-cross-linking (Figure A.8C). This result indicates that a modification at this base does not interfere with recognition of the platinum adduct and that it is positioned favorably for photo-cross-linking of proteins bound to the damage site. Preparative-scale photo-cross-linking experiments need to be completed for the 15G-BP probe to identify these proteins. Moreover, the complementary strand to 15G-BP should be synthesized with different platinum compounds, such as oxaliplatin, to determine whether the nature of the platinum compound dictates the binding of damage recognition proteins.

## V. REFERENCES

1. Zdraveski, Z. Z.; Mello, J. A.; Farinelli, C. K.; Essigmann, J. M.; Marinus, M. G., *J. Biol. Chem.* **2002**, 277, 1255-1260.
2. Buterin, T.; Meyer, C.; Giese, B.; Naegeli, H., *Chem. Biol.* **2005**, 12, 913-922.
3. Berens, C.; Courtoy, P. J.; Sonveaux, E., *Bioconjugate Chem.* **1999**, 10, 56-61.
4. Jamieson, E. R.; Jacobson, M. P.; Barnes, C. M.; Chow, C. S.; Lippard, S. J., *J. Biol. Chem.* **1999**, 274, 12346-12354.

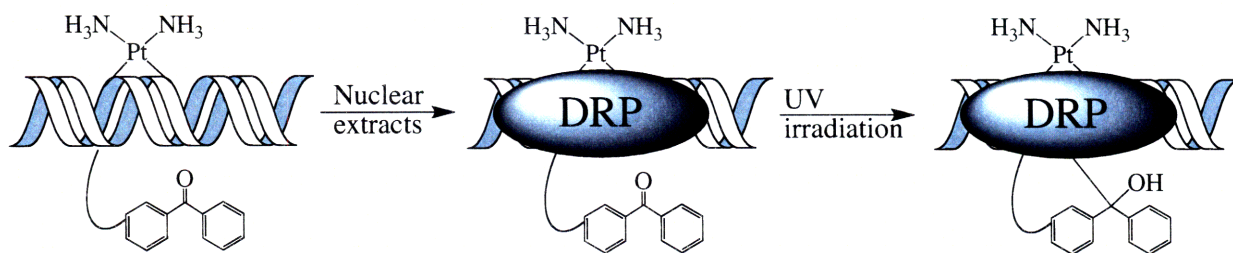
## VI. SCHEMES



Scheme A.1. Synthesis of benzophenone-modified DNA from commercially available starting materials.

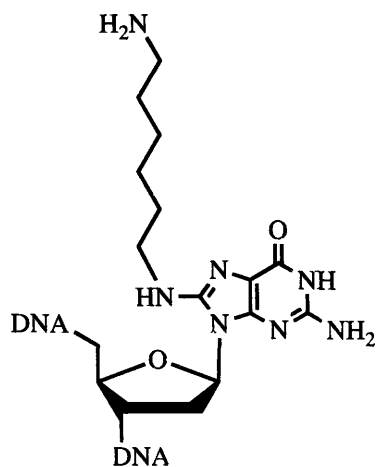


VII. FIGURES

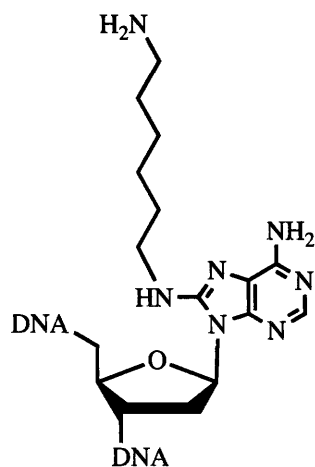


DRP = damage response protein

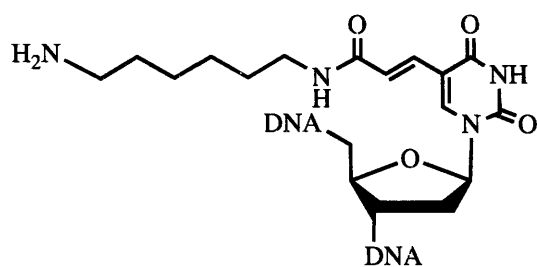
Figure A.1. Photo-cross-linking using benzophenone-modified DNA.



**Amino-modified  
guanine**



**Amino-modified  
adenine**



**Amino-modified  
thymine**

Figure A.2. Amino-modified bases prepared from commercially available starting materials.

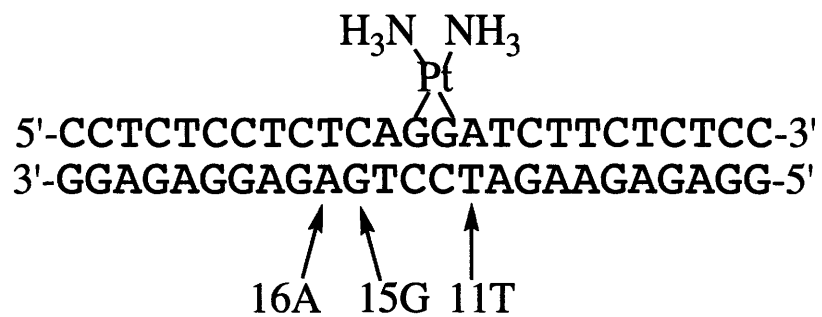


Figure A.3. The sites of benzophenone attachment used in these experiments.

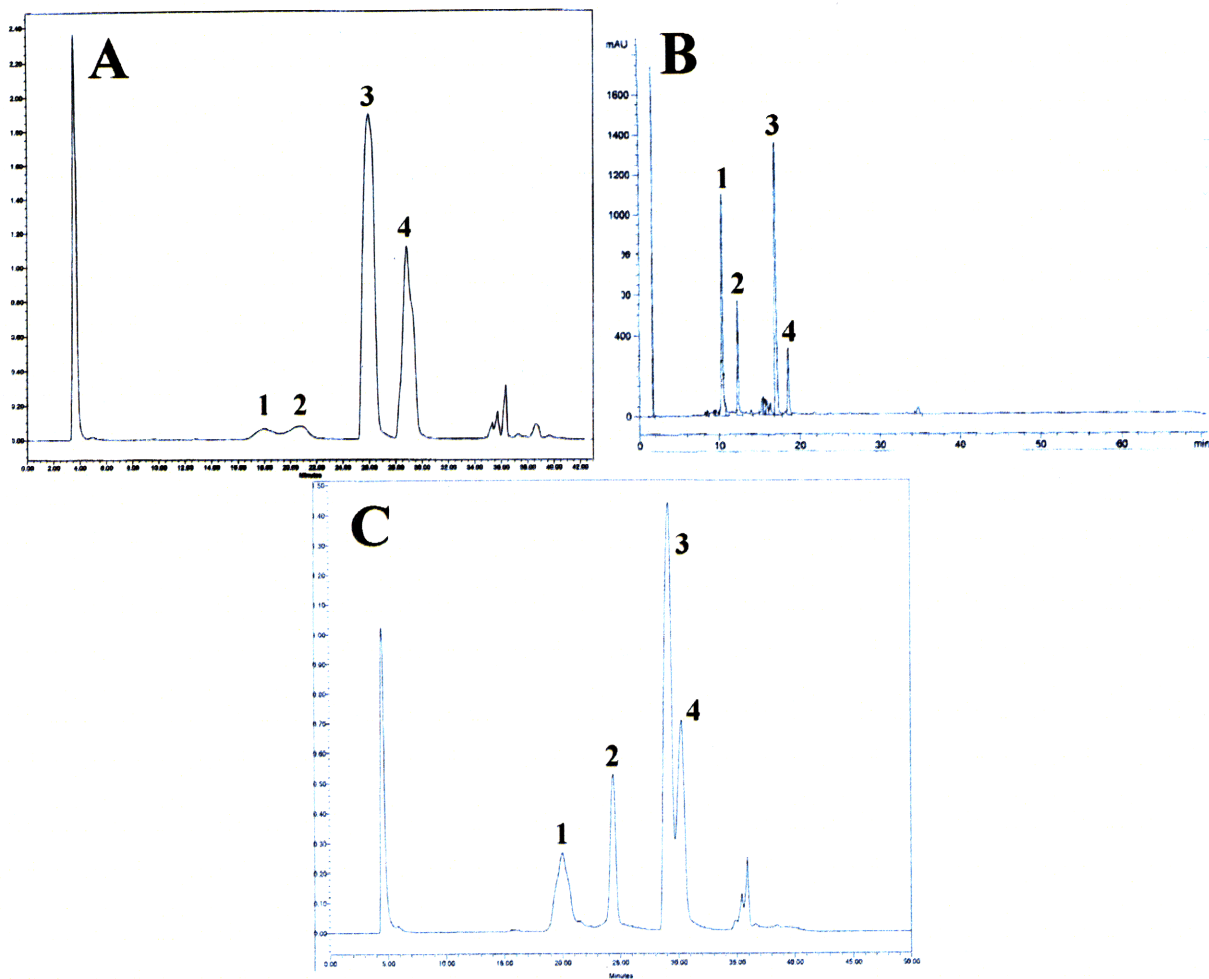
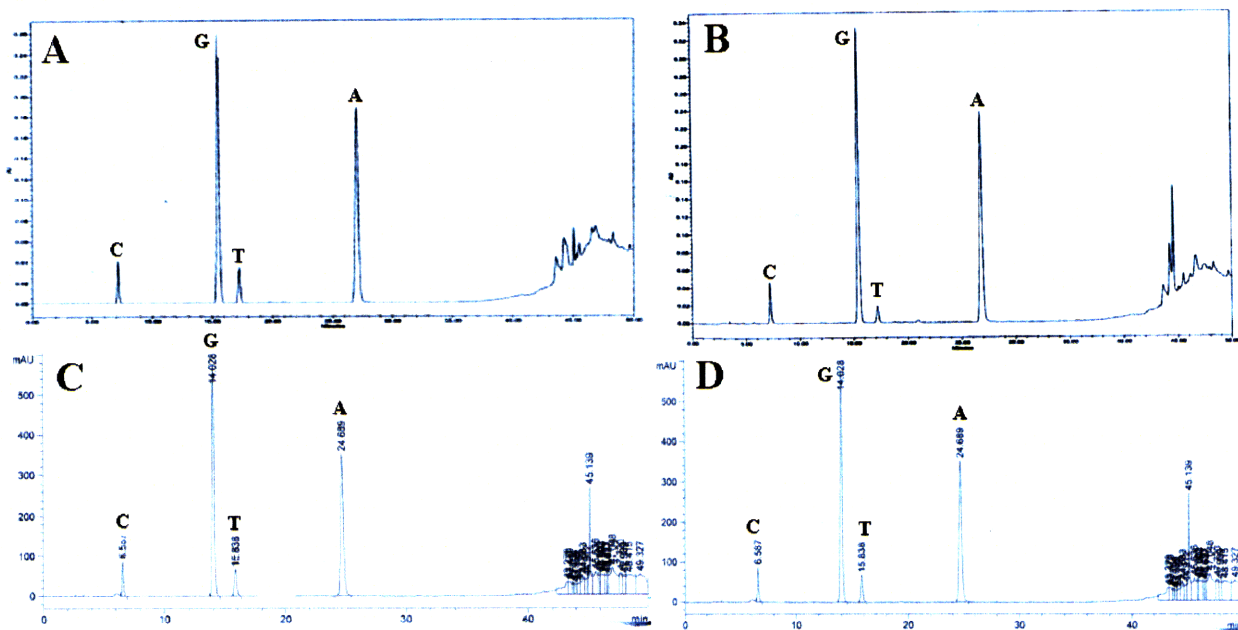


Figure A.4. RP-HPLC purification of benzophenone-modified DNA.

The RP-HPLC purification of the 11T-BP (**A**), 15G-BP (**B**), and 16A-BP (**C**) reactions. In each trace, peak 1 contains amino-modified starting material (Figure A.2), peak 2 contains the benzophenone-modified product. Following dialysis at a MWCO of 3500, no UV-vis signal was present for peaks 3 and 4, indicating that these peaks contain reaction byproducts of low molecular weight.



Base	Expected	Unmodified	11T-BP	15G-BP	16A-BP
C	2	1.9	2.1	2.2	2.1
G	12	12.0	12.4	10.7	11.8
T	2	2.0	0.9	2.0	8.2
A	9	9.1	8.7	9.0	8.1

Figure A.5. Nuclease digestion analysis of unmodified and benzophenone-modified DNA probe.

Unmodified (A), 11T-BP (B), 15G-BP (C), and 16A-BP (D) DNA. The table indicates the calculated values for each modified DNA.

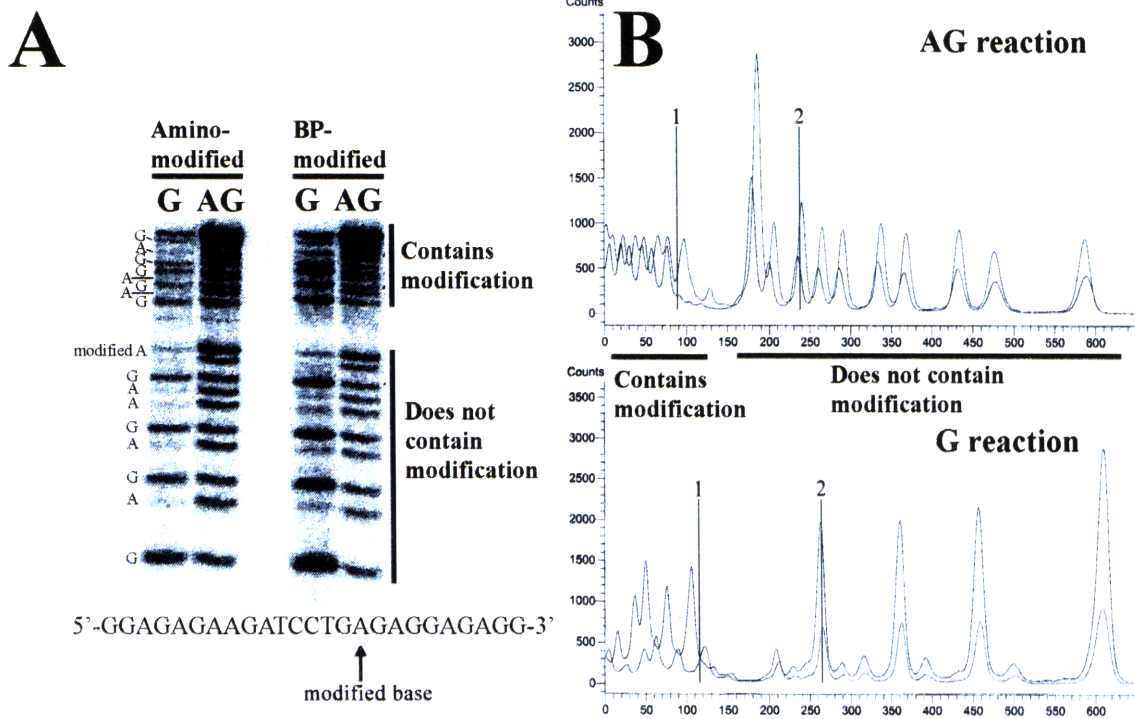
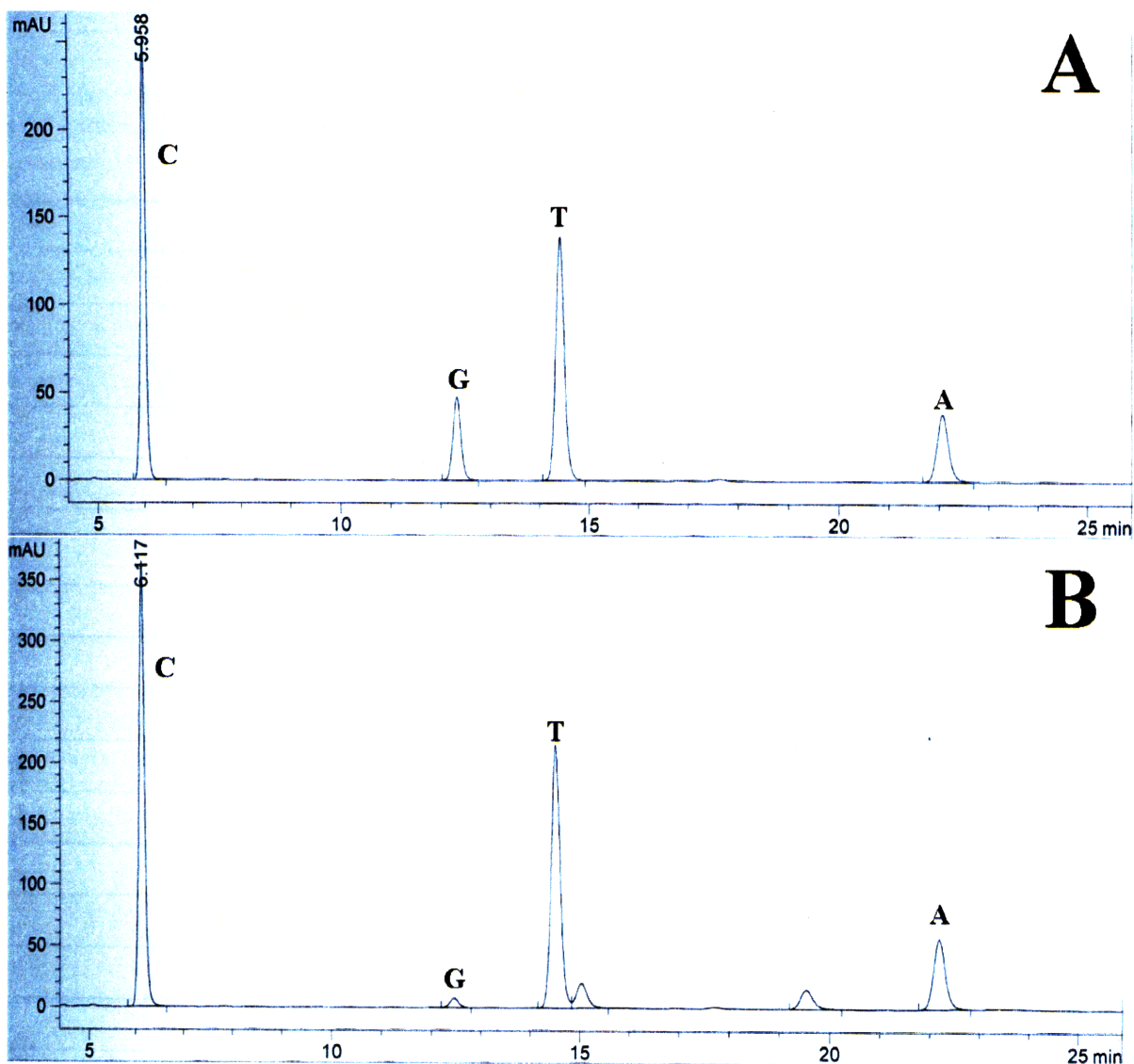


Figure A.6. Maxam-Gilbert analysis of amino- versus benzophenone-modified DNA.

A) 20% urea-PAGE analysis of the Maxam-Gilbert sequencing reactions. The benzophenone-modified probe contains a larger modification, which slightly retards the gel mobility of the digested DNA containing the modification. The DNA that does not contain the modified base migrates through the gel with equal mobility. A graphical representation of the gel (B) illustrates the difference in gel mobility between a band containing the benzophenone-modification (1) and one that does not (2).



Base	Expected	Unplatinated	Cisplatin-DNA
C	12	12.0	12.0
G	2	2.1	0.2
T	9	9.0	9.0
A	2	2.0	1.8

Figure A.7. Nuclease digestion analysis of cisplatin-modified DNA.

The digestion of the unplatinated strand (A) matched the expected peak areas for each base. The digestion of the platinated probe (B) indicated that the two guanines of the DNA were bound by platinum.

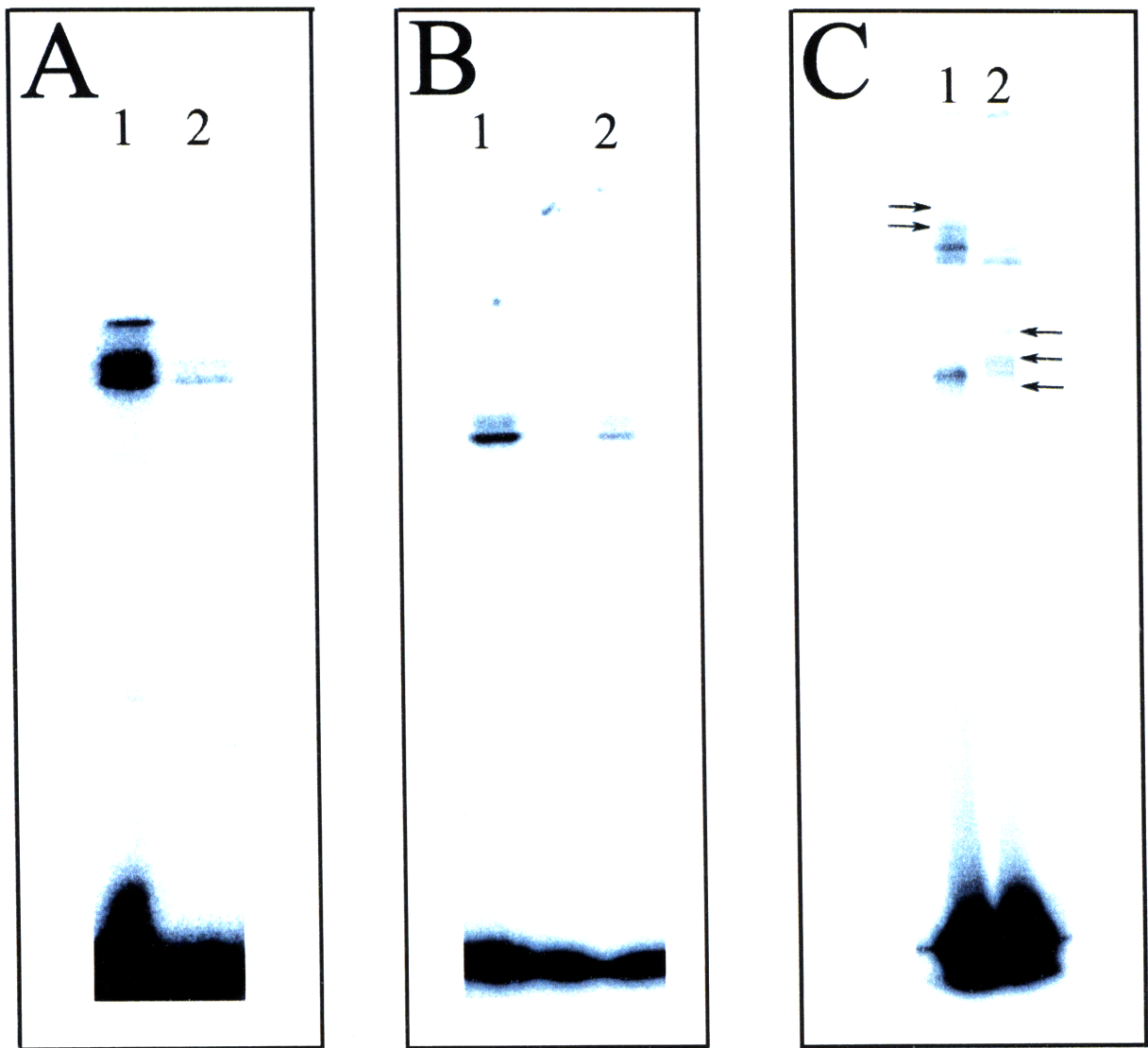


Figure A.8. Photo-cross-linking of DNA-BP duplexes.

The photo-cross-linking of the 11T-BP (**A**), 16A-BP (**B**), and 15G-BP (**C**) probes are presented. Lane 1: Probe annealed to unplatinated DNA. Lane 2: Probe annealed to cisplatin-modified DNA. The arrows in **C** indicate protein-DNA complexes containing proteins photo-cross-linked exclusively by either the unplatinated or platinated DNA. The differences between lanes 1 and 2 in **C** indicate that the 15G-BP probe is able to photo-cross-link to cisplatin-damaged DNA-binding proteins.



**Appendix B: Synthesis and characterization of a benzophenone-modified 157-base pair probe.**

## I. INTRODUCTION

The success of the 25-bp duplex and 90-base probes for photo-cross-linking and identification of proteins that bind to platinum-modified DNA, described in Chapters 2-4, led us to investigate an even longer DNA probe. Such a probe would increase the distance between DNA end-binding proteins and the photo-cross-linker, perhaps providing a more realistic environment of damaged DNA in cells. Work from our lab has demonstrated our ability to use 146-bp site-specifically platinated duplex probes to reconstitute nucleosomes from both native and recombinant histones.<sup>1-4</sup> The synthesis of such a long PtBP6-modified duplex would therefore allow photo-cross-linking experiments to take place on nucleosomal DNA in the future. In the present work, a PtBP6-modified 157-bp probe was synthesized. Analytical-scale photo-cross-linking experiments using this DNA were carried out.

## II. MATERIALS AND METHODS

All solvents and chemical reagents were purchased from commercial sources. DNA strands were synthesized on an Applied Biosystems ABI 392 DNA/RNA synthesizer using solvents and reagents supplied by Glen Research. Enzymes were purchased from New England BioLabs and Promega. UV-vis spectra were obtained on an HP 8453 UV-visible spectrometer. UV irradiation was conducted in a Stratagene Stratalinker UV Crosslinker.

### *Synthesis and characterization of a site-specifically platinated 25-base DNA*

Synthesis and characterization of a 25-base DNA containing a 1,2-d(GpG) adduct of PtBP6 were carried out as described in Chapter 2.

*Synthesis of other DNA strands.* A set of 48-, 49-, 60-, 63-, and 69-base DNA strands of the desired sequence, shown in Figure B.1, were prepared on the DNA synthesizer and purified by 6% urea-PAGE as described for the 65-base DNA in Chapter 4.

*Synthesis of a 157-bp duplex containing a 1,2-d(GpG) intrastrand adduct of PtBP6*

PtBP6-platinated or unplatinated 25-base DNA was radiolabeled using T4 PNK and  $\gamma$ -<sup>32</sup>P-ATP as described in Chapter 2. The 48-, 49-, and 69-base DNA strands were phosphorylated using standard T4 PNK protocols in 10 mM ATP. In an eppendorf tube, 100 pmol of radiolabeled 25-base DNA, phosphorylated 48-, 49-, and 69-base DNAs and unmodified 60- and 63-base DNAs were combined in 100  $\mu$ L of NEBuffer 3 (New England BioLabs, 50 mM Tris-HCl pH 7.9, 100 mM NaCl, 10 mM MgCl<sub>2</sub>, 1 mM DTT). The DNA was heated to 90 °C for 5 min and cooled to 16 °C over 4 h. To each tube was added 100  $\mu$ L of ligation reaction buffer (50 mM Tris-HCl, 10 mM MgCl<sub>2</sub>, 1 mM ATP, 10 mM DTT pH 7.5, 400 units T4 DNA ligase). The solutions were incubated at 16 °C overnight. The DNA was then ethanol precipitated, dried by vacuum centrifugation, and analyzed and subsequently purified by 6% urea-PAGE. The DNA was visualized by autoradiography and extracted from the gel by the crush and soak method. Following purification, the DNA strands were reannealed.

*Analytical-scale photo-cross-linking of 157-bp duplex containing a 1,2-d(GpG) intrastrand adduct of PtBP6*

To 1 pmol of a 157-bp duplex was added 20  $\mu$ g of HeLa nuclear extracts in 20  $\mu$ L of protein binding buffer (10 mM Tris pH 7.5, 10 mM KCl, 10 mM MgCl<sub>2</sub>, 1 mM EDTA,

0.05% NP-40, 0.2 µg/mL BSA). The solution was incubated on ice for 30 min and then exposed to UV irradiation for 2 h on ice. The cross-linking was analyzed by 5% SDS-PAGE with a 4% stacking gel.

*Exonuclease digestion of 157-bp duplex*

To each of four eppendorf tubes containing 20 µL of binding buffer was added 2 pmol of radiolabeled PtBP6-platinated or unplatinated 157-bp duplex. Next, 0.5 µL of 0.05 M dithiothreitol and 0, 0.5, 1 or 1.5 µL of ExoIII (New England BioLabs) was added to the tubes. The DNA was incubated at 37 °C for 30 min and the reactions were then ethanol precipitated and analyzed by 5% urea-PAGE.

*Enzymatic digestion-coupled analytical-scale photo-cross-linking of 157-bp duplex containing a 1,2-d(GpG) intrastrand adduct of PtBP6*

To 1 pmol of 157-bp duplex was added 20 µg of nuclear extract and 20 µL of binding buffer (10 mM Tris-HCl pH 7.5, 10 mM MgCl<sub>2</sub>, 50 mM KCl, 1 mM EDTA, 0.05% NP-40, 0.2 µg/mL BSA). The samples were UV irradiated for 2 h on ice. To the sample was added 0.5 µL of 0.05 M dithiothreitol and 0.5 µL of ExoIII. The reactions were incubated at 37 °C for 20 min and then analyzed by 5% SDS-PAGE.

### III. RESULTS

A 157-bp duplex site-specifically platinated with a 1,2-d(GpG) adduct of PtBP6 was synthesized and used for preliminary photo-cross-linking experiments. This probe was built from six separate DNA fragments, including a 25-base platinated DNA (Figure B.1). The synthesis and characterization of this DNA fragment are described in Chapter 2.

*Synthesis of a 157-bp duplex containing a 1,2-d(GpG) intrastrand adduct of PtBP6*

A 157-bp duplex containing a 1,2-d(GpG) intrastrand adduct of PtBP6 was synthesized from six DNA fragments using standard methodology. The DNA was phosphorylated, annealed, and ligated using commercially available enzymes. The DNA was analyzed by 6% urea-PAGE (Figure B.2). This gel indicates that a significant amount of 157-base DNA was formed in the reaction, and this DNA was then purified by preparative 6% urea-PAGE.

*Analytical-scale photo-cross-linking of 157-bp duplex containing a 1,2-d(GpG) intrastrand adduct of PtBP6*

Standard analytical-scale photo-cross-linking experiments, described in Chapter 2, were carried out using this 157-bp duplex. The protein-platinum-DNA complexes were not resolved and a long smear is visible on the gel (Figure B.3). Photo-cross-linking experiments using shorter probes, described in Chapters 2-4, resolved into distinct protein-platinum-DNA complexes. These results indicate that shorter DNA strands lead to better resolution of the bands. In order to shorten the 157-bp probe following photo-cross-linking but before the gel was carried out, the DNA was digested with an exonuclease.

*Exonuclease digestion of 157-bp duplex*

To decrease the size of the DNA and increase the resolution of the photo-cross-linking experiments, we digested the 157-bp duplex with exonuclease III. In initial experiments, the DNA was digested without exposure to nuclear extracts to ensure that this method would sufficiently degrade the DNA. Urea-PAGE analysis of the digested

DNA shows that the protocol was effective in producing a smaller DNA strand (Figure B.4). The band at about 80 bases in lane 4 indicates that the platination site is able to block the nuclease from completely degrading the DNA. This property is important because the radiolabel and the photo-cross-linker must remain tethered in order to visualize protein-platinum-DNA adducts by PAGE.

#### *Exonuclease digestion-coupled photo-cross-linking*

The duplex was then used in photo-cross-linking experiments, followed by incubation with exonuclease III prior to SDS-PAGE analysis. The gel revealed a number of more clearly resolved bands (Figure B.5), although the resolution still needs to be improved before preparative-scale experiments can be carried out.

## IV. DISCUSSION

Chapters 2-4 describe the photo-cross-linking and identification of proteins with an affinity for platinum-modified DNA using a photo-activatable cisplatin analogue, PtBP6. In that work, 25-bp and 90-base dumbbell probes were site-specifically modified with a platinum adduct. In the present work, a site-specifically platinated 157-bp duplex was synthesized and used in preliminary photo-cross-linking experiments. The longer DNA probe provides a better mimic of the environment of DNA damage inside a cell. Further, this type of duplex could be synthesized and used to reconstitute nucleosomes, and the proteins that bind to platinum-modified nucleosomal DNA could be identified.

Initial photo-cross-linking experiments using this 157-bp probe indicated that the protein-platinum-DNA complexes will not separate well by SDS-PAGE (Figure B.3). Exonuclease digestion of the DNA following UV irradiation but prior to gel analysis

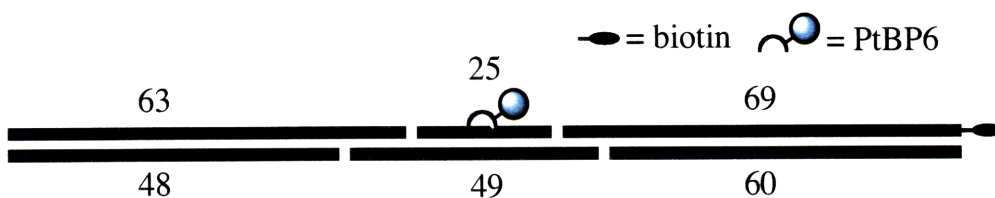
leads to better resolution of complexes (Figure B.5). The resolution of the DNA-platinum-protein complexes needs to be improved further before photo-cross-linking experiments on nucleosomal DNA will be possible, which may require other DNA digestion techniques to shorten the DNA prior to analysis.

## V. REFERENCES

1. Danford, A. J.; Wang, D.; Wang, Q.; Tullius, T. D.; Lippard, S. J., *Proc. Natl. Acad. Sci. U.S.A.* **2005**, 102, 12311-12316.
2. Ober, M.; Lippard, S. J., *J. Am. Chem. Soc.* **2007**, 129, 6278-6286.
3. Ober, M.; Lippard, S. J., *J. Am. Chem. Soc.* **2008**, 130, 2851-2861.
4. Wang, D.; Hara, R.; Singh, G.; Sancar, A.; Lippard, S. J., *Biochemistry* **2003**, 42, 6747-6753.



VI. FIGURES



63-base DNA:

5'-ATCAATATCCACCTGCAGATTCTACCAAAAGTGTATTTGGAA  
ACTGCTCCATCAAAGGCATG-3'

69-base DNA:

5'-CCTCAACATCGGAAAACCTCGTCAAAGGTTTATGTGAAA  
ACCATCTTAGACGTCCACCTATAACTA-biotin-3'

25-base DNA:

5'-CCTCTCCTCTCAGGATCTTCTCTCC-3'

60-base DNA:

5'-TAGTTATAGGTGGACGTCTAAGATGGTTTTACATAAACCTT  
TGACGAGGTAGTTTTCCG-3'

49-base DNA:

5'-ATGTTGAGGGGAGAGAAGATCCTGAGAGGAGAGGCATGCC  
TTTTGATGG-3'

48-base DNA:

5'-AGCAGTTTCAAATACACTTTTGGTAGAATCTGCAGGTGGAT  
ATTGAT-3'

Figure B.1. The 157-bp duplex is synthesized from six shorter DNA fragments.

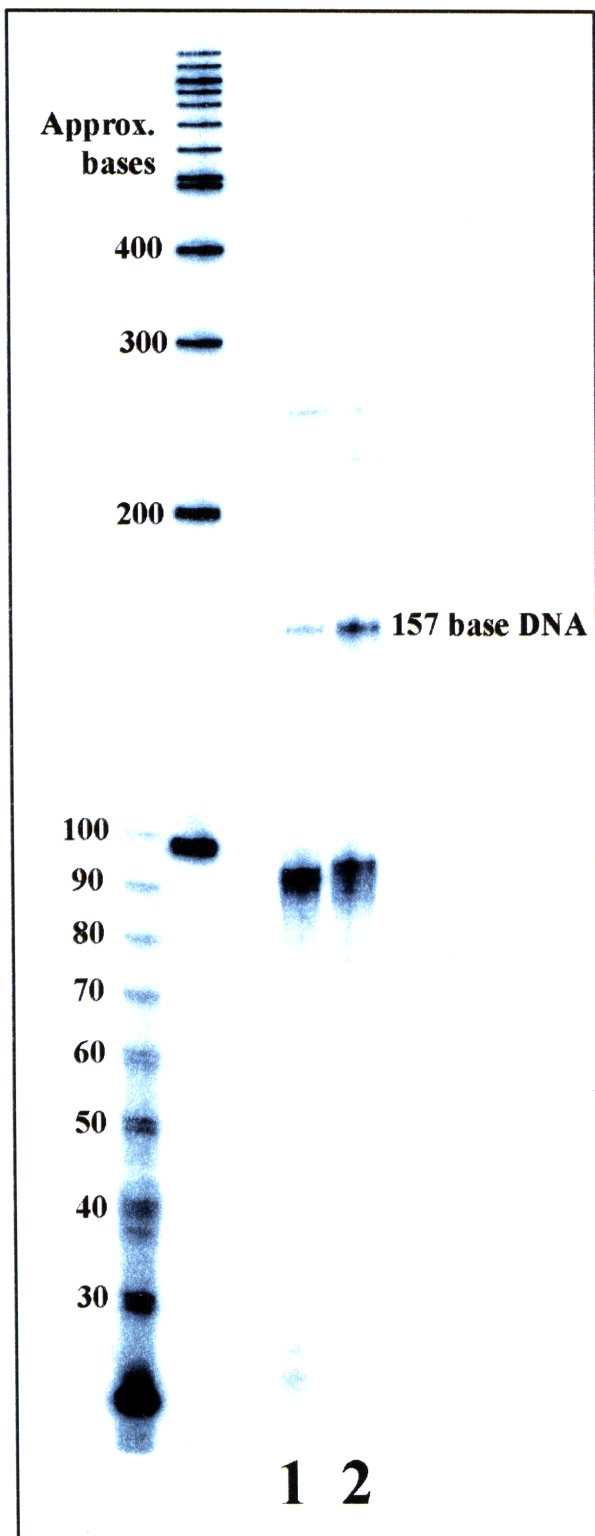


Figure B.2. 6% urea-PAGE analysis of 157-base DNA probe.

1) Unplatinated DNA. 2) PtBP6-modified DNA.

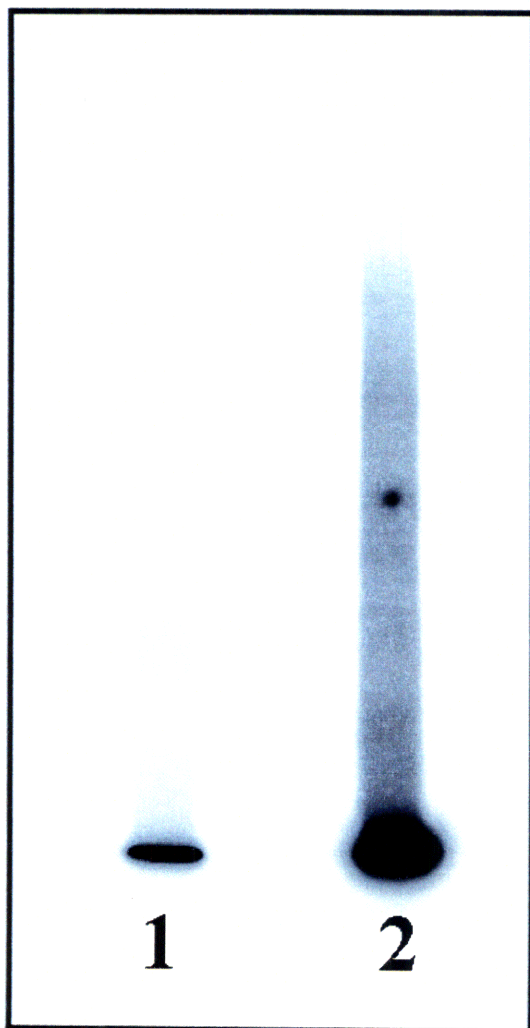


Figure B.3. Analytical-scale photo-cross-linking of 157-bp probe with HeLa nuclear extracts.

Lane 1: Unplatinated DNA. Lane 2: PtBP6-modified DNA. The PtBP6-modified probe photo-cross-links to several proteins, however, these protein-platinum-DNA complexes are not resolved on the gel.

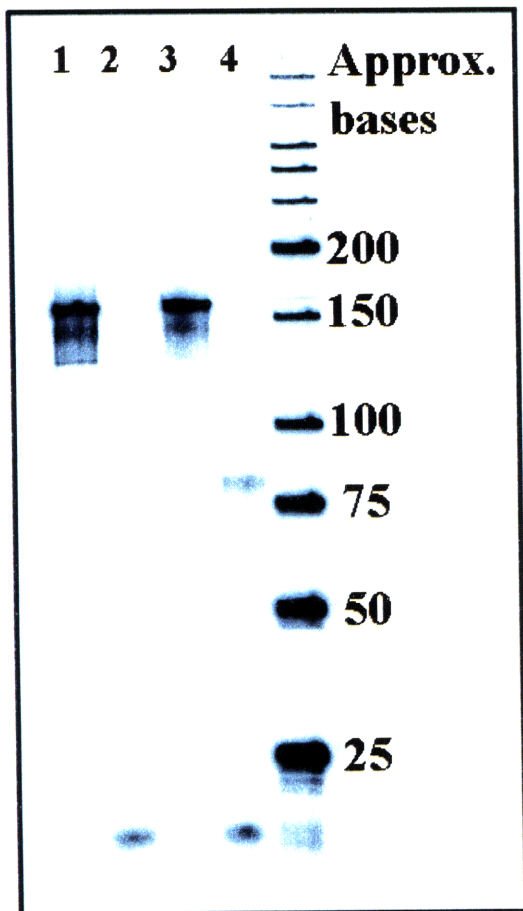


Figure B.4. Exonuclease III digestion of 157-bp duplexes.

Lane 1: Unplatinated duplex. Lane 2: Exonuclease III digested unplatinated 157-bp duplex. Lane 3: PtBP6-modified 157-bp duplex. Lane 4: Exonuclease III digested PtBP6-modified 157-bp duplex. The exonuclease is stalled at the platination site, resulting in a band at 81 bases.

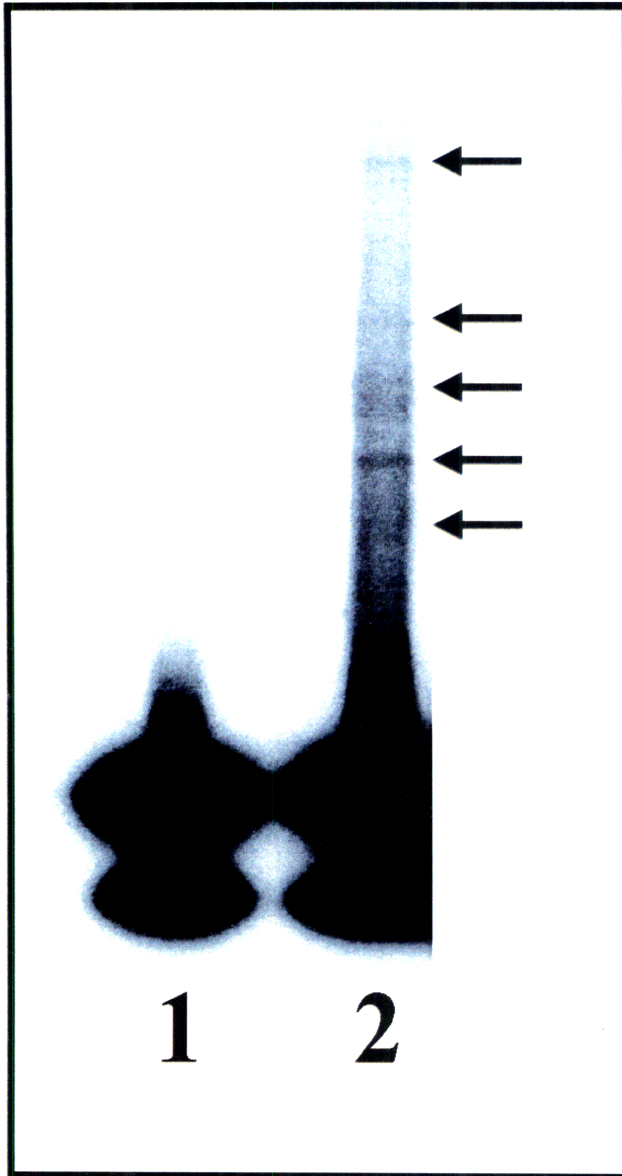


Figure B.5. Exonuclease-coupled photo-cross-linking experiment with 157-bp duplex.  
Lane 1: Unplatinated DNA. Lane 2: PtBP6-modified DNA. The arrows indicate protein-platinum-DNA complexes.

## **Appendix C: Synthesis of PtBP6-modified d(GpG).**

## I. INTRODUCTION

Chapters 2-4 describe the identification of nuclear proteins that bind to platinum-modified DNA using the photoactive cisplatin analogue *cis*-[Pt(NH<sub>3</sub>)(*N*-(6-aminohexyl)-4-benzophenonamide)Cl<sub>2</sub>] (PtBP6). The binding of this molecule to DNA should afford two orientational isomers as demonstrated with similarly asymmetric platinum compounds. The orientational isomers of *cis*-[Pt(NH<sub>3</sub>)(C<sub>6</sub>H<sub>11</sub>NH<sub>2</sub>){d(GpG)}]<sup>+1</sup> were investigated using a d(GpG) containing an <sup>15</sup>N-labeled N7 atom on the 3'-guanine.<sup>1</sup> The study of *cis*-[Pt(NH<sub>3</sub>)(4-aminoTEMPO){d(GpG)}]<sup>+2</sup> was aided by the presence of the paramagnetic nitroxide moiety.<sup>2</sup> These studies demonstrated that an asymmetric *cis*-[Pt(NH<sub>3</sub>)(NH<sub>2</sub>R)<sup>2+</sup>{d(GpG)}] cross-link can have the RNH<sub>2</sub> ligand oriented toward either the 5'- or 3'-end of the DNA (Figure C.1).

The d(pGpG) dinucleotide itself can also align into different conformers.<sup>3-8</sup> In order to characterize these conformers, platinum compounds containing bulky amine ligands were synthesized that slow the dynamic motion of the dinucleotide. Using 2-2'-bipiperidine-modified<sup>6</sup> and *N,N'*-dimehtyl-2,4-diaminopentane-modified<sup>8</sup> platinum compounds, the structures of several such conformers were established (Figure C.2). In the present study, *cis*-[Pt(NH<sub>3</sub>)(*N*-(6-aminohexyl)-4-benzophenonamide){d(GpG)}]<sup>+1</sup> was prepared and preliminary NMR spectroscopy experiments were performed to characterize the platinated DNA.

## II. MATERIALS AND METHODS

Solvents and chemical reagents were purchased from commercial sources. The d(GpG) molecule was prepared using solvents and reagents supplied by Glen Research. UV-vis spectra were obtained on an HP 8453 UV-visible spectrometer. Analytical and preparative HPLC work was performed either on an HP Waters or an Agilent 1200 HPLC system. LC/MS was performed on an Agilent 1100 Series LC/MSD system. NMR spectroscopy was performed on a Bruker

AVANCE-400 NMR spectrometer at the MIT department of chemistry instrumentation facility (DCIF).

*Synthesis of d(GpG) dinucleotide*

This synthesis is outlined in Scheme C.1. In a column containing a frit was placed 1.0 g of d(G)-CPG high load glass bead tethered guanine oligonucleotide (Glen Research) and a small stir bar. The column was sealed with a septum through which a tube flowing  $N_2(g)$  was inserted. On the bottom of the column, a stopcock was attached such that the column could either be closed or open to a line of tubing passing through a septum into a curved glass connector attached to a vacuum line and a round-bottom flask. In this manner, with the stopcock open and the vacuum on, the solution in the column would flow into the round-bottom flask. The column was positioned over a stir plate.

After purging the column with  $N_2(g)$  for five min, 10 mL of acetonitrile was injected into the column and the beads were stirred for five min. The acetonitrile was evacuated from the column and 10 mL of 3% trichloroacetic acid in dichloromethane was added. The solution was stirred for five min and the supernatant was removed by vacuum. This step was repeated three times. A 10 mL portion of acetonitrile was added to the column and it was stirred for one min before evacuation. This step was repeated three times.

To the column was added 4 mL of 0.45 M tetrazole in anhydrous acetonitrile and 0.25 g of d(G) phosphoramidite. The slurry was stirred for five min before removing the solvent by vacuum. This step was repeated three times. In total, 40 molar equivalents of tetrazole were added together with 10 equivalents of the phosphoramidite. A 10 mL portion of 0.2 M  $I_2$  in pyridine/THF/water was added and the suspension was stirred for one min and removed by



vacuum. This step was repeated once. Next, 10 mL of acetonitrile was added to the column and the solution was stirred for one min before evacuation. This step was repeated four times.

To the column was added 10 mL of 3% trichloroacetic acid in dichloromethane. The solution was stirred for five min and the supernatant was removed by vacuum. This step was repeated three times. Next, 10 mL of acetonitrile was added to the column and was stirred for one min before evacuation. This step was repeated three times. To the column was then added 20 mL of 30%  $\text{NH}_4\text{OH}$  and the beads were stirred for one h. The round-bottom flask was then replaced and the  $\text{NH}_4\text{OH}$  solution was collected. The column was washed with 5 mL of 30%  $\text{NH}_4\text{OH}$  that was combined with to the previously collected aliquot. The solution was heated to 55 °C overnight. The solution was then cooled on ice and the  $\text{NH}_4\text{OH}$  was removed by vacuum centrifugation. The DNA pellet was then dissolved in 25 mL of ddH<sub>2</sub>O and syringe filtered to remove insoluble particles.

#### *Purification of the d(GpG) dinucleotide*

The solution was analyzed by LC/MS. The larger of two LC peaks corresponded to an ESI-MS reading of 595.5 m/z in accord with the expected value for the  $\text{d}(\text{GpG})^-$  of to 595.1 m/z. The mixture was then purified by C18 RP-HPLC, the method employed 20% - 40% B, where solvent A was 0.1 M ammonium acetate in water and solvent B was 0.1 M ammonium acetate in 50% water and 50% acetonitrile. The peak corresponding to the product eluted at 7.0 min and was collected and lyophilized. The lyophilized compound was then dissolved in water and dialyzed against water with a molecular weight cutoff of 500. A total of 14.1  $\mu\text{mol}$  of DNA was collected, a 14.1% yield from the d(G)-CPG high load glass bead starting material.

#### *Characterization of d(GpG) dinucleotide*

The concentration of DNA was determined by UV-vis spectroscopy. The product was characterized by  $^1\text{H}$  NMR spectroscopy; ( $\text{D}_2\text{O}$ , pH 5.0): 8.01 (1H, s), 7.75 (1H, s), 6.162 (1H, t), 6.02 (1H, dd), 4.18 (2H, m), 4.11 (2H, m), 2.76 (1H, m), 2.45 (2H, m), 2.25 (1H, m). The DNA was also characterized by ESI-MS, with a peak at 595.5 m/z and the expected value for the  $\text{d}(\text{GpG})^-$  equal to 595.1 m/z.

#### *Synthesis of PtBP6-modified d(GpG) dinucleotide*

PtBP6 was activated as described in Chapter 2. To a solution of 14.1  $\mu\text{mol}$  of  $\text{d}(\text{GpG})$  was added 28  $\mu\text{mol}$  activated PtBP6 in 10 mM  $\text{Na}_2\text{HPO}_4$  buffer. The solution was incubated with mixing at 37° C overnight in the dark. The reaction was then purified by RP-HPLC, 5 - 95% B over 60 min where solvent A was 0.1% TFA in water and solvent B was 0.1% TFA in acetonitrile.

#### *Characterization of PtBP6-modified d(GpG) dinucleotide*

The concentration of DNA was determined by UV-vis spectroscopy. The mass of the platinated dinucleotide was determined by ESI-MS and showed peaks at 566.4 and 1131.2 m/z with the expected platinum isotope pattern. For a  $\text{d}(\text{GpG})$  dinucleotide in which PtBP6 was cross-linked to both guanines, the expected mass for  $[\text{M}+\text{H}]^{2+}$  is 565.7 m/z and for  $[\text{M}]^+$  is 1130.3 m/z. The compound was characterized by  $^1\text{H}$  NMR spectroscopy ( $\text{D}_2\text{O}$ , pH 5.0): 8.60 (1H, s, br), 8.41 (1H, s), 8.29 (1H, s), 8.08 (1H, s), 7.84-7.68 (7H, m), 7.54 (2H, td), 6.13 (2H, m), 4.70 (1H, s, br), 4.55 (1H, s, br), 4.15 (1H, s), 4.00, (3H, m), 3.72 (1H, t), 3.45 (1H, s, br), 3.34 (2H, q), 2.78-2.45 (6H, m), 1.69 (2H, m), 1.55 (2H, m), 1.28 (4H, m).  $^1\text{H}$  NMR spectroscopy experiments were repeated at pH values 4, 5, 7, 10 using DCl and NaOD solutions (Cambridge Isotope Labs) to adjust the pH. The DNA was further characterized by COSY NMR spectroscopy.

### III. RESULTS

#### *Synthesis and characterization of d(GpG) dinucleotide*

A total of 14.1  $\mu$ mole of purified dinucleotide was synthesized by this method, a 14.1% yield. ESI-MS analysis shows a mass of 595.5 m/z, with the calculated mass for  $[M]^-$  being 595.1 m/z. NMR spectroscopy of the product showed the expected peaks for this compound (Figure C.3).

#### *Synthesis of PtBP6-modified d(GpG) dinucleotide*

Platination of the dinucleotide with PtBP6 was carried out using standard methodology for this type of reaction. The reaction was purified by RP-HPLC with two major products corresponding to the unreacted dinucleotide and the platinated dinucleotide (Figure C.4). A 3.3  $\mu$ mole portion of platinated dinucleotide was collected as determined by UV-vis spectroscopy, a 23.4% yield.

#### *Characterization of PtBP6-modified d(GpG) dinucleotide*

The product was analyzed by ESI-MS, and showed peaks at 566.4 and 1131.2 m/z with the expected platinum isotope pattern. For a d(GpG) dinucleotide in which PtBP6 was cross-linked to both guanines, the expected mass for  $[M+H]^{2+}$  is 565.7 m/z and for  $[M]^+$  it is 1130.3 m/z. The purified compound was analyzed by  $^1\text{H}$  NMR spectroscopy (Figure C.5). All the peaks were assigned except for the H8 atoms of the guanine bases. There were four peaks in the region where the H8 proton peaks are expected at 8.07, 8.28, 8.42, and 8.60 ppm. It is likely that the H8 peaks are split due to multiple conformers of the compound in the solution.<sup>6,8,9</sup> pH-Dependent NMR spectroscopy was also carried out to determine whether these peaks showed similar pH-dependent values to other platinated DNA in the literature (Figure C.6).<sup>10-14</sup> No shift of the H8

peaks occurs from pH 4 to 5 (Figure C.6A and C.6B). At pH 7 (Figure C.6C), one small broad peak is visible at 8.29 ppm. At pH 10 (Figure C.6D), the peak at 8.29 ppm remains, and four small peaks at 7.95, 8.58, 8.88 and 9.28 ppm, which integrate to less than one fourth of a proton each, and a larger peak at 7.90 ppm appear. The significance of these shifts is discussed in the next section.

COSY analysis confirms the peaks assignments from the 1D NMR spectroscopy (Figure C.7). All of the expected cross-peaks are present except a B1  $\rightarrow$  A1, A1' cross-peak. This omission is most likely due to the separate broad signals from the two A1 protons. For comparison, the two analogous A2 proton signals create a single sharp peak at 4.0 ppm, and the cross-peak with the B2 proton at 4.15 ppm is weak. Since the A1 peaks are broad and separated, the cross-peaks are not strong enough to show up by COSY at this concentration. Every other through-bond interaction results in a strong cross-peak, as indicated in Figure C.7.

#### IV. DISCUSSION

The major DNA adduct of the anticancer drug cisplatin is a 1,2-d(GpG) intrastrand cross-link in which the platinum binds to the N7 of adjacent guanine bases. The NMR structures of platinum-modified short oligomers have been reported extensively in the literature.<sup>1-3,5,6,8-10,13,15</sup> In the work described in Chapters 2-4, a new platinum compound, *cis*-[Pt(NH<sub>3</sub>)(*N*-(6-aminohexyl)-4-benzophenonamide)Cl<sub>2</sub>] (PtBP6), containing a photoactive benzophenone moiety tethered to a platinum amine ligand through a six-carbon linker was used to identify proteins that bind to platinum-modified DNA. The binding of this compound to DNA should afford orientational isomers in which the benzophenone is directed towards either the 3' or 5'-end of the DNA (Figure C.1). This type of isomerism was demonstrated for the DNA-bound forms of

the compounds *cis*-[Pt(NH<sub>3</sub>)(C<sub>6</sub>H<sub>11</sub>NH<sub>2</sub>)Cl<sub>2</sub>] and *cis*-[Pt(NH<sub>3</sub>)(4-aminoTEMPO)Cl]<sub>2</sub>,<sup>1,2</sup> which also have two different N-donor ligands. Here, NMR spectroscopic studies were carried out on PtBP6-modified d(GpG).

#### *Assignment of NMR spectroscopic peaks*

All expected peaks were identified in the NMR spectroscopic analysis of the unplatinated d(GpG) (Figure C.3). Signals from protons on the 3'- or 5'-guanosine were assigned tentatively based on literature values for small unplatinated oligomers.<sup>9,10,13</sup> The dinucleoside monophosphate was allowed to react with PtBP6 and the product was purified by RP-HPLC, yielding one major species (Figure C.4, Peak 2). The binding of platinum to d(GpG) draws the guanine bases closer to one another, and proton resonance are generally shifted downfield.<sup>3,5</sup> One characteristic chemical shift in platinated DNA is the H8 proton. A downfield shift in H8 is a benchmark of platinum-DNA binding interactions.<sup>11-13</sup> The two H8 peaks in d(GpG), which shift downfield upon binding to PtBP6 (Figures C.3 and C.5), split into four peaks. This splitting could be caused by the presence of two orientational isomers in solution (Figure C.1). The two isomers of the compound *cis*-[(Pt)(NH<sub>3</sub>)(NH<sub>2</sub>CH<sub>2</sub>CH<sub>3</sub>){r(GpG)}]<sup>+</sup> resulted in H8 resonances of 8.10, 8.20, 8.79 and 8.82 ppm,<sup>16</sup> whereas the present work reveals resonances of 8.07, 8.28, 8.42, and 8.60 ppm. Conversely, the four H8 resonances could be due to conformers of the dinucleoside monophosphate (Figure C.2). Platination also causes the H8 protons to exchange more readily with deuterium from the aqueous solvent,<sup>17</sup> and the four peaks integrate into less than one-half proton each. The H8 resonance at 8.60 ppm is broader than the other three peaks. This behavior could be due to either slow interconversion of conformers of the d(GpG) (Figure C.2) or faster exchange with the solvent of one H8 proton from a specific orientational isomer (Figure C.1).

The sample was also analyzed by COSY (Figure C.7) to ensure that the peaks were correctly attributed. All the expected cross-peaks were seen, showing that the spectrum was correctly assigned. No cross-peaks were found for the peaks assigned to the H8 protons, indicating that they are assigned correctly, since no through-bond interactions are expected.

#### *pH-Dependent NMR of PtBP6-d(GpG)*

In order to further characterize the four H8 peaks for this compound, pH-dependent NMR spectroscopy experiments were carried out. At higher pH, H8 peaks on platinated DNA will shift upfield.<sup>10-14</sup> This shift is attributed to the deprotonation of the N1 of guanine.<sup>13</sup> For the d(GpG)-PtBP6 complex, raising the pH from 4 to 5 does not shift the peaks (Figures C.6A and C.6B). At pH 7 only a small broad peak at 8.29 ppm is visible (Figure C.6C). At pH 10, this peak remains and four small peaks, at 7.95, 8.58, 8.88 and 9.28 ppm, and a larger peak at 7.90 ppm appear (Figure C.6D). NMR studies of the orientational isomers of platinum compounds with asymmetric ammine ligands bound to DNA have been reported in the literature. One orientational isomer of the compound  $cis\text{-}[(Pt)(NH_3)(C_6H_{11}NH_2)\{d(GpG)\}]^+$  showed H8 resonance of 8.3 and 8.1 ppm at pH 6, which shifted to 8.2 and 7.4 at pH 12.<sup>1</sup> The orientational isomers of to  $cis\text{-}[(Pt)(NH_3)(NH_2CH_2CH_3)\{r(GpG)\}]^+$  were also isolated and analyzed by NMR spectroscopy.<sup>16</sup> The H8 chemical shifts of one isomer deviate from 8.82 and 8.10 to 8.55 and 7.62 ppm from pH 5 to pH 10. The other orientational isomer has shifts of 8.79 and 8.20 that change to 8.25 and 8.00 from pH 2 to pH 10. These shifts are depicted in Figure C.8. All of these data exhibit an inflection point at pH 8.5, corresponding to deprotonation of N1.

The four H8 peaks for d(GpG)-PtBP6 are present at pH 5 and only one is present at pH 7. The aromatic signal from the benzophenone moiety could potentially overlap with these peaks if they shifted upfield, but its integration remains constant, suggesting that the H8 hydrogen atoms

exchange with the solvent at increased pH (Figure C.6C). At pH 10 (Figure C.6D), small peaks appear downfield of the four peaks at pH 4 and 5, and one peak is present upfield very close to the aromatic signal. According to the literature, at pH 10 the H8 signals should have shifted upfield, which is not the case for this molecule. The pH-dependent NMR experiments were unable to yield any new structural information on the isomers present in solution.

## V. CONCLUSIONS AND FUTURE DIRECTIONS

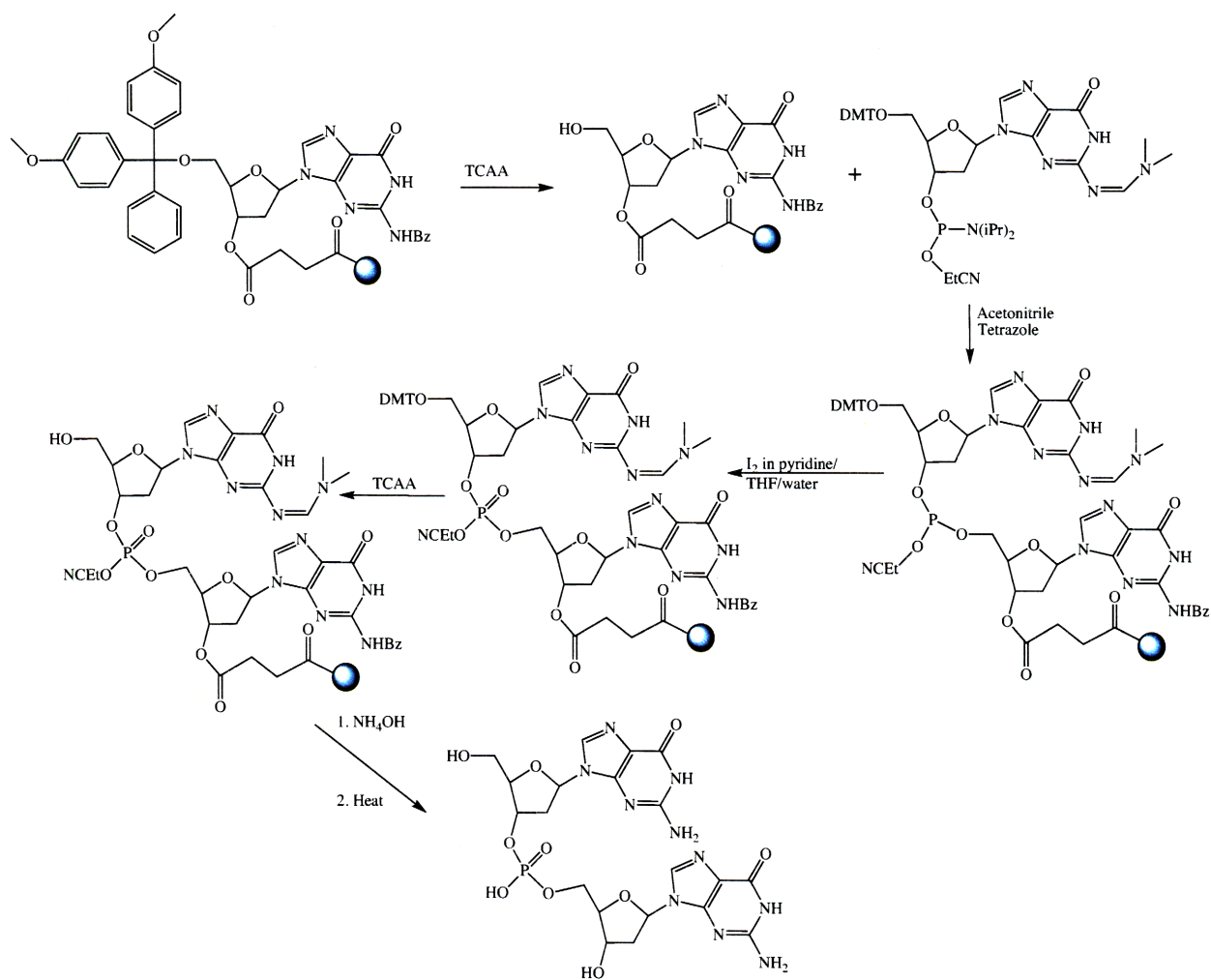
The compound *cis*-[Pt(NH<sub>3</sub>)(*N*-(6-aminohexyl)-4-benzophenonamide){d(GpG)}]<sup>+</sup> was synthesized and purified by RP-HPLC. ESI-MS indicates that the desired compound was formed. It was analyzed by <sup>1</sup>H NMR spectroscopy and COSY, but these methods were unable to fully characterize the orientational isomers. Four H8 resonances were revealed, indicating the presence of either two orientational isomers (Figure C.1) or multiple d(GpG) conformers (Figure C.2). pH-Dependent NMR experiments did not give any new structural information about these isomers because the behavior of the compound at basic pH did not reflect that of similar complexes from the literature. In the future, low temperature NMR experiments will determine whether the one broad H8 signal at 8.60 ppm is due to slow interconversion of multiple conformers or faster exchange with the solvent of one H8 proton of a specific orientational isomer. If the signal splits into multiple peaks at low temperature, we will know that there are multiple conformers present (Figure C.2). If the signal sharpens without splitting, the broadening is due to exchange with the solvent, making it more likely that orientational isomers are present (Figure C.1). NOESY studies will also be performed to characterize the through-space interactions between the two bases, and possibly interactions between the benzophenone moiety and one of the bases, depending on the orientational isomer.

## VI. REFERENCES

1. Hartwig, J. F.; Lippard, S. J., *J. Am. Chem. Soc.* **1992**, 114, 5646-5654.
2. Dunham, S. U.; Lippard, S. J., *J. Am. Chem. Soc.* **1995**, 117, 10702-10712.
3. Den Hartog, J. H. J.; Altona, C.; Chottard, J.-C.; Girault, J.-P.; Lallemand, J.-Y.; De Leeuw, F. A. A. M.; Marcelis, A. T. M.; Reedijk, J., *Nucleic Acids Res.* **1982**, 10, 4715-4730.
4. Elizondo-Riojas, M.-A.; Kozelka, J., *J. Mol. Biol.* **2001**, 314, 1227-1243.
5. Kozelka, J.; Fouchet, M.-H.; Chottard, J.-C., *Eur. J. Biochem.* **1992**, 205, 895-906.
6. Marzilli, L. G.; Ano, S. O.; Intini, F. P.; Natile, G., *J. Am. Chem. Soc.* **1999**, 121, 9133-9142.
7. Sherman, S. E.; Gibson, D.; Wang, A. H.-J.; Lippard, S. J., *J. Am. Chem. Soc.* **1988**, 110, 7368-7381.
8. Williams, K. M.; Scarcia, T.; Natile, G.; Marzilli, L. G., *Inorg. Chem.* **2001**, 40, 445-454.
9. Fouts, C. S.; Marzilli Luigi, G.; Byrd, R. A.; Summers, M. F.; Zon, G.; Sinozuka, K., *Inorg. Chem.* **1988**, 27, 366-376.
10. Neumann, J.-M.; Tran-Dinh, S.; Girault, J.-P.; Chottard, J.-C.; Huynh-Dinh, T.; Igolen, J., *Eur. J. Biochem.* **1984**, 141, 465-472.
11. Girault, J.-P.; Chottard, G.; Lallemand, J.-Y.; Chottard, J.-C., *Biochemistry* **1982**, 21, 1352-1356.
12. Marcelis, A. T. M.; Den Hartog, J. H. J.; Van Der Marel, G. A.; Wille, G.; Reedijk, J., *Eur. J. Biochem.* **1983**, 135, 343-349.
13. Caradonna, J. P.; Lippard, S. J., *J. Am. Chem. Soc.* **1982**, 104, 5793-5795.
14. Inagaki, K.; Sawaki, K., *Bull. Chem. Soc. Jpn.* **1993**, 66, 1822-1825.
15. Over, D.; Bertho, G.; Elizondo-Riojas, M.-A.; Kozelka, J., *J. Biol. Inorg. Chem.* **2006**, 11, 139-152.
16. Inagaki, K.; Nakahara, H.; Alink, M.; Reedijk, J., *J. Chem. Soc., Dalton Trans.* **1991**, 1337-1341.
17. Lippert, B., Platinum Nucleobase Chemistry. In Progress in Inorganic Chemistry, Lippard, S. J., Ed. John Wiley & Sons, Inc.: Hoboken, NJ, 1989; Vol. 37, pp 1-97.



## VII. SCHEMES



Scheme C.1. Synthesis of d(GpG).

TCAA, 3% trichloroacetic acid in dichloromethane.

VIII. FIGURES

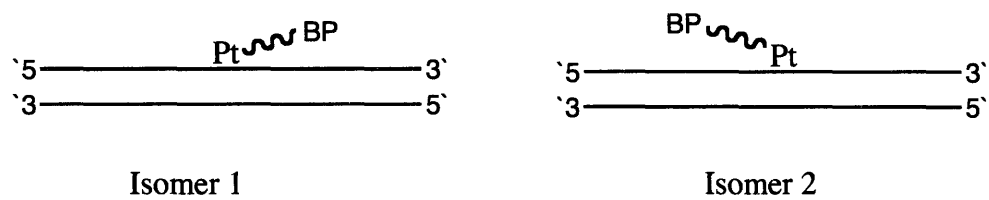


Figure C.1. Orientational isomers of PtBP6 on DNA.

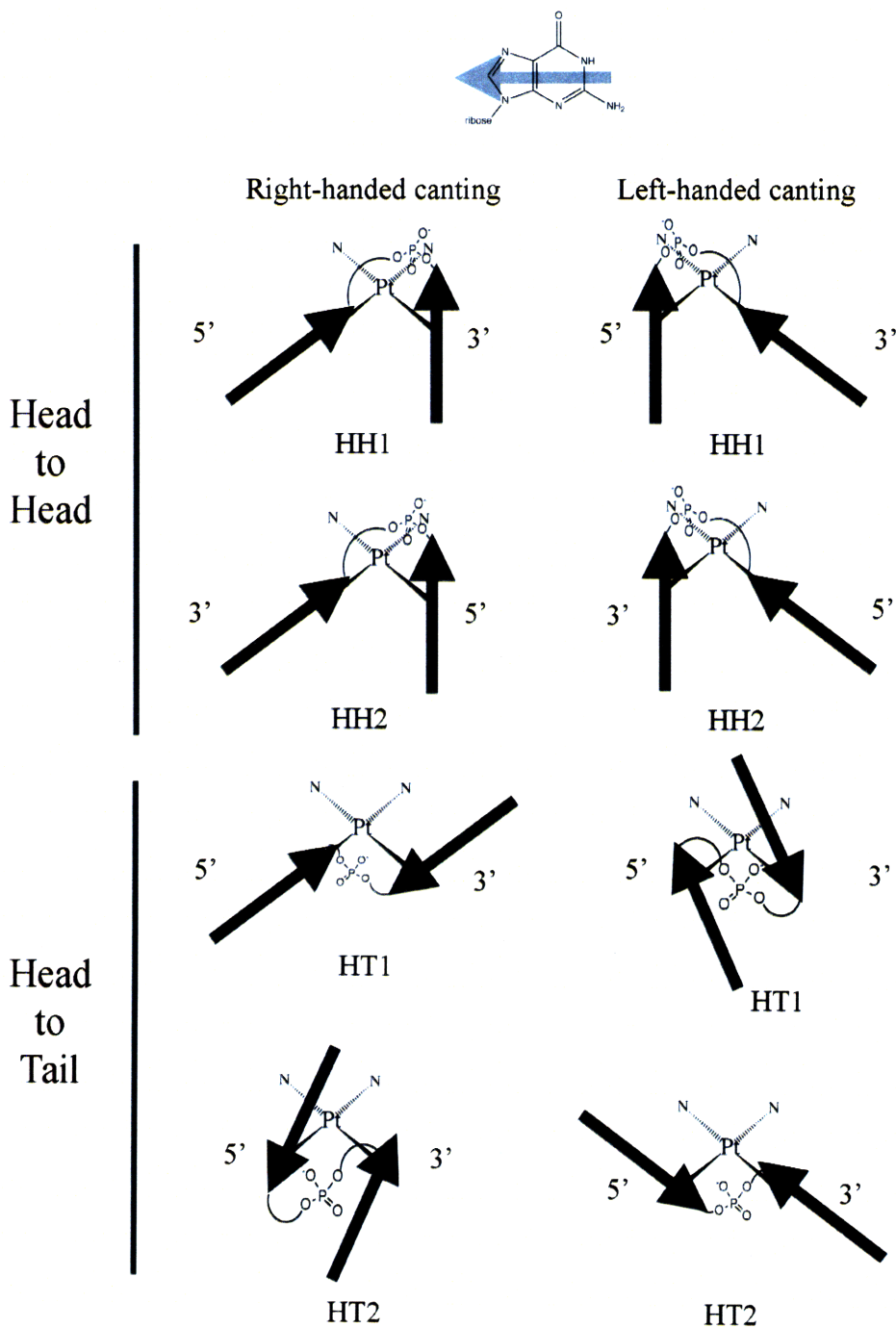


Figure C.2. Conformers of d(GpG).

Adapted from Williams *et al.*<sup>8</sup> The “N” ligands of the platinum are either ammine or BP6, depending on the orientation of the BP6 ligand illustrated in Figure C.1. The orientation of the guanine represented by the arrows is shown at the top of the figure.

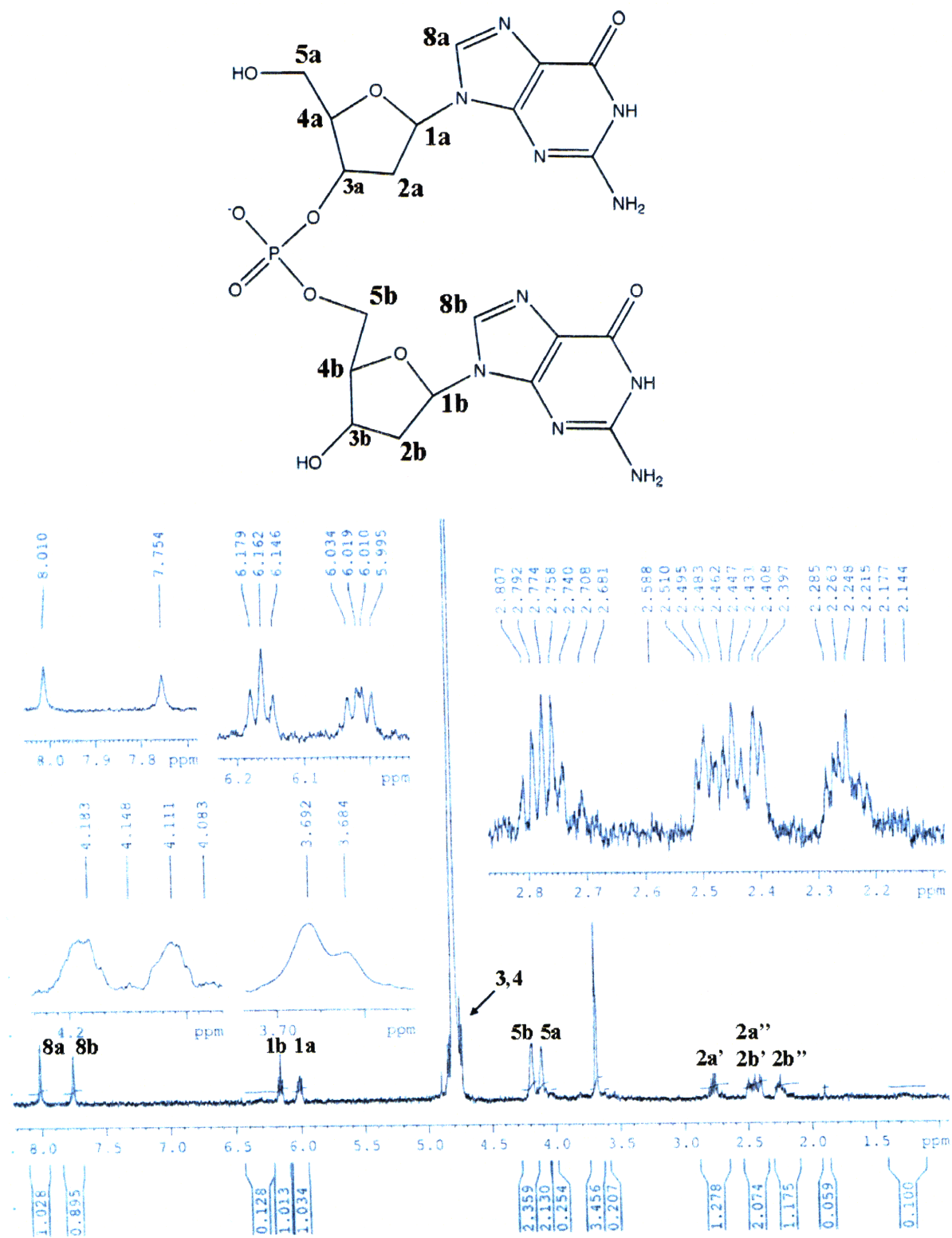


Figure C.3. <sup>1</sup>H NMR spectrum of d(GpG).

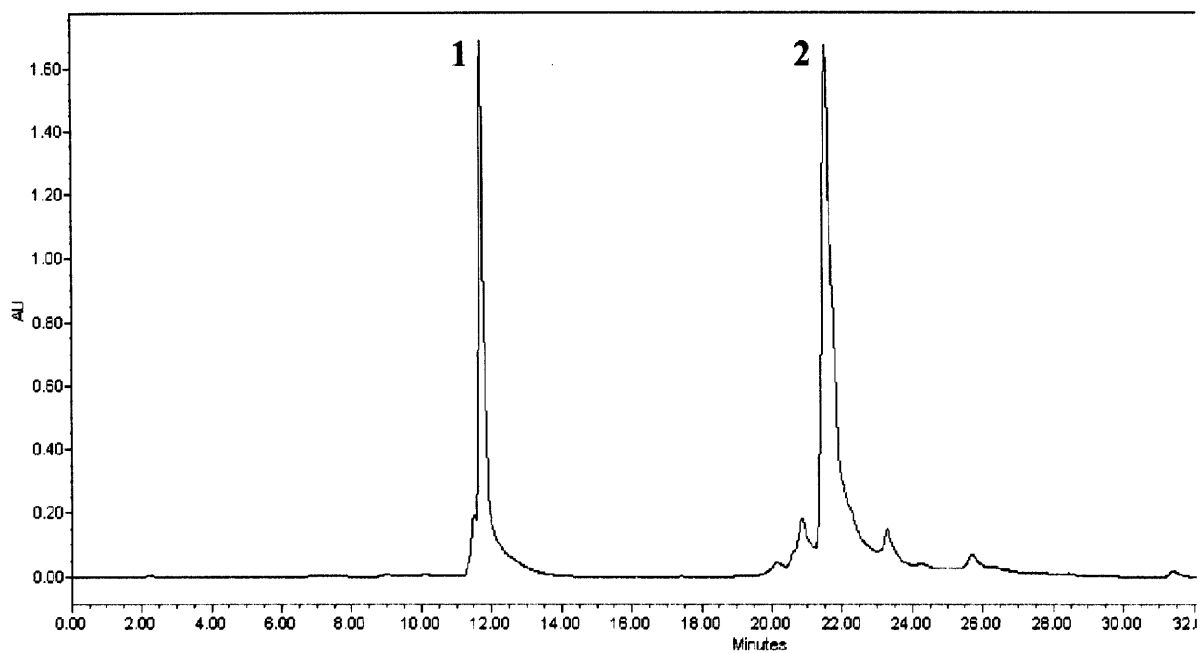


Figure C.4. RP-HPLC purification of d(GpG)-PtBP6.

Peak 1 is unreacted d(GpG) and peak 2 is the product, d(GpG)-PtBP6.

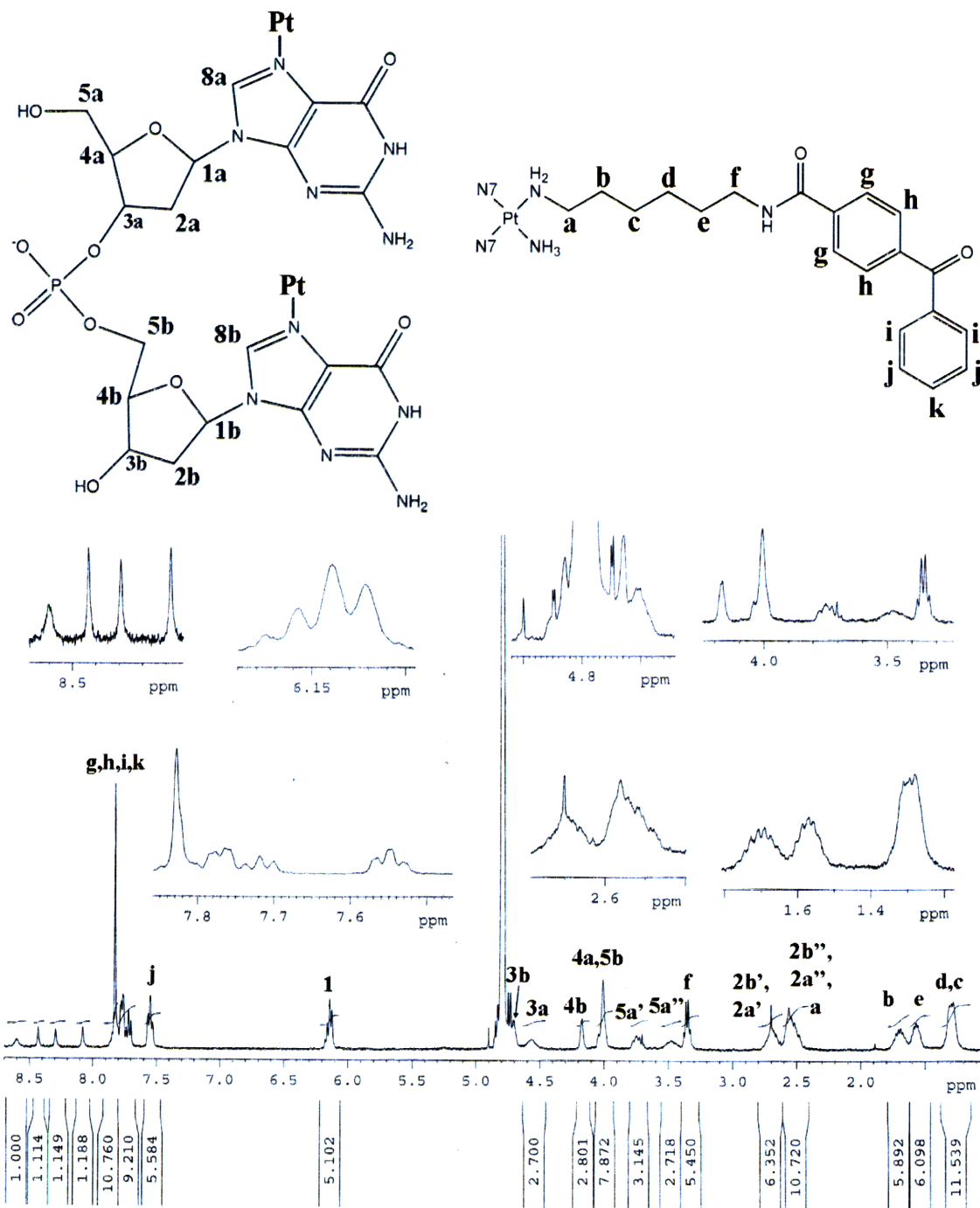


Figure C.5. <sup>1</sup>H NMR spectrum of d(GpG)-PtBP6.

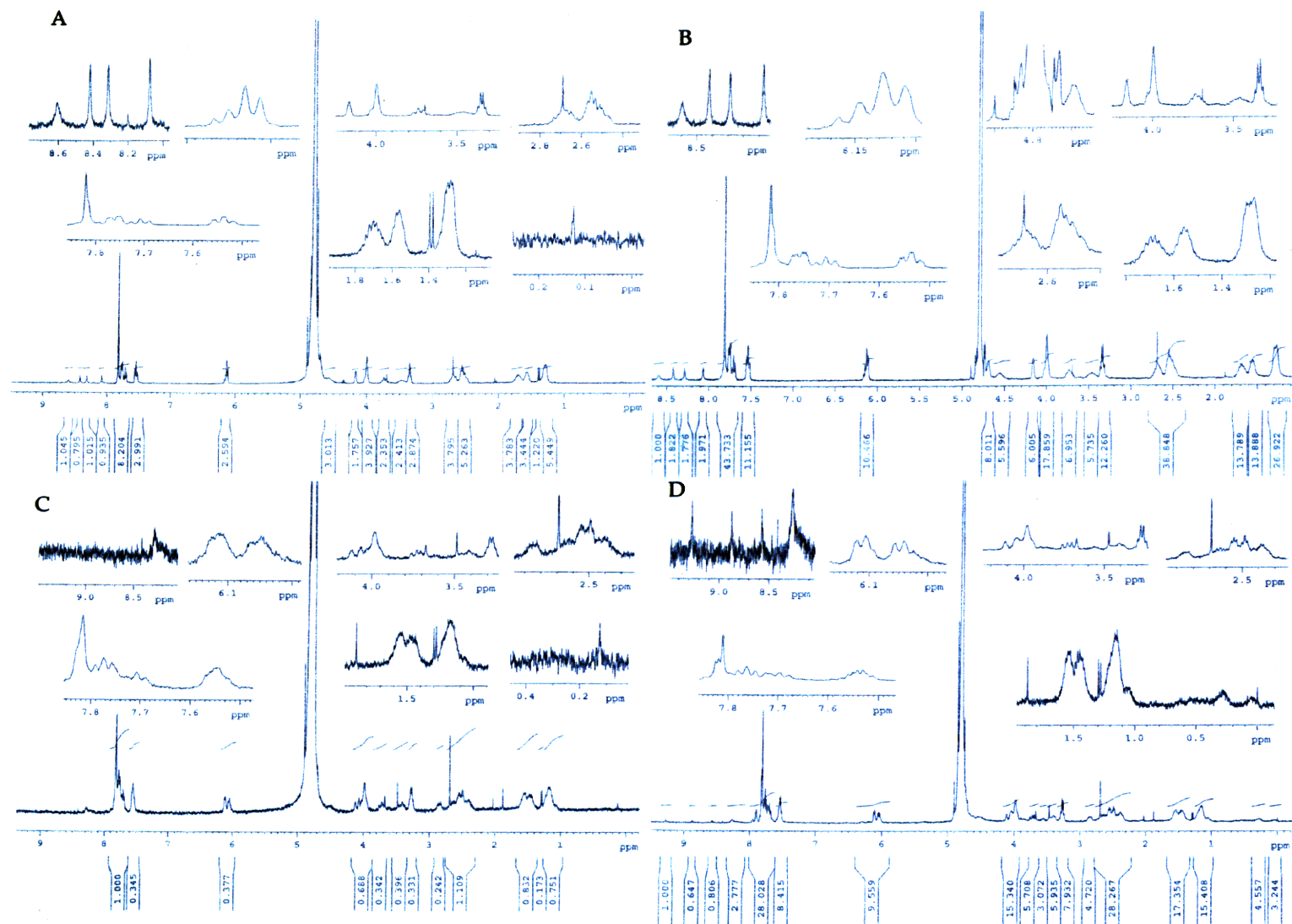


Figure C.6. pH-dependent  $^1\text{H}$  NMR spectra of d(GpG)-PtBP6.

A) pH 4. B) pH 5. C) pH 7. D) pH 10.

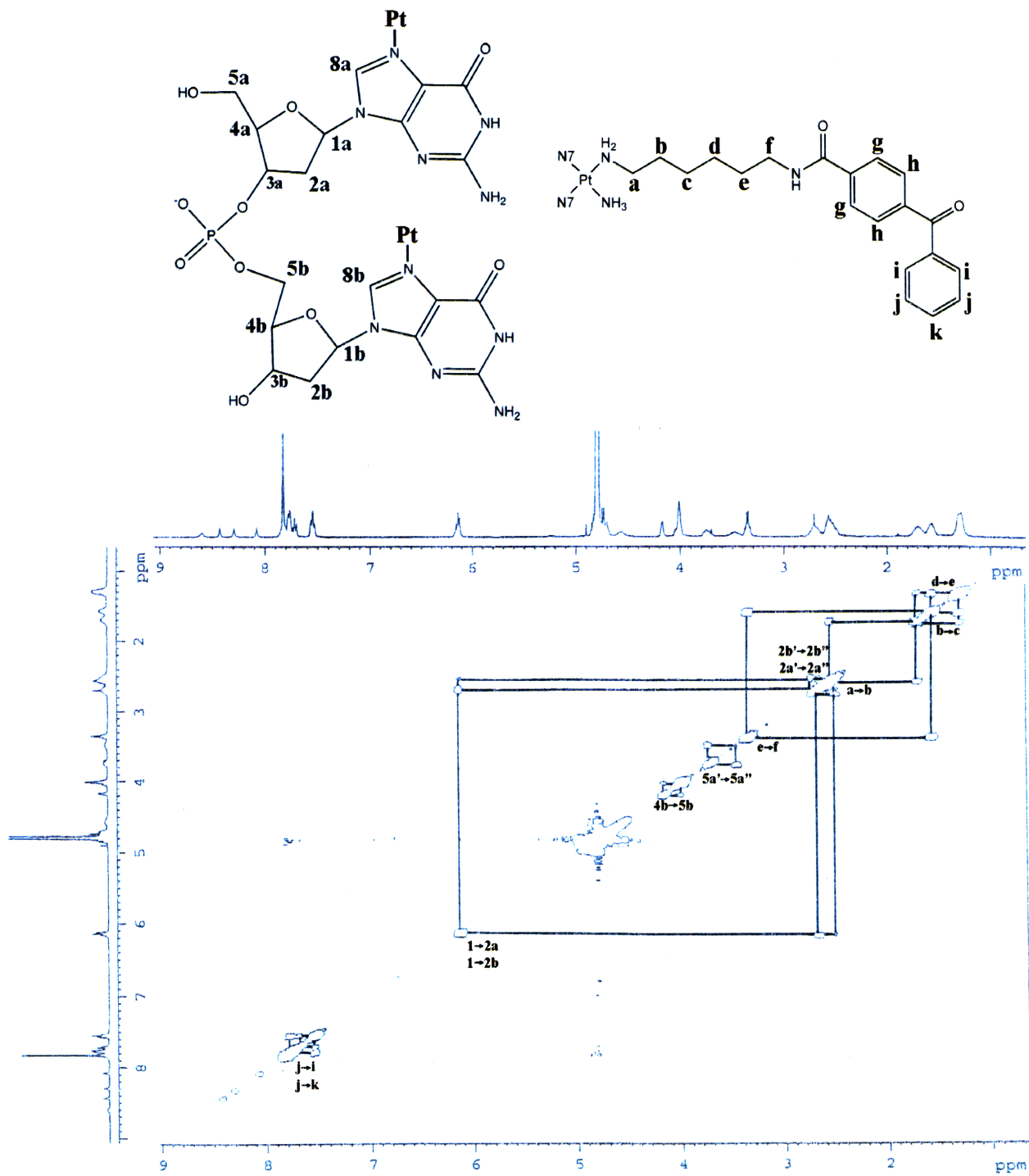


Figure C.7.  $^1\text{H}$  COSY of d(GpG)-PtBP6.



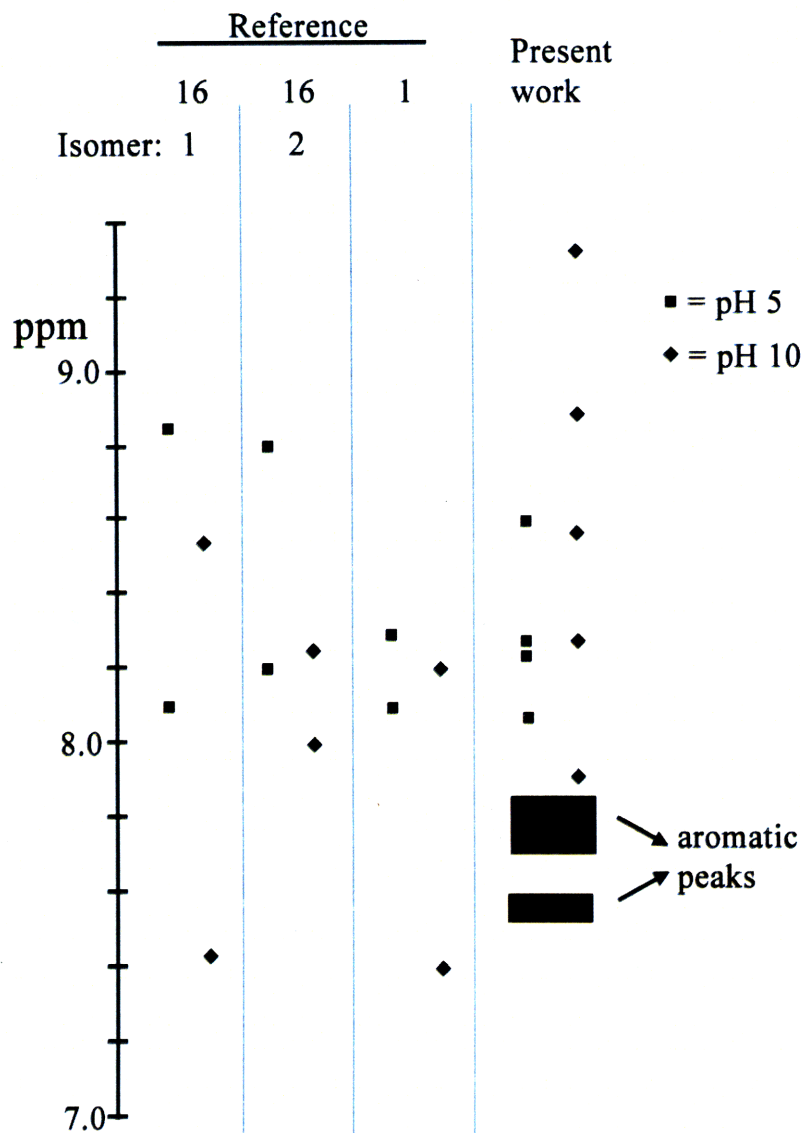


Figure C.8. H8 proton chemical shifts at low and high pH.

The chemical shifts of the H8 protons of a dinucleotide containing an asymmetric platinum compound have a distinct upfield shift at elevated pH, with an inflection point at pH 8.5. This behavior was not exhibited by the H8 protons of the compound *cis*-[Pt(NH<sub>3</sub>)(*N*-(6-aminohexyl)-4-benzophenonamide){d(GpG)}]<sup>+</sup>. These data suggest that the isomers present are a product of dinucleotide positioning (Figure C.2) and not orientation of the asymmetric platinum ligand (Figure C.1).

## Curriculum Vitae

### Evan Guggenheim

32 Vassar Street  
Building 18 Room 425  
Cambridge, MA 02139

Phone (860) 778-9644  
e-mail: [evanross@mit.edu](mailto:evanross@mit.edu)

---

### EDUCATION

- 2008 MASSACHUSETTS INSTITUTE OF TECHNOLOGY: Ph.D. in Inorganic Chemistry in the laboratory of Dr. Stephen J. Lippard
- 2003 BRANDEIS UNIVERSITY: B.S. in Chemistry with High Honors, Senior Thesis, "Studies toward gamma irradiation-induced reactivity of uranium methacrylate compounds."

### AWARDS AND HONORS

- 2006-2007 Koch Graduate Fellowship
- 2006 International Precious Metals Institute (IPMI) Student Award
- 2004-2005 MIT Cancer Training Grant Research Fellowship
- 2002-2003 Selected for undergraduate research in the lab of Dr. Bruce M. Foxman, Brandeis University
- 2002 NSF Solid-State Chemistry Summer Research Grant for work done in the lab of Dr. Bruce Foxman
- 2001 Selected for Undergraduate Summer Research Program in Biological and Biomedical Sciences, University of Connecticut Health Center, in the lab of Dr. David Papermaster

### RESEARCH GOALS

My research has been focused on understanding the mechanisms by which platinum-based chemotherapeutic compounds are able to kill cancer cells. Cisplatin has been used to treat cancer for almost thirty years. The cytotoxicity of cisplatin derives from an ability to bind DNA. I have sought to identify proteins that have an affinity for platinum-modified DNA in order to better understand the initial signaling pathways that can eventually lead to either DNA repair or cell death.

### TEACHING EXPERIENCE

- 2004 Massachusetts Institute of Technology: Teaching Assistant for Profs. Joseph Sadighi and Richard Schrock, Principles of Inorganic Chemistry I
- 2003 Teaching Assistant for Prof. Janet Schrenk, Introductory Chemical Experimentation, Massachusetts Institute of Technology
- 2003 Summer Teaching Assistant for Prof. Timothy Rose, Undergraduate General Chemistry Lab, Brandeis University
- 2002-2003 Teaching Assistant for Prof. Milos Dolnik, Undergraduate General Chemistry Lab, Brandeis University

### PUBLICATIONS

1. Guo, C.; Hickey, M. B.; Guggenheim, E. R.; Enkelmann, V.; Foxman, B. M. Conformational Polymorphism of Methacrylamide. *Chem. Commun.* **2005**, 2220-2222.

2. Guggenheim, E. R.; Xu, D.; Zhang, C. X.; Chang, P. V; Lippard, S. J. "Photo-Affinity Isolation and Identification of Proteins in Cancer Cell Extracts that Bind to Platinum-Modified DNA," *submitted*.
3. Guggenheim, E. R.; Ondrus, A. E.; Movassaghi, M.; Lippard, S. J. "Poly(ADP-ribose) Polymerase-1 Facilitates the Dissociation of Nuclear Proteins from Platinum-Damaged DNA," *submitted*.

#### **RESEARCH SEMINARS**

- MIT Center for Cancer Research Focus Seminar Series, February 2, 2007.
- American Chemical Society 234<sup>th</sup> National Meeting and Exposition, Poster Presentation, "Photo-cross-linking and identification of proteins that bind to platinum-modified DNA in cancer cell extracts," August 19, 2007; Boston, MA.
- International Symposium on Platinum Coordination Compounds in Cancer Chemotherapy, Oral Presentation, "Photo-cross-linking and identification of proteins that bind to platinum-modified DNA in cancer cell extracts," December 1, 2007; Verona, Italy.

#### **ACTIVITIES**

While at Brandeis University, I spent four years on the Brandeis Men's Rugby Team, two of those years as captain. I was also involved in the Intramural Softball League and the Intramural Flag Football League. Since arriving at MIT, I have participated in the MIT Intramural Softball League, MIT Chemistry Intramural Volleyball League as well as MIT Chemistry Pick-up Basketball.